



Uinta Basin Composition Study

Comprehensive Final Report

Prepared by

Trang Tran, PhD
Seth Lyman, PhD
Bingham Research Center
Utah State University
320 N Aggie Blvd
Vernal, UT 84078

Mike Pearson
Alliance Source Testing, LLC
5530 Marshall Street
Arvada, CO 80002

Tom McGrath
Innovative Environmental Solutions, Inc.
PO Box 177
Cary, IL 60013-017

Lexie Wilson & Bart Cubrich
Utah Department of Environmental Quality
Division of Air Quality
195 North 1950 West
Salt Lake City, UT 84116

UtahStateUniversity
BINGHAM RESEARCH CENTER



Submitted on March 31, 2020

Assembled by Lexie Wilson

lexiewilson@utah.gov
(801) 536-0022

Table of Contents

Cooperating Agents	5
Definitions	5
Executive Summary.....	8
Project Organization and Reports.....	9
Report A: Hydrocarbon Sampling	11
Summary	16
Uinta Basin Composition Study – Hydrocarbon Sampling - Purpose.....	16
Sampling and Analysis Description	16
Quality Assurance and Reporting.....	17
Testing Methodology	20
GPA 2166: Obtaining Natural Gas Samples for Analysis by Gas Chromatography	20
GPA 2174: Obtaining Liquid Hydrocarbon Samples for Analysis by Gas Chromatography	20
GPA 2286: Method for the Extended Analysis of Natural Gas and Similar Gaseous Mixtures by Temperature Programmed Gas Chromatography.....	20
GPA 2103M/2186M: Tentative Method for the Analysis of Natural Gas Condensate Mixtures Containing Nitrogen and Carbon Dioxide by Gas Chromatography	21
Flash Gas Composition by VMGThermo EOS/PSM	21
Report B: Hydrocarbon Sampling Data Quality	22
Report C: Measurement of Carbonyls, Speciation Profile Analysis, and High Flow Emissions Sampling & Analysis	30
Contents.....	31
List of Tables	31
List of Figures	33
Introduction	35
Carbonyl Speciation in Flash Gas	36
Methodology.....	36
Results.....	38
Development of Composition Speciation Profiles	43
Methodology.....	43

Hydrocarbon Speciation in Raw Gas: Grouping Results	46
Hydrocarbon Speciation in Flash Gas: Grouping Results	47
Incorporating Carbonyl Data into Flash Gas Speciation Profiles	52
Ozone Reactivities of Raw Gas and Flash Gas Profiles.....	54
Compiling Composition Profiles with SPTOOL and Application of SPECIATE Profiles	56
SPTOOL Configurations	56
Application of SPECIATE Profiles.....	57
Direct Measurements of Emissions from Oil Wells	62
Methodology.....	62
Results.....	68
Data Availability	78
Acknowledgments.....	78
References	79
Report D: Supplemental Speciation Profile Analysis	82
Introduction	82
Methods.....	86
Results.....	89
Discussion.....	95
Report E: Speciation Profile Comparison.....	97
Speciation Profile Introduction.....	97
Comparison.....	100
Report F: Verification Sampling	105
Summary.....	107
Uinta Basin Composition Study - Verification Sampling - Purpose.....	107
Results.....	107
Testing Methodology	112
GPA 2174: Obtaining Liquid Hydrocarbon Samples for Analysis by Gas Chromatography	112
GPA 2286: Method for the Extended Analysis of Natural Gas and Similar Gaseous Mixtures by Temperature Programmed Gas Chromatography	112
GPA 2103M/2186M: Tentative Method for the Analysis of Natural Gas Condensate Mixtures Containing Nitrogen and Carbon Dioxide by Gas Chromatography	112
Flash Gas Composition by VMGThermo EOS/PSM	113

Flash Gas to Oil Ratio – Modified Physical Flash.....	113
Report G: Process Simulator Comparison and Analysis.....	114
Comparison of EOS/PSM Tank Emissions Estimations	117
Sensitivity Testing	122
Comparison of Vasquez-Beggs Equation & AP-42 Tank Emissions Estimations	126
Comparison to Utah Air Agencies Oil and Gas 2017 Emissions Inventory.....	128
Summary	133
Key Findings	134
Sampling and Composition Analysis in the Uinta Basin.....	134
Sampling.....	134
Analysis	134
Chemical Composition of Oil and Gas Well Emissions.....	134
Flash Gas	135
Raw gas	135
Grouping of Composition Data & Application of Speciation Profiles	135
Comparison of Direct (High Flow) to Indirect (Separator) Emissions Measurement	136
EOS/PSM Use for Flash Gas Emissions in the Uinta Basin	136
Composition Results Compared to 2017 Utah Air Agencies Oil and Gas Emissions Inventory	137
Uinta Basin Oil and Gas Speciation Profiles	137
Next Steps	140
Acknowledgements.....	140
Appendices.....	141
Appendix A: Calibration Checks	141
Appendix B: Calibration Gas Certificates of Analysis	141
Appendix C: Sample Collection, LHC Composition, and EOS Calculations Data	142
Appendix D: AST Hydrocarbon Composition Data.....	145
Appendix E: Uinta Basin Profiles as Column-wise and Throughput-Weighted Averages.....	159
Appendix F: EOS/PSM Comparison Tables.....	161

Cooperating Agents

Lexie Wilson

Utah Division of Air Quality

Project Manager

Mike Natchees

Ute Indian Tribe

Cooperating Agency

Trang Tran

USU Bingham Research Center

Cooperating Agency

Minnie Grant

Ute Indian Tribe

Cooperating Agency

Seth Lyman

USU Bingham Research Center

Cooperating Agency

Mike Pearson

Alliance Source Testing

Contracted Laboratory

Cindy Beeler

US Environmental Protection Agency Region 8

Cooperating Agency

Andrew Marmo

Alliance Source Testing

Contracted Laboratory, Field

Bart Cubrich

Utah Division of Air Quality

Data Analysis

Tom McGrath

Innovative Environmental Solutions, Inc.

Contracted Data Quality Assessment

Dave McNeill

Utah Division of Air Quality

Cooperating Agency

Whitney Oswald

Utah Division of Air Quality

Project Oversight

Definitions

Several oil and gas-related terms and acronyms are defined for use throughout this report.

API gravity	A specific gravity scale developed by the American Petroleum Institute (API) for measuring the relative density of various petroleum liquids
AST	Alliance Source Testing
ASTM	"American Society for Testing and Materials"; typically followed by a 5-character alphanumeric code describing a particular standardized method for analysis
Blowdown	To vent gas from production/process equipment or pipelines before performing work on the equipment
BTEX	"Benzene, Toluene, Ethylbenzene, Xylenes"; aromatic compounds often emphasized for their ozone reactivity
Bubble point	The pressure and temperature conditions at which the first bubble of gas comes out of solution in oil
Completion	A generic term used to describe the events and equipment necessary to bring a wellbore into production once drilling operations have been concluded, including but not limited to the assembly of downhole tubulars and equipment required to enable safe and efficient production from an oil or gas well
Condensate	Hydrocarbon liquids from gas wells

Dump valve	Moderates the flow of liquid between the separator and the storage tank, etc.
EOS/PSM	"Equation of State / Process Simulation Model"
FGOR	"Flash Gas-Oil Ratio"
FID	"Flame Ionization Detector"; part of the gas chromatograph
Flash gas	Gas released from entrainment within oil or condensate as the liquids are depressurized when routed from the separator to the storage tank or the temperature increases from the separator to the storage tank
Fugitives	Unintended emissions or leaks from pressurized oil and gas equipment
Gauge pressure	Pressure of the separator at the time of sampling according to the pressure gauge on the separator
Gauge temperature	Temperature of the separator at the time of sampling according to the temperature gauge on the separator
GC	"Gas Chromatograph"
GPA	"Gas Processors Association"; typically followed by a four-digit code indicating a particular analytical method
HC	"hydrocarbon"
Heater Treater	See "Separator"
LHC	"Liquid Hydrocarbon"
Mod-FLA	"Modified Flash", indicates a laboratory method for simulating flash gas generation at the storage tank
OGEI	Acronym for "Oil and Gas Emissions Inventory," specifically referring to the Utah Air Agencies Oil and Gas Emissions Inventory; This is a triennial inventory that includes equipment and activity data from oil and gas operators across all jurisdictions in Utah
Oil	Hydrocarbon liquids from oil wells
Oil leg/oil leg dump valve	Tubing or point through which oil or condensate passes from the separator to the storage tank
PBP/PSC	The ratio of the bubble point pressure of a sample to the sample collection pressure
PIONA	"Paraffins, Isoparaffins, Olefins, Naphthenes, Aromatics"; a PIONA characterization describes the approximate amount of each category included in higher hydrocarbons not explicitly speciated through gas chromatography; exclusively modeled in EOS/PSM usage
Pneumatic Controllers	Natural gas-powered controllers associated with process operations on oil or gas well sites
Pneumatic Pumps	Natural gas-powered pumps associated with process operations on oil or gas well sites
Pressurized liquid	Liquids from the well in a pressurized vessel, with vessel pressure equivalent to the separator pressure
Probe pressure	Pressure of the separator at the time of sampling according to a calibrated highly accurate external pressure gauge
Probe temperature	Temperature of the separator at the time of sampling according to a calibrated highly accurate thermocouple
PTE	"Potential to Emit"; a regulatory estimation of a new source's annual emissions

Raw gas	Gas sampled off the pressurized separator following the well and upstream of the storage tanks. This gas can be used on-site to power pneumatic controllers and pumps, provide fuel gas for combustor pilots and engines, etc.
RVP	"Reid Vapor Pressure"
Sample port	Port on a separator from which a pressurized liquid sample can be drawn
scf/bbl	"Standard Cubic Feet per Barrel"; standard unit for FGOR
Separator	A vessel that separates the well fluids into gas and liquids. See "Two-Phase Separator" and "Three-phase Separator"
Sight glass	Glass window installed on the separator to view the separation point between liquids
STDEV	Standard Deviation
Storage tank	Tank receiving fluids from the separator; in this study, "storage tank" refers to the oil or condensate tank, not the water tank
Storage tank temperature	Temperature of the oil or condensate storage tank at the time of separator sampling according to the temperature gauge on the tank
SWB	"Standing Working Breathing" Emissions; acronym for emissions emanating from a storage tank due to small temperature and pressure changes in the tank's environment and the type of tank; this does not include flash emissions
TCD	"Thermal Conductivity Detector"; part of the gas chromatograph
Three-phase separator	A vessel that separates the well fluids into gas and two types of liquids: oil and water, using pressure and temperature, often associated with oil wells
Two-phase separator	A vessel that separates the well fluids into gas and total liquid using pressure and temperature, often associated with gas wells
U&O Reservation	Uintah & Ouray Reservation
UBCS	Uinta Basin Composition Study (this study)
VBE	Vasquez-Beggs Equation
VMG	"Virtual Materials Group"; often in reference to the particular Process Simulation Model employed during the Hydrocarbon & Verification Sampling portions of this study
VMGThermo	EOS/PSM used in Hydrocarbon & Verification sampling portions of this study
Waxy crude	Unrefined oil that is solid at room temperature, often resembling the texture of peanut butter, due to high paraffin content
Well liquid unloading	A well with decreasing production may be shut in for a period of time in order for pressure to increase, at which point the well is blown down to remove accumulated liquids at the bottom of the well that are hampering gas flow. The pressurized stream is routed to a tank where the inhibiting liquid can drop out, bypassing the separator.
WRAP	Western Regional Air Partnership

Executive Summary

The Uinta Basin Composition Study was designed to gain a better understanding of the chemical components that make up air emissions from oil and gas production facilities. Oil and gas emissions contain volatile organic compounds (VOCs) which are precursors to ozone. The Uinta Basin's recent designation as an ozone non-attainment area prompted the Utah Division of Air Quality to fund this study in an effort to better speciate VOCs from these sources. The study included an extensive sampling campaign from 78 oil and gas wells across the Uinta Basin, in which pressurized liquids and raw gas samples were collected from the separator at each facility. These samples were then analyzed by gas chromatography to describe the different hydrocarbons present in each gas sample. Utah State University (USU) engaged in an additional analysis to measure carbonyl content in a subset of ten oil and gas well samples, because carbonyls are especially reactive for ozone production. Special analytical methods were deployed in the laboratory in order to accurately process waxy Uinta Basin crude in the gas chromatograph. USU also directly measured the composition of emissions detected by infrared camera on producing oil or gas well sites in the Basin and compared these results to the separator-sampled composition reports.

Flash gas hydrocarbon composition was simulated using an Equation of State/Process Simulation Model (EOS/PSM), rather than being physically flashed and measured in the laboratory.

Following an in-depth quality control review of the data, a new statistical technique was applied to all the composition data and summarized the reports into six speciation profiles. The results include four profiles describing the composition of: i) flashed gas from oil wells, ii) flashed gas from gas wells, iii) raw gas from oil wells, and iv) raw gas from gas wells in the Uinta Basin. The two remaining profiles describe flashed gas from oil and gas wells including carbonyls.

EOS/PSM performance was tested on a subset of 5 wells from the study. EOS/PSM are often used by operators in the Uinta Basin to prepare emissions estimations for permit applications and oil and gas emissions inventory submissions. Testing of an EOS/PSM on the samples collected in this study revealed that accurately modeling a heated tank environment is crucial to accurate VOC emission rate and gas-oil ratio estimations. Most oil-producing tanks in the Uinta Basin are heated to keep the waxy crude in a liquid state during storage, and this heating can greatly increase VOC emission rates.

The speciation profiles developed in this study will have an impact on photochemical modeling exercises, the triennial oil and gas emissions inventory, and oil and gas permit application processes.

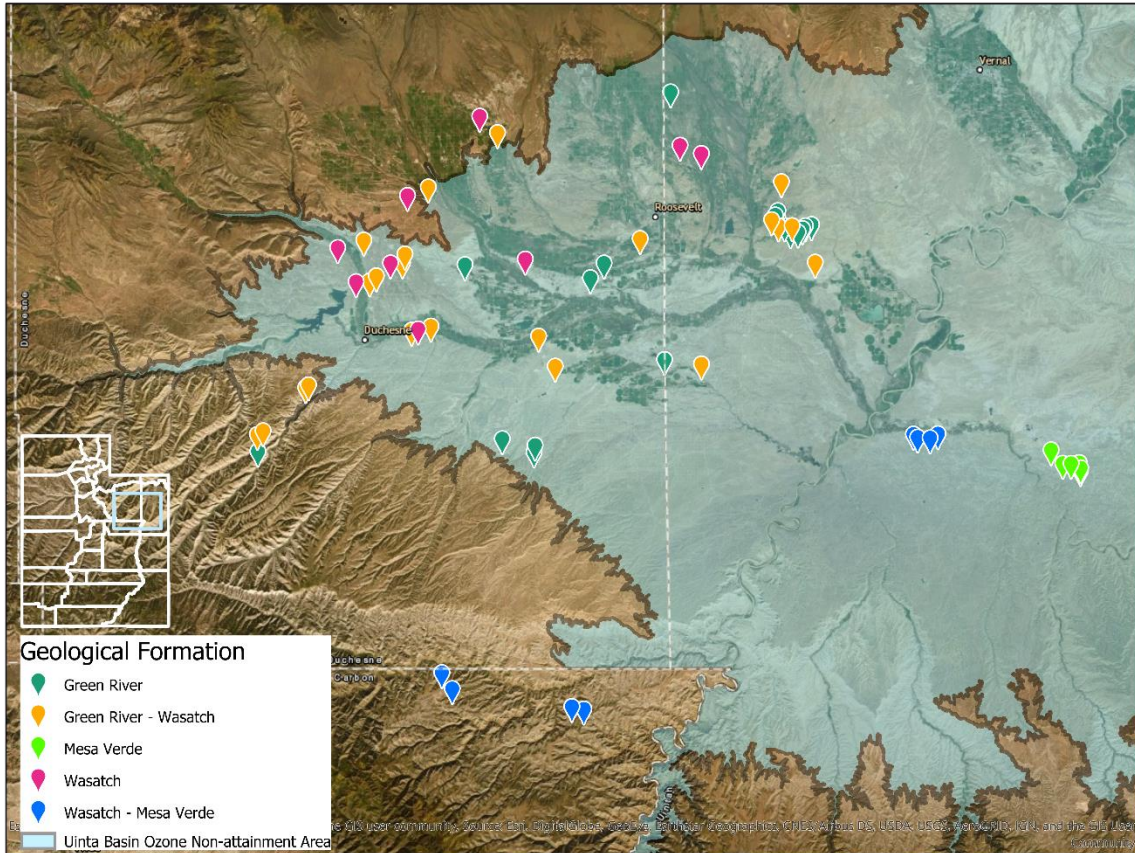


Figure 1: Location and geological formation associated with oil and gas wells sampled in this study.

Project Organization and Reports

The Uinta Basin Composition Study includes contributions from several institutions (see Figure 2), and their results are in the final report accordingly:

- **Report A: Hydrocarbon Sampling** – Alliance Source Testing (AST) describes their process in sampling and analyzing the original selection of 78 wells across the Uinta Basin, including details about standardized analytical methods used and notes about best sampling practices.
- **Report B: Hydrocarbon Sampling Data Quality** – Innovative Environmental Solutions performs a statistical analysis on AST's results from Report A, and identifies samples to remove from the dataset using a bubble point analysis.
- **Report C: Measurement of Carbonyls, Speciation Profile Analysis, and High Flow Emissions Sampling & Analysis** – Utah State University reports on their analysis of carbonyls found in raw and flash gas from a subset of 10 wells also sampled by AST, the grouping of sample results into several speciation profiles to be used in photochemical modeling, and comparing speciation profiles to measured emissions composition using the high-flow device.
- **Report D: Supplemental Speciation Profile Analysis** – UDAQ proposes an alternative method to group composition data into speciation profiles.

- **Report E: Speciation Profile Comparison** – Previous Uinta Basin speciation profiles are compared to the profiles generated in this study.
- **Report F: Verification Sampling** – AST re-sampled 5 wells of the original 78 in order to perform physical flash gas composition analysis. Modified physical flash gas analysis methods (specific to Uinta Basin waxy crude) are described.
- **Report G: Process Simulator Comparison and Analysis** – EOS/PSM results from various popular models are compared based on the composition data from Report F, with the intent to determine model input and set-up impact on air emissions estimates. The resulting air emissions estimates are then compared to data in the Utah Air Agencies 2017 Oil and Gas Emissions Inventory.

Uinta Basin Composition Study Comprehensive Sampling & Analysis Outline

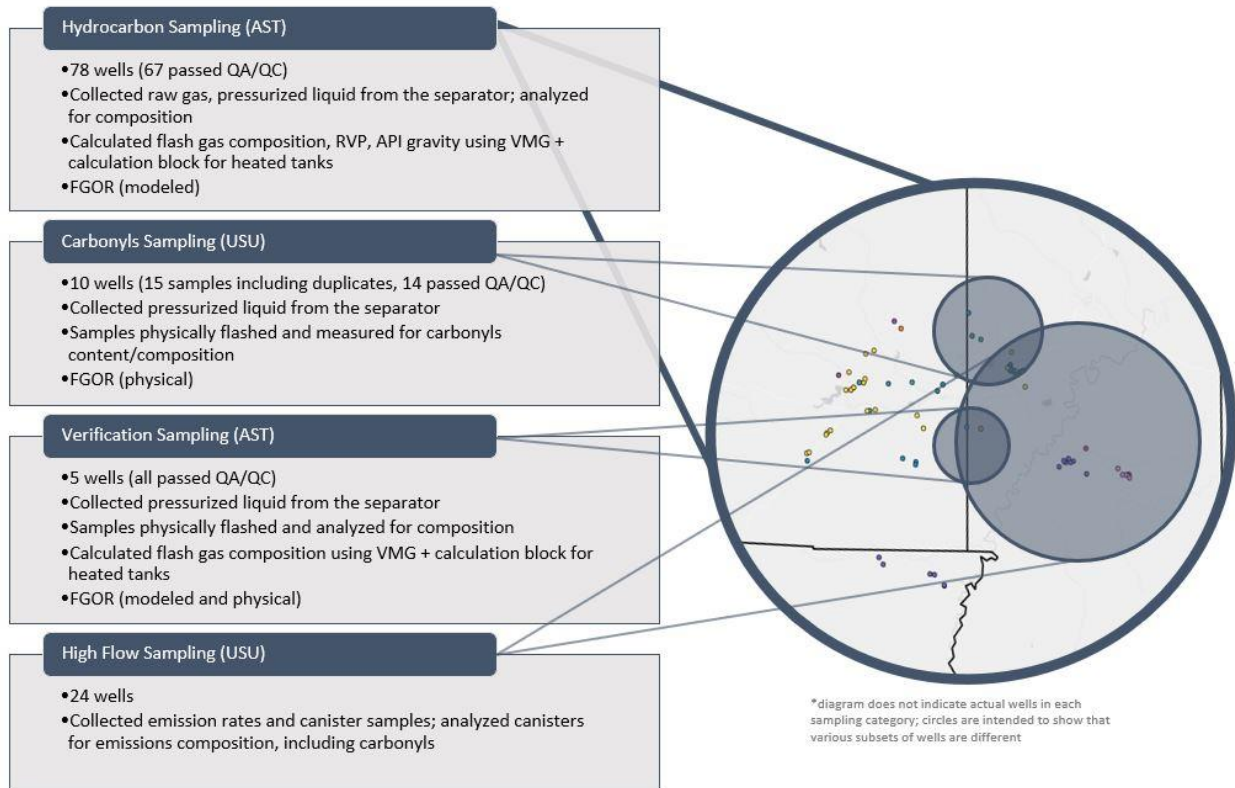


Figure 2: Diagram illustrating the four sampling campaigns under the Uinta Basin Composition Study. The circle diagram on the right alludes to subsetting; of the 78 wells included in initial hydrocarbon sampling, various subsets were taken for carbonyls, verification, and high flow sampling events with some overlap in wells sampled

Report A: Hydrocarbon Sampling

Alliance Source Testing

The top half of the page features a background image of an industrial refinery or chemical plant at sunset. The sky is a mix of orange, yellow, and blue. In the foreground, there are several tall distillation columns and a complex network of pipes and scaffolding. The Alliance Source Testing logo is overlaid on the left side of this image. The logo consists of the word "Alliance" in a large, bold, white sans-serif font, with a stylized flame or wave icon above the letter 'i'. Below "Alliance" is the text "SOURCE TESTING" in a smaller, all-caps, white sans-serif font.

Alliance
SOURCE TESTING

Uinta Basin Report

Utah Division of Air Quality

195 North 1950 West

Salt Lake City, Utah

Test Dates:

October 2018 – January 2019

Test Program

Uinta Basin Composition Study

Source Information

Test Location
Uinta Basin

Sources Tested
78 Wells

Test Parameters
Pressurized Liquid & Raw Gas
Samples

Contact Information

Test Company

Alliance Source Testing, LLC
5530 Marshall Street
Arvada, CO 80002

Project Manager
Mike Pearson
Michael.pearson@stacktest.com
(720) 457-9512

Field Team Leader
Andrew Marmo
Andrew.marmo@stacktest.com
(720) 457-9512

Innovative Environmental Solutions, Inc.
Data Analysis, QA review
Tom McGrath
Tmcgrath.me@gmail.com
(714) 315-4040

Cooperating Agents

Lexie Wilson
Utah Division of Air Quality
195 North 1950 West
Salt Lake City, Utah
Lexiewilson@utah.gov
(801) 536-0022

Whitney Oswald
Utah Division of Air Quality
195 North 1950 West
Salt Lake City, Utah
Whitneyoswald@utah.gov
(801) 536-0022

Seth Lyman
USU Bingham Research Center
320 N. Aggie Blvd.
Vernal, UT
Seth.lyman@usu.edu
(435) 722-1740

Cindy Beeler
US Environmental Protection Agency
1595 Wynkoop St.
Denver, CO 80202
Beeler.Cindy@epa.gov
(303) 312-6204

Alliance Source Testing, LLC (AST) has completed the analytical testing as described in this report. Results apply only to the wells tested and operating conditions for the specific test dates and times identified within this report. All results are intended to be considered in their entirety, and AST is not responsible for use of less than the complete test report without written consent. This report shall not be reproduced in full or in part without written approval from the customer.

To the best of my knowledge and abilities, all information, facts and test data are correct. Data presented in this report has been checked for completeness and is accurate, error-free and legible. Onsite testing was conducted in accordance with approved internal Standard Operating Procedures. Any deviations or problems are detailed in the relevant sections on the test report.

This report is only considered valid once an authorized representative of AST has signed in the space provided below; any other version is considered draft. This document was prepared in portable document format (.pdf) and contains pages as identified in the bottom footer of this document.



Mike Pearson, Oil & Gas Lab Manager
Alliance Source Testing, LLC

1/27/20

Date

TABLE OF CONTENTS

Summary..... 16

Uinta Basin Composition Study – Hydrocarbon Sampling - Purpose 16

Sampling and Analysis Description..... 16

Quality Assurance and Reporting 17

Testing Methodology 20

GPA 2166: Obtaining Natural Gas Samples for Analysis by Gas Chromatography 20

GPA 2174: Obtaining Liquid Hydrocarbon Samples for Analysis by Gas Chromatography..... 20

GPA 2286: Method for the Extended Analysis of Natural Gas and Similar Gaseous Mixtures by Temperature Programmed Gas Chromatography 20

GPA 2103M/2186M: Tentative Method for the Analysis of Natural Gas Condensate Mixtures Containing Nitrogen and Carbon Dioxide by Gas Chromatography 21

Flash Gas Composition by VMGThermo EOS/PSM..... 21

LIST OF TABLES AND FIGURES

TABLE A-1 TESTING METHODOLOGY..... 16

FIGURE A-1 SOURCE PORT MODIFICATION **Error! Bookmark not defined.**17

APPENDICES

- Appendix A Calibration Checks
- Appendix B Calibration Gas Certificates of Analysis

Summary

Summary

Uinta Basin Composition Study – Hydrocarbon Sampling - Purpose

This report summarizes the results from the compositional analysis of raw gas & pressurized liquid samples collected from 78 wells across Utah state jurisdiction in the Uinta Basin. The purpose of the study was to provide a robust set of compositional data to the Utah Department of Air Quality (UDAQ) to be used to create improved speciation profiles for use in modeling, inventory collection, and permit distribution and ultimately establish emission factors that better represent the specific products in the Basin.

Alliance Source Testing (AST) utilized the analyses shown in Table A-1. Section 2 provides a more comprehensive presentation and discussion of the testing methodology.

TABLE A-1
TESTING METHODOLOGY

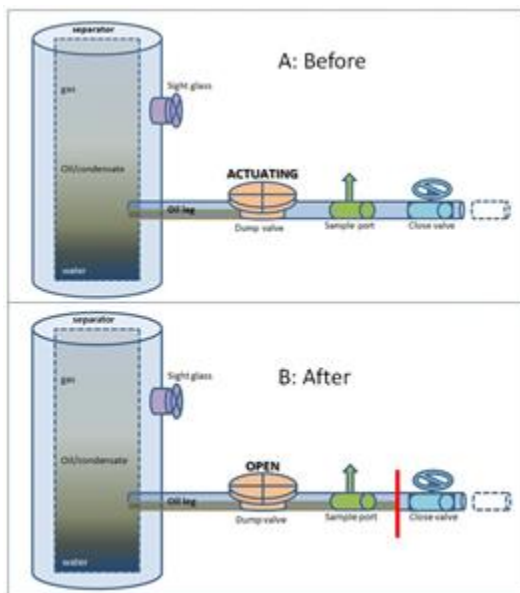
Parameter	GPA Test Methods	Notes/Remarks
Pressurized Gas Collection	GPA 2166	Obtaining Natural Gas Samples
Pressurized Liquid Collection	GPA 2174	Obtaining Liquid Hydrocarbon samples
Raw Gas Composition	GPA 2286	Extended Gas Analysis by Gas Chromatography
Pressurized Liquid Composition	GPA 2103M/2186M	Extended Liquid Hydrocarbon Analysis by Gas Chromatography
Flash Gas Composition & FGOR	NA	VMG – EOS/PSM
Reid Vapor Pressure (Flashed Liquid)	NA	VMG – EOS/PSM
API Gravity (Flashed Liquid)	NA	VMG – EOS/PSM

Sampling and Analysis Description

The pressurized liquids fell into two categories: a thick yellow or black “waxy crude” oil from oil wells and a lighter condensate from gas wells. The waxy crude oil associated with the oil wells solidified at ambient temperatures and the onsite production equipment had to be heated to a range of 110°F – 180°F to keep the product flowing. The lighter condensate associated with the gas wells was mostly clear and colorless.

Both types of well sites presented unique liquid sampling challenges. In the case of the oil wells, the solid wax can plug both the sampling equipment in the field and the laboratory instrumentation. Keeping the sample probe warm and maintaining a constant liquid flow rate during the probe purging process helped avoid the solidification of the oil during sample collection. This was especially important during the winter sampling. Most of the waxy crude oil samples were collected from the oil leg of the separator. At certain locations the only available sample point was on the oil leg after the dump valve. To collect a representative pressurized sample, in those instances, a valve downstream of the sample port was closed and the oil leg was purged (Fig. A-1). The gas wells in the Basin produce a small amount of condensate relative to the gas and water. Some of the gas well separators were operated as two-phase systems and did not separate the oil and water onsite. The sample collection difficulty for the gas wells was that a relatively large volume of water had to be drained before the liquid hydrocarbon could be collected from either a sight glass or leg of the separator.

FIGURE A-1
SAMPLE PORT MODIFICATION



Modifications were made to the laboratory instrumentation for the analysis of the pressurized waxy crude oil. AST added a heat traced network of tubing to the gas chromatograph's (GC) plumbing. Heat traced tubing temperatures were set to the temperature of the well's heated storage tank to guarantee the sample was a flowing liquid right before injection but not hot enough to become two phases (gas/liquid) in the plumbing. The methodology modifications to quantify the waxy crude oil samples' heavy decanes plus component can be found in the Testing Methodology section.

The heat traced GC was not used for the gas well condensate samples. Several of the condensate samples had a low bubble point bias that could be due to the draining process disturbing the liquid/gas equilibrium of the samples directly before sample collection. Further quality assurance discussion can be found in Section 1.3 and REPORT B: HYDROCARBON SAMPLING DATA QUALITY.

VMGThermo Process Simulation Model/Equation of State (PSM/EOS) calculations based on the analytical results from the pressured liquid samples were used to estimate the flash gas composition, flash gas to oil ratio (FGOR), flashed liquid Reid Vapor Pressure (RVP), and flashed liquid API gravity. VMG was selected instead of the physical flash, vapor pressure, and density measurements because of the waxy crude analysis difficulties explained above. AST worked directly with VMG to generate the best model to handle the waxy crude compositions. More detail on VMG can be found in the Testing Methodology section.

The raw gas samples were collected and analyzed using standard GPA methodology. More detail about the collection and analysis of the gas samples can be found in the Testing Methodology section.

Quality Assurance and Reporting

Analytical results for liquid hydrocarbon (LHC) samples were initially and primarily evaluated by reviewing the ratio of the bubble point pressure of a sample to the sample collection pressure (P_{BP}/P_{SC}). P_{BP}/P_{SC} ratios close to 1.0 (e.g., about 0.7 to 1.3) are considered an indication that the LHC samples were collected at or near gas/liquid equilibrium conditions and that the analytical results are accurate. The bubble point pressure is calculated using Equation of State

(EOS) process simulation software using the analytical results (i.e., LHC composition). LHC samples were classified as either condensate or waxy crude. The waxy crudes are solid at ambient temperatures whereas the condensate remains a liquid. Due to these compositional differences and different separator designs and operation for the two types of LHCs, the data analysis evaluated the condensate and waxy crude samples separately. REPORT B: HYDROCARBON SAMPLING DATA QUALITY gives a detailed discussion of the data evaluation.

Twenty-seven condensate samples were collected, and ten of the condensate samples have P_{BP}/P_{SC} values ranging from 0.157 to 0.614, and P_{BP}/P_{SC} values this low are likely caused by the loss of light HCs (e.g., methane, ethane, propane). This contention is supported by a cursory review of the compositional data and FGOR estimates based on these samples would be expected to have a low bias. It is strongly suspected that the separation equipment and operation at many condensate production sites contributed to the low P_{BP}/P_{SC} values. Several of the condensate production sites employed vertical two-phase separators with the sight glass and dump valve either near the bottom or midpoint of the vertical column, and had very high water-to-oil ratios. Quite often, before condensate samples could be collected at the sight glass, large volumes of water needed to be drained from the separators to bring the condensate to the sight glass level for sample collection. It is suspected that the rapid separator headspace volume increase created by this water removal caused light HCs to volatilize into the headspace and disturbed the gas/condensate equilibrium. Loss of light ends would depress EOS-calculated values of bubble point pressure and FGORs. Considering the separator operation anomalies and the low P_{BP}/P_{SC} values, the analytical results for these 10 condensate samples are likely not reasonable representations of the LHCs at equilibrium at the sample collection temperature and pressure. Thus, use of these particular samples for air quality analyses is not recommended. The remaining 17 condensate samples do appear to be reasonable representations of the LHCs at equilibrium at the sample collection temperature and pressure. In addition, a lesson learned from the condensate sample collection is that specific guidelines should be developed for collection of samples from two-phase separators with high water-to-oil ratios. For example, select separators with sight glasses near the mid-level rather than the bottom of a vertical column and coordinate with operators to manage several pre-sample well cycles to maximize oil and minimize water in the separator prior to sample collection.

Fifty-one waxy crude samples were collected, and one waxy crude sample had the largest P_{BP}/P_{SC} value (1.44), as well as the largest FGOR and ethane and propane concentrations despite an average separator pressure. Taken together, these anomalies suggest the analytical results for this sample may not be a reasonable representation of the LHCs at equilibrium at the sample collection temperature and pressure, and use of this sample for air quality analyses is not recommended. The remaining 50 waxy crude samples do appear to be reasonable representations of the LHCs at equilibrium at the sample collection temperature and pressure.

Calibration checks were performed on GC's to confirm instrument precision. Certified 'natural' liquid standards were used for the liquid GC's and certified natural gas standards were used for the gas GC's. Precision limit checks and certificates of analysis can be found in Appendix A:

Testing Methodology

Testing Methodology

The testing program was conducted in accordance with the test methods listed in Table A-1. Method descriptions are provided below while quality assurance/quality control data is provided in APPENDIX A:

GPA 2166: Obtaining Natural Gas Samples for Analysis by Gas Chromatography

The purge and trap method was used to transfer gas from the source into a leak-free, stainless steel, single cavity, double valve gas container. The gas vessels were kept heated prior to each sampling event to avoid any condensation due to a cold cylinder. The gas sampling assembly included a short probe, highly accurate pressure gauge, gas vessel, pigtail extension, and several valves. The source valve was opened to blow out any accumulated material a few times and the gas container assembly was connected to the source. The source valve was opened, then the sample container was slowly purged. The outlet (pigtail) was then closed allowing the pressure to build up rapidly. The sample cylinder inlet valve was closed and then the outlet was opened allowing the container to vent to almost atmospheric pressure. The outlet was closed, and the steps were repeated until the number of cycles complied with the method to effectively purge the container and fill it with source gas. Well names, probe pressure, pipe temperature, gauge pressure, gauge temperature, ambient conditions, sample times, sampler's initials, dates, number of tanks onsite, and any important sampling notes or changes were recorded.

GPA 2174: Obtaining Liquid Hydrocarbon Samples for Analysis by Gas Chromatography

Samples were collected from a location (e.g., sample probe, sight glass fitting) with routine oil circulation to avoid collecting stagnate HC liquids from the bottom of the separator. Several of the samples were collected from a sample port on the oil leg upstream of the dump valve on the heater treater described in Section 1.2. A sample collection rate of 60 ml/min or less (start sample collection at a slow rate and increase to target sampling rate) was used for all sampling. The sample collection temperature and pressure were monitored and recorded at the start and conclusion of each sample collection event using highly calibrated gauges on the sample probe. No anomalous pressure changes occurred during the sampling. All samples were collected in constant pressure cylinders. The sample probe was completely purged before introduction of the liquid into the cylinder. The cylinders were filled to approximately 80% volume. An onsite compressibility check was performed by pressurizing the back-pressure side of the cylinder with helium after the cylinder was filled to ensure that an unseen gas plug was not introduced into the sample. None of the samples compressed to any extent. The probe assembly and constant pressure cylinders were kept around 70°F until the sampling occurred.

The separator pressure and temperature were measured using a sample probe with highly accurate gauges. The approximate time of the last dump cycle was recorded. The beginning and end time of the sampling event was recorded. The storage tank temperature was recorded for the waxy crude samples that required heated storage tanks. Well names, probe pressure, probe temperature, gauge pressure, gauge temperature, ambient conditions, sample times, sampler's initials, dates, number of tanks onsite, and any important sampling notes or changes were recorded.

GPA 2286: Method for the Extended Analysis of Natural Gas and Similar Gaseous Mixtures by Temperature Programmed Gas Chromatography

The gas samples were analyzed on a GC equipped with a flame ionization detector (FID) and a thermal conductivity detector (TCD). The GC was calibrated with several certified external standards and response factors for both detectors were determined. The required components measured were C1-C10, N₂, O₂, CO₂, and BTEX. A calibration check with a certified natural gas standard was performed on the GC before running a batch of gases. The

calibration checks complied with reproducibility requirements of GPA 2261 and can be found in Appendix A:. The cylinders were heated to approximately 200^oF by a heated oven and line assembly. The gas was introduced into the GC sample loop at a constant purge rate. The gas cylinder was closed and the gas in the sample loop was allowed to relax to atmospheric pressure before injection into the GC. The gas concentrations were reported in mole % and mass %.

GPA 2103M/2186M: Tentative Method for the Analysis of Natural Gas Condensate Mixtures Containing Nitrogen and Carbon Dioxide by Gas Chromatography

The pressurized liquid sample analysis was done by an AST modified version of GPA 2103M/2186M. The AST modifications included an ASTM D7169 simulated distillation analysis to extend the report to C36+, an ASTM D6730 detailed hydrocarbon analysis on the flame ionization detector (FID) for improved speciation, the thermal conductivity detector (TCD) analysis was C1 - C6+ and CO2 with the air removed, and the C10+ molecular weight and density fractions were calculated from the GC analysis.

The waxy crude liquid samples were heated to the storage tank temperatures, pressurized to 1000 psig, and injected on the GC. The C1 - C6+ and CO2 concentrations were measured on the TCD. The C6+ peak on the TCD is back flushed. A calibration curve and response factors for C1 - C5 and CO2 were established on the TCD using a pressurized ‘natural’ liquid calibration standard made from a sample in the Denver-Julesburg Basin. The C1 - C5 and CO2 sample concentrations were determined by multiplying the sample peak areas and the individual response factors from the calibration curve. The C6 – C10 concentrations are determined by an ASTM D6730 detailed hydrocarbon analysis run on the FID. A small amount of the pressurized liquid was flashed, diluted with carbon disulfide, and run on a second GC-FID by ASTM D7169. The ASTM D7169 simulated distillation run extended out to C100 and allowed the final report to be extended to C36+.

Flash Gas Composition by VMGThermo EOS/PSM

VMGThermo was used to determine the flash gas composition, Reid Vapor Pressure (RVP) &API gravity of flashed liquids, and FGOR from the pressurized liquid. Using VMGThermo’s Advanced Peng Robinson and Advanced Peng Robinson for Natural Gas 2 property packages the calculations were performed for reporting purposes and quality assurance checks (bubble points) of laboratory analysis.

Using VMGThermo’s advanced fluid characterization methodology, PIONA, the complete fluid could be modeled accurately from the pure component ‘light ends’ through the carbon number analysis to C36+. For quality assurance the calculated bubble point was compared to the measured separator conditions in the field. VMGThermo was then used to flash the fluid to storage tank conditions which determined the flash gas composition, and various properties of the flashed liquid. Results of this analyses are discussed in REPORT G: PROCESS SIMULATOR COMPARISON AND ANALYSIS.

Report B: Hydrocarbon Sampling Data Quality

Innovative Environmental Solutions, Inc.



innovative environmental solutions, inc.

MEMORANDUM

Date: March 14, 2019

To: Mike Pearson, Alliance Source Testing (AST)

From: Tom McGrath, Innovative Environmental Solutions, Inc.

Re: Review of AST Analytical Results for Liquid Hydrocarbon Samples Collected in Utah

Introduction

In 2018 and 2019 AST collected and analyzed 78 liquid hydrocarbon (LHC) samples in Utah. 78 samples were collected from 78 production sites operated by seven Companies, and 27 were classified as condensate (C) samples and 51 were classified as waxy crude (W) samples. The waxy crudes are solid at ambient temperatures; thus, the production separators and storage tanks are heated (e.g., ~ 110-180°F) to handle the waxy crude as a liquid. Due to the waxy crude properties, the AST sample analytical systems required heat tracing. The condensate production equipment operated at lower temperatures and large volumes of water needed to be drained from some condensate separators prior to LHC sample collection. As will be further discussed, it is suspected that the separator headspace created by this water removal impacted the gas/LHC equilibrium in some condensate separators. Table B-1 summarizes the samples collected, the ranges of process/sample collection conditions, and the ranges of calculated flash gas-to-oil ratios (FGOR).

Table B-1. Summary of Samples Collected and Process Conditions

Production Company	Number of Samples	Condensate (C) or Waxy Crude (W)	Sample Collection Temperature (°F)	Sample Collection Pressure (psia)	FGOR (scf/bbl)
I	10	C	49 - 86	89 - 339	10 - 49
II	9	C	60 - 116	37 - 203	5 - 33
III	8	C	64 - 72	204 - 357	77 - 154
IV	6	W	115 - 135	44 - 67	5 - 74
V	15	W	111 - 185	48 - 94	9 - 63
VI	15	W	110 - 163	44 - 64	10 - 30
VII	15	W	111 - 159	44 - 88	7 - 43

Bubble Point Pressure / Sample Collection Pressure Data for All Samples

The ratio of the bubble point pressure of a sample to the sample collection pressure (P_{BP}/P_{SC}) is used to evaluate the quality of analytical results for LHC samples. P_{BP}/P_{SC} ratios close to 1.0 are considered an indication that the LHC samples were collected at or near gas/liquid equilibrium conditions and that the analytical results are accurate. The bubble point pressure is calculated using Equation of State (EOS) process simulation software using the analytical results (i.e., LHC composition).

Figure B-1 graphs P_{BP}/P_{SC} values for all the project samples ordered from the smallest to the largest P_{BP}/P_{SC} . Condensate samples have blue symbols and waxy crude samples have red symbols. The condensate samples generally have much lower P_{BP}/P_{SC} values. Due to these data trends and the different separator designs and operation for the two types of LHCs, further data analysis evaluated the condensate and waxy crude samples separately.

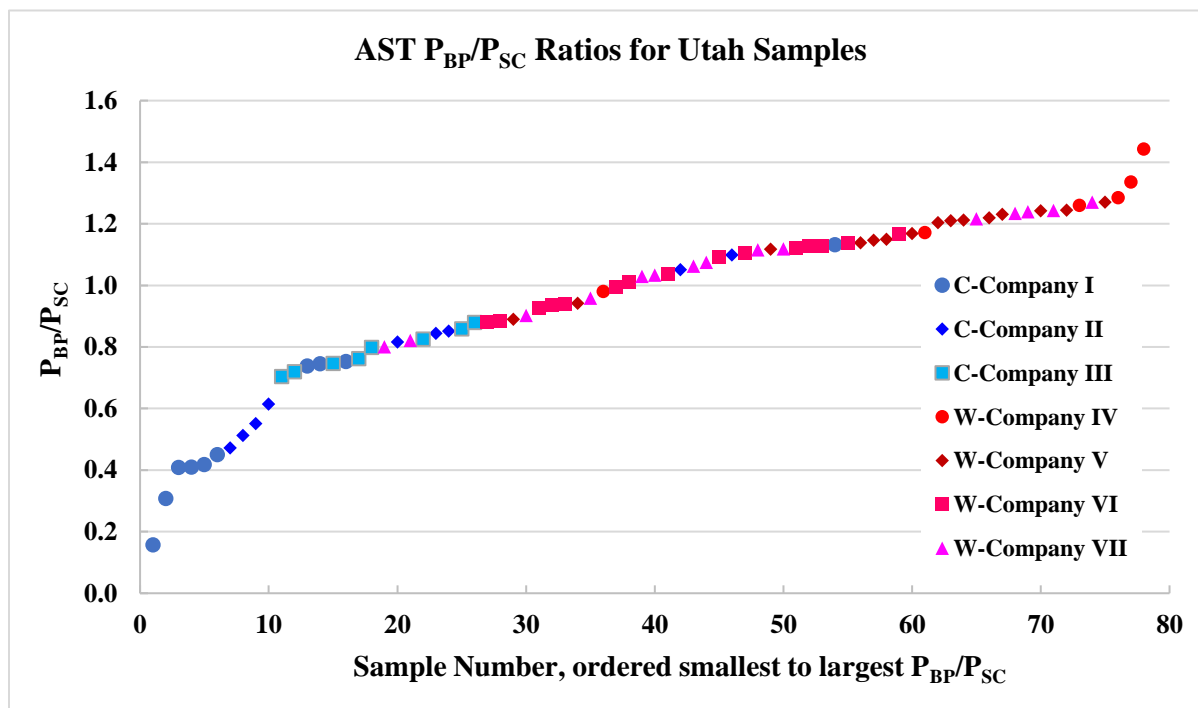


Figure B-1. P_{BP}/P_{SC} for all samples

Waxy Crude Samples

Figure B-2 graphs P_{BP}/P_{SC} values for the project waxy crude samples ordered from the smallest to the largest P_{BP}/P_{SC} . P_{BP}/P_{SC} values ranged from 0.800 to 1.442. Based on inspection, the samples with the two smallest and two largest P_{BP}/P_{SC} values were analyzed to determine if they are statistical outliers for this data set.

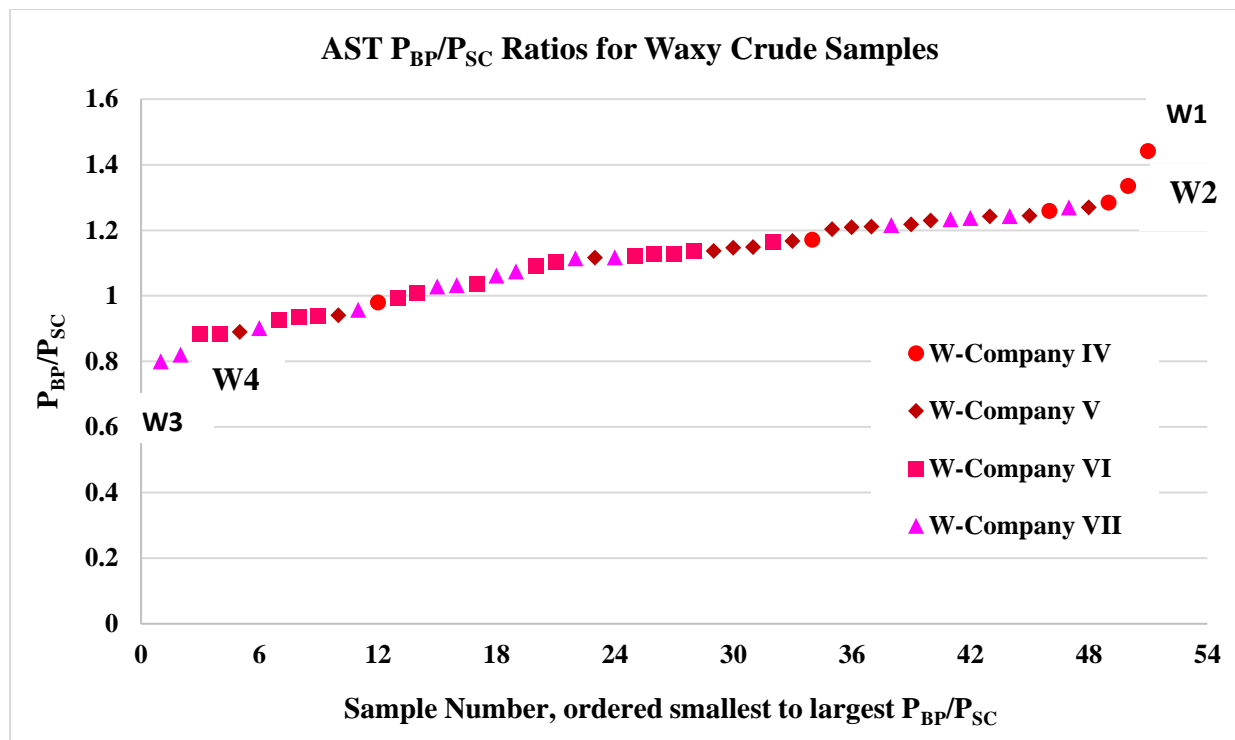


Figure B-2. P_{BP}/P_{SC} values for waxy crude samples

The basic steps for the data review and statistical analysis include:

1. Calculate basic statistics for the data set.
2. Determine if data set has a normal probability distribution.
3. Identify possible outlier samples by two methods: Grubbs Outlier Test with Rosen Procedure¹ and Dixons Q test.²
4. Consider other parameters associated with the sample (e.g., FGOR, composition)
5. Summary and recommendation

Basic Statistics: Table B-2 summarizes the basic statistics for the waxy crude samples data set. The average P_{BP}/P_{SC} value is about 1.11 and the median is 1.13; thus, although the data set has a normal probability distribution, its center is offset from 1.0.

Table B-2. Summary Statistics for the Waxy Crude Samples Data

Number of Samples	P _{BP} /P _{SC}				
	Average	Median	STDEV	Max	Min
51	1.11	1.13	0.142	1.44	0.800

¹ Based on ASTM D7915-14 "Standard Practice for Application of Generalized Extreme Studentized Deviate (GESD) Technique to Simultaneously Identify Multiple Outliers in a data Set." and α = 0.05 (2-sided) values from http://www.statistics4u.com/fundstat_eng/ee_grubbs_outliertest.html

²Outlier Test – Dean and Dixon, http://www.statistics4u.com/fundstat_eng/cc_outlier_tests_dixon.html

Probability Distribution: The data set has a normal probability distribution as determined by goodness of fit test for a normal probability distribution based on chi-square (χ^2) distribution³ and illustrated by the histogram in Figure B-3.

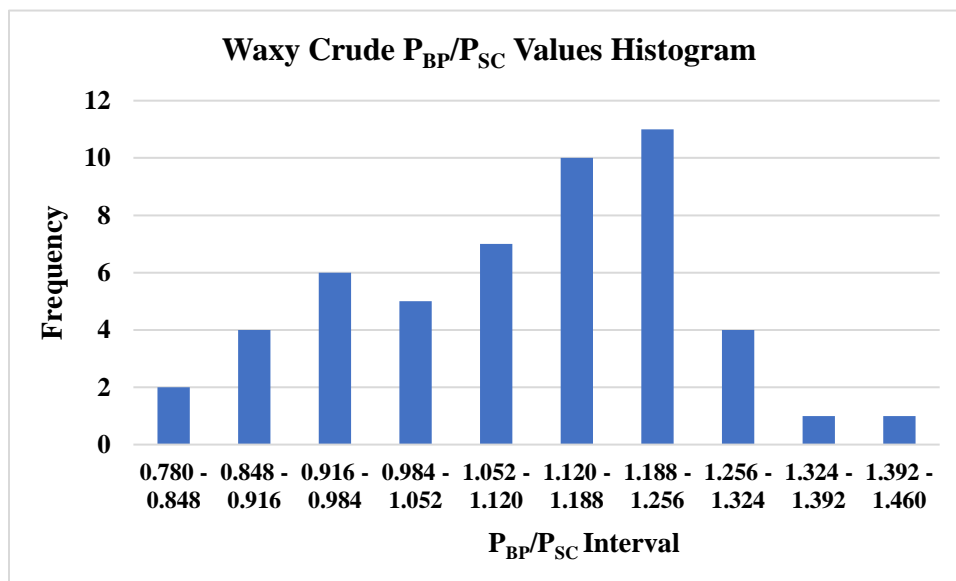


Figure B-3. Histogram for the waxy crude samples data

Outlier Tests: Table B-3 lists the four samples identified as potential outliers, and the results of the outlier tests calculations. None of four samples were determined to be outliers by either the Grubbs Outlier Test with Rosen Procedure or the Dixons Q test. Also listed in Table B-3 is a Z value calculated as the difference between the PBP/PSC value and the average PBP/PSC divided by the standard deviation. Some quality control programs track Z values and flag measurements with values greater than 2 for further scrutiny. Based on this criterion, further review of samples W1, W3, and W4 was conducted.

Table B-3. Outlier Analysis Results for Waxy Crude Samples

Sample	PBP/PSC	Grubbs Test Outlier? ($\alpha = 0.05$)	Dixons Q Test Outlier? ($\alpha = 0.05$)	Z = (PBP/PSC - Avg)/ STDEV
W1 – IV-5	1.442	No	No	2.36
W2 – IV-4	1.336	No	No	1.61
W3 – VII-8	0.800	No	No	2.15
W4 – VII-5	0.821	No	No	2.01

Other Parameters: APPENDIX C: SAMPLE COLLECTION, LHC COMPOSITION, AND EOS CALCULATIONS DATA is a tabulation of sample collection data (e.g., temperature and pressure), LHC composition data (e.g., mole %), and EOS calculations data (i.e., bubble point pressure and FGOR) for all the project samples. Analysis of FGOR values can sometimes be used to evaluate the reliability of

³ Anderson, Sweeney, & Williams, "Statistics for Business and Economics, 8th Edition". 2002 by South-Western/Thomson Learning

LHC analytical results. However, quantitative analysis of the FGOR results for this project is limited because samples were collected over a wide range of temperatures and pressures (e.g., refer to Table B-1), and both parameters strongly impact the FGOR of LHCs. A review of the sample composition and EOS calculated parameters did not find any anomalies for samples W3 and W4. In addition to the high P_{BP}/P_{SC} ratio (i.e., 1.44), sample W1 anomalies included the highest FGOR of all the waxy crude samples (despite an average sample collection pressure) and the highest concentrations of the light end compounds ethane and propane of all the samples. Figure B-4 graphs ethane + propane concentrations for the waxy crude samples ordered from highest to lowest concentration, and it appears that sample W1 is an outlier (confirmed by the Grubbs and Dixons outlier tests). Adjusting the concentrations for sample collection temperature and pressure did not change this conclusion.

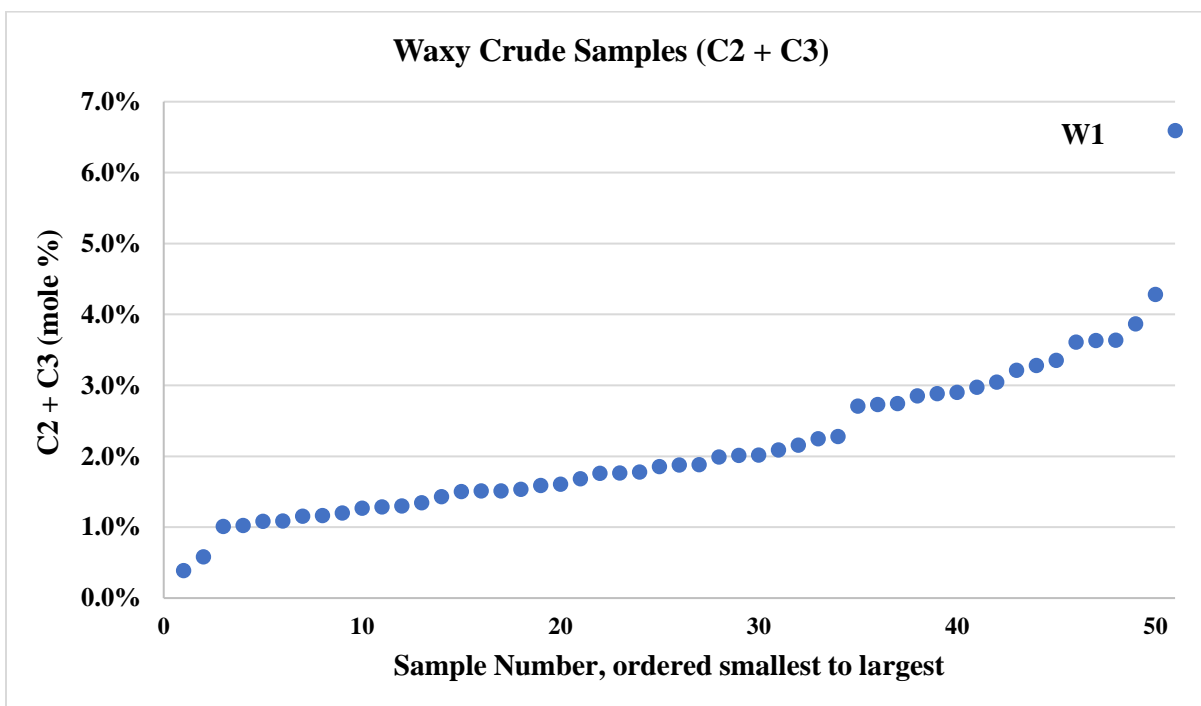


Figure B-4. Ethane + Propane Concentrations for Waxy Crude Samples Ordered from Highest to Lowest Concentration

Summary and recommendation: FGORs for these samples are very low (i.e., maximum of 74.0 scf/bbl). None of the samples P_{BP}/P_{SC} values were identified as statistical outliers and all but two samples had P_{BP}/P_{SC} values within the 0.7 to 1.3 range. As noted above, Sample W1 had the largest P_{BP}/P_{SC} value (1.44), as well as the largest FGOR and ethane and propane concentrations (refer to Figure B-4) despite an average separator pressure. Taken together, these anomalies suggest the W1 analytical results may not be a reasonable representation of the LHCs at equilibrium at the sample collection temperature and pressure, and use of this sample for air quality analyses is not recommended. In APPENDIX C: SAMPLE COLLECTION, LHC COMPOSITION, AND EOS CALCULATIONS DATA, sample W1 has strike-through text to indicate this recommendation. For all other waxy crude samples, the P_{BP}/P_{SC} values and other data suggest the analytical results are reasonable representations of the LHCs at equilibrium at the sample collection temperature and pressure.

Condensate Samples

Figure B-5 graphs P_{BP}/P_{SC} values for the project condensate samples ordered from the smallest to the largest P_{BP}/P_{SC} . P_{BP}/P_{SC} ranged from 0.157 to 1.131.

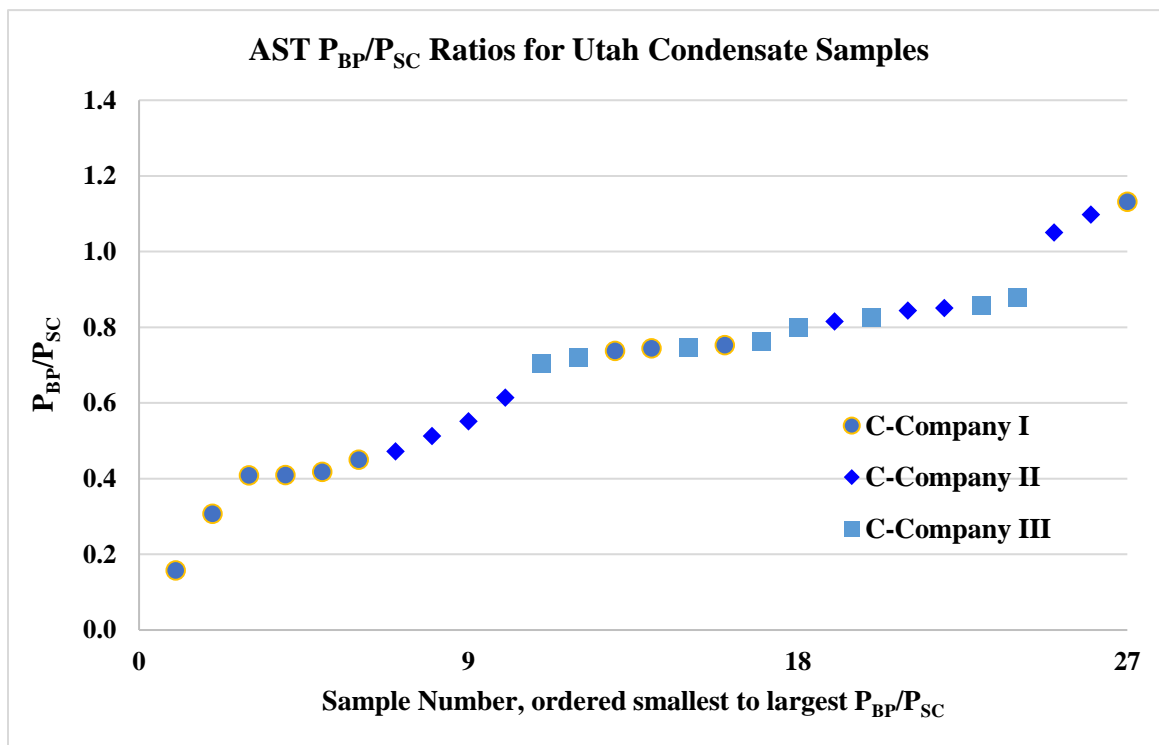


Figure B-5. P_{BP}/P_{SC} values for condensate samples

Basic Statistics: Table B-4 summarizes the basic statistics for the condensate samples data set. The average P_{BP}/P_{SC} value is about 0.689 and the median is 0.744. The P_{BP}/P_{SC} values for the condensate samples are generally much lower than the P_{BP}/P_{SC} values for the waxy crude samples (e.g., average of 0.689 vs. 1.11).

Table B-4. Summary Statistics for the Condensate Samples Data

Number of Samples	P_{BP}/P_{SC}				
	Average	Median	STDEV	Max	Min
27	0.689	0.744	0.240	1.13	0.157

Probability Distribution: The data set does not have a normal probability distribution as determined by goodness of fit test for a normal probability distribution based on chi-square (χ^2) distribution⁴ and illustrated by the histogram in Figure B-6. Thus, the outlier tests used for the

⁴ Anderson, Sweeney, & Williams, "Statistics for Business and Economics, 8th Edition". 2002 by South-Western/Thomson Learning

waxy crude samples, the Grubbs Outlier Test with Rosen Procedure and the Dixons Q test, are not applicable for this data set.

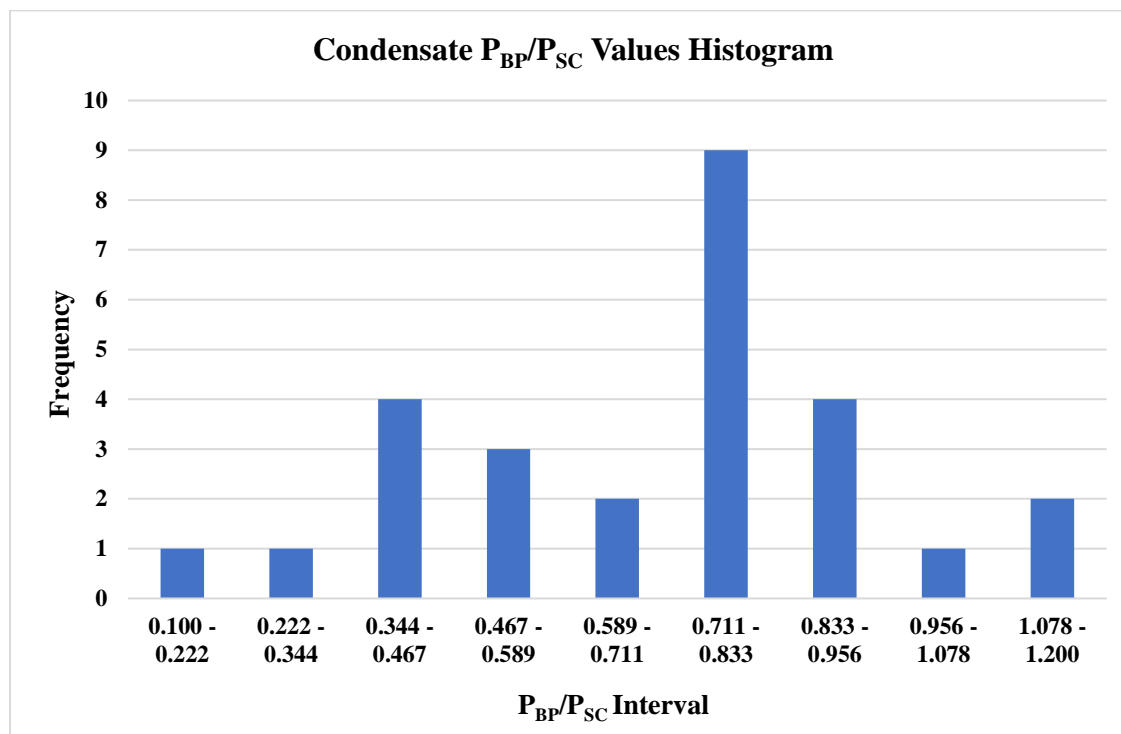


Figure B-6. Histogram for the condensate samples data

Outlier Analysis/Data Review and Analysis: Ten of the condensate samples have P_{BP}/P_{SC} values ranging from 0.157 to 0.614, and P_{BP}/P_{SC} values this low are likely caused by the loss of light HCs (e.g., methane, ethane, propane). This contention is supported by a cursory review of the compositional data and FGOR estimates based on these samples would be expected to have a low bias. It is strongly suspected that the separation equipment and operation at many condensate production sites contributed to the low P_{BP}/P_{SC} values. The condensate production sites employed vertical two-phase separators with the sight glass and dump valve either near the bottom or midpoint of the vertical column, and had very high water-to-oil ratios. Quite often, before condensate samples could be collected at the sight glass, large volumes of water needed to be drained from the separators to bring the condensate to the sight glass level for sample collection. It is suspected that the rapid separator headspace volume increase created by this water removal caused light HCs to volatilize into the headspace and disturbed the gas/condensate equilibrium. Loss of light ends would depress EOS calculated values of bubble point pressure and FGORs.

Under such conditions, bubble point pressure depression would be expected to be greater for higher separator pressures because the light ends fraction (and potential light ends loss to separator headspace) of HC liquids increases with pressure. Figure B-7 compares P_{BP}/P_{SC} values with sample collection (i.e., separator) pressure and shows a distinct P_{BP}/P_{SC} reduction with increasing P_{SC} for the C-Company I and C-Company II samples. This trend is not observed for the C-Company III samples. Discussion with lab and sample collection personnel determined

that much less water was drained from the C-Company III separators prior to sample collection than from the C-Company I and C-Company II separators. These observations and the P_{BP}/P_{SC} vs P_{SC} trend in Figure B-7 suggest the C-Company III samples were much less biased by the separator water removal.

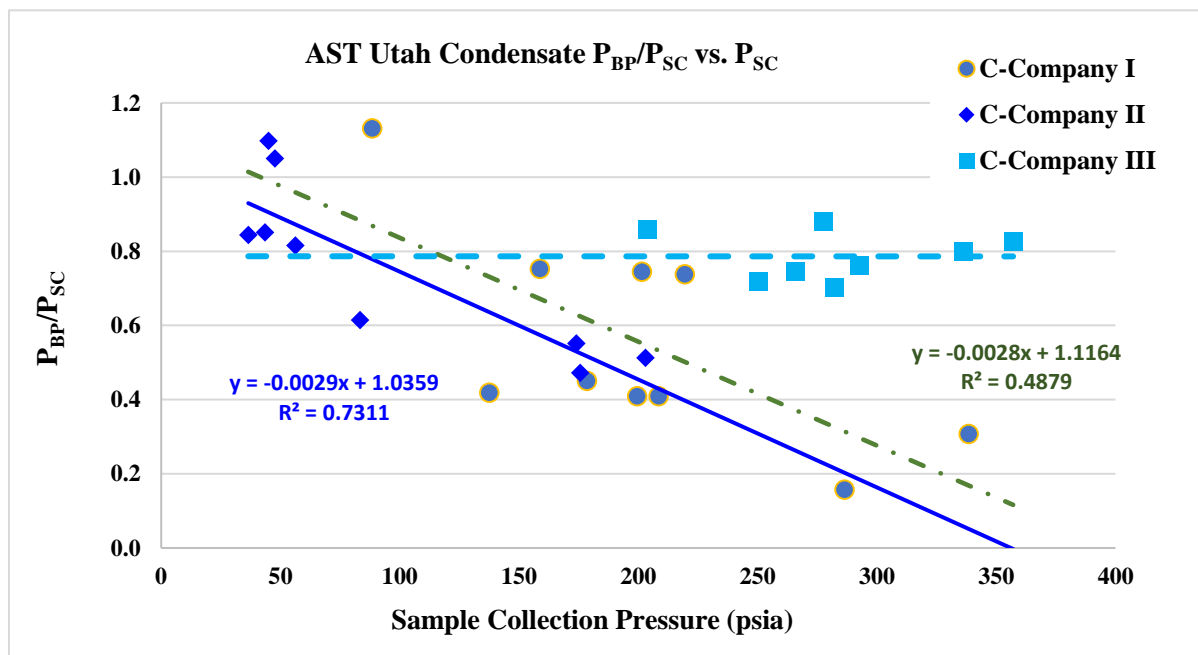


Figure B-7. P_{BP}/P_{SC} vs. P_{SC} for the condensate samples

Summary and recommendation: A lesson learned from the condensate sample collection is that specific guidelines should be developed for collection of samples from two-phase separators with high water-to-oil ratios. For example, select separators with sight glasses near the mid-level rather than the bottom of a vertical column and coordinate with operators to manage several pre-sample well cycles to maximize oil and minimize water in the separator prior to sample collection.

The 10 condensate samples with P_{BP}/P_{SC} values less than 0.70 very likely have a low bias in the concentration of light end HCs. Considering the separator operation anomalies and the low P_{BP}/P_{SC} values, the analytical results for these 10 samples are likely not reasonable representations of the LHCs at equilibrium at the sample collection temperature and pressure. Thus, use of these samples for air quality analyses is not recommended. These samples are indicated by strike-through text in APPENDIX C: SAMPLE COLLECTION, LHC COMPOSITION, AND EOS CALCULATIONS DATA. The P_{BP}/P_{SC} values for the other condensate samples suggest the analytical results are reasonable representations of the LHCs at equilibrium at the sample collection temperature and pressure.



Report C: Measurement of Carbonyls, Speciation Profile Analysis, and High Flow Emissions Sampling & Analysis

Utah State University Bingham Research Center



COMPOSITION OF VOLATILE ORGANIC COMPOUND EMISSIONS FROM OIL AND GAS WELLS IN THE UINTA BASIN

FINAL REPORT

Submitted to:

Lexie Wilson

Utah Division of Air Quality

195 N 1950 W

Salt Lake City, UT 84114

Submitted by:

Trang Tran, PhD

Seth Lyman, PhD

Huy Tran, PhD

Bingham Research Center

Utah State University

320 N Aggie Blvd

Vernal, UT 84078

DOCUMENT NUMBER: BRC192608A

REVISION: VERSION 2

DATE: 14 NOVEMBER 2019

Contents

List of Tables	31
List of Figures	33
1. Introduction	35
2. Carbonyl Speciation in Flash Gas	36
2.1. Methodology.....	36
2.2. Results.....	38
3. Development of Composition Speciation Profiles	43
3.1. Methodology.....	43
3.2. Hydrocarbon Speciation in Raw Gas: Grouping Results	46
3.3. Hydrocarbon Speciation in Flash Gas: Grouping Results	47
3.4. Incorporating Carbonyl Data into Flash Gas Speciation Profiles	52
3.5. Ozone Reactivities of Raw Gas and Flash Gas Profiles.....	54
4. Compiling Composition Profiles with SPTOOL and Application of SPECIATE Profiles	56
4.1. SPTOOL Configurations	56
4.2. Application of SPECIATE Profiles.....	57
5. Direct Measurements of Emissions from Oil Wells	62
5.1. Methodology.....	62
5.2. Results.....	68
5.3. Data Availability	78
6. Acknowledgments.....	78
7. References	79

List of Tables

Table C2-1. Concentrations of carbonyls in flash gas from pressurized oil samples, in ppm (vol/vol).	38
Table C2-2. Concentrations of carbonyls in flash gas from pressurized condensate samples, in ppm (vol/vol).....	39
Table C2-3. Carbonyl detection limits, reported by mass and concentration.	41
Table C3-1. Grouping of sampled wells by geological formation.	44

Table C3-2. Jarque-Bera normality test *p*-values (two-tailed) for raw gas composition data for each geological formation. 45

Table C3-3. Jarque-Bera normality test *p*-values (two-tailed) for flash gas composition data for each geological formation. 46

Table C3-4. Mean (\bar{X}) weight percent and relative standard deviation (RSD) calculated for raw gas composition for each geological formation. 47

Table C3-5. Mean (\bar{X}) weight percent and relative standard deviation (RSD) calculated for the flash gas composition of each geological formation. 48

Table C3-6. Mean (\bar{X}) weight percent and relative standard deviation (RSD) calculated for the flash gas composition of the Green River–Wasatch subgroups. 49

Table C3-7. Mean (\bar{X}) weight percent and relative standard deviation (RSD) calculated for the flash gas composition of the Wasatch subgroups. 50

Table C3-8. Final flash gas hydrocarbon composition profiles for oil wells (weight percent). 51

Table C3-9. Final flash gas hydrocarbon composition profiles (weight percent) for gas wells. 52

Table C3-9. Flash gas hydrocarbon and carbonyl composition profiles (weight percent) for sampled oil wells. 53

Table C3-10. Flash gas hydrocarbon and carbonyl composition profiles (weight percent) for sampled gas wells that draw from the Mesa Verde (MV) formation. 54

Table C4-1. Organic compound speciation profiles developed from hydrocarbon and carbonyl measurements of flash gas and raw gas from oil and gas wells in the Uinta Basin. 58

Table C4-2a. Organic compound raw gas speciation profiles used as input for SPTOOL, in weight percent. 59

Table C4-2b. Organic compound flash gas speciation profiles used as input for SPTOOL, in weight percent. 60

Table C4-3. Organic compound speciation profiles produced by SPTOOL (in split factor). 61

Table C5-4. List of organic compounds measured with the high flow system, the compound type, the analytical method used by USU, and whether the compounds were analyzed for by AST. 64

Table C5-5. Summary of emission plumes detected at each well visited. 69

Appendix Table E-1a. Hydrocarbon composition of flash gas (weight percent) at oil wells associated with the Green River formation. 145

Appendix Table E-1b. Z-scores calculated for hydrocarbon composition of flash gas at oil wells associated with the Green River formation. 146

Appendix Table E-2a. Hydrocarbon composition of flash gas (weight percent) at oil wells associated with the Green River - Wasatch formation. 147

Appendix Table E-2b. Z-scores calculated for hydrocarbon composition of flash gas at oil wells associated with the Green River-Wasatch formation..... 148

Appendix Table E-2. Hydrocarbon composition of flash gas (weight percent) at oil wells associated with the Wasatch formation. 149

Appendix Table E-3. Hydrocarbon composition of flash gas (weight percent) at gas wells associated with the Mesa Verde formation. 150

Appendix Table E-4. Hydrocarbon composition of flash gas (weight percent) at gas wells associated with the Wasatch - Mesa Verde formation. 151

Appendix Table E-5a. Hydrocarbon composition of raw gas (weight percent) at oil wells associated with the Green River formation..... 152

Appendix Table E-6b. Z-scores calculated for hydrocarbon composition of raw gas at oil wells associated with the Green River formation..... 153

Appendix Table E-6a. Hydrocarbon composition of raw gas (weight percent) at oil wells associated with the Green River - Wasatch formation..... 154

Appendix Table E-7b. Z-scores calculated for hydrocarbon composition of raw gas at oil wells associated with the Green River formation..... 155

Appendix Table E-7. Hydrocarbon composition of raw gas (weight percent) at oil wells associated with the Wasatch formation. 156

Appendix Table E-8. Hydrocarbon composition of raw gas (weight percent) at gas wells associated with the Mesa Verde formation. 157

Appendix Table E-9. Hydrocarbon composition of raw gas (weight percent) at gas wells associated with the Wasatch - Mesa Verde formation. 158

List of Figures

Figure C2-1. Comparison of gas-oil ratios of flash gas measured from pressurized liquid samples analyzed in the laboratory by USU and gas-oil ratios modeled by AST 38

Figure C2-2. Average carbonyl composition of gas flashed from oil samples. 40

Figure C2-3. Average carbonyl composition of gas flashed from pressurized condensate samples..... 40

Figure C2-4. Box and whisker plots of total carbonyl concentrations in oil samples and associated blanks. 42

Figure C2-5. Box and whisker plots of total carbonyl concentrations in all condensate samples and associated blanks. 42

Figure C3-1. Ozone maximum incremental reactivities of five raw gas formation-averaged composition profiles. 55

Figure C3-2. Ozone maximum incremental reactivities of eight flash gas formation-averaged composition profiles. 56

Figure C5-1. Diagram of high flow sampling system..... 62

Figure C5-2. Box and whisker plot of emissions from well pad sources measured with the high flow system. 69

Figure C5-3. Emissions composition by carbon number for oil tank emissions measured with the high flow system and flash gas modeled by AST. 70

Figure C5-4. Percent difference between the emissions composition from high flow system measurements of oil tanks and flash gas emissions modeled by AST ($[\text{direct measurement} - \text{AST modeled}]/\text{average of the two methods}$). 71

Figure C5-5. Emission composition by carbon number for non-tank emissions measured with the high flow system and raw gas samples analyzed by AST..... 72

Figure C5-6. Percent difference between the emissions composition from high flow system measurements of raw gas and raw gas sampled analyzed by AST ($[\text{emissions measurement} - \text{AST raw gas sample}]/\text{average of the two methods}$)..... 72

Figure C5-7. Emissions composition from wellhead sources by compound type. 73

Figure C5-8. Emissions composition from oil tank sources by compound type. 74

Figure C5-9. Carbonyl composition of emissions measurements..... 75

Figure C5-10. Emissions composition from water tank sources by compound type..... 75

Figure C5-11. Percent difference between the emissions composition of a few select compounds from high flow system measurements of water tank emissions in this study and similar measurements collected in Wyoming ($[\text{this study} - \text{Wyoming study}]/\text{average of the two studies}$). 76

Figure C5-12. Emission rate of total alkanes and total aromatics versus water production..... 77

Figure C5-13. Comparison of total organic compound emissions measured directly by our high flow system against emissions measured with the quantitative optical gas imaging software..... 78

Introduction

Regulatory agencies, industry, and academic researchers have worked for the past nine years to better understand organic compound emission rates and composition from oil and gas facilities and equipment in the Uinta Basin. These efforts have included top-down estimates of whole-basin emissions (Ahmadov et al., 2015; Foster et al., 2017; Karion et al., 2013), facility-level and equipment-level emissions measurement campaigns (Lyman, 2015; Lyman and Mansfield, 2018; Lyman et al., 2018; Lyman et al., 2017; Mansfield et al., 2018; Robertson et al., 2017; Tran et al., 2017; Warneke et al., 2014), intercomparisons of modeled and measured emissions (Ahmadov et al., 2015; Edwards et al., 2014; Mansfield, 2014; Matichuk et al., 2017; Tran et al., 2014) and emissions inventory efforts (Lyman et al., 2013; Stoeckenius, 2015; UDAQ, 2018). These efforts have filled in knowledge gaps and allowed industry and regulators to develop emissions reduction strategies that are based on sound scientific information.

This document reports on Utah State University's contribution to a new effort to improve estimates of the speciation of organic compound emissions from Uinta Basin oil and gas wells. This effort, led by the Utah Division of Air Quality (UDAQ) entailed:

Work completed by Alliance Source Testing (AST):

1. Collection and analysis of pressurized gas and liquid samples from separators at 78 oil and gas wells and data analysis and modeling to determine the hydrocarbon compositions of raw gas and flash gas (flash gas is the vapor emitted when liquid petroleum samples are depressurized or heated). This work and its results are described in the Appendices.

Work completed by Utah State University:

2. Collection of pressurized liquid samples from eleven oil and gas wells, followed by laboratory analysis to determine the carbonyl compound composition of flash gas. This work is described in Section 2.
3. Use of composition data to develop speciation profiles that can be used in air quality modeling. This work is described in Sections 3 and 4.
4. Direct, speciated organic compound emissions measurements from some of the same wells at which pressurized gas and liquid samples were collected. This work is described in Section 5.

We use the following data from AST in Sections 2 through 5 of this report:

- Raw gas composition determined by method GPA 2286
- Flash gas composition determined by VMG—EOS/PSM
- Gas-oil ratio determined by VMG—EOS/PSM

Information about the methods used by AST can be found in REPORT A: HYDROCARBON SAMPLING.

Carbonyl Speciation in Flash Gas

Methodology

Field Sample Collection

We collected fifteen pressurized liquid samples from separators at six oil and five gas wells (at least one sample from each well, as well as four additional quality control samples). One of the oil well samples was compromised during analysis and discarded. The ten wells at which we collected the remaining samples were a subset of the wells from which raw gas and pressurized liquid samples were collected and analyzed by AST. We collected pressurized liquid samples with a floating piston cylinder according to GPA 2174 (GPA, 2014) at the same times and locations and from the same equipment at which AST collected samples, and we used the same sampling ports and lines that they used. We used Durasite 500 cc floating piston cylinders, manufactured by YZ systems, to collect pressurized liquid samples. The samples were all filled with 400 cc of oil.

Laboratory Sample Processing

We analyzed the pressurized liquid samples for flash gas content following PS Memo 17-01 from the Colorado Department of Public Health and Environment, *Flash Gas Liberation Analysis Method for Pressurized Liquid Hydrocarbon Samples* (CDPHE, 2017). This method involved the following steps:

1. We used silicone heat tape and a temperature controller to heat the sample cylinder to the temperature of the well-site separator at the time of field sample collection (separator temperatures were measured by AST), and we allowed the cylinder to equilibrate at the set temperature for at least 30 minutes before analyzing the sample.
2. We used helium to pressurize the sample cylinder to at least the pressure of the well-site separator at the time of field sample collection (separator pressures were measured by AST).
3. We connected the cylinder to 3 mm-diameter PFA Teflon tubing that led to a sealed, 700 mm PFA flask. A manual PFA needle valve was placed between the cylinder and the flask to regulate the flow of liquid from the cylinder.
4. The flask connected via another 3 mm PFA Teflon tube to a trans-1,2-bis-(4-pyridyl) ethylene/2,4-dinitrophenylhydrazine (BPE-DNPH) cartridge followed by an Alicat MC-Series totalizing mass flow controller. The BPE-DNPH cartridge retained carbonyls from the gas sample, and the mass flow controller regulated and recorded gas flow. We corrected gas flow for the hydrocarbon composition of flash gas, following the method provided by Alicat Scientific (Alicat, 2018). We calculated the viscosity of the gas mixtures using calculations available at <https://www.beta-strumentazione.it/en/documents/spreadsheets/>. We used flash gas composition data from AST.
5. As we opened the cylinder and the needle valve, hydrocarbon liquid slowly transferred into the flask and depressurized. The evolved gas passed from the flask, through the DNPH cartridge, through the mass flow controller, and to exhaust. We did not heat the 3 mm tube that connected the sample cylinders to the PFA Teflon flask. Some of the oil samples we collected

solidified in the tube or the needle valve before reaching the flask, preventing liquid flow. We used a heat gun in these cases to heat the sample line and needle valve, melting the sample and allowing flow to resume.

6. After all the flash gas exhausted, we recorded the total volume of gas exhausted and then flushed ~1 L of ultra-high purity air through the flask to flush remaining flash gas out of the flask and through the BPE-DNPH cartridge.
7. We analyzed the BPE-DNPH cartridge and divided the carbonyl content of the cartridge by the volume of flash gas to determine the carbonyl content of the flashed gas.
8. After each sample, we cleaned all components of the sampling system with reagent-grade n-hexane.

We analyzed duplicate samples in two ways to determine the reproducibility of our methods. First, for ten samples, we analyzed the sample twice during the same analytical batch. Second, for four samples, we collected duplicate samples in the field and analyzed both samples separately. We calculated the percent difference among duplicates as the difference between the duplicates, divided by the average of the two.

We analyzed blanks in two ways to determine the level of system contamination. First, we analyzed unsampled BPE-DNPH cartridges as a test of contamination in the analytical system. Second, we sampled 2 L of ultra-high purity air through the flash gas vessel and into BPE-DNPH cartridges to assess the combined contamination in our sampling and analytical systems.

Analysis of BPE-DNPH Cartridges

We analyzed BPE-DNPH cartridges following Uchiyama et al. (2009). We kept used and unused cartridges refrigerated or on ice, except when installed for sampling. We analyzed cartridges within 14 days of sampling. To prepare samples for analysis, we flushed cartridges with a 5 mL solution of 75% acetonitrile and 25% dimethyl sulfoxide to release DNPH-carbonyls into solution. We collected the solution into 5 mL volumetric flasks and brought the flasks to a volume of 5 mL using 0.5-1 mL of the acetonitrile/dimethyl sulfoxide solution. Finally, we pipetted a 1 mL aliquot from the 5 mL flask into a 1.5 mL autosampler vial for analysis by High-Performance Liquid Chromatography (HPLC).

We analyzed samples using a Hewlett Packard series 1050 HPLC with a Restek Ultra AQ C18 column and a diode array detector. We used a mixture of acetonitrile and water as the eluent. We prepared standards by diluting commercially available carbonyl-DNPH standards, and we calibrated the instrument on each analysis day with a five-point calibration curve. We ran at least one additional standard at the beginning and end of each analysis batch to check for retention time drift or other errors.

Results

Gas-Oil Ratio

We calculated the gas-oil ratio of the samples we analyzed as the volume of gas evolved divided by the volume of liquid originally collected. The slope of the relationship was 1.02, indicating generally good agreement among the two methods, though considerable scatter was observed (Figure C2-1).

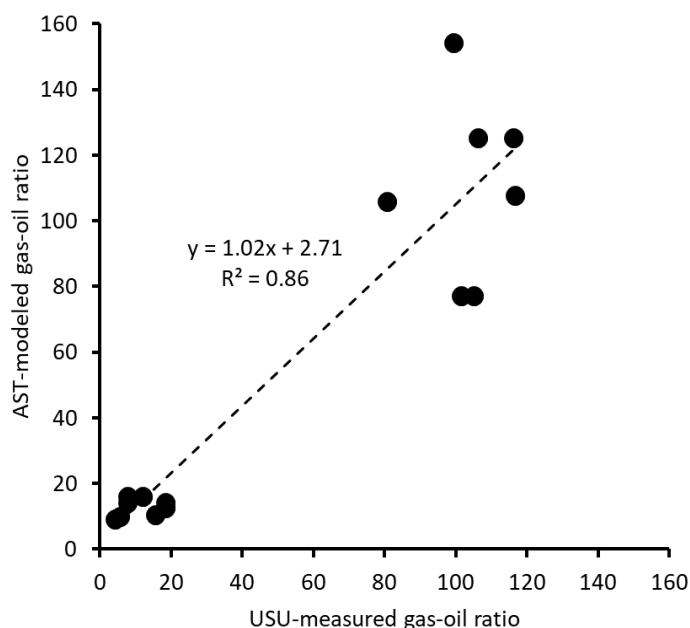


Figure C2-1. Comparison of gas-oil ratios of flash gas measured from pressurized liquid samples analyzed in the laboratory by USU and gas-oil ratios modeled by AST in units of standard cubic feet per barrel. Duplicate USU samples are included. The linear regression equation and r^2 value of the relationship is shown.

Carbonyl Composition of Flash Gas

Tables C2-1 and C2-2 show the carbonyl concentrations in flash gas from pressurized oil and condensate samples, respectively. Figure C2-2 and Figure C2-3 show the relative concentrations of different carbonyl compounds. We were unable to quantify acetone in these samples because acetone was used to clean the floating piston cylinders before they came into our possession, and the cylinders were thus contaminated with acetone.

Table C2-1. Concentrations of carbonyls in flash gas from pressurized oil samples, in ppm (vol/vol). The volume of gas evolved from each liquid sample is also shown. N.D. means not detected. Well names have been anonymized.

	V-9	V-14	V-5	V-15	V-10
Gas evolved (L)	1.04	0.28	0.81	1.24	0.38
Formaldehyde	0.26	1.46	0.63	1.00	2.38
Acetaldehyde	0.29	2.58	0.77	0.70	1.43
Acetone	--	--	--	--	--
Acrolein	N.D.	N.D.	N.D.	N.D.	N.D.

	V-9	V-14	V-5	V-15	V-10
Propionaldehyde	N.D.	N.D.	N.D.	N.D.	0.28
Crotonaldehyde	N.D.	N.D.	N.D.	0.09	N.D.
Methacrolein/ butyraldehyde/ 2-butanone	N.D.	N.D.	N.D.	0.60	N.D.
Benzaldehyde	N.D.	N.D.	N.D.	0.11	N.D.
Valeraldehyde	N.D.	N.D.	N.D.	0.40	0.24
p-Tolualdehyde	N.D.	N.D.	N.D.	N.D.	N.D.
Hexaldehyde	N.D.	N.D.	N.D.	0.07	N.D.
Total carbonyls	0.55	4.04	1.40	2.97	4.33

Table C2-2. Concentrations of carbonyls in flash gas from pressurized condensate samples, in ppm (vol/vol). The volume of gas evolved is also shown. N.D. means not detected. Well names have been anonymized.

	III-6	III-3	III-2	III-4	III-1
Gas evolved (L)	6.71	7.87	7.84	5.44	7.09
Formaldehyde	0.03	0.13	0.01	0.01	0.06
Acetaldehyde	0.04	0.24	19.80	0.09	0.21
Acetone	--	--	--	--	--
Acrolein	N.D.	N.D.	N.D.	N.D.	N.D.
Propionaldehyde	N.D.	N.D.	0.08	N.D.	N.D.
Crotonaldehyde	N.D.	N.D.	N.D.	N.D.	0.01
Methacrolein/ butyraldehyde/ 2-butanone	0.02	0.02	0.02	0.01	0.07
Benzaldehyde	N.D.	N.D.	N.D.	N.D.	N.D.
Valeraldehyde	0.01	N.D.	N.D.	N.D.	0.02
p-Tolualdehyde	N.D.	N.D.	N.D.	N.D.	0.01
Hexaldehyde	N.D.	N.D.	N.D.	N.D.	0.01
Total carbonyls	0.09	0.39	19.90	0.10	0.39

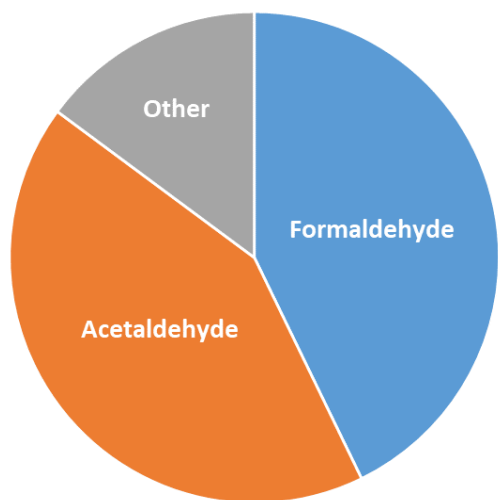


Figure C2-2. Average carbonyl composition of gas flashed from oil samples.

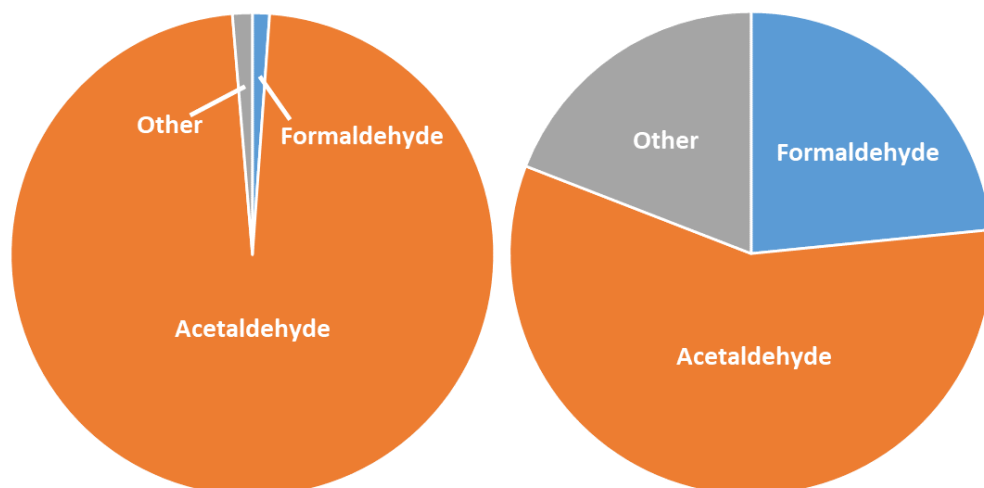


Figure C2-3. Average carbonyl composition of gas flashed from pressurized condensate samples. The left chart utilizes data from all samples. The right chart excludes data from one well (III-2) that had much higher acetaldehyde concentrations than other samples.

Detection Limits

We calculated analytical detection limits as three times the standard deviation of repeat measurements of a low-concentration calibration standard. The detection limit results are shown in Table C2-3.

Table C2-3. Carbonyl detection limits, reported by mass and concentration. Average flash gas volumes for oil (0.75 L) and condensate (6.99 L) samples, respectively, were used to determine concentrations from the mass detection limits.

	Oil			Condensate	
	µg	mg m ⁻³	ppm	mg m ⁻³	ppm
Formaldehyde	0.05	0.07	0.05	0.01	0.01
Acetaldehyde	0.08	0.11	0.06	0.01	0.01
Acetone	0.05	0.07	0.14	0.01	0.01
Acrolein	0.26	0.35	0.03	0.01	0.003
Propionaldehyde	0.20	0.26	0.10	0.03	0.01
Crotonaldehyde	0.07	0.10	0.03	0.01	0.003
Methacrolein/ butyraldehyde/ 2-butanone	0.17	0.22	0.07	0.02	0.01
Benzaldehyde	0.29	0.39	0.08	0.04	0.01
Valeraldehyde	0.11	0.15	0.04	0.02	0.004
p-Tolualdehyde	0.18	0.24	0.05	0.02	0.005
Hexaldehyde	0.18	0.24	0.05	0.03	0.01
Total carbonyls	1.65	2.20	0.69	0.24	0.07

Duplicates

We only consistently detected formaldehyde and acetaldehyde in duplicate samples, so we only report data from those two compounds here. For sample eluent analyzed twice during the same analytical batch, the percent difference between duplicates was $5 \pm 18\%$ (mean \pm 95% confidence interval) for formaldehyde and $7 \pm 18\%$ for acetaldehyde. For field duplicates, the percent differences for formaldehyde and acetaldehyde were $43 \pm 86\%$ and $44 \pm 100\%$. Field duplicate oil samples had higher percent differences than condensate samples. The percent difference for all compounds from oil sample field duplicates was $76 \pm 53\%$, compared to $24 \pm 27\%$ for condensate sample field duplicates.

Blanks

Total carbonyl concentrations in analytical blanks, calculated using average flash gas volumes, were 0.47 ± 0.20 and 0.07 ± 0.03 ppm for oil and condensate samples, respectively. Sampling system blanks, calculated using the actual volumes of purified air sampled, were 0.37 ± 0.39 ppm. Figure C2-4 shows box and whisker plots comparing oil sample results to blank values, and Figure C2-5 shows a similar figure for condensate samples.

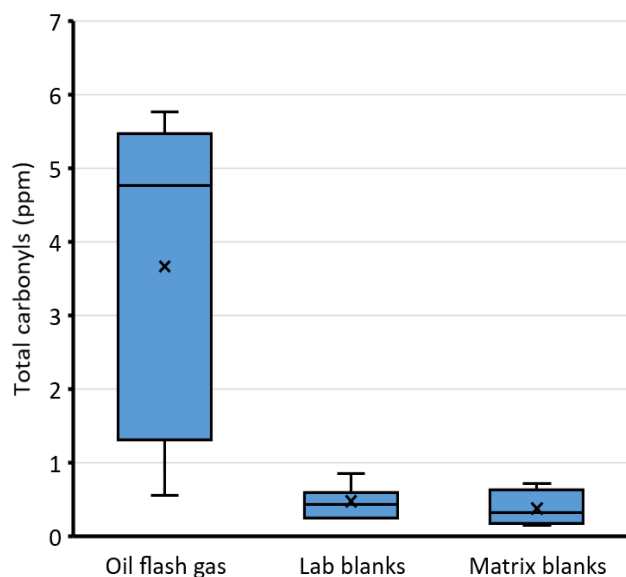


Figure C2-4. Box and whisker plots of total carbonyl concentrations in oil samples and associated blanks. The line within each box is the median. X's represent the mean. The upper and lower bounds of each box represent the first and third quartiles. The whiskers represent maxima and minima.

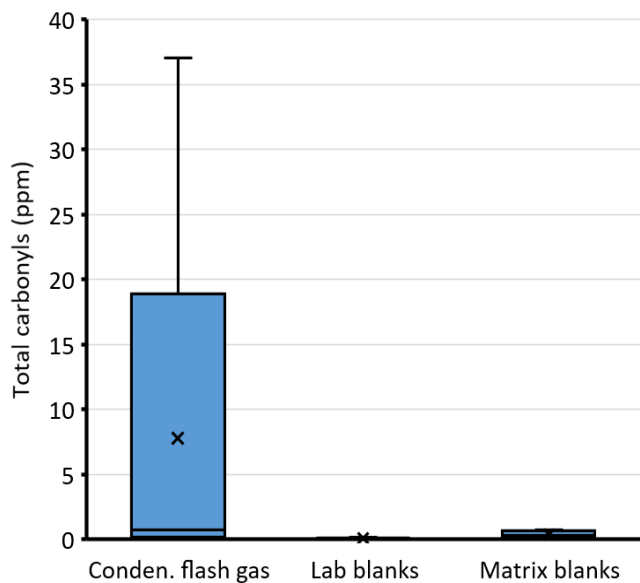


Figure C2-5. Box and whisker plots of total carbonyl concentrations in all condensate samples and associated blanks. The line within each box is the median. X's represent the mean. The upper and lower bounds of each box represent the first and third quartiles. The whiskers represent maxima and minima.

Development of Composition Speciation Profiles

Between 8 October and 5 December 2018, AST collected raw gas and pressurized liquid samples from separators at 78 wells across five geological formations in the Uinta Basin. They analyzed the raw gas samples for hydrocarbon composition, including a suite of C1 to C10 alkanes (C1 is methane, C2 is ethane, C6 denotes alkanes with six carbons, etc.) and benzene, toluene, ethylbenzene, and xylenes. They analyzed the pressurized liquid samples for C1 through C36 hydrocarbons and used those results to simulate flash gas composition for the same suite of compounds analyzed in the raw gas samples. Details about the methods used by AST are presented in REPORT A: HYDROCARBON SAMPLING. AST recommended discarding data from 11 wells that failed quality assurance tests performed by their lab. Therefore, we only included data from the remaining 67 wells in this analysis. As described in Section 2, we collected additional pressurized liquid samples at eleven of the 67 wells, and we analyzed these samples for the carbonyl composition of flash gas.

The goal of this study was to develop raw and flash gas organic compound speciation profiles for wells producing oil and gas from five studied geological formations, based on these hydrocarbon and carbonyl composition measurements. The speciation profiles consist of the average weight percent of the compounds and compound groups analyzed by AST, and the average weight percent of 11 carbonyls and carbonyl groups analyzed by USU (when those data were available), averaged by formation. We created average compositions for different (1) geological formations, (2) well types (oil or gas), and (3) gaseous emission sources (raw gas or flash gas). The developed composition profiles will be used to speciate total organic compound emissions from oil and gas production for photochemical modeling of Uinta Basin winter ozone.

Methodology

We grouped composition data from all sampled wells into five geological formations and two well types. Table C3-1 presents information about the samples collected that correspond to the five geological formations. The sampling locations were selected to best represent the major geologic formations from which the majority of wells in Uinta and Duchesne Counties extract oil and gas. The geological formation and well type information associated with studied wells were obtained from the Utah Division of Oil, Gas, and Mining (UDOGM, 2018). We calculated flash and raw gas speciation profiles for each geological formation as the averaged weight percent of groups of samples.

Identifying Outliers

We calculated statistical scores (mean (\bar{X}) and standard deviation (SD)) for formation-grouped raw and flash gas compositions. We considered mean (i.e., average) values to be representative of the whole sample group if standard deviations of the three most abundant components of the composition were less than one-third of corresponding mean values (i.e., if relative standard deviation, $RSD = 100\% \times \frac{SD}{|\bar{X}|}$, was less than 33.3%).

Table C3-0-1. Grouping of sampled wells by geological formation.

Geological formation	Number of sampled wells (for hydrocarbons for carbonyls)	Well type	Number of Outliers (raw gas flash gas)
GREEN RIVER (GR)	19 0	Oil	2 1
GREEN RIVER-WASATCH (GRWA)	22 3	Oil	0 2
WASATCH (WA)	9 2	Oil	0 2
MESA VERDE (MV)	8 5	Gas	0 0
WASATCH-MESA VERDE (WAMV)	9 0	Gas	1 1
TOTAL passing lab QA	67 10		3 6

Some extreme outliers led to RSD values notably larger than 33.3%, meaning that the resulting average values were not representative for the whole dataset. Therefore, we detected those outliers and discarded them from further analysis. For geological formations with sample sizes larger than twelve (e.g., Green River and Green River–Wasatch formations, Table C3-1), we detected outliers by calculating z-scores across the sample set for each analyzed compound using the outlier-detecting method. The outliers are the data points that are in the tails of the distribution and therefore far from the mean. How far depends on a set threshold z_{th} for the normalized data points z_i calculated with the formula:

$$z_i = \frac{x_i - \bar{X}}{SD}$$

where x_i is a data point, \bar{X} is the mean of all x_i , and SD is the standard deviation of all x_i . An outlier is then a normalized data point which has an absolute value greater than z_{th} . That is:

$$|z_i| > z_{th}$$

We chose the commonly used z_{th} value of 3.0 for detecting outliers, which then were discarded from the dataset. Calculated z-scores are shown in Appendix D. We also experimented with another outlier detecting method called box-and-whisker plot IQR (interquartile range). This method frequently detected more outliers than the z-score method. Therefore, we chose the z-score method over the IQR method for outlier detecting to minimize the number of samples that were discarded since the sample sizes were already small. From the z-score outlier detecting method, we discarded two raw gas and three flash gas outlier samples. These outliers are shown in red in the corresponding tables in Appendix D.

For geological formations with sample sizes less than twelve (e.g., Wasatch, Mesa Verde, and Wasatch-Mesa Verde), neither the z-score nor the IQR outlier detecting methods worked well. In these situations, we considered outliers as upper bound or lower bound values of the dataset that caused the RSD of the three most abundant components to be larger than 33.3%. From this analysis, we discarded one raw gas and three flash gas samples that were determined to be outliers (i.e., exclusion of these samples resulted in RSD values that were smaller than 33.3%). These outliers are shown in red in the corresponding tables in Appendix D.

Tests of Normality

After outlier removal, we analyzed the speciation profiles for each geological formation using the Jarque-Bera test for normality (Jarque and Bera, 1980) (Tables C3-2 and C3-3). The Jarque-Bera test results showed that compounds in the profiles for the five geological formations followed a normal distribution, except octanes, nonanes, and decanes-plus in some of the raw gas profiles. However, these compounds were minor components of the raw gas composition (i.e., they had small weight percents), so we judged that statistical analyses designed for normally-distributed datasets were appropriate for all profiles. For data that have a normal distribution, analysis using statistical scores such as mean, standard deviation, and relative standard deviation are valid.

Table C3-0-2. Jarque-Bera normality test *p*-values (two-tailed) for raw gas composition data for each geological formation. *p*-values greater than the significance level of 0.05 indicate data with a normal distribution. Red indicates *p*-values less than 0.05.

Compound	GR	GRWA	WA	MV	WAMV
Methane	0.50	0.91	0.74	0.69	0.50
Ethane	0.59	0.74	0.70	0.84	0.35
Propane	0.95	0.37	0.38	0.13	0.54
Isobutane	0.67	0.70	0.75	0.49	0.65
n-Butane	0.73	0.71	0.86	0.42	0.86
Isopentane	0.37	0.41	0.71	0.77	0.95
n-Pentane	0.56	0.74	0.76	0.61	0.83
Cyclopentane	0.32	0.26	0.75	0.57	0.06
n-Hexane	0.58	0.63	0.62	0.86	0.36
Cyclohexane	0.26	0.47	0.51	0.63	0.60
Other hexanes	0.31	0.52	0.46	0.06	0.43
Heptanes	0.57	0.18	0.24	0.12	0.36
Methylcyclohexane	0.69	0.47	0.74	0.05	0.32
2,2,4 Trimethylpentane	0.62	0.39	0.48	0.34	0.41
Benzene	0.42	0.53	0.52	0.95	0.75
Toluene	0.84	0.60	0.74	0.05	0.65
Ethylbenzene	0.45	0.88	0.82	0.08	0.05
Xylenes	0.27	0.18	0.77	0.18	0.55
Octanes	0.01	0.86	0.59	0.04	0.09
Nonanes	0.55	< 0.01	0.81	0.66	0.01
Decanes plus	0.12	0.61	0.73	0.14	0.01

Table C3-3. Jarque-Bera normality test *p*-values (two-tailed) for flash gas composition data for each geological formation. *p*-values greater than the significance level of 0.05 indicate data with a normal distribution.

Compound	GR	GRWA	WA	MV	WAMV
Methane	0.72	0.54	0.47	0.74	0.80
Ethane	0.75	0.05	0.56	0.68	0.90
Propane	0.39	0.93	0.80	0.78	0.84
Isobutane	0.06	0.65	0.85	0.69	0.69
n-Butane	0.53	0.56	0.79	0.72	0.78
Isopentane	0.90	0.69	0.80	0.59	0.74
n-Pentane	0.91	0.82	0.65	0.72	0.79
Cyclopentane	0.86	0.34	0.45	0.73	0.88
n-Hexane	0.05	0.65	0.93	0.92	0.78
Cyclohexane	0.60	0.62	0.19	0.76	0.66
Heptanes	0.88	0.42	0.58	0.21	0.72
Methylcyclohexane	0.80	0.89	0.48	0.84	0.68
2,2,4 Trimethylpentane	0.52	0.68	0.48	0.73	0.87
Benzene	0.07	0.16	0.52	0.91	0.77
Toluene	0.81	0.15	0.69	0.73	0.84
Ethylbenzene	0.80	0.25	0.66	0.69	0.64
Xylenes	0.53	0.55	0.66	0.63	0.56
Octanes	0.82	0.19	0.63	0.66	0.59
Nonanes	0.15	0.08	0.69	0.40	0.63
Decanes plus	0.24	0.12	0.05	0.85	0.62

Hydrocarbon Speciation in Raw Gas: Grouping Results

We normalized raw gas composition data (weight percent) using the 21 compounds shown in Table C3-2 for speciation profiles (i.e., we excluded hydrogen sulfide, carbon dioxide, and nitrogen, which were measured by AST). Anonymized well-specific composition data are given in Appendix D. Table C3-4 shows the mean and relative standard deviation (RSD) of raw gas compositions calculated for the five geological formations. RSD of the three most abundant components of all five formation-grouped datasets passed screening thresholds (RSD < 33.3%), which indicate that the data points were adequately clustered around the mean, meaning that formation-averaged compositions were representative. Each geological formations was thus represented by a single organic compound speciation profile for raw gas emissions.

Table C3-4. Mean (\bar{X}) weight percent and relative standard deviation (RSD) calculated for raw gas composition for each geological formation. N = sample size. Blue indicates RSD of the three most abundant components passing the screening threshold (RSD < 33.3%).

Compound	GR Oil well N = 17		GRWA Oil well N = 22		WA Oil well N = 9		MV Gas well N = 8		WAMV Gas well N = 8	
	\bar{X}	RSD	\bar{X}	RSD	\bar{X}	RSD	\bar{X}	RSD	\bar{X}	RSD
Methane	49.530	13.4%	57.210	22.1%	51.760	14.3%	71.034	4.5%	77.038	6.8%
Ethane	10.631	21.0%	11.202	25.8%	13.227	18.6%	10.367	4.2%	9.627	18.6%
Propane	10.490	14.9%	8.575	29.3%	9.523	16.5%	6.956	7.6%	4.485	28.2%
Isobutane	2.506	27.3%	1.933	39.8%	2.223	17.8%	1.801	7.5%	1.448	49.8%
n-Butane	5.832	20.5%	4.330	39.7%	4.710	24.0%	2.575	9.7%	1.556	38.8%
Isopentane	2.904	33.3%	1.996	52.0%	2.249	28.5%	1.114	13.0%	0.832	40.2%
n-Pentane	3.868	32.7%	2.748	50.2%	3.011	33.8%	0.957	16.1%	0.668	48.9%
Cyclopentane	0.365	44.4%	0.197	69.1%	0.152	41.7%	0.060	22.2%	0.040	59.5%
n-Hexane	2.536	44.8%	1.983	55.7%	2.212	46.7%	0.526	23.9%	0.380	50.1%
Cyclohexane	0.704	41.5%	0.508	53.5%	0.542	43.9%	0.301	35.9%	0.230	35.2%
Other hexanes	3.226	41.8%	2.176	54.4%	2.360	39.5%	0.880	20.8%	0.707	39.9%
Heptanes	2.631	35.7%	2.352	60.8%	2.700	66.0%	0.783	82.7%	0.583	53.4%
Methylcyclohexane	0.852	28.1%	0.743	47.0%	0.838	47.2%	0.776	98.4%	0.520	46.5%
2,2,4- Trimethylpentane	0.002	48.9%	0.001	72.9%	0.001	66.8%	0.000	116.6%	0.000	73.0%
Benzene	0.156	45.5%	0.161	61.6%	0.246	66.5%	0.062	26.1%	0.098	40.9%
Toluene	0.236	30.7%	0.256	58.4%	0.396	59.9%	0.240	108.9%	0.284	53.4%
Ethylbenzene	0.026	40.7%	0.026	53.9%	0.030	45.7%	0.015	95.8%	0.019	69.7%
Xylenes	0.173	31.8%	0.216	57.4%	0.291	40.8%	0.152	79.7%	0.190	45.0%
Octanes	1.737	24.0%	1.750	46.4%	1.917	35.0%	0.792	115.3%	0.576	60.0%
Nonanes	0.253	26.5%	0.426	93.7%	0.443	35.7%	0.136	75.3%	0.165	63.8%
Decanes plus	1.342	37.7%	1.209	41.1%	1.168	35.6%	0.472	80.7%	0.553	54.8%

Hydrocarbon Speciation in Flash Gas: Grouping Results

We normalized flash gas composition data (weight percent) using the 20 compounds shown in Table C3-3 for speciation profiles (i.e., we excluded hydrogen sulfide, carbon dioxide, and nitrogen, which were measured by AST). Details of composition data for each well are shown in Appendix D. Table C3-5 shows means and relative standard deviations (RSD) calculated for flash gas composition, grouped by geological formation. RSD of the three most abundant components for the Green River (GR), Mesa Verde (MV), and Wasatch-Mesa Verde (WAMV) formations passed screening thresholds of 33.3%, indicating that formation-averaged compositions were representative. RSD of methane from the Green River-Wasatch (GRWA) formation failed screening thresholds (Table C3-5), indicating that formation-averaged composition profiles were not representative of the entire dataset. Thus, we sorted this dataset with respect to methane weight percent and separated composition data into subgroups, ensuring that the RSD of each subgroup passed screening thresholds. For the Wasatch (WA) formation, we separated composition data into two subgroups based on casing perforation information sourced

originally from the DOGM database: group 1 (WA_sP) included wells that extracted oil from a single Wasatch perforation and group 2 (WALWR_mP) included wells that extracted oil from multiple Wasatch-Green River (LWR) perforations (Table C3-6 and Table C3-7).

In summary, we compiled flash gas hydrocarbon composition data from 61 wells (six outliers excluded) associated and five geological formations into eight different speciation profiles, as shown in Table C3-8 and Table C3-9.

Table C3-5. Mean (\bar{X}) weight percent and relative standard deviation (RSD) calculated for the flash gas composition of each geological formation. N = sample size. Blue (red) indicates RSD of the three most abundant components passing (failing) the screening threshold (RSD < 33.3%).

Compound	GR Oil well N = 18		GRWA Oil well N = 20		WA Oil well N = 8		MV Gas well N = 8		WAMV Gas well N = 8	
	\bar{X}	RSD	\bar{X}	RSD	\bar{X}	RSD	\bar{X}	RSD	\bar{X}	RSD
Methane	12.095	29.5%	15.649	45.3%	10.529	33.9%	31.190	16.5%	60.851	23.0%
Ethane	9.632	14.9%	11.868	25.7%	11.132	16.5%	19.556	5.6%	17.683	20.9%
Propane	17.016	13.3%	15.621	16.2%	14.727	9.6%	24.265	7.7%	8.553	32.8%
Isobutane	5.078	26.0%	4.365	23.4%	4.854	17.4%	7.110	12.6%	2.329	40.8%
n-Butane	13.158	15.6%	11.214	25.3%	11.411	17.7%	9.706	15.3%	2.523	44.8%
Isopentane	6.273	15.5%	5.397	31.7%	5.883	18.7%	3.443	21.5%	1.249	56.1%
n-Pentane	8.123	13.9%	7.542	28.3%	7.779	24.1%	2.588	23.1%	0.840	57.2%
Cyclopentane	0.787	25.3%	0.527	47.1%	0.386	45.9%	0.120	21.6%	0.054	79.6%
n-Hexane	6.785	24.7%	6.485	25.4%	6.512	12.2%	0.760	25.5%	0.780	91.4%
Cyclohexane	1.661	15.4%	1.611	25.3%	1.697	17.1%	0.358	25.1%	0.358	72.8%
Heptanes	11.321	38.0%	10.958	46.7%	15.873	24.4%	0.135	43.0%	2.317	185.2%
Methylcyclohexane	1.792	15.1%	2.042	27.0%	2.299	23.6%	0.463	31.1%	0.732	101.0%
2,2,4-Trimethylpentane	0.052	41.3%	0.045	35.6%	0.025	138.2%	0.006	42.8%	0.007	143.7%
Benzene	0.292	29.3%	0.415	53.2%	0.709	59.5%	0.063	29.6%	0.163	85.6%
Toluene	0.425	24.3%	0.544	50.0%	0.909	43.6%	0.092	40.1%	0.414	126.7%
Ethylbenzene	0.069	60.6%	0.035	118.5%	0.037	81.0%	0.003	35.6%	0.024	139.0%
Xylenes	0.339	34.4%	0.356	37.7%	0.441	42.5%	0.030	28.8%	0.264	148.1%
Octanes	1.965	29.5%	2.082	27.2%	1.683	23.9%	0.048	36.6%	0.349	109.7%
Nonanes	2.766	22.3%	2.748	36.1%	2.786	20.9%	0.058	32.1%	0.461	148.9%
Decanes plus	0.371	48.7%	0.497	68.4%	0.327	24.0%	0.009	18.9%	0.050	93.7%

Table C3-6. Mean (\bar{X}) weight percent and relative standard deviation (RSD) calculated for the flash gas composition of the Green River–Wasatch subgroups. N = sample size. Blue indicates RSD of the three most abundant components passing the screening threshold (RSD < 33.3%).

Compound	GRWA1 N = 4		GRWA2 N = 9		GRWA3 N = 7	
	\bar{X}	RSD	\bar{X}	RSD	\bar{X}	RSD
Methane	26.387	6.0%	16.822	14.9%	8.006	18.9%
Ethane	15.189	25.8%	11.746	23.9%	10.127	6.4%
Propane	14.631	13.0%	15.045	16.8%	16.927	15.3%
Isobutane	3.346	15.0%	3.947	15.2%	5.484	9.5%
n-Butane	7.959	11.5%	10.582	21.7%	13.886	10.2%
Isopentane	3.224	28.5%	5.091	22.3%	7.031	12.2%
n-Pentane	4.965	23.8%	7.239	20.3%	9.404	15.7%
Cyclopentane	0.435	69.6%	0.569	45.6%	0.524	43.1%
n-Hexane	5.417	28.8%	6.542	19.2%	7.021	29.2%
Cyclohexane	1.333	47.5%	1.676	18.6%	1.687	21.4%
Heptanes	9.805	40.0%	11.311	49.9%	11.165	50.4%
Methylcyclohexane	1.767	46.2%	2.029	20.6%	2.216	25.2%
2,2,4 Trimethylpentane	0.042	50.0%	0.046	35.9%	0.044	32.3%
Benzene	0.280	55.6%	0.371	54.6%	0.548	41.6%
Toluene	0.428	40.9%	0.497	47.7%	0.670	50.2%
Ethylbenzene	0.031	170.3%	0.042	113.1%	0.029	108.1%
Xylenes	0.312	46.9%	0.358	40.0%	0.378	34.5%
Octanes	2.055	39.2%	2.253	28.1%	1.877	13.0%
Nonanes	1.924	86.5%	3.299	16.8%	2.512	23.6%
Decanes plus	0.471	125.8%	0.533	48.9%	0.465	66.5%

Table C3-7. Mean (\bar{X}) weight percent and relative standard deviation (RSD) calculated for the flash gas composition of the Wasatch subgroups. N = sample size. Blue indicates RSD of the three most abundant components passing the screening threshold (RSD < 33.3%).

Compound	WA_sP N = 5		WALWR_mP N = 2	
	\bar{X}	RSD	\bar{X}	RSD
Methane	10.245	42.19%	11.238	2.3%
Ethane	11.367	19.22%	10.543	2.3%
Propane	14.853	8.79%	14.412	15.5%
Isobutane	5.093	15.56%	4.257	20.9%
n-Butane	12.078	16.46%	9.743	9.7%
Isopentane	6.165	19.46%	5.179	7.2%
n-Pentane	8.371	22.80%	6.300	10.4%
Cyclopentane	0.313	27.98%	0.568	44.7%
n-Hexane	6.869	6.40%	5.622	16.1%
Cyclohexane	1.683	20.94%	1.733	4.0%
Heptanes	13.982	16.85%	20.600	11.0%
Methylcyclohexane	2.252	28.98%	2.418	5.3%
2,2,4 Trimethylpentane	0.016	101.09%	0.048	141.4%
Benzene	0.735	66.53%	0.645	49.0%
Toluene	0.864	51.47%	1.022	33.6%
Ethylbenzene	0.024	103.94%	0.069	1.8%
Xylenes	0.425	47.24%	0.480	44.0%
Octanes	1.676	21.96%	1.699	38.6%
Nonanes	2.683	25.31%	3.042	2.1%
Decanes plus	0.306	26.61%	0.381	12.8%

Table C3-8. Final flash gas hydrocarbon composition profiles for oil wells (weight percent). N = sample size.

Compound	GR N = 18	GRWA1 N = 4	GRWA2 N = 9	GRWA3 N = 7	WA_sP N = 5	WALWR _mP N = 2
Methane	12.095	26.387	16.822	8.006	10.245	11.238
Ethane	9.632	15.189	11.746	10.127	11.367	10.543
Propane	17.016	14.631	15.045	16.927	14.853	14.412
Isobutane	5.078	3.346	3.947	5.484	5.093	4.257
n-Butane	13.158	7.959	10.582	13.886	12.078	9.743
Isopentane	6.273	3.224	5.091	7.031	6.165	5.179
n-Pentane	8.123	4.965	7.239	9.404	8.371	6.300
Cyclopentane	0.787	0.435	0.569	0.524	0.313	0.568
n-Hexane	6.785	5.417	6.542	7.021	6.869	5.622
Cyclohexane	1.661	1.333	1.676	1.687	1.683	1.733
Heptanes	11.321	9.805	11.311	11.165	13.982	20.600
Methylcyclohexane	1.792	1.767	2.029	2.216	2.252	2.418
2,2,4- Trimethylpentane	0.052	0.042	0.046	0.044	0.016	0.048
Benzene	0.292	0.280	0.371	0.548	0.735	0.645
Toluene	0.425	0.428	0.497	0.670	0.864	1.022
Ethylbenzene	0.069	0.031	0.042	0.029	0.024	0.069
Xylenes	0.339	0.312	0.358	0.378	0.425	0.480
Octanes	1.965	2.055	2.253	1.877	1.676	1.699
Nonanes	2.766	1.924	3.299	2.512	2.683	3.042
Decanes plus	0.371	0.471	0.533	0.465	0.306	0.381

Table C3-9. Final flash gas hydrocarbon composition profiles (weight percent) for gas wells. N = sample size.

Compound	MV N = 8	WAMV1 N = 8
Methane	31.190	60.851
Ethane	19.556	17.683
Propane	24.265	8.553
Isobutane	7.110	2.329
n-Butane	9.706	2.523
Isopentane	3.443	1.249
n-Pentane	2.588	0.840
Cyclopentane	0.120	0.054
n-Hexane	0.760	0.780
Cyclohexane	0.358	0.358
Heptanes	0.135	2.317
Methylcyclohexane	0.463	0.732
2,2,4- Trimethylpentane	0.006	0.007
Benzene	0.063	0.163
Toluene	0.092	0.414
Ethylbenzene	0.003	0.024
Xylenes	0.030	0.264
Octanes	0.048	0.349
Nonanes	0.058	0.461
Decanes plus	0.009	0.050

Incorporating Carbonyl Data into Flash Gas Speciation Profiles

We only collected and analyzed carbonyl samples for flash gas composition at ten wells. We collected carbonyl samples at two and three oil wells associated with the Wasatch (WA) and Green River–Wasatch (GRWA) formations, respectively, and at five gas wells associated with the Mesa Verde (MV) formation. We converted hydrocarbon and carbonyl gas densities (g/m³) sampled at the same wells to weight percentages for composition profiles. Table C3-9 and Table C3-10 show flash gas composition profiles that include 20 measured hydrocarbons and 11 carbonyls. The percentage of total carbonyls was between 0.001 and 0.002% of total organics. These speciation percentages are small but should be included in emission calculations for photochemical modeling of ozone because carbonyls are important precursors to ozone production.

Table C3-9. Flash gas hydrocarbon and carbonyl composition profiles (weight percent) for sampled oil wells. Well IDs are anonymized. (*) indicates well ID that was identified as an outlier and excluded from the formation-specific profiles above.

Compound	GRWA Well V-9	GRWA Well V-14	GRWA Well V-5	WA Well V-15	WA(*) Well V-10
Methane	15.69	24.77	17.60	11.05	22.65
Ethane	13.97	12.07	10.29	10.37	10.51
Propane	15.26	13.49	9.71	15.99	14.82
Isobutane	3.66	3.58	2.78	4.89	3.81
n-Butane	9.35	8.57	6.73	10.41	8.52
Isopentane	4.48	4.51	4.11	5.44	3.89
n-Pentane	6.07	5.98	5.95	5.84	4.76
Cyclopentane	0.35	0.88	0.32	0.75	0.53
n-Hexane	6.20	6.62	8.92	4.98	4.03
Cyclohexane	1.46	2.17	1.87	1.68	1.46
Heptanes	14.63	5.08	19.19	18.99	15.69
Methylcyclohexane	1.87	2.84	2.72	2.33	1.85
2,2,4- Trimethylpentane	0.05	0.05	0.03	0.10	0.05
Benzene	0.47	0.41	0.67	0.42	0.24
Toluene	0.64	0.68	1.00	0.78	0.41
Ethylbenzene	0.05	0.11	0.04	0.07	0.09
Xylenes	0.34	0.52	0.56	0.33	0.43
Octanes	2.00	2.70	2.53	2.16	2.47
Nonanes	3.10	3.63	4.49	3.00	3.30
Decanes plus	0.38	1.33	0.47	0.42	0.49
Formaldehyde	3.08E-05	2.03E-04	7.28E-05	1.06E-04	3.12E-04
Acetaldehyde	4.95E-05	5.27E-04	1.29E-04	1.09E-04	2.75E-04
Acetone	0	0	0	0	0
Acrolein	1.31E-04	0	3.05E-03	1.21E-03	1.91E-03
Propionaldehyde	0	0	0	0	7.16E-05
Crotonaldehyde	0	0	0	2.19E-05	0
Methacrolein/2-butanone	0	0	0	1.50E-04	0
Benzaldehyde	0	0	0	4.00E-05	0
Valeraldehyde	0	0	0	1.21E-04	9.16E-05
p-Tolualdehyde	0	0	0	0	0
Hexaldehyde	0	0	0	2.45E-05	0

Table C3-10. Flash gas hydrocarbon and carbonyl composition profiles (weight percent) for sampled gas wells that draw from the Mesa Verde (MV) formation. Well IDs are anonymized.

Compound	MV Well III-6	MV Well III-3	MV Well III-2	MV Well III-4	MV Well III-1
Methane	26.12	30.17	31.54	27.50	33.58
Ethane	17.47	19.79	18.49	19.75	20.30
Propane	26.54	24.58	23.72	25.71	23.33
Isobutane	8.14	7.18	7.24	7.69	6.37
n-Butane	11.32	9.98	10.07	10.57	8.62
Isopentane	4.15	3.58	3.86	4.01	3.19
n-Pentane	3.37	2.75	2.84	2.83	2.42
Cyclopentane	0.15	0.15	0.12	0.12	0.13
n-Hexane	1.09	0.76	0.89	0.71	0.72
Cyclohexane	0.49	0.34	0.36	0.32	0.35
Heptanes	0.15	0.12	0.16	0.13	0.20
Methylcyclohexane	0.65	0.37	0.44	0.38	0.44
2,2,4- Trimethylpentane	0.00	0.01	0.01	0.01	0.00
Benzene	0.08	0.05	0.06	0.06	0.06
Toluene	0.12	0.06	0.07	0.08	0.09
Ethylbenzene	0.00	0.00	0.00	0.00	0.00
Xylenes	0.03	0.02	0.03	0.02	0.04
Octanes	0.05	0.04	0.05	0.05	0.07
Nonanes	0.06	0.06	0.06	0.05	0.08
Decanes plus	0.01	0.01	0.01	0.01	0.01
Formaldehyde	3.86E-06	1.58E-05	1.04E-06	1.29E-06	7.80E-06
Acetaldehyde	5.30E-06	4.47E-05	3.67E-03	1.54E-05	3.93E-05
Acetone	0	0	0	0	0
Acrolein	8.82E-05	1.97E-04	2.33E-05	4.51E-04	2.61E-03
Propionaldehyde	0	0	1.90E-05	0	0
Crotonaldehyde	0	0	0	0	4.29E-06
Methacrolein/2-butanone	6.01E-06	6.14E-06	6.10E-06	2.25E-06	2.18E-05
Benzaldehyde	0	0	0	0	0
Valeraldehyde	3.13E-06	0.00E+00	0.00E+00	0.00E+00	8.01E-06
p-Tolualdehyde	0	0	0	0	4.08E-06
Hexaldehyde	0	0	0	0	3.46E-06

Ozone Reactivities of Raw Gas and Flash Gas Profiles

Different organic compounds have different ability to react in the atmosphere and form ozone. Carter (2009) provided ozone maximum incremental reactivities (MIR) for many organic compounds. The higher the MIR value for a compound, the abler that compound is to form ozone. Some light, stable compounds such as methane or ethane have low MIR because they are relatively inert. Heavier alkanes in the range of C4 to C7, aromatics, and carbonyls are more reactive and have larger MIR values. Here we utilized Carter (2009) MIRs to provide a coarse estimate of the ozone-forming potential of organic

compound speciation profiles. To accomplish this, we multiplied MIR values for the compounds and compound groups in each developed profile by the weight percent of each compound or compound group. Carter MIR values are in units of g ozone formed per g of an emitted compound, and we assumed total organic compound emissions of 100 g.

Figure C3-1 indicates that assuming same amount of total organics emitted into the atmosphere, raw gas emissions from oil wells would produce more ozone than raw gas emissions from gas wells. The majority of ozone formed was due to alkanes with between three and seven carbon atoms. This was true for both oil and gas wells. Although MIR values for aromatics are higher than those for alkanes, aromatics were less important because they had smaller weight percentages. Raw gas profiles for oil wells that produce from the Green River (GR) formation were the most reactive, while gas wells that produce from the Wasatch-Mesa Verde formation were the least reactive.

Figure C3-2 shows the same analysis as Figure C3-1 but for flash gas emissions. As with the raw gas profiles, flash gas profiles from oil wells were more reactive than profiles from gas wells. Aromatics and carbonyls from both oil and gas wells resulted in much less formed ozone than was formed from alkanes because of lower weight percentages in the profiles.

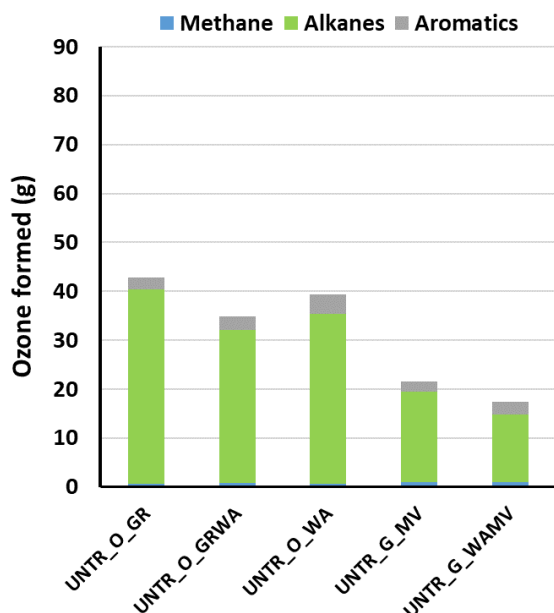


Figure C3-1. Ozone that would be formed from emissions of 100 g of total organics from each of the raw gas speciation profiles indicated. The leftmost three bars are profiles for oil wells, and the rightmost two bars are profiles for gas wells. These values were calculated by multiplying the weight percentage of each compound or compound group in each profile by the MIR for that compound or group, resulting in the mass of ozone formed (g) per 100 g of total organic compounds emitted.

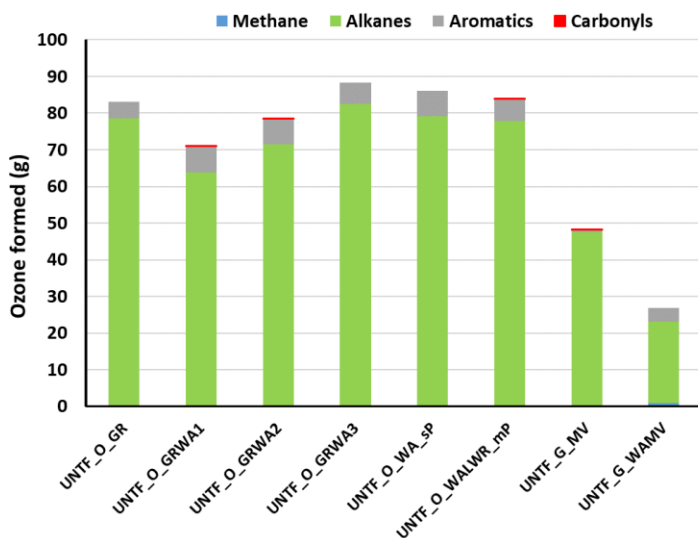


Figure C3-2. Ozone that would be formed from emissions of 100 g of total organics from each of the flash gas speciation profiles indicated. The leftmost six bars are profiles for oil wells, and the rightmost two bars are profiles for gas wells. These values were calculated by multiplying the weight percentage of each compound or compound group in each profile by the MIR for that compound or group, resulting in the mass of ozone formed (g) per 100 g of total organic compounds emitted.

Compiling Composition Profiles with SPTOOL and Application of SPECIATE Profiles

SPTOOL Configurations

We processed the organic compound speciation profiles developed in Section 0 with Speciation Tool 4.0 (SPTOOLv4.0) (Jimenez et al., 2016) to create SPECIATE organic compound profiles that can be utilized by the Sparse Matrix Operator Kernel Emissions Model (SMOKE) and are compatible with Carbon Bond 6 (CB6) chemistry in the Comprehensive Air Quality Model with extensions (CAMx). Table C4-1 lists names and brief descriptions of the 13 organic compound speciation profiles we developed for oil and gas wells in the Uinta Basin. Table C4-2a and Table C4-2b. show these 13 speciation profiles as the input and output, respectively, of SPTOOL processing.

Preparing inputs for SPTOOL included the following steps:

1. Assigning compound names to “species_ID” following the EPA SPECIATE 4.5 database (Table C4-1) (Hsu et al., 2016).
2. Creating a “tbl_gas_profile_weights” SPTOOL input table to include developed speciation profiles in the required format.
3. Calculating “VOC_to_TOG” conversion factors for each developed speciation profile and formatting them in the SPTOOL input table “tbl_gas_profiles” (EPA, 2017), using a VOC_to_TOG

conversion factor of $100/(\text{sum of organic compound weight \%}; \text{excluding the sum of methane and ethane})$

SPTOOL produced SMOKE-ready formatted mechanism-specific profiles and “GSPRO” and “GSCNV” ancillary files, storing split factors of modeled species and VOC_to_TOG for each profile, respectively.

Application of SPECIATE Profiles

The developed SPECIATE profiles in Table C4-2(a,b) are applicable for oil and gas emissions within Uintah and Duchesne counties. They differ by geological formations and by the type of gas emitted, which are two attributes of a well available from DOGM (UDOGM, 2018). Applications of these profiles for emissions processing in SMOKE are summarized as below and in Table C4-1:

- **Raw** gas profiles developed for **oil** wells: Applied to vented source emissions from non-CBM oil wells for source categories such as equipment and pipeline blowdowns, pigging, pneumatic controllers, pneumatic pumps, associated gas venting, and fugitive leaks.
- **Raw** gas profiles developed for **gas** wells: Applied to vented source emissions from non-CBM gas wells for source categories such as equipment and pipeline blowdowns, pigging, pneumatic controllers, pneumatic pumps, and fugitive leaks.
- **Flash** gas profiles developed for **oil** wells: Applied to emissions from oil tanks, casinghead gas venting, and truck loading.
- **Flash** gas profiles developed for **gas** wells: Applied to emissions from condensate tanks, gas venting associated with well liquid unloading, and truck loading.

Among the three flash gas profiles developed for oil wells that produce from the mixed Green River-Wasatch formation, the profile with the lowest percentage of methane (UNTF_O_GRWA3) is more able to form ozone than the others (UNTF_O_GRWA1, UNTF_O_GRWA2) (Figure C3-2). Locations of wells associated with each of these three profiles showed a random spatial distribution (not shown). Thus, the middle-range profile UNTF_O_GRWA2 is recommended to represent for flash gas emissions from oil tanks on the Green River- Wasatch formation.

Table C4-1. Organic compound speciation profiles developed from hydrocarbon and carbonyl measurements of flash gas and raw gas from oil and gas wells in the Uinta Basin. () indicates the number of wells at which both hydrocarbons and carbonyls were measured.**

Profile_ID	Name and application	Number of individual profiles
UNTF_O_GR	Flash gas profiles for oil tank emissions associated with the Green River formation	18
UNTF_O_GRWA1	Flash gas profiles for oil tank emissions associated with the Green River-Wasatch formation (highest Methane)	1 (**)
UNTF_O_GRWA2	Flash gas profiles for oil tank emissions associated with the Green River-Wasatch formation (2nd highest Methane) (recommended)	2 (**)
UNTF_O_GRWA3	Flash gas profiles for oil tank emissions associated with the Green River-Wasatch formation (3rd highest Methane)	7
UNTF_O_WA_sP	Flash gas profiles for oil tank emissions associated with the Wasatch formation	5
UNTF_O_WALWR_mP	Flash gas profiles for oil tank emissions associated with the Wasatch-Lower Green River formation	2 (**)
UNTF_G_MV	Flash gas profiles for condensate tank emissions associated with the Mesa Verde formation	5 (**)
UNTF_G_WAMV	Flash gas profiles for condensate tank emissions associated with the Wasatch-Mesa Verde formation (higher methane)	8
UNTR_O_GR	Raw gas profiles for oil-well vented source emissions associated with the Green River formations	17
UNTR_O_GRWA	Raw gas profiles for oil-well vented source emissions associated with the Green River-Wasatch formations	22
UNTR_O_WA	Raw gas profiles for oil-well vented source emissions associated with the Wasatch formations	9
UNTR_G_MV	Raw gas profiles for gas-well vented source emissions associated with the Mesa Verde formation	8
UNTR_G_WAMV	Raw gas profiles for gas-well vented source emissions associated with the Wasatch-Mesa Verde formation	8

Table C4-2a. Organic compound raw gas speciation profiles used as input for SPTOOL, in weight percent.

Compound	EPA SPECIATE species_ID	Oil well			Gas well	
		UNTR_O_GR	UNTR_O_GRWA	UNTR_O_WA	UNTR_G_MV	UNTR_G_WAMV
Methane	529	49.530	57.210	51.760	71.034	77.038
Ethane	438	10.631	11.202	13.227	10.367	9.627
Propane	671	10.490	8.575	9.523	6.956	4.485
Isobutane	491	2.506	1.933	2.223	1.801	1.448
n-Butane	592	5.832	4.330	4.710	2.575	1.556
Isopentane	508	2.904	1.996	2.249	1.114	0.832
n-Pentane	605	3.868	2.748	3.011	0.957	0.668
Cyclopentane	390	0.365	0.197	0.152	0.060	0.040
n-Hexane	601	2.536	1.983	2.212	0.526	0.380
Cyclohexane	385	0.704	0.508	0.542	0.301	0.230
Other hexanes	600	3.226	2.176	2.360	0.880	0.707
Heptanes	600	2.631	2.352	2.700	0.783	0.583
Methylcyclohexane	550	0.852	0.743	0.838	0.776	0.520
2,2,4- Trimethylpentane	118	0.002	0.001	0.001	0.000	0.000
Benzene	302	0.156	0.161	0.246	0.062	0.098
Toluene	717	0.236	0.256	0.396	0.240	0.284
Ethylbenzene	449	0.026	0.026	0.030	0.015	0.019
Xylenes	522	0.173	0.216	0.291	0.152	0.190
Octanes	604	1.737	1.750	1.917	0.792	0.576
Nonanes	603	0.253	0.426	0.443	0.136	0.165
Decanes plus	598	1.342	1.209	1.168	0.472	0.553
VOC_to_TOG	-NA-	2.510	3.166	2.856	5.377	7.499

Table C4-2b. Organic compound flash gas speciation profiles used as input for SPTOOL, in weight percent. ()** indicates that profiles only include wells from which both hydrocarbons and carbonyls were measured.

Compound	EPA SPECIATE species_ID	Oil well						Gas well	
		UNTF_O_GR	UNTF_O_GRW A1 (**)	UNTF_O_GRW A2 (**)	UNTF_O_GRW A3	UNTF_O_WA_sP	UNTF_O_WAL_WR_mP (**)	UNTF_G_MV (**)	UNTF_G_WA_MV
Methane	529	12.095	24.771	16.645	8.006	10.245	11.055	29.781	60.851
Ethane	438	9.632	12.073	12.131	10.127	11.367	10.370	19.158	17.683
Propane	671	17.016	13.492	12.484	16.927	14.853	15.990	24.774	8.553
Isobutane	491	5.078	3.578	3.218	5.484	5.093	4.886	7.324	2.329
n-Butane	592	13.158	8.570	8.039	13.886	12.078	10.413	10.111	2.523
Isopentane	508	6.273	4.506	4.293	7.031	6.165	5.444	3.756	1.249
n-Pentane	605	8.123	5.981	6.012	9.404	8.371	5.836	2.842	0.840
Cyclopentane	390	0.787	0.875	0.338	0.524	0.313	0.748	0.133	0.054
n-Hexane	601	6.785	6.621	7.559	7.021	6.869	4.983	0.834	0.780
Cyclohexane	385	1.661	2.172	1.665	1.687	1.683	1.684	0.374	0.358
Heptanes	600	11.321	5.083	16.909	11.165	13.982	18.992	0.154	2.317
Methylcyclohexane	550	1.792	2.835	2.299	2.216	2.252	2.328	0.455	0.732
2,2,4- Trimethylpentane	118	0.052	0.051	0.044	0.044	0.016	0.097	0.005	0.007
Benzene	302	0.292	0.413	0.569	0.548	0.735	0.422	0.061	0.163
Toluene	717	0.425	0.684	0.819	0.670	0.864	0.779	0.082	0.414
Ethylbenzene	449	0.069	0.111	0.045	0.029	0.024	0.068	0.003	0.024
Xylenes	522	0.339	0.515	0.446	0.378	0.425	0.330	0.028	0.264
Octanes	604	1.965	2.704	2.262	1.877	1.676	2.163	0.051	0.349
Nonanes	603	2.766	3.629	3.795	2.512	2.683	2.996	0.063	0.461
Decanes plus	598	0.371	1.334	0.424	0.465	0.306	0.415	0.009	0.050
Formaldehyde	465		2.03E-04	5.18E-05			1.06E-04	5.96E-06	
Acetaldehyde	279		5.27E-04	8.92E-05			1.09E-04	7.55E-04	
Acetone	281								
Acrolein	283			1.59E-03			1.21E-03	6.73E-04	
Propionaldehyde	673							3.79E-06	
Crotonaldehyde	382						2.19E-05	8.58E-07	
Methacrolein/2-butanone	188						1.50E-04	8.45E-06	
Benzaldehyde	301						4.00E-05		
Valeraldehyde	845						1.21E-04	2.23E-06	
p-Tolualdehyde	1462							8.17E-07	
Hexaldehyde	840						2.45E-05	6.91E-07	
VOC_to_TOG	-NA-	1.278	1.583	1.404	1.221	1.276	1.273	1.958	4.659

Table C4-3. Organic compound speciation profiles produced by SPTOOL (in split factor). Species IDs follow CAMx CB6 mechanism (Yarwood et al., 2010; Yarwood et al., 2005).

Species_ID Profile_ID	ALD2	ALDX	BENZ	CH4	ETHA	FORM	OLE	PAR	PRPA	TOL	UNR	XYL
UNTF_O_GR			2.92E-03	0.121	0.096			0.601	0.170	4.85E-03	6.50E-05	3.39E-03
UNTF_O_GRWA1	5.29E-06		4.13E-03	0.248	0.121	2.10E-06		0.480	0.135	7.81E-03	6.37E-05	5.15E-03
UNTF_O_GRWA2	8.81E-07	1.05E-05	5.69E-03	0.167	0.121	6.01E-07	5.23E-06	0.569	0.125	8.58E-03	5.50E-05	4.46E-03
UNTF_O_GRWA3			5.48E-03	0.080	0.101			0.633	0.169	6.95E-03	5.50E-05	3.78E-03
UNTF_O_WA_sP			7.35E-03	0.102	0.114			0.615	0.149	8.85E-03	2.00E-05	4.52E-03
UNTF_O_WALWR_mP	8.81E-07	9.27E-06	4.22E-03	0.111	0.104	1.20E-06	4.46E-06	0.610	0.160	8.39E-03	1.21E-04	3.30E-03
UNTF_G_MV	7.49E-06	4.49E-06	6.10E-04	0.298	0.192		2.24E-06	0.261	0.248	8.46E-04	6.28E-06	2.80E-04
UNTF_G_WAMV			1.63E-03	0.609	0.177			0.120	0.086	4.35E-03	8.71E-06	2.64E-03
UNTR_O_GR			1.58E-03	0.500	0.107			0.280	0.106	2.61E-03	2.57E-06	1.75E-03
UNTR_O_GRWA			1.61E-03	0.572	0.112			0.224	0.086	2.79E-03	1.29E-06	2.16E-03
UNTR_O_WA			2.64E-03	0.518	0.132			0.245	0.095	4.22E-03	1.29E-06	2.91E-03
UNTR_G_MV			6.20E-04	0.710	0.104			0.112	0.070	2.53E-03		1.52E-03
UNTR_G_WAMV			9.80E-04	0.770	0.096			0.083	0.045	3.01E-03		1.90E-03

Direct Measurements of Emissions from Oil Wells

We visited 24 oil wells in Duchesne County to detect and directly quantify organic compound emissions. Each of the wells we visited was a well at which raw gas samples and pressurized liquid samples were collected and analyzed by AST (see REPORT A: HYDROCARBON SAMPLING).

Methodology

Emissions detection

We used a FLIR GF320 optical gas imaging camera to detect emissions at each well pad. Most potential emission sources were quantified from a distance of ~3 m or less. In most cases, if an emission source was accessible and safe, we used a high flow emissions measurement system to quantify organic compound emissions from the source. When possible, we also used quantitative optical gas imaging software as a secondary quantification method. Funding available for the study did not allow us to quantify every detected emission source.

High Flow Emissions Measurements

High flow samplers have been utilized in many scientific studies to quantify natural gas emissions (Allen et al., 2013; Johnson et al., 2015) and are approved by EPA for emissions quantification (CFR Title 40, part 98, Subpart W (98.233)). However, commercial high flow samplers do not distinguish among different organic compounds and have been shown to suffer from bias (Howard et al., 2015). Additionally, they are generally only able to quantify smaller emission plumes (<0.5 m³ min⁻¹). We developed a high flow sampling system that overcomes these challenges. Figure C5-1 shows a diagram of this system. Johnson et al. (2015) deployed a similar system to measure methane emissions from compressor stations and calculated an overall measurement uncertainty of about 5%. Our actual measurement uncertainty for methane, calculated from measurements of a controlled methane emission source, is about 10%.

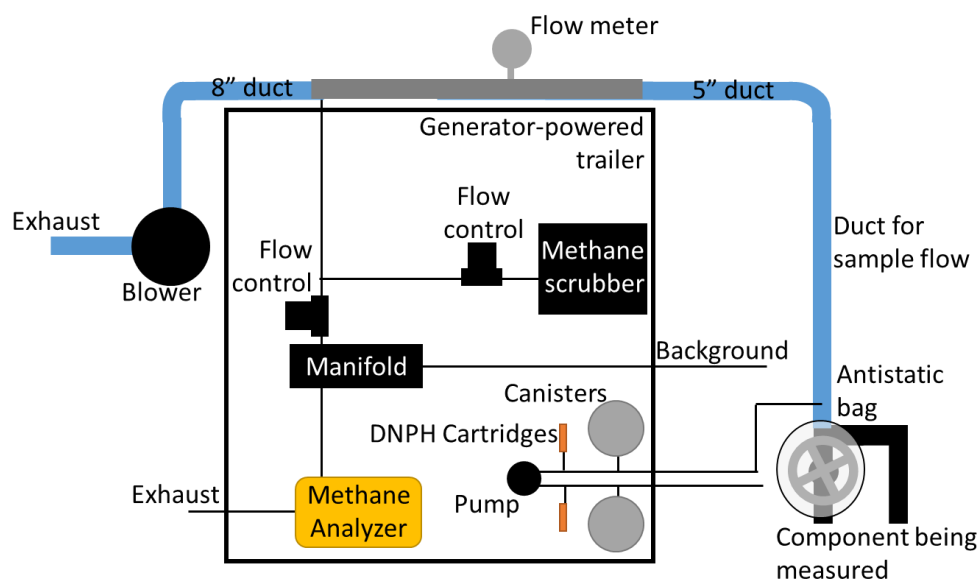


Figure C5-1. Diagram of the high flow sampling system.

To measure a leaking component with our high flow sampler, we wrapped an antistatic polymer bag around the component to contain the emission plume and connected the bag to a 38 m length of 13 cm-diameter conductive ducting. An explosion-proof blower pulled gas (between 0.5 and 3 m³ min⁻¹, adjustable) from the bag, through the ducting, and into a flow measurement tube (3 m length of 10 cm diameter stainless steel tubing). We used a Fox Thermal Instruments Model FT1 mass flow meter to measure the flow rate through the measurement tube. We corrected the flow for temperature, pressure, water vapor, and organic compound concentrations. The sampled gas contained ambient air from the vicinity of the bagged emission source in addition to the emitted stream of hydrocarbon gas. We calculated the emission rate as the concentration of a given organic compound in the sampled gas (in mg m⁻³; corrected for the concentration of the compound in ambient air) multiplied by the total flow rate (m³ min⁻¹). We measured ambient concentrations of the compounds of interest through a 6 mm-diameter PFA Teflon tube, the inlet of which we placed within 0.3 m of the component being measured. A flush pump kept the flow through this tube at at least 4 L min⁻¹.

We used a handheld natural gas detector (Bascom Turner Gas Rover; detection limit for total combustible hydrocarbons of 10 ppm) to check that the antistatic bag and duct fully contained each emission plume. We used a Los Gatos Research Greenhouse Gas Analyzer to measure methane and carbon dioxide concentrations in sample gas and background air. The analyzer can detect methane concentrations of up to 10% in air. For methane at higher concentrations, we used a mass flow controller to dilute the analyzer flow (analyzer flow rate is 0.5 sL min⁻¹) with methane-free air to keep within the analyzer's range. We generated methane-free air with a custom-built air scrubber system in the trailer.

We calibrated the methane analyzer for methane and carbon dioxide at at least three points along its measurement range, including one zero point, on each field measurement day. We used a scrubber system to generate methane and carbon dioxide-free air, and we diluted NIST-traceable compressed gas standards with calibrated mass flow controllers for span calibrations. Calibration zero points were 76 ± 3 and 8 ± 15 ppb (mean ± 95% confidence interval) for methane and carbon dioxide, respectively. Carbon dioxide recovery for non-zero points was 99 ± 2%. The analyzer has two lasers for methane, one for 0-1000 ppm, and one for concentrations greater than 1000 ppm. The calibration recovery was 99 ± 2 and 99 ± 1% for the low and high lasers, respectively. We also injected methane into the measurement duct on each sampling day as a calibration check of the entire measurement system. Methane recovery was 91 ± 2% for these checks.

In addition to methane and carbon dioxide, we determined the emission rate of a suite of C2-C10 hydrocarbons, light alcohols, and carbonyls. A list of all compounds measured with the high flow system is shown in Table C5-1.

For C2-C10 hydrocarbons and alcohols, we collected 6-L silonite-coated stainless steel canister samples. For carbonyls, we collected BPE-DNPH cartridge samples. Because the 13 cm sampling duct was not inert, we installed a stainless steel port 3 m downstream from the duct inlet, and we pulled 4 L min⁻¹ of sample gas from this port, through a 6 mm-diameter PFA Teflon tube, to the measurement trailer, and

we collected canister and DNPH cartridge samples from this tube. We installed this port 3 m downstream from the duct inlet, rather than at the inlet, to allow the emitted gas and ambient air to mix thoroughly prior to sampling. To determine that 3 m was adequate to ensure thorough mixing, we injected methane at the duct inlet and measured the methane concentration at different points in the duct. Methane concentrations in the duct were stable when measured 3 m or more downstream from the inlet. The residence time of methane and carbon dioxide in the 13-cm duct was 19 sec, and the residence time of other measured compounds in the duct and the PFA tubing was 10 sec.

We grounded all components of the system to the trailer, and we attached the trailer to a ground rod to dissipate buildup of static electricity. All components that came into contact with sample gas were antistatic and/or explosion-proof. The interior of the trailer was not rated for environments that are rich in flammable gases. Thus, we placed the trailer and the generators that powered it at least 10 m from any potential source of flammable gas.

Table C5-1. List of organic compounds measured with the high flow system, the compound type, the analytical method used by USU, and whether the compounds were analyzed for by AST. Acetylene was assigned to the alkene category even though it is an alkyne.

Compound	Type	USU analytical method	Analyzed by AST?
Methane	Methane	LGR analyzer	Yes
Ethane	Alkane	GC/GC/MS	Yes
Ethylene	Alkene	GC/GC/MS	No
Propane	Alkane	GC/GC/MS	Yes
Propylene	Alkene	GC/GC/MS	No
Isobutane	Alkane	GC/GC/MS	Yes
n-Butane	Alkane	GC/GC/MS	Yes
Acetylene	Alkene	GC/GC/MS	No
Trans-2-butene	Alkene	GC/GC/MS	No
1-Butene	Alkene	GC/GC/MS	No
Cis-2-butene	Alkene	GC/GC/MS	No
Isopentane	Alkene	GC/GC/MS	Yes
N-Pentane	Alkane	GC/GC/MS	Yes
Trans-2-pentene	Alkene	GC/GC/MS	No
1-Pentene	Alkene	GC/GC/MS	No
Cis-2-pentene	Alkene	GC/GC/MS	No
2,2-Dimethylbutane	Alkane	GC/GC/MS	No
Cyclopentane	Alkane	GC/GC/MS	Yes
2,3-Dimethylbutane	Alkane	GC/GC/MS	No
2-Methylpentane	Alkane	GC/GC/MS	No
3-Methylpentane	Alkane	GC/GC/MS	No
Isoprene	Alkene	GC/GC/MS	No
1-Hexene	Alkene	GC/GC/MS	No

Compound	Type	USU analytical method	Analyzed by AST?
n-Hexane	Alkane	GC/GC/MS	Yes
Methylcyclopentane	Alkane	GC/GC/MS	No
2,4-Dimethylpentane	Alkane	GC/GC/MS	Yes, as heptanes
Benzene	Aromatic	GC/GC/MS	Yes
Cyclohexane	Alkane	GC/GC/MS	Yes
2-Methylhexane	Alkane	GC/GC/MS	Yes, as heptanes
2,3-Dimethylpentane	Alkane	GC/GC/MS	Yes, as heptanes
3-Methylhexane	Alkane	GC/GC/MS	Yes, as heptanes
2,2,4-Trimethylpentane	Alkane	GC/GC/MS	Yes
n-Heptane	Alkane	GC/GC/MS	Yes, as heptanes
Methylcyclohexane	Alkane	GC/GC/MS	Yes
2,3,4-Trimethylpentane	Alkane	GC/GC/MS	Yes, as heptanes
Toluene	Aromatic	GC/GC/MS	Yes
2-Methylheptane	Alkane	GC/GC/MS	Yes, as octanes
3-Methylheptane	Alkane	GC/GC/MS	Yes, as octanes
n-Octane	Alkane	GC/GC/MS	Yes, as octanes
Ethylbenzene	Aromatic	GC/GC/MS	Yes
m/p-Xylene	Aromatic	GC/GC/MS	Yes, as xylenes
Styrene	Alkene	GC/GC/MS	No
o-Xylene	Aromatic	GC/GC/MS	Yes, as xylenes
n-Nonane	Alkane	GC/GC/MS	Yes, as nonanes
Isopropylbenzene	Aromatic	GC/GC/MS	No
n-Propylbenzene	Aromatic	GC/GC/MS	No
1-Ethyl-3-methylbenzene	Aromatic	GC/GC/MS	No
1-Ethyl-4-methylbenzene	Aromatic	GC/GC/MS	No
1,3,5-Trimethylbenzene	Aromatic	GC/GC/MS	No
1-Ethyl-2-methylbenzene	Aromatic	GC/GC/MS	No
1,2,4-Trimethylbenzene	Aromatic	GC/GC/MS	No
n-Decane	Alkane	GC/GC/MS	Yes, as decanes+
1,2,3-Trimethylbenzene	Aromatic	GC/GC/MS	No
1,3-Diethylbenzene	Aromatic	GC/GC/MS	No
1,4-Diethylbenzene	Aromatic	GC/GC/MS	No
Methanol	Alcohol	GC/GC/MS	No
Ethanol	Alcohol	GC/GC/MS	No
Isopropanol	Alcohol	GC/GC/MS	No
Formaldehyde	Carbonyl	HPLC	No
Acetaldehyde	Carbonyl	HPLC	No
Acrolein	Carbonyl	HPLC	No
Acetone	Carbonyl	HPLC	No

Compound	Type	USU analytical method	Analyzed by AST?
Propionaldehyde	Carbonyl	HPLC	No
Crotonaldehyde	Carbonyl	HPLC	No
Butyraldehyde	Carbonyl	HPLC	No
Methacrolein	Carbonyl	HPLC	No
2-Butanone	Carbonyl	HPLC	No
Benzaldehyde	Carbonyl	HPLC	No
Valeraldehyde	Carbonyl	HPLC	No
Tolualdehyde	Carbonyl	HPLC	No
Hexaldehyde	Carbonyl	HPLC	No

Analysis of Canister Samples

After sampling, we analyzed canisters within 60 days. If the concentrations of organic compounds in canister samples were too high for our analytical calibration curve, we used an Entech 4600 dynamic diluter to dilute canister samples in ultra-high purity nitrogen to the desired concentration range for analysis. All samples, regardless of concentration, were diluted with the Entech 4600 to at least 1034 mbar (absolute pressure; ~150 mbar above ambient) when they were returned to the laboratory.

We used an Entech 7200 preconcentrator and 7016D autosampler to concentrate samples and introduce them to a gas chromatograph (GC) system for analysis. We used cold trap dehydration to reduce water vapor in the sample, as described by Wang and Austin (2006). The GC system consisted of two Shimadzu GC-2010 GCs with a flame ionization detector (FID) and a Shimadzu QP2010 Mass Spectrometer (MS), respectively.

For cold trap dehydration with the Entech 7200 preconcentrator, hydrocarbons and alcohols passed through an empty deactivated fused silica-coated tube kept at -40°C to remove most water and then were collected on a subsequent Tenax-filled trap kept at -110°C. The empty tube was then heated to 10°C as helium passed over it to transfer additional hydrocarbons and alcohols into the Tenax-filled trap. Next, the Tenax-filled trap was heated to 230°C to transfer hydrocarbons and alcohols to an empty silonite-coated tube kept at -195°C. Finally, that tube was heated rapidly to 75°C to introduce the trapped compounds into the GC system.

Sample introduced to the GC system from the Entech preconcentrator first passed through a Restek rtx1-ms column (60 m, 0.25 mm ID) and then entered a VICI four-port GC valve with a Valcon E rotor. For the first 6.5 min after injection, the sample passed into a Restek Alumina BOND/Na₂SO₄ PLOT column (50 m, 0.32 mm ID) and into an FID. After 6.5 min, the valve position changed and the sample was directed into another Restek rtx1-ms column (30 m, 0.25 mm ID). Light hydrocarbons (ethane, ethylene, acetylene, propane, and propylene) were quantified by FID, while all other compounds were quantified by MS. Bromochloromethane, 1,4-difluorobenzene, chlorobenzene-d₅, and 1-bromo-4-fluorobenzene were added to each sample during the preconcentration step and used as internal standards.

At the beginning of every batch analyzed, we established a five-point calibration curve, and we conducted two calibration checks, a duplicate sample analysis, and a blank check at the end of each batch. We prepared calibration and internal standards by diluting NIST-traceable compressed gas standards in high-purity nitrogen using an Entech 4600 diluter. We cleaned canisters with an Entech 3100, which heats them to 80°C and repeatedly evacuates and then pressurizes them with humidified high-purity nitrogen (5 repetitions).

Calibration curve r^2 values were 0.997 ± 0.001 (mean \pm 95% confidence interval). Duplicate samples were $0.2 \pm 0.8\%$ different from each other. Recovery of calibration checks was $95.2 \pm 0.4\%$.

Analysis of DNPH Cartridges

DNPH cartridges were analyzed in the same way as was described in Section 2.1.3.

Meteorological Measurements

At each location where we collected measurements with the high flow sampler, we measured ambient temperature, and relative humidity (New Mountain NM150WX), wind speed and direction (Gill WindSonic), and barometric pressure (Campbell CS100) on a tower extended from the measurement trailer to a height of 6 m.

Quantitative Optical Gas Imaging

We used a Providence Photonics QL320 tablet with quantitative optical gas imaging software, connected to the FLIR GF320 camera, to quantify emissions where possible. The QL320 tablet is not intrinsically safe, so we kept it and the attached camera at least 10 m from any potential source of combustible gases. Because of this limitation, many of the sampled emission sources were unresolvable with the QL320 tablet, either because they were too small to be seen from 10 m or because they were blocked from view, and we were only able to collect successful measurements with the quantitative software from a minority of the emission plumes we observed.

The software requires the user to input ambient temperature, wind speed, and distance of the GF320 camera from the emission source. We used meteorological measurements from the tower connected to the trailer for temperature and wind speed, and we measured the distance with a range finder. We collected at least five software-based measurements of each emission source and averaged the values. We only included results for further analysis if the average result was larger than the 95% confidence interval. We also did not use any results for emissions within buildings (since the camera with the tablet attached could not safely enter buildings) or results in which the camera operator indicated they had low confidence.

We used the software's default calibration for methane, and we corrected the methane results for the composition of measured emissions determined from high flow sampling, following the method recommended by the manufacturer (Providence, 2019; Zeng et al., 2017).

Comparison with Results from AST

We compared our high flow system results to raw gas and flash gas data from AST (see Introduction for information about which AST data were used). In all cases, we used only the AST data for the specific wells at which we collected measurements with the high flow system. We did not make any comparisons of our measurement results against aggregated profiles from Section DEVELOPMENT OF COMPOSITION SPECIATION PROFILES.

Results

Emissions measured from liquid storage tanks tended to be higher than those from other sources (Figure C5-2). Twenty-three of the 24 wells we visited routed tank vapors to combustors. Emissions from tanks were usually from leaking thief hatches, but some were also from pressure relief valves. We detected emissions from five oil tanks, five water tanks, and two other tanks (Table C5-2). One of the other tanks was an overflow tank (total organic compound emissions of 3.9 g h^{-1}) and the other held fluid used by an electric jet pump, which uses the force of the tank fluid to move oil from the underground oil reservoir to the surface (total organic compound emissions from this tank were 1482.4 g h^{-1}). We detected emissions from a vent at the center of the tank top at some other overflow tanks. These vents were inaccessible with the high flow system, and we did not quantify them.

We measured emissions from nine sources on separator equipment, including connections, pneumatic devices, valves, and regulators. We collected four measurements from wellheads, including connections, a valve, and an actuator. We also measured emissions from other connections and equipment at the wells visited. We did not measure every observed emission source. We tried to obtain measurements from a variety of sources at many wells. The maximum number of emissions we quantified at any well was three.

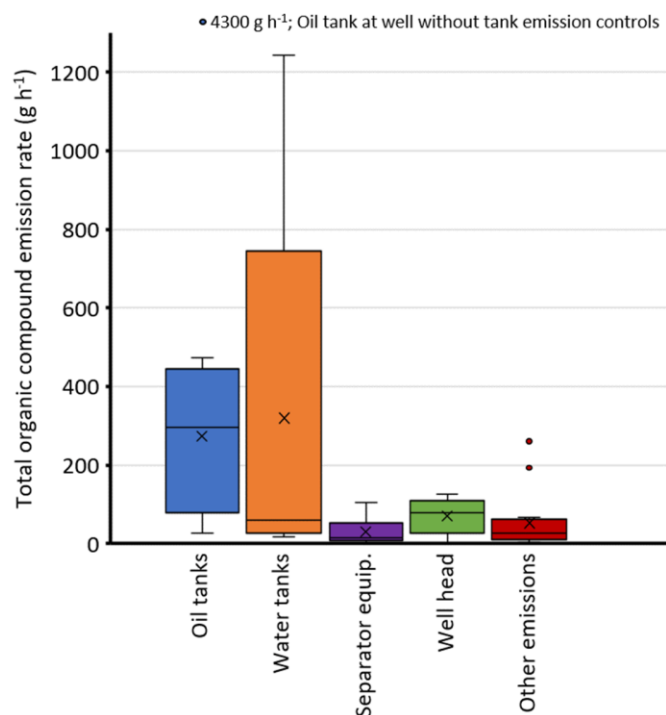


Figure C5-2. Box and whisker plot of emissions from well pad sources measured with the high flow system. X's show means. The lower and upper bounds of the boxes show first and third quartiles. Lines in boxes show medians. Whiskers represent minima and maxima, and dots beyond whiskers show outliers (>1.5 times the interquartile range).

Table C5-2. Summary of emission plumes detected at each well visited. Each plume detected with the optical gas imaging camera is shown with an X. A bold X indicates the detected emission plume was quantified with the high flow sampling system.

Anonymized well name	Oil tank	Water tank	Other tank	Separator equipment	Well head	Other
V-1				X X		
V-2						
V-4				X		X
V-5	X					X
V-6				X	X	
V-7	X			X	X	
V-8	X			X		X
V-9		X				
V-10		X	X			X
V-11			X			
V-12						X
V-13		X	X			
V-14				X		
V-15						
VII-2						X X
VII-3					X X	X
VII-6					X X	X
VII-7		X		X X		
VII-8		X				X

Anonymized well name	Oil tank	Water tank	Other tank	Separator equipment	Well head	Other
VII-9			X			X X
VII-10	X			X		X
VII-11				X X		X X
VII-14	X X	X		X X X X	X	X X X X
VII-15						

Comparison with AST Composition Results

The composition of emissions measured directly from oil tanks was different from the flash gas composition modeled by AST (Figure C5-3). While biases in the methods could have caused this discrepancy, some or all of the difference could also be due to the fact that the two methods measured different phenomena. AST modeled flash gas emissions, or the release of gases from a liquid when the pressure of the liquid decreases or temperature increases as liquid moves from the separator to the tank. Our direct emissions measurements, on the other hand, likely included a combination of flash gas emissions and evaporation of the liquid while it resides in the heated tank. We were not able to discern whether our tank emissions measurements occurred during periods when separators deposited pressurized liquids into tanks (i.e., when they flashed). We also could not discern if there was a malfunction, for example, of a dump valve, that could allow for separator raw gas to seep continuously into the tanks.

Methane as a percent of total composition was not significantly different between the direct emissions measurements and the AST results (Figure C5-4). The percent of total emissions comprised by most C2-C6 compounds, however, was significantly lower for the direct measurement method than for the AST results, and the percent of emissions comprised by aromatics was higher for the direct emissions measurements.

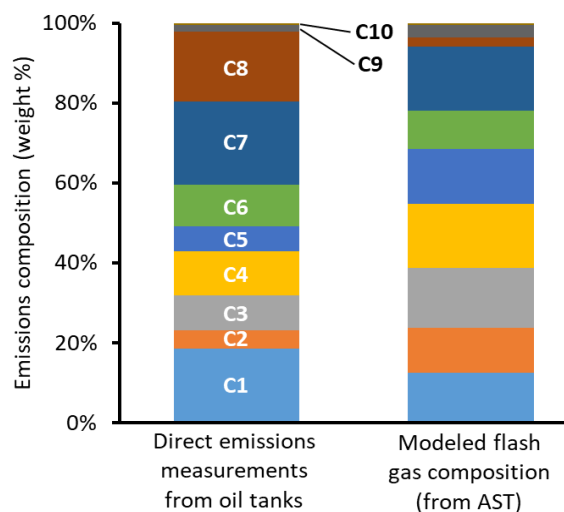


Figure C5-3. Average emissions composition by carbon number for oil tank emissions measured with the high flow system and flash gas modeled by AST. Only compounds included in both methods were used to make this figure. For the AST data, only data from wells sampled with the high flow system are included.

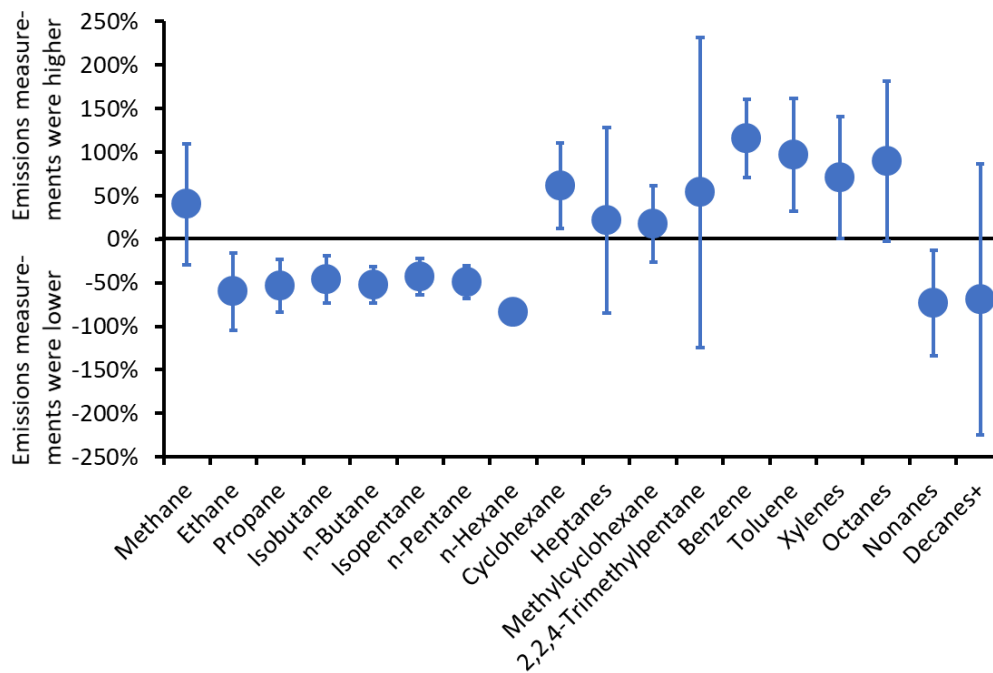


Figure C5-4. Average percent difference between the emissions composition from the direct measurements of oil tanks and flash gas emissions modeled by AST ($[\text{direct measurement} - \text{AST modeled}] / \text{average of the two methods}$). Values below zero indicate the direct emissions measurements were lower than the AST results, while values above zero indicate the opposite. Whiskers represent 95% confidence intervals, and whiskers overlapping the zero line indicate no significant difference.

The composition of the average of all non-tank emission sources we measured with the high flow system was dominated by methane and was not similar to raw gas samples collected and analyzed by AST (Figure C5-5). Some of the wells we visited used processed, rather than raw, gas in the wells' pneumatic devices and burners. This likely explains why the composition of emitted gas from non-tank sources did not always match raw gas samples analyzed by AST. The composition of emissions measured at well heads was similar to AST raw gas samples, probably because gas emitted at well heads had not been processed.

Figure C5-6 shows that, while the comparison of direct emission measurements against raw gas samples analyzed by AST shows similar trends to the comparison of direct measurements against AST flash gas results, the differences between the two methods were not statistically significant for raw gas (except propane).

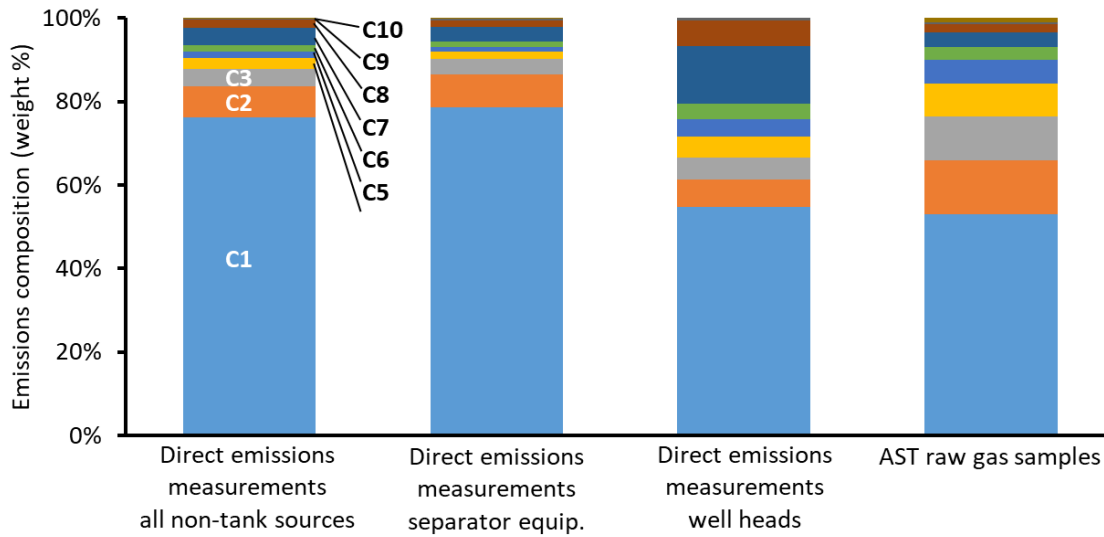


Figure C5-5. Average emission composition by carbon number for non-tank emissions measured with the high flow system and raw gas samples analyzed by AST. Only compounds utilized by both methods were used to create this figure. For the AST data, only data from wells sampled with the high flow system are included.

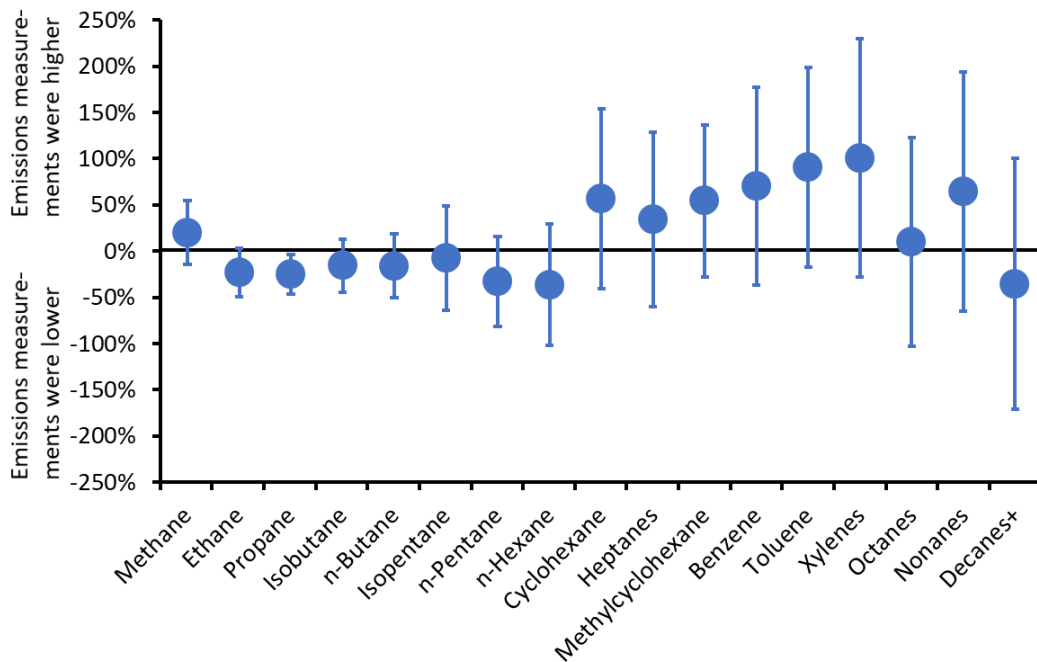


Figure C5-6. Average percent difference between the emissions composition from high flow system measurements of raw gas and raw gas sampled analyzed by AST ($[\text{emissions measurement} - \text{AST raw gas sample}] / \text{average of the two methods}$). Values below zero indicate the direct emissions measurements were lower than the raw gas sample results, while values above zero indicate the opposite. Whiskers represent 95% confidence intervals, and whiskers overlapping the zero line indicate no significant difference.

Ozone Reactivities of Emissions Compositions

The differences between the compositions of our direct measurements of emissions and the AST results are atmospherically relevant. Methane and other light hydrocarbons (ethane, propane) are relatively unreactive, while heavier hydrocarbons and aromatics are very active in ozone production. One way to compare the reactivity of different ozone-forming organics is maximum incremental reactivity (MIR). Maximum incremental reactivity is the change in ozone, calculated by a box model, for a given change in the amount of an organic compound in the atmosphere, when other conditions for ozone production are optimized (the units for maximum incremental reactivity are grams of ozone per gram of the organic compound) (Carter, 2009). Maximum incremental reactivities are specific to a set of meteorological conditions. We used values from Carter (2009). We adjusted emissions for maximum incremental activity by multiplying the emissions composition weight percent for each compound by the incremental reactivity of that compound.

While methane made up the majority of total organic compound emissions from wellheads, it was only 1% of the total incremental reactivity (Figure C5-7). In other words, of the total amount of ozone that would be formed from those emissions during a winter inversion episode, only 1% would be formed from the emitted methane. In contrast, 14% of any ozone formed would be due to emitted aromatics, even though the weight percent of aromatics emissions was 2.4%. Using this method, emissions of alcohols and carbonyls from wellheads would only be responsible for 0.05 and 0.02% of ozone formation, respectively. Figure C5-8 shows similar information for oil tank samples.

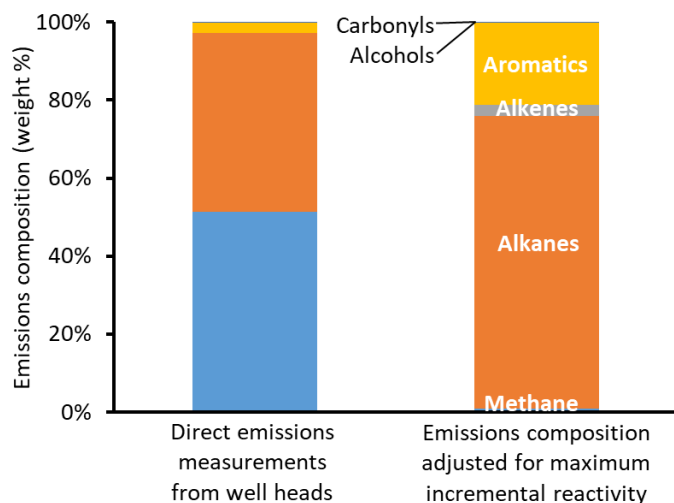


Figure C5-7. Average emissions composition from wellhead sources by compound type. The left bar shows the actual composition, and the right bar shows the composition weight percent values adjusted for maximum incremental reactivity.

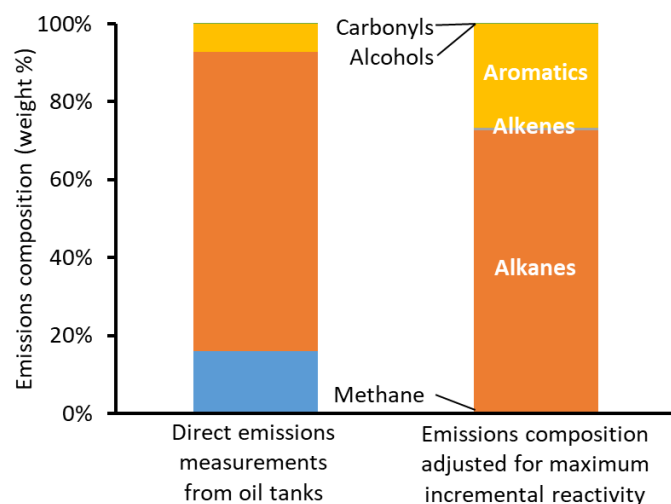


Figure C5-8. Average emissions composition from oil tanks by compound type. The left bar shows the actual composition, and the right bar shows the composition weight percent values adjusted for maximum incremental reactivity.

C6-C10 hydrocarbons comprised 51% of total hydrocarbon emissions in our direct measurements of oil tanks, compared to 31% in AST flash gas results (this comparison only included wells for which data were available for both methods). Similarly, aromatics comprised 7.8% of emissions in our direct oil tank measurements, compared to 1.8% in AST results. C6-C10 alkanes and aromatics are relatively reactive, and the total incremental reactivity of our direct emission measurements was 51% higher than the AST flash gas model results. The total incremental reactivity of our well head emission measurements was 35% higher than AST raw gas results.

Comparison with Carbonyl Speciation in Laboratory Flash Gas Measurements

The composition of our direct emissions measurements from oil tanks had much lower formaldehyde than we found in our laboratory analysis of flash gas composition (Figure C5-9; also see Section 2). Direct emissions measurements collected in this study and a previous direct measurement study (Lyman, 2015) both showed that less than 5% of total carbonyl emissions from oil tanks was due to formaldehyde. As discussed above, the laboratory flash gas analysis measured flash emissions, or the emissions that occur when a pressurized liquid is depressurized or heated as the liquid moves from the separator to the tank., while the direct measurements likely contained a mix of flash emissions and evaporative losses from the liquid in the tanks. This could be the reason for the difference between the results of the two methods. Alternatively, the difference could be due to a bias in one or both of the sampling methods.

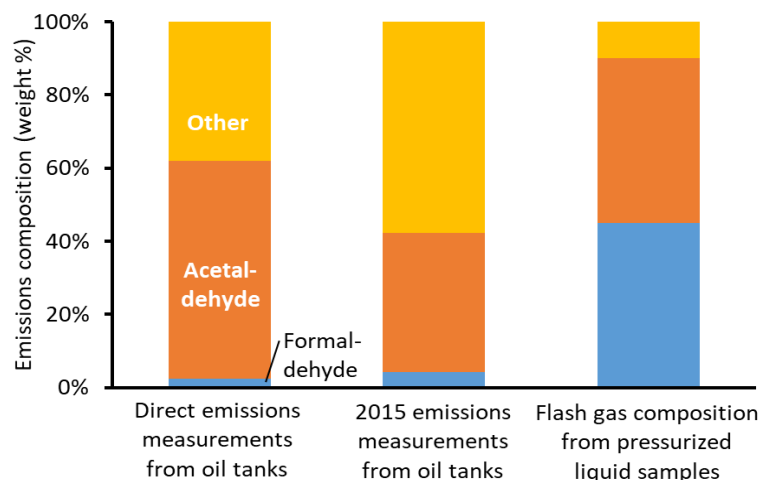


Figure C5-9. Average carbonyl composition of emissions measurements. The left bar shows direct emissions measurements from oil tanks from this study. The center bar shows direct emissions measurements from Lyman (2015). The right bar shows flash gas composition measured by USU in the laboratory from liquid samples collected in this study (see Figure C2-2).

Emissions from Water Tanks

As Figure C5-2 shows, we measured significant emissions from water tanks in this study. The composition of water tank emissions was similar to emissions from wellhead sources (Figure C5-10), with more methane and fewer heavier hydrocarbons and aromatics than emissions from oil tanks. This may be indicative of malfunctioning dump valves or liquid level controllers leading to unintentional gas carry-through. Because of this, the total incremental reactivity of the composition of oil tank emissions was 3.0 times greater than the value for water tank emissions.

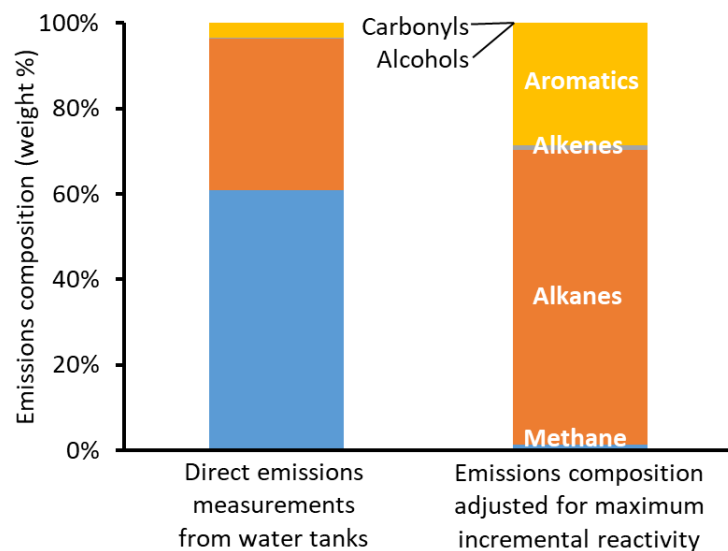


Figure C5-10. Average emissions composition from water tank sources by compound type. The left bar shows the actual composition, and the right bar shows the composition weight percent values adjusted for maximum incremental reactivity.

Emissions from produced water tanks at seven natural gas wells were measured in a study led by the Wyoming Department of Environmental Quality (Airtech, 2014). The Wyoming study measured total organics and speciated measurements of a few select compounds. Figure C5-11 shows a comparison of the produced water tank emissions composition in this study and the composition of direct emissions measurements collected in the Wyoming study. Except for hexane, the composition for the compounds measured in the Wyoming study was not significantly different.

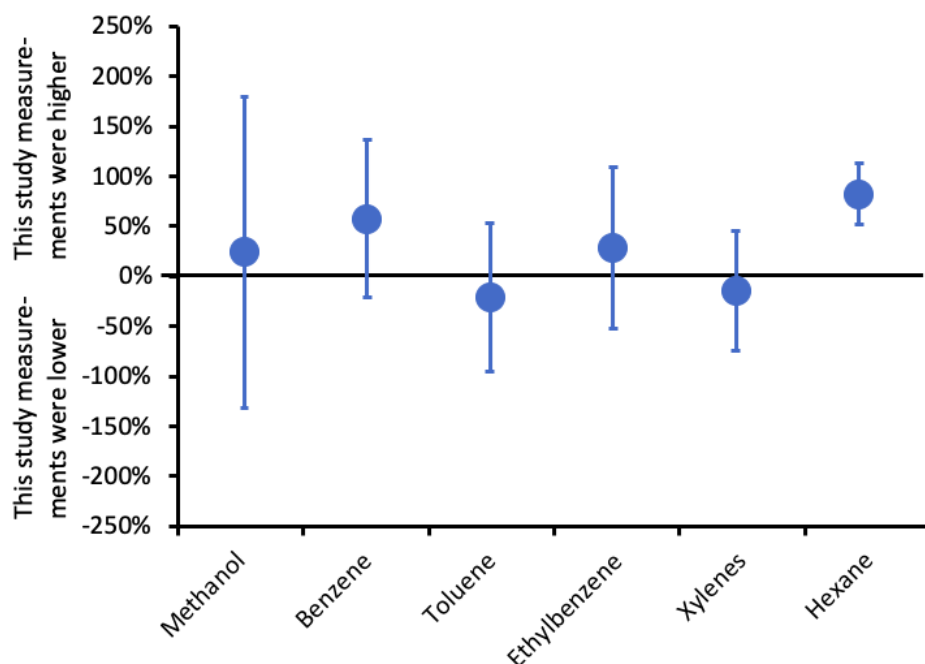


Figure C5-11. Average percent difference between the emissions composition of a few select compounds from high flow system measurements of water tank emissions in this study and similar measurements collected in Wyoming ($[\text{this study} - \text{Wyoming study}]/\text{average of the two studies}$). Values below zero indicate values from this study were lower than the results of the Wyoming study, while values above zero indicate the opposite. Whiskers represent 95% confidence intervals, and whiskers overlapping the zero line indicate no significant difference.

While our dataset for water tanks is very small, and more measurements are needed, we found that emissions from water tanks correlated with the amount of water produced by wells (Figure C5-12). When we applied this relationship to wells that produced water in the Uinta Basin (we obtained produced water data from the Utah Division of Oil, Gas and Mining (UDOGM, 2018) and information about water tank locations from the 2014 Utah Air Agencies Oil and Gas Emissions Inventory (UDAQ, 2018)), we calculated annual organic compound emissions from water tanks of 2451 tons yr^{-1} . If we assumed that only 25% of water tanks had emissions (the percentage observed in this study), the total VOC emissions would be 613 tons yr^{-1} . The 2014 Utah Air Agencies Oil and Gas Emissions Inventory estimates emissions totaled 338 tons yr^{-1} from produced water tanks at well pads.

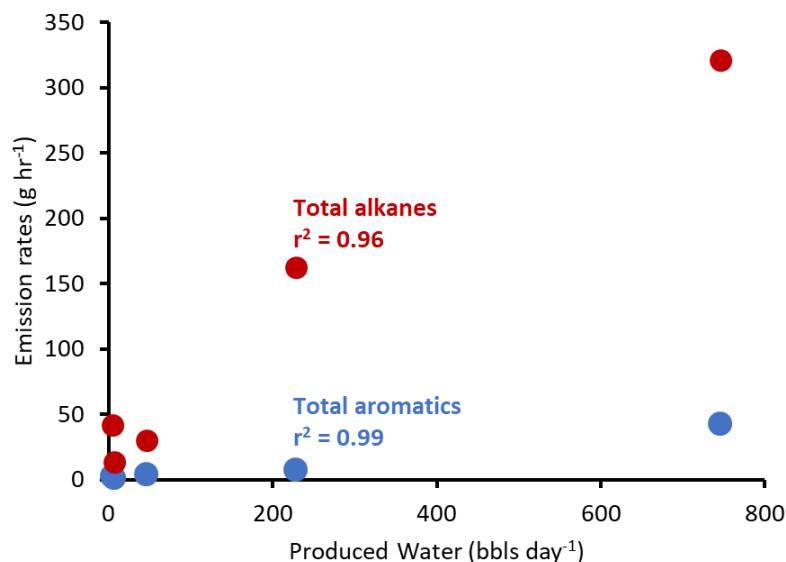


Figure C5-12. Emission rate of total alkanes and total aromatics measured with the high flow sampling system versus water production.

Comparison with Quantitative Optical Gas Imaging Software

Total organic compound emissions measured with the quantitative optical gas imaging software were correlated with measurements collected with the high flow system (Figure C5-13; $r^2 = 0.59$ with one outlier removed, 0.09 with the outlier). The measurements in Figure C5-13 include leaking fittings and flanges, tanks, and pneumatics. Figure C5-13 shows results from the quantitative software that used the factory calibration for methane, corrected for emissions of non-methane organics. A calibration for the actual measurement range, in real field conditions, would likely result in a slope closer to the 1:1 line shown in Figure C5-13.

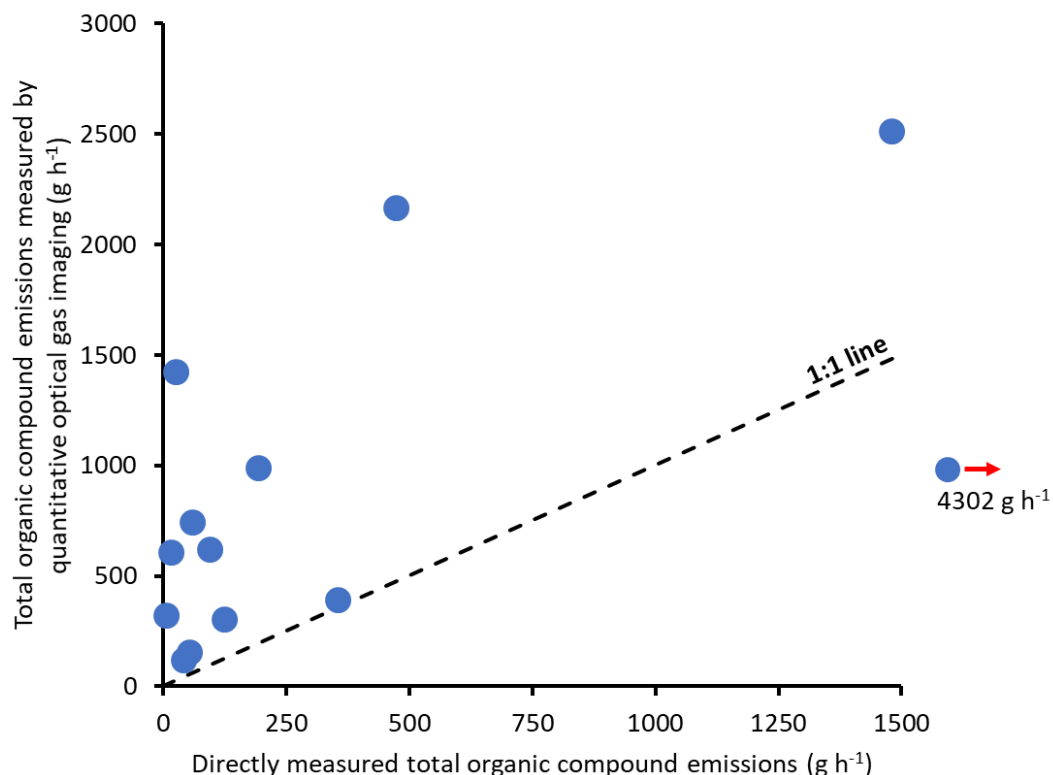


Figure C5-13. Comparison of total organic compound emissions measured directly by our high flow system against emissions measured with the quantitative optical gas imaging software.

Data Availability

An anonymized dataset of the high flow emission measurements is available here:

<https://usu.box.com/s/y271plw15q0ew2hf91a2hxvfc9qnk0wd>.

Acknowledgments

This work was funded by the Utah Division of Air Quality, the Uintah Impact Mitigation Special Service District, and the Utah Legislature. We are grateful to many oil and gas companies that allowed us to access and collect samples at their facilities, and we are grateful to the Ute Indian Tribe for allowing access to facilities on Tribal land. The optical gas imaging camera and quantitative optical gas imaging software used in this project were made available to us by the Utah Division of Air Quality. Alliance Source Testing, with funding from the Utah Division of Air Quality, collected and analyzed the raw gas samples and pressurized liquid samples used in this project to determine hydrocarbon composition of raw and flash gas, and they helped us obtain the pressurized liquid samples we analyzed for the carbonyl composition of flash gas. Questar Energy Services of Rock Springs, Wyoming, donated the floating piston cylinders we used for the analysis of carbonyl composition in flash gas. Representatives from the Environmental Protection Agency and the Ute Indian Tribe provided guidance on this project and comments on the report.

References

Ahmadov, R., McKeen, S., Trainer, M., Banta, R., Brewer, A., Brown, S., Edwards, P.M., de Gouw, J.A., Frost, G.J., Gilman, J., Helmig, D., Johnson, B., Karion, A., Koss, A., Langford, A., Lerner, B., Olson, J., Oltmans, S., Peischl, J., Petron, G., Pichugina, Y., Roberts, J.M., Ryerson, T., Schnell, R., Senff, C., Sweeney, C., Thompson, C., Veres, P.R., Warneke, C., Wild, R., Williams, E.J., Yuan, B., Zamora, R., 2015. Understanding high wintertime ozone pollution events in an oil- and natural gas-producing region of the western US. *Atmos. Chem. Phys.* 15, 411-429.

Airtech, 2014. Report on the Upper Green River Basin Closed Top Produced Water Tank Emission Study. Wyoming Department of Environmental Quality, Cheyenne, Wyoming, http://deq.wyoming.gov/media/attachments/Air%20Quality/Winter%20Ozone/Technical%20Documents/2015-0331_AQD_Produced-Water-Tank-Study-Final-Report.pdf.

Alicat, 2018. Operating Manual: Precision Gas Mass Flow Controllers. Alicat Scientific, Tucson, Arizona, https://documents.alicat.com/manuals/Gas_Flow_Controller_Manual.pdf.

Allen, D.T., Torres, V.M., Thomas, J., Sullivan, D.W., Harrison, M., Hendler, A., Herndon, S.C., Kolb, C.E., Fraser, M.P., Hill, A.D., 2013. Measurements of methane emissions at natural gas production sites in the United States. *Proc. Natl. Acad. Sci. U. S. A.* 110, 17768-17773.

Carter, W.P., 2009. Updated maximum incremental reactivity scale and hydrocarbon bin reactivities for regulatory applications, <https://ww3.arb.ca.gov/regact/2009/mir2009/mir10.pdf>.

CDPHE, 2017. PS Memo 17-01: Flash gas liberation analysis method for pressurized liquid hydrocarbon samples. Colorado Department of Public Health & Environment, Denver, Colorado, <https://www.colorado.gov/pacific/sites/default/files/AP-Memo-17-01-Flash-Gas-Liberation-Analysis.pdf>.

Edwards, P.M., Brown, S.S., Roberts, J.M., Ahmadov, R., Banta, R.M., deGouw, J.A., Dube, W.P., Field, R.A., Flynn, J.H., Gilman, J.B., Graus, M., Helmig, D., Koss, A., Langford, A.O., Lefer, B.L., Lerner, B.M., Li, R., Li, S.-M., McKeen, S.A., Murphy, S.M., Parrish, D.D., Senff, C.J., Soltis, J., Stutz, J., Sweeney, C., Thompson, C.R., Trainer, M.K., Tsai, C., Veres, P.R., Washenfelder, R.A., Warneke, C., Wild, R.J., Young, C.J., Yuan, B., Zamora, R., 2014. High winter ozone pollution from carbonyl photolysis in an oil and gas basin. *Nature* 514, 351-354.

EPA, 2017. SPECIATE and using the Speciation Tool to prepare VOC and PM chemical speciation profiles for air quality modeling, Baltimore, Maryland, https://www.epa.gov/sites/production/files/2017-10/documents/speciate_speciationtool_training.pdf.

Foster, C., Crosman, E., Holland, L., Mallia, D., Fasoli, B., Bares, R., Horel, J., Lin, J., 2017. Confirmation of Elevated Methane Emissions in Utah's Uintah Basin With Ground-Based Observations and a High-Resolution Transport Model. *J. Geophys. Res. Atmos.* 122, 13026-13044.

GPA, 2014. Method GPA 2174: Obtaining Liquid Hydrocarbon Samples for Analysis by Gas Chromatography. Gas Processors Association, Tulsa, Oklahoma, https://infostore.saiglobal.com/en-us/standards/gpa-2174-2014-557722_SAIG_GPA_GPA_1272275/.

Howard, T., Ferrara, T.W., Townsend-Small, A., 2015. Sensor transition failure in the high flow sampler: implications for methane emission inventories of natural gas infrastructure. *J. Air Waste Manage. Assoc.* 65, 856-862.

Hsu, S., Divita, F., Dorn, J., 2016. SPECIATE Version 4.5. Abt Associates, Bethesda, Maryland, https://www.epa.gov/sites/production/files/2016-09/documents/speciate_4.5.pdf.

Jarque, C.M., Bera, A.K., 1980. Efficient tests for normality, homoscedasticity and serial independence of regression residuals. *Economics letters* 6, 255-259.

Jimenez, M., Nopmongcol, U., Yarwood, G., 2016. Speciation Tool User's Guide Version 4.0. Environ, Novato, California, https://www.cmascenter.org/help/model_docs/speciation_tool/4.0/Speciation_Tool_Users_Guide_v4.0.pdf.

Johnson, D.R., Covington, A.N., Clark, N.N., 2015. Methane emissions from leak and loss audits of natural gas compressor stations and storage facilities. *Environ. Sci. Technol.* 49, 8132-8138.

Karion, A., Sweeney, C., Petron, G., Frost, G., Hardesty, R.M., Kofler, J., Miller, B.R., Newberger, T., Wolter, S., Banta, R., Brewer, A., Dlugokencky, E., Lang, P., Montzka, S.A., Schnell, R., Tans, P., Trainer, M., Zamora, R., Conley, S., 2013. Methane emissions estimate from airborne measurements over a western United States natural gas field. *Geophys. Res. Lett.* 40, 4393-4397.

Lyman, S., 2015. Measurement of Carbonyl Emissions from Oil and Gas Sources in the Uintah Basin. Utah State University, Vernal, Utah, http://binghamresearch.usu.edu/files/CarbonylEmiss_FnlRprt_31jul2015.pdf.

Lyman, S., Shorthill, H., Eds., 2013. Final Report: 2012 Uinta Basin Winter Ozone Study, <http://rd.usu.edu/htm/reports>.

Lyman, S.N., Mansfield, M.L., 2018. Organic compound emissions from a landfarm used for oil and gas solid waste disposal. *J. Air Waste Manage. Assoc.* DOI: 10.1080/10962247.2018.1459327.

Lyman, S.N., Mansfield, M.L., Tran, H.N., Evans, J.D., Jones, C., O'Neil, T., Bowers, R., Smith, A., Keslar, C., 2018. Emissions of organic compounds from produced water ponds I: Characteristics and speciation. *Sci. Total Environ.* 619, 896-905.

Lyman, S.N., Watkins, C., Jones, C.P., Mansfield, M.L., McKinley, M., Kenney, D., Evans, J., 2017. Hydrocarbon and Carbon Dioxide Fluxes from Natural Gas Well Pad Soils and Surrounding Soils in Eastern Utah. *Environ. Sci. Technol.* 51, 11625-11633.

Mansfield, M.L., 2014. Kerogen maturation data in the Uinta Basin, Utah, USA, constrain predictions of natural hydrocarbon seepage into the atmosphere. *J. Geophys. Res. Atmos.* 119, 3460-3475.

Mansfield, M.L., Tran, H.N.Q., Lyman, S.N., Smith, A., Bowers, R., Keslar, C., 2018. Emissions of organic compounds from produced water ponds III: mass-transfer coefficients, composition-emission correlations, and contributions to regional emissions. *Sci. Total Environ.* 627, 860-868.

Matichuk, R., Tonnesen, G., Luecken, D., Gilliam, R., Napelenok, S.L., Baker, K.R., Schwede, D., Murphy, B., Helmig, D., Lyman, S.N., 2017. Evaluation of the Community Multiscale Air Quality Model for Simulating Winter Ozone Formation in the Uinta Basin. *J. Geophys. Res. Atmos.* 122, 13545–13572.

Providence, 2019. Advanced Training on Quantitative Optical Gas Imaging, <https://www.providencephotonics.com/news/flir-webinar-advanced-training-on-qogi>.

Robertson, A.M., Edie, R., Snare, D., Soltis, J., Field, R.A., Burkhart, M.D., Bell, C.S., Zimmerle, D., Murphy, S.M., 2017. Variation in Methane Emission Rates from Well Pads in Four Oil and Gas Basins with Contrasting Production Volumes and Compositions. *Environ. Sci. Technol.* 51, 8832-8840.

Stoeckenius, T., 2015. Final Report: 2014 Uinta Basin Winter Ozone Study, http://binghamresearch.usu.edu/files/UBWOS_2014_Final.pdf.

Tran, H., Tran, T., Crosman, E., Mansfield, M., Lyman, S., 2014. Impacts of Oil and Gas Production on Winter Ozone Pollution in the Uintah Basin Using Model Source Apportionment, AGU Fall Meeting, San Francisco, California.

Tran, H.N.Q., Lyman, S.N., Mansfield, M.L., O'Neil, T., Bowers, R.L., Smith, A.P., Keslar, C., 2017. Emissions of organic compounds from produced water ponds II: evaluation of flux-chamber measurements with inverse-modeling techniques. *J. Air Waste Manage. Assoc.* DOI: 10.1080/10962247.2018.1426654.

Uchiyama, S., Naito, S., Matsumoto, M., Inaba, Y., Kunugita, N., 2009. Improved measurement of ozone and carbonyls using a dual-bed sampling cartridge containing trans-1, 2-bis (2-pyridyl) ethylene and 2, 4-dinitrophenylhydrazine-impregnated silica. *Anal. Chem.* 81, 6552-6557.

UDAQ, 2018. Uinta Basin: 2014 Air Agencies Oil and Gas Emissions Inventory, <https://deq.utah.gov/legacy/destinations/u/uintah-basin/air-agencies-emissions-inventory/index.htm>.

UDOGM, 2018. Data Research Center, http://oilgas.ogm.utah.gov/Data_Center/DataCenter.cfm.

Warneke, C., Geiger, F., Edwards, P.M., Dube, W., Petron, G., Kofler, J., Zahn, A., Brown, S.S., Graus, M., Gilman, J.B., Lerner, B.M., Peischl, J., Ryerson, T.B., de Gouw, J.A., Roberts, J.M., 2014. Volatile organic compound emissions from the oil and natural gas industry in the Uintah Basin, Utah: oil and gas well pad emissions compared to ambient air composition. *Atmos. Chem. Phys.* 14, 10977-10988.

Yarwood, G., Jung, J., Whitten, G.Z., Heo, G., Mellberg, J., Estes, M., 2010. Updates to the Carbon Bond mechanism for version 6 (CB6), 2010 CMAS Conference, Chapel Hill, North Carolina.

Yarwood, G., Rao, S., Yocke, M., Whitten, G., 2005. Final Report: Updates to the Carbon Bond chemical mechanism: CB05. Yocke and Company, Novato, California, http://www.camx.com/files/cb05_final_report_120805.aspx.

Zeng, Y., Morris, J., Sanders, A., Mutyala, S., Zeng, C., 2017. Methods to determine response factors for infrared gas imagers used as quantitative measurement devices. *J. Air Waste Manage. Assoc.* 67, 1180-1191.

Report D: Supplemental Speciation Profile Analysis

Utah Division of Air Quality

Introduction

For photochemical modeling and other air quality analytical assessments, it is necessary to apply the results from the few wells sampled in this study to the more than 11,000 wells in the Uinta Basin. To accomplish this, the composition data from this study are grouped into composite speciation profiles based on some generic characteristics. Previous grouping efforts⁵ (outside those discussed in REPORT C: DEVELOPMENT OF COMPOSITION SPECIATION PROFILES) made no effort to demonstrate the statistical validity or representativeness of their groupings. This supplemental analysis poses a statistically robust methodology for grouping the compositional data collected in this study, and presents alternative profiles from the initial speciation profile analysis (see Report C: DEVELOPMENT OF COMPOSITION SPECIATION PROFILES).

This report details the findings of research answering two specific challenges of working with composition data:

- 1) in general, what statistics can be used to tell if a specific grouping schema adequately divides the data into distinct groups, and
- 2) statistical challenges in dealing with datasets in which each individual sample is represented by percentages, rather than amounts, of components.

Composition data refer to a set of values describing the percentage each species contributes to the overall composition of the substance. While in three dimensions composition data may be referred to as ternary, and are plotted on a ternary (triangular) diagram, and in four dimensions they may be called tetrahedral, and are plotted on a tetrahedral diagram, the compositional geometry is generally referred to as simplex geometry. A simplex is the generalization of the notion of a triangle or tetrahedron to many arbitrary dimensions. In such a geometry, each vertex represents a composition made up 100% of one component, and 0% of the rest. Anywhere else in the simplex must be a mixture of components.

In the case of this study, the composition data describe the weight fraction (or percentage) of each chemical specie found in hydrocarbon gases from upstream oil and gas production. The primary challenge with composition data is that the sample space (simplex space) is non-Euclidian. Specifically, the space is not infinitely continuous because compositions are bounded between 0 and 1 by definition. This violates the assumptions of many statistical tests. In order to define a statistically robust analysis for these data, it is necessary to transform the data into a Euclidian space. Many transformations are

⁵ Matichuk, R., G. Tonnesen, A. Eisele, E. Thoma, Mike Kosusko, M. Strum, AND C. Beeler. Advancing Understanding of Emissions from Oil and Natural Gas Production Operations to Support EPA's Air Quality Modeling of Ozone Non-Attainment Areas; Final Summary Report. U.S. Environmental Protection Agency, Washington, DC, EPA/600/R-17/224, 2016. https://cfpub.epa.gov/si/si_public_file_download.cfm?p_download_id=531121&Lab=NRMRL

available, the most common being the additive log-ratio transformation (ALR⁶), centered log-ratio transformation (CLR⁷), and the isometric log-ratio transformation (ILR⁸). The ILR transformation is the one we chose to adopt in order to accomplish a transformation to a Euclidian space. The ILR transformation scales the composition by dividing all columns by their geometric means, then taking the log of each value. The resultant geometry is confined to in an n-dimensional hyperplane with a user defined orthonormal basis (default is Helmert Matrix). See the associated references for details on why this transformation was used, what the drawbacks and advantages are, and for visualizations of the geometry of composition space.⁹ The R package “compositions” was used to implement the ILR transformation and its inversion¹⁰.

Assuming normal distributions for the columns in the data causes the uncertainty envelope to include negative values, which does not make sense because compositional data are inherently bounded between 0 and 1. A model like a log-normal distribution is needed to prevent this. The uncertainty of means of each group can be found and evaluated in the ILR space, however, the confidence interval of n-dimensional composition data in ILR space will be a hyper-spheroid or hyper-ellipse. Such a confidence interval cannot be easily expressed as a set of uncertainties around the mean of each component in composition space, and, as such, we cannot give a meaningful representation of the uncertainties in the group averages using these methods. Confidence testing of membership to these groups for new points, like those that will be submitted by oil and gas companies in the future to UDAQ for permitting purposes, can be done with the transformed data in ILR space.

Profile averages can also be generated by calculating the average profiles in the standard weight percent format (we refer to this method as “Column-wise Average,” which was the approach used in REPORT C: MEASUREMENT OF CARBONYLS, SPECIATION PROFILE ANALYSIS, AND HIGH FLOW EMISSIONS SAMPLING & ANALYSIS). These methods vary only slightly in the final result, and underlying this choice is an assumption about whether the data are normally distributed in ILR space or standard composition space. Because the standard deviations in composition space are not physically possible (lead to negative weight percentages), we assume the data are normally distributed in ILR space. To see the differences in each averaging method, compare the ILR based profiles (Tables D-3 and D-4**Error! Reference source not found.**) to the Column-wise Averaging (APPENDIX E: UINTA BASIN PROFILES AS COLUMN-WISE AND THROUGHPUT-WEIGHTED AVERAGES). While this analysis cannot include uncertainty estimates in ILR space, the uncertainty given for column-averaged data can be used to qualitatively understand the spread of the data. Also included is a table showing Column-wise averaging weighted by facility throughput (APPENDIX E: UINTA BASIN PROFILES AS COLUMN-WISE AND

⁶ Aitchison, J. (1982), The Statistical Analysis of Compositional Data. Journal of the Royal Statistical Society: Series B (Methodological), 44: 139-160. doi:10.1111/j.2517-6161.1982.tb01195.x

⁷ Aitchison, J. 1986. The statistical analysis of compositional data. London: Chapman and Hall.

⁸ Egozcue, J.J., Pawlowsky-Glahn, V., Mateu-Figueras, G. et al. Mathematical Geology (2003) 35: 279. <https://doi.org/10.1023/A:1023818214614>

⁹ Aitchison, J. 1986. The statistical analysis of compositional data. London: Chapman and Hall.

¹⁰ <https://cran.r-project.org/web/packages/compositions/index.html>

THROUGHPUT-WEIGHTED AVERAGES). This is included because previous studies used this method of reporting¹¹.

Now that the composition data is in a Euclidian space, apply typical statistical techniques to achieve grouping. There are multiple answers to the question of how to statistically assess grouping schemes: the most common of these are Multivariate Analysis of Variance (MANOVA), Multi-Response Permutation Procedures (MRPP), Analysis of Group Similarities (ANOSIM¹²), and Mantel's Test. Of these tests ANOSIM is the best for our application. The ANOSIM test uses distances from randomly chosen points within each group (intra-group distance) and compares those with distances of randomly chosen points between groups (inter-group distance). If the groups are distinct, intra-group distances will be much smaller than inter-group distances. The distribution of these distances is analyzed to create the ANOSIM score (Figure D-1 [*top*]). While any concept of distance may be used (e.g. Euclidian, Bray-Curtis, Jaccard), a distance metric has to be specified during the analysis. Euclidian distance is one of the concepts that is restored with an ILR transformation, so Euclidian distance was the metric used in this study because it is easy to interpret.

The ANOSIM test has the advantage over the other tests in that it yields a degree of group differences. Its R score ranges from 0 to 1 (for real composition datasets) with 0 meaning the groups are all very similar and with 1 meaning the groups are all very different (Figure D-1 [*bottom*]). This degree of difference allows us to choose the best grouping scheme of the available options, even if that scheme does not create the most perfect possible separation of the data. This has advantages with oil and gas data specifically, because these data show evidence of an evolution of compositions from raw gas to flash gas, suggesting that there may be no perfect cutoff to split the data into groups (see results, esp. Figure D-3).

¹¹ Matichuk, R., G. Tonnesen, A. Eisele, E. Thoma, Mike Kosusko, M. Strum, AND C. Beeler. Advancing Understanding of Emissions from Oil and Natural Gas Production Operations to Support EPA's Air Quality Modeling of Ozone Non-Attainment Areas; Final Summary Report. U.S. Environmental Protection Agency, Washington, DC, EPA/600/R-17/224, 2016.

https://cfpub.epa.gov/si/si_public_file_download.cfm?p_download_id=531121&Lab=NRMRL

¹² Warton, D.I., Wright, T.W., Wang, Y. 2012. Distance-based multivariate analyses confound location and dispersion effects. *Methods in Ecology and Evolution*, 3, 89–101

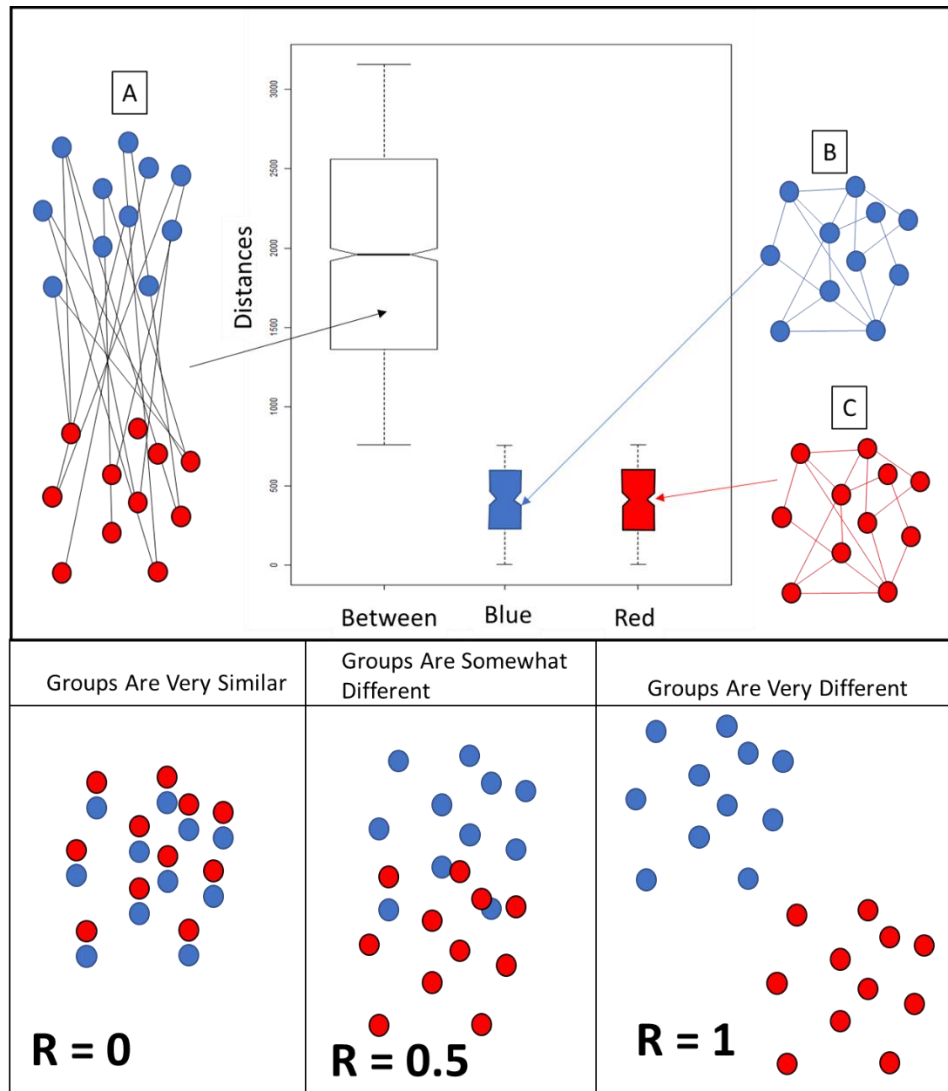


Figure D-1:

TOP: Example of the distribution of intra vs inter-group distance analyzed to create the ANOSIM score in two dimensions. In this example the R value would be close to 1 because the intra group distances are on average much smaller than the intragroup distances. R score ranges from 0 to 1 (for real composition datasets) with 0 meaning the groups are all very similar and with 1 meaning the groups are all very different. In this analysis, a higher R score indicated a more distinct grouping scheme for the composition data.

BOTTOM: Illustration of how ANOSIM R values indicates the degree of difference between groups. Colored points represent two groups of points in arbitrary X, Y coordinates. R score ranges from 0 to 1 (for real composition datasets) with 0 meaning the groups are all very similar and with 1 meaning the groups are all very different.

The importance of using the ILR transformation for statistical tests is demonstrated in Figure D-2. In the compositional domain, comparing A to B shows essentially no difference in the R score, meaning that these two datasets would be considered equally distinct. After applying the ILR transformation and comparing C to D, the ANOSIM score of (A) goes down, but the ANOSIM score of B is unchanged. This means that in ILR space these two cases can be distinguished.

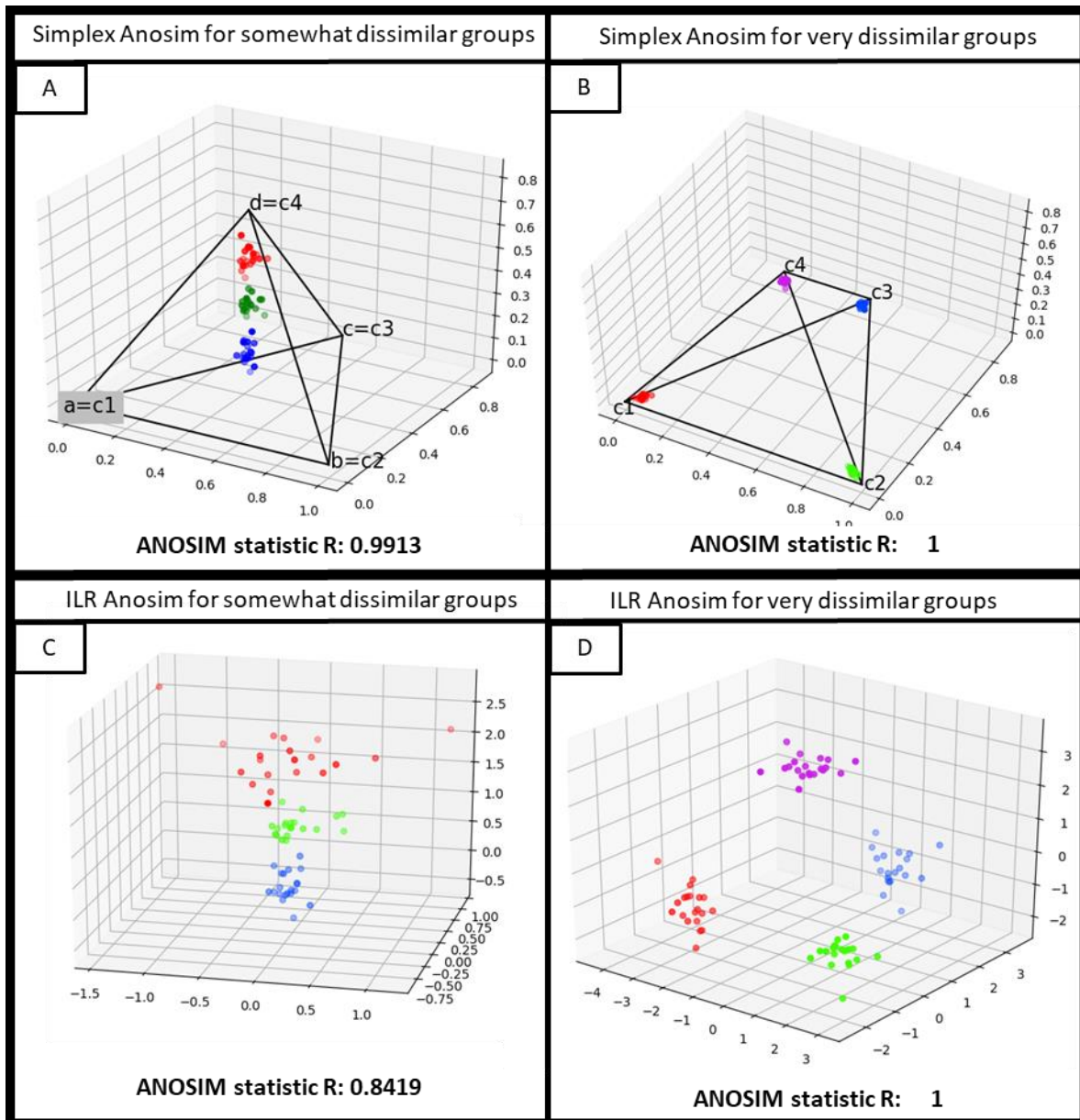


Figure D-2: A) Visualization of 4D (4 component) compositional data which are separated into distinct groups, but are not as distinct as possible in compositional space. The accompanying R value is the ANOSIM statistic R value for the data before transformation into ILR space. B) Visualization of 4D compositional data that are close to as distinct of groups that are possible in a 4D compositional domain. C) ILR transformation of (A) into 3-dimensional Euclidian space. D) ILR transformation of (B) into 3-dimensional Euclidian space.

Methods

The method designed in this study is meant to be repeatable, such that the same analysis can be performed with new data or groupings and can also be compared with the results presented here. Composition data typically speciate out to C10 and often out to C36, meaning that analysis would include 36+ dimensions in compositional space. One part of the methods we consider necessary is subsetting or amalgamating the data to reduce the number of dimensions. Subsetting only considers a few key species and renormalizes those compositions, and amalgamating adds several species together

into representative compositions. The first reason to subset the data is that certain transformations like ALR, CLR, and ILR do not allow true zero values, and zeroes often occur in composition space when a chemical component is completely absent from a sample. While this can normally be overcome by adding very small quantities to all true zeroes (usually method detectable limit values) in certain cases having too many zeroes does cause issues with the ANOSIM statistic.¹³ As such, using subsets and amalgamations are the best methods to test the robustness of results from the ANOSIM statistics. Subsets and amalgamations both have drawbacks, but our usage of them assumes that if a grouping scheme is the highest performer on the raw data as well as in subsets and amalgamations of the data, then that result is more robust. The specific subsets and amalgamations were selected for components that have the greatest influence on the photochemical model. In the subsetting test, we used the three most abundant components (methane, ethane, and propane), benzenes and hexanes, and C10+. In the amalgamation approach we amalgamated based on number of carbons per molecule, which is generally related to ozone production.¹⁴ We amalgamated BTEX components, which are regularly grouped and measured as an estimated potential for ozone formation. We also performed another amalgamation based on the amalgamation used for Carbon Bond 6 (CB6) modeling preparation of the data (this is the format that composition data are entered for use in the SMOKE model). A table of how the conversions from composition data to CB6 parameters is given in Table D-1).

The method used here is performed as follows:

- 1) Fill all zeroes in the dataset with a small number. In this analysis, 1e-9 was used.
- 2) Normalize each measurement to sum to 1.
- 3) Parse out the subset and calculate the following amalgamations and summations on the data:
 - a. Subset (Methane, Ethane, Propane, N-Hexane, Benzene, Decanes)
 - b. Amalgamation (C1, C2, C3, C6, BTEX, C8)
 - c. CB6 (BENZ, PRPA, PAR, TOL, XYL, NR, CH4) (see Table D-1)
- 4) Apply the isometric log-ratio (ILR) transform to the raw data as well as each amalgamation/subset. This was done by using the [compositions package](#) in R.

¹³ Future work will include the exploration the the Box-Cox transformation. Tsagris et al. (2011) generalize the CLR by using a Box-Cox transformation, which generalizes the logarithm (ILR) transformation. The ILR transformation is a Box-Cox transformation with parameter 1. Purportedly, this Box-Cox parameter can be varied, and some values match certain data conditions better than other. Essentially, the Box-Cox parameter specifies how much to apply the transformation, so zero would be no transformation, 1 would be the ILR transformation, and $\frac{1}{2}$ would be halfway between no transformation and a logarithmic transformation. Preliminary reading suggests that one way to deal with true zeroes would be to use a transformation closer to the halfway value, but we have not been able to test this concept yet.

¹⁴ Yarwood, Greg, et al. "Updates to the Carbon Bond mechanism for version 6 (CB6)." 9th Annual CMAS Conference, Chapel Hill, NC. 2010.

Table D-1: CB6 conversion table. Cells grayed when value present for ease of reading. This shows how the conversions of composition data to CB6 parameters was performed to amalgamate compounds for modeling preparation of the data for use in the SMOKE model.

	NASN	ACET	KET	ETHY	BENZ	PRPA	PAR	OLE	TOL	XYL	FORM	ALD2	ETH	ISOP	MEOH	ETOH	NR	CH4	ETHA	IOLE	ALDX	TERP	MW	#carbons
2,2,4 TRIMETHYLPENTANE	0	0	0	0	0	0	7	0	0	0	0	0	0	0	0	0	1	0	0	0	0	0	114.23	7
ISOPENTANE	0	0	0	0	0	0	5	0	0	0	0	0	0	0	0	0	0	0	0	0	0	0	72.15	5
BENZENE	0	0	0	0	6	0	0	0	0	0	0	0	0	0	0	0	0	0	0	0	0	0	78.11	1
CYCLOPENTANE	0	0	0	0	0	0	5	0	0	0	0	0	0	0	0	0	0	0	0	0	0	0	70.14	5
ETHANE	0	0	0	0	0	0	0	0	0	0	0	0	0	0	0	0	0	0	1	0	0	0	30.07	2
ETHYLBENZENE	0	0	0	0	0	0	1	0	1	0	0	0	0	0	0	0	0	0	0	0	0	0	106.17	8
DECANES	0	0	0	0	0	0	9.25	0	0	0	0	0	0	0	0	0	0.75	0	0	0	0	0	142.29	9.25
HEPTANES	0	0	0	0	0	0	6.81	0	0	0	0	0	0	0	0	0	0.19	0	0	0	0	0	100.21	6.81
NONANES	0	0	0	0	0	0	8.75	0	0	0	0	0	0	0	0	0	0.25	0	0	0	0	0	128.26	8.75
OCTANES	0	0	0	0	0	0	7.62	0	0	0	0	0	0	0	0	0	0.38	0	0	0	0	0	114.23	7.62
XYLENES	0	0	0	0	0	0	0.25	0	0.25	0.75	0	0	0	0	0	0	0	0	0	0	0	0	106.17	8
METHANE	0	0	0	0	0	0	0	0	0	0	0	0	0	0	0	0	0	1	0	0	0	0	16.04	1
METHYLCYCLOHEXANE	0	0	0	0	0	0	7	0	0	0	0	0	0	0	0	0	0	0	0	0	0	0	98.19	7
N-BUTANE	0	0	0	0	0	0	4	0	0	0	0	0	0	0	0	0	0	0	0	0	0	0	58.12	4
N-HEXANE	0	0	0	0	0	0	6	0	0	0	0	0	0	0	0	0	0	0	0	0	0	0	86.18	6
N-PENTANE	0	0	0	0	0	0	5	0	0	0	0	0	0	0	0	0	0	0	0	0	0	0	72.15	5
PROPANE	0	0	0	0	0	3	0	0	0	0	0	0	0	0	0	0	0	0	0	0	0	0	44.1	1.5
TOLUENE	0	0	0	0	0	0	0	0	1	0	0	0	0	0	0	0	0	0	0	0	0	0	92.14	7
ISOBUTANE	0	0	0	0	0	0	4	0	0	0	0	0	0	0	0	0	0	0	0	0	0	0	58.12	4
CYCLOHEXANE	0	0	0	0	0	0	6	0	0	0	0	0	0	0	0	0	0	0	0	0	0	0	84.16	6

- 5) Create a column for each grouping scheme. Additionally, permute all combinations of the grouping methods. For example, if one column was a well type consisting of $x=[\text{'oil well'}, \text{'gas well'}]$ and the other columns was sample type consisting of $y=[\text{'raw gas'}, \text{'flash gas'}]$, then a new column is created where $z=[\text{'oil well raw gas'}, \text{'oil well flash gas'}, \text{'gas well raw gas'}, \text{'gas well flash gas'}]$.
- 6) Look at how many members there are per group (N). For each grouping scheme, ideally, there would be at least twenty measurements per group for the ANOSIM method to work well. The $N > 20$ number is based on simulated data, where the underlying effects were known, and the ANOSIM parameters were explored by varying them in controlled ways.¹⁵
- 7) Calculate the ANOSIM R for each amalgamation/subset and the total data for each grouping scheme. These can be compiled into a table as shown in Table D-2. The R package [‘vegan’ was used for this analysis.](#)
- 8) Define the best grouping scheme as the one that has the highest ANOSIM score while still having at least 20 samples per group. The R statistic can be interpreted like a correlation value with these rough guidelines for interpretation:
 - 0.75 < R < 1.00 - highly different
 - 0.50 < R < 0.75 - different
 - 0.25 < R < 0.50 - different with some overlap
 - 0.10 < R < 0.25 - similar with some differences (or high overlap)
 - 0.00 < R < 0.10 - similar
- 9) Calculate the average for each column in the ILR transformation once a grouping scheme is chosen. Reverse the transformation with the compositions package in R by using the function “`IlrInv`”¹⁶. Profile averages can also be generated by calculating the average profiles in the standard weight percent format.

Results

The results of the ANOSIM analysis are given in Table D-2. The only grouping scheme which has both a high enough sample count per group ($N > 20$ samples per group) and significant ANOSIM score is the “Well Type – Sample Type” grouping. Our findings indicate that this is the best possible grouping given the currently available data and the categorical variables available (factors). Grouping by formation was not valid because of sample size.

¹⁵ <https://www.umass.edu/landeco/teaching/multivariate/schedule/discriminate1.pdf>

¹⁶ <https://cran.r-project.org/web/packages/compositions/compositions.pdf>, page 98

Table D-2: The table highlights grouping schemes that have enough samples per group (N>20) in blue. Those that are very close are shown in orange. The ANOSIM results are color-coded from yellow (groupings are not distinct from each other) to green (groupings are more distinct). Although sample-type and formation groupings have high ANOSIM scores, there are too few samples per group to be statistically valid, though this grouping scheme is close to having enough samples (indicated by orange highlight). A color key is provided below the table.

Grouping	Number of Groups	Average Samples Per Group	ANOSIM Scores				
			Total	CB6	Amalgamated	Subsetted	Average ANOSIM
Company	7	19.0	0.27	0.37	0.39	0.34	0.34
Well Type	2	66.5	0.24	0.54	0.61	0.56	0.49
Sample Type	2	66.5	0.37	0.44	0.47	0.59	0.47
Field	13	10.2	0.30	0.32	0.33	0.28	0.31
Formation	5	26.6	0.22	0.38	0.31	0.27	0.29
USU Groups	13	10.2	0.81	0.73	0.82	0.82	0.80
USU Groups (no sub groups)	9	14.8	0.73	0.77	0.82	0.82	0.79
'Company' 'well_type'	7	19.0	0.27	0.37	0.39	0.34	0.34
'Company' 'sample_type'	14	9.5	0.56	0.72	0.77	0.76	0.70
'Company' 'Field'	14	9.5	0.35	0.38	0.38	0.33	0.36
'Company' 'formation'	13	10.2	0.30	0.36	0.33	0.28	0.32
'well_type' 'sample_type'	4	33.3	0.46	0.71	0.79	0.82	0.70
'well_type' 'Field'	13	10.2	0.30	0.32	0.33	0.28	0.31
'well_type' 'formation'	5	26.6	0.22	0.38	0.31	0.27	0.29
'sample_type' 'Field'	26	5.1	0.59	0.66	0.70	0.73	0.67
'sample_type' 'formation'	10	13.3	0.47	0.64	0.63	0.65	0.60
'Field' 'formation'	22	6.0	0.37	0.37	0.32	0.26	0.33

					ANOSIM Scores				
Grouping			Number of Groups	Average Samples Per Group					
					Total	CB6	Amalgamated	Subsetted	Average ANOSIM
'Company'	'well_type'	'sample_type'	14	9.5	0.56	0.72	0.77	0.76	0.70
'Company'	'well_type'	'Field'	14	9.5	0.35	0.38	0.38	0.33	0.36
'Company'	'well_type'	'formation'	13	10.2	0.30	0.36	0.33	0.28	0.32
'Company'	'sample_type'	'Field'	28	4.8	0.65	0.74	0.77	0.77	0.73
'Company'	'sample_type'	'formation'	26	5.1	0.60	0.71	0.73	0.74	0.69
'Company'	'Field'	'formation'	22	6.0	0.37	0.37	0.32	0.26	0.33
'well_type'	'sample_type'	'Field'	26	5.1	0.59	0.66	0.70	0.73	0.67
'well_type'	'sample_type'	'formation'	10	13.3	0.47	0.64	0.63	0.65	0.60
'well_type'	'Field'	'formation'	22	6.0	0.37	0.37	0.32	0.26	0.33
'sample_type'	'Field'	'formation'	44	3.0	0.69	0.75	0.74	0.76	0.73

Color Coding Key

Samples Per Group	ANOSIM Score	
Nearly Sufficient Samples Per Group	0.16	Low R
	0.33	
	0.49	
Sufficient Samples Per Group	0.65	High R
	0.82	

The composite profiles created from this method are given in Table D-3 and Table D-4. These profiles are not the column-wise average of the raw data by group, but instead, the centroid in ILR space reverted into the simplex space (see INTRODUCTION).

Table D-3: New Uinta Basin composition profiles represented as ILR Centroids. These are the new composition profiles calculated by finding the average of each profile in the ILR transformed data, then using the ILR inverse function to return the profiles to standard composition weight percentages.

	Oil Well – Flash Gas	Oil Well – Raw Gas	Gas Well – Flash Gas	Gas Well – Raw Gas
<i>Profile Name</i>	<i>UNTF_OW</i>	<i>UNTR_OW</i>	<i>UNTF_GW</i>	<i>UNTR_GW</i>
METHANE	13.01%	53.38%	47.76%	73.76%
ETHANE	10.74%	11.49%	20.57%	10.39%
PROPANE	16.48%	9.68%	15.68%	5.92%
ISOBUTANE	4.85%	2.22%	4.37%	1.67%
N-BUTANE	12.38%	4.99%	5.25%	2.12%
ISOPENTANE	6.07%	2.32%	2.16%	1.01%
N-PENTANE	8.12%	3.13%	1.52%	0.83%
CYCLOPENTANE	0.61%	0.23%	0.08%	0.05%
N-HEXANE	6.76%	2.14%	0.75%	0.46%
CYCLOHEXANE	1.73%	0.57%	0.37%	0.26%
HEPTANES	10.47%	4.99%	0.33%	1.45%
METHYLCYCLOHEXANE	2.09%	0.81%	0.56%	0.55%
2,2,4 TRIMETHYLPENTANE	0.022%	0.0012%	0.0022%	0.000012%
BENZENE	0.38%	0.16%	0.10%	0.07%
TOLUENE	0.53%	0.26%	0.17%	0.20%
ETHYLBENZENE	0.0005%	0.03%	0.01%	0.01%
XYLENES	0.36%	0.21%	0.08%	0.14%
OCTANES	2.04%	1.81%	0.11%	0.54%
NONANES	2.94%	0.34%	0.12%	0.13%
DECANES+	0.42%	1.26%	0.02%	0.44%
TOTAL	100.00%	100.00%	100.00%	100.00%

Table D-4: New Uinta Basin composition profiles featuring carbonyls. Only flash gas samples were analyzed for carbonyls.

	Oil Well – Flash Gas + carbonyl	Gas Well – Flash Gas + carbonyl
<i>Profile Name</i>	<i>UNTF_OW_C=O</i>	<i>UNTF_GW_C=O</i>
methane	18.352449%	29.781276%
ethane	11.442717%	19.158171%
propane	13.853831%	24.774409%
isobutane	3.743012%	7.324207%
n-butane	8.717217%	10.111346%
isopentane	4.485868%	3.755852%
n-pentane	5.720342%	2.841874%
cyclopentane	0.566515%	0.132872%
n-hexan	6.150359%	0.834259%
cyclohexane	1.728527%	0.373549%
heptanes	14.715750%	0.153740%
methylcyclohexane	2.321627%	0.455461%
2,2,4 trimethylpentane	0.057637%	0.005366%
benzene	0.442477%	0.061007%
toluene	0.702816%	0.082497%
ethylbenzene	0.071685%	0.002748%
xylenes	0.433246%	0.027933%
octanes	2.372057%	0.050819%
nonanes	3.503362%	0.062586%
decanes plus	0.616783%	0.008577%
Formaldehyde	0.000145%	0.000006%
Acetaldehyde	0.000218%	0.000755%
Acetone	0.000000%	0.000000%
Acrolein	0.001259%	0.000673%
Propionaldehyde	0.000014%	0.000004%
Crotonaldehyde	0.000004%	0.000001%
Methacrolein/2-butanone	0.000030%	0.000008%
Benzaldehyde	0.000008%	0.000000%
Valeraldehyde	0.000042%	0.000002%
p-Tolualdehyde	0.000000%	0.000001%
Hexaldehyde	0.000005%	0.000001%
TOTAL	100.00%	100.00%

One important point for this dataset is that the total raw data contained many zeroes because some species were not represented across all the samples in the dataset. For example, 13/135 samples reported zero for their 2,2,4 trimethylpentane concentration and 15/135 reported zero for their ethylbenzene concentration. As such, the ANOSIM score for well type/sample type is low on the total data. The “Well Type – Sample Type” grouping had a score of 0.46 on the total composition data, which is interpreted as “different with some overlap.” However, it is still the highest ANOSIM score of grouping schemes with N>20 samples per group (most grouping methods with N>20 samples per group have ANOSIM score from 0.2-0.3). The reason we performed a CB6-style amalgamation/subset was to ensure that the grouping method we chose was effective in the sample space in which the data product – the speciation profile – would be applied.

This methodology, like most statistical analyses, depends on sufficiently large sample sizes for success. Too few samples per group will inflate the ANOSIM R. In the extreme case, if you have one sample per group, then the intragroup distances will all be zero and all the intergroup distances will be non-zero, which will give an ANOSIM score of 1. With this in mind, ‘well type—sample type—formation’ and ‘sample type—formation’ also show a high ANOSIM score, but these groupings do not have the N>20 sample samples per group to be needed to be valid (see METHODS). Though a major hypothesis of this study was that composition data could be grouped according to geological formation, not enough samples were collected from each group to definitively answer this question.

One solution is to focus future work on adding representative sampling from each formation so that geological formation could be added to the grouping regime. One reason to do this is the performance of the USU groupings, heretofore undiscussed in this section of the report. The USU grouping used a combination of well type and geological formation, in addition to some statistical methods of outlier rejections, to split the data into either 9 or 13 groups (some groups could either be split or combined, see REPORT C: DEVELOPMENT OF COMPOSITION SPECIATION PROFILES). The same methodology described here (see METHODS) was used to evaluate the “Well Type - Sample Type – Geologic Formation” grouping. It is the best performing grouping scheme available based on the ANOSIM score alone (ANOSIM scores range from 0.7-0.8 across the various subsets, Table D-2), but neither grouping method has enough samples per group to be valid for the ANOSIM statistic. Thus, future work could include sampling from more wells in the Uinta Basin again to provide 20 samples for each of these groups. Aside from the cost of this (would need about 135 more samples), there is compelling evidence that this is not the best approach. The geological formation categorical variable is fraught with problems, so that even if perfect samples could be collected for the study, it would be difficult to ensure that new data received from companies could be clearly classified. This is because producing formation can easily be mischaracterized. Oil resides in each formation as a result of oil migration and trapping, and is not intrinsically connected to formation except over small areas. Also, many wells are completed in multiple zones with commingled production, and this is not always reported accurately. Even when it is reported accurately, it is difficult to know the percent contribution from each formation to the final product in comingled production. The amount of oil or gas coming from each completion is not well known, and can change over time, so an unmixing of this information is impossible. As such, even if very

strong groups were created by using formation as part of the grouping, it is dubious those groups will shed much light on new unknowns.

“Company – Sample Type” is another grouping that provided a high ANOSIM score, but without enough samples per category. It would not be worthwhile to pursue this combination as a grouping method because companies will change over time, and that will make the results hard to generalize to future data. Nonetheless, it is worth speculating that the significance of this grouping method could be related to several causes. First, some companies specialize in either oil or gas production alone, making “Company– Sample Type” a similar result to “Well Type – Sample Type.” Second, some companies also produce from a specific geological formation, particularly because oil and gas companies often work based on “plays,” which are specific regions of specific basins that are known to have traps. Plays are typically related to formation, and smaller companies often only work with a single play. This grouping was examined because all oil and gas emissions inventory data are submitted on a per-company basis.

The most robust grouping to generate composite profiles of Uinta Basin oil or gas composition data is a combination of well type and sample type. These four composite profiles—Gas Well Raw Gas, Oil Well Flash Gas, Gas Well Raw Gas, and Oil Well Raw Gas—are recommended for use in photochemical modeling and other applicable analyses in the Uinta Basin. Two additional composite profiles were generated for Gas Well Flash Gas and Oil Well Flash Gas groupings that include the carbonyls data collected and analyzed by USU in REPORT C: DEVELOPMENT OF COMPOSITION SPECIATION PROFILES). These profiles are shown in Table D-4. Future work will include testing the carbonyls profiles against the non-carbonyls profiles to identify their ability to produce ozone in the photochemical model.

Discussion

One key finding from this study is that oil and gas data show a linear evolution in the simplex (Figure D-3:a). This evolution is very hard to visualize in the 23-dimensional space of the total composition data, but can be viewed in certain subsets of the data (e.g. Methane, Ethane, Propane, N-Butane). The curve seen in Figure D-3:a, and its transformation to a line in Figure D-3:b, is characteristic of straight lines in simplex space. Such a line is a straight-line geodesic with respect to the Aitchison Distance: that is, it is the shortest path through the simplex as measured by the Aitchison Distance¹⁷. Grouping based on the “Well Type – Sample Type” grouping discussed above shows that one explanation for this evolution is an evolution from “Gas Well Raw Gas” to “Oil Well Raw Gas” to “Gas Well Flash Gas” to “Oil Well Flash Gas.” The compounds show an evolution from lighter, low-carbon-number compounds in the raw gas to heavier, high-carbon-number compounds in the oil well flash gas.

Findings from this study indicate five reasons why this analysis should be the preferred method for grouping composition data:

- 1) Composition data have a complex geometry which we handle by transforming the composition data to a Euclidian space using the ILR transformation.

¹⁷ Egozcue, J.J., Pawlowsky-Glahn, V., Mateu-Figueras, G. et al. *Mathematical Geology* (2003) 35: 279. <https://doi.org/10.1023/A:1023818214614>

- 2) To test a grouping method a consistent statistic and set of criteria need to be established. For these we use the ANOSIM statistic with the requirement of ~20 samples per-group, and no groups with very few samples.
- 3) The ANOSIM statistic provides a degree of difference. Thus, future grouping methods can be evaluated against the current one. This is better than statistics which only provide binary results (this grouping scheme is or is not significant).
- 4) Oil and gas data show linear evolution trends in ILR space, which means that grouping methods will likely be unable to perfectly split the data into groups (Figure D-3). The degree of difference provided by the ANOSIM R score allows evaluation of the relative success of imperfect grouping methods.

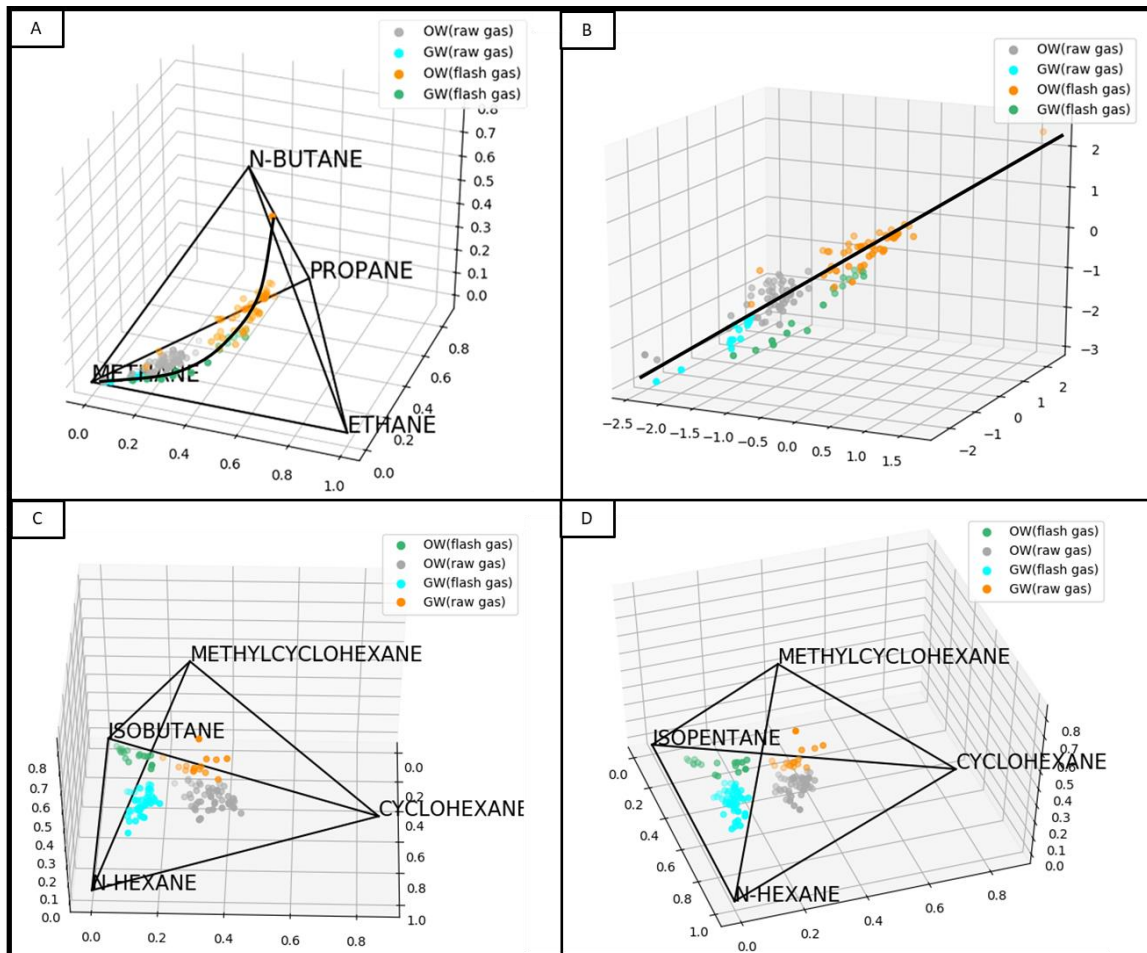


Figure D-3: A) A projection of the composition study data in to a 4D subset composition (Methane, Ethane, Propane, N-Butane). These data show a linear evolution in simplex space B) ILR transformation of A. These data make a 3D line. This suggests an evolution from the raw gas from gas wells to the flash gas from oil wells. The evolution is a trend towards higher carbon number compounds. from “Gas Well - Raw Gas” with the lowest carbon number to “Oil Well - Flash Gas” with the highest number. C-D) The plots in C and D show 4D projections where the study data do form distinct groups. This is shown to illustrate the challenges of analysis high dimensional data for groups. In the subset in A, the data show a continuous evolution, but in C and D the groups are very distinct. The reality is somewhere in between, as indicated by the ANOSIM score of 0.7 for this grouping scheme (“Well Type – Sample Type”).

Report E: Speciation Profile Comparison

Utah Division of Air Quality

Speciation Profile Introduction

The speciation profiles in this report are not the first of their kind to be developed for ozone modeling purposes in the Uinta Basin. This report summarizes these previous efforts and compares them to the profiles developed in this study (see Table E-1). For ease of comparison, we use the profiles described and developed according to

REPORT D: SUPPLEMENTAL SPECIATION PROFILE ANALYSIS rather than those in

REPORT C: MEASUREMENT OF CARBONYLS, SPECIATION PROFILE ANALYSIS, AND HIGH FLOW EMISSIONS SAMPLING & ANALYSIS, because none of the previous speciation profiles used geological formation as a grouping identifier. As such, all the profiles compared herein can be grouped according to the type of well (oil well or gas well) and sample type (flash gas/tank emissions or raw gas/other emissions). Additionally, carbonyls were not included in the speciation profiles in the figures below, because, as noted in

REPORT C: MEASUREMENT OF CARBONYLS, SPECIATION PROFILE ANALYSIS, AND HIGH FLOW EMISSIONS SAMPLING & ANALYSIS, carbonyls made up a very small percentage of the total speciation. Table E-1 describes the profiles that are compared in this report.

Table E-1: Description of Uinta Basin speciation profiles to be compared

Data Type	Count gas wells, raw gas	Count oil wells, raw gas	Count gas wells, flash gas	Count oil wells, flash gas	Data Source	Date Range	Composite Profile Technique
WRAP¹⁸	28	gas & oil wells combined	5	1	WRAP Phase III survey	before 2007	Weighted average according to gas or oil throughput by company, then column averaged by well type/sample type
TMSR¹⁹	59	gas & oil wells combined	127	66	U&O Tribal registration data mining effort - EPA R8	August 2011 to March 2015	Weighted average according to 2014 gas or oil throughput (UDOGM) by company, then

¹⁸ Memo on WRAP Phase III oil and gas speciation profiles, August 27, 2015
https://www.wrapair2.org/pdf/WRAP_P3_OG_speciation_rev27Aug2015.pdf

¹⁹ Matichuk, R., G. Tonnesen, A. Eisele, E. Thoma, Mike Kosusko, M. Strum, AND C. Beeler. Advancing Understanding of Emissions from Oil and Natural Gas Production Operations to Support EPA’s Air Quality Modeling of Ozone Non-Attainment Areas; Final Summary Report. U.S. Environmental Protection Agency, Washington, DC,

					column averaged by well type/sample type		
Data Type	Count gas wells, raw gas	Count oil wells, raw gas	Count gas wells, flash gas	Count oil wells, flash gas	Data Source	Date Range	Composite Profile Technique
DAQ Data	23	18	10	49	Composition data mined from DAQ permits, registration, inventories, other	samples taken by various labs from 2001 to 2017	Weighted average according to 2017 gas or oil throughput (UDOGM) by company, then column averaged by well type/sample type
UBCS	17	50	17	50	Uinta Basin Composition Study	November 2018 to February 2019	Averaged by well type/sample type in ILR space according to UDAQ statistical analysis of compositional data method and weighted by throughput (annual value collected from 6/2018 to 05/2019) for each well

All speciation profiles compared in this report contain data only from the Uinta Basin region of Utah. All are composite reports representing composition data from several wells, weighted by annual throughput values from UDOGM for each well in the profile. Not all throughput data correspond to the same timeframe. All profiles were made composite by completing a simple column average (averaging methane weight %, then ethane weight %, etc. from each well in the composite), except the final profiles from this study, which were averaged in the ILR space described in

EPA/600/R-17/224, 2016.

https://cfpub.epa.gov/si/si_public_file_download.cfm?p_download_id=531121&Lab=NRML

REPORT D: SUPPLEMENTAL SPECIATION PROFILE ANALYSIS.

Starting in 2007, the Western Regional Air Partnership (WRAP) began its Phase III oil and gas inventory, which included a data request for composition data that various oil and gas companies had collected. “The data are based on oil and gas companies taking Gas Chromatography/Mass Spectrometry (GC/MS) analyses of their produced gas or in some cases running models such as E&P TANK using input measured compositions (again derived from GC/MS tests of hydrocarbon liquids).”²⁹ The WRAP profiles combined raw gas composition for oil and gas wells.

From 2014 to 2016, EPA Region 8 deployed an intensive data mining project designed to extract composition data from Uintah & Ouray Tribal Minor Source Registrations (TMSR). Region 8 is currently responsible for collecting Tribal Minor Source Registrations (TSMR) for oil and gas sources located on Uintah & Ouray Indian Reservation (U&O Reservation) in the Uinta Basin. The U&O Reservation produces the majority of gas in the Uinta Basin, but registrations from oil production areas were submitted as well, and so oil-tank-versus-condensate-tank emission profiles were developed. Speciation data were mined from the tank emission estimate output provided in the registrations, and included flash as well as standing/working/breathing (SWB) emissions. The TMSR profiles also combined raw gas composition data for oil and gas wells.

In 2017, UDAQ mined its own permits for composition data reports submitted by oil and gas operators as part of their permit applications. These composition data represent the counterpart to EPA R8’s TMSR analysis for state lands in the Uinta Basin. State lands are primarily associated with oil production.

All three of these prior speciation profile developments relied on the integrity of composition data submitted by the operators and the emission estimating software used which produced the composition of the emission streams. The Uinta Basin Composition Study profiles have the benefit of being collected by the same field technician and analyzed under the same laboratory and model conditions with attention paid to consistent quality procedures to maximize the integrity of sample collection and lab analysis and using the same process simulator to estimate the emissions and their composition. While the composite profiles comprise fewer total data points than the TMSR or DAQ Permit profiles, the sample and analysis conditions are assumed to be less variable within these profiles and are more current.

Comparison

Figure E-1 shows a comparison of raw gas profiles, including 2 profiles each for the Uinta Basin Composition Study (UBCS) and UDAQ Permits – one for oil wells and one for gas wells. TMSR and WRAP profiles combined oil and gas wells into one raw gas profile each. Generally speaking, for well pad facilities, it was assumed that raw gas coming from fugitives, equipment and pipeline blowdowns, pneumatic controllers, pneumatic pumps, etc. are similar in composition. Results from the UBCS, however, indicate that raw gas from oil-producing wells are defined by higher weight percentages of VOCs and the statistical grouping discussed in REPORT D: SUPPLEMENTAL SPECIATION PROFILE ANALYSIS support grouping raw gas samples by well type.

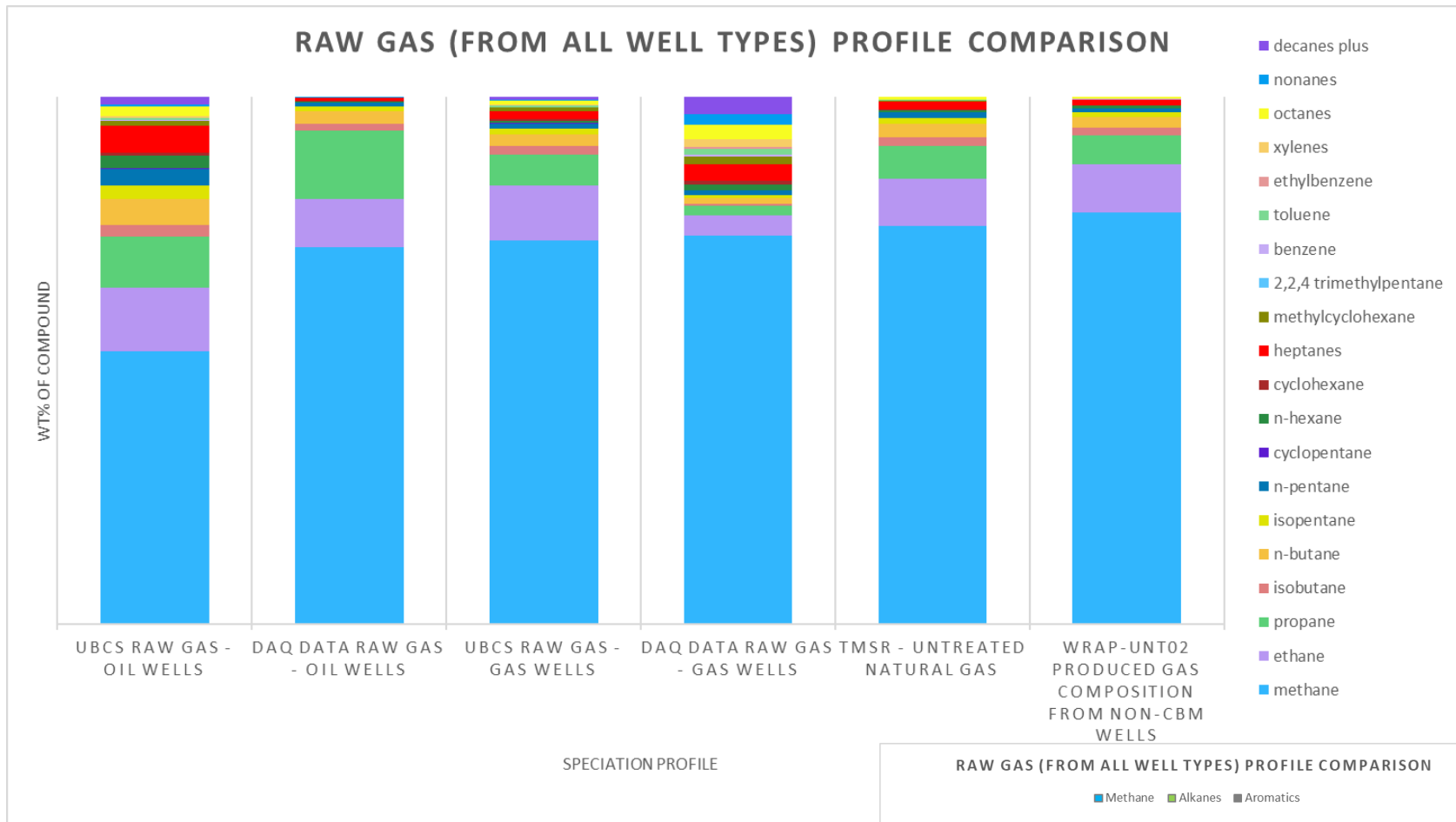


Figure E-1: Raw gas composition from both oil and gas wells in the Uinta Basin speciation profile comparison. Full speciation (above) and Methane-alkanes-aromatics (right).

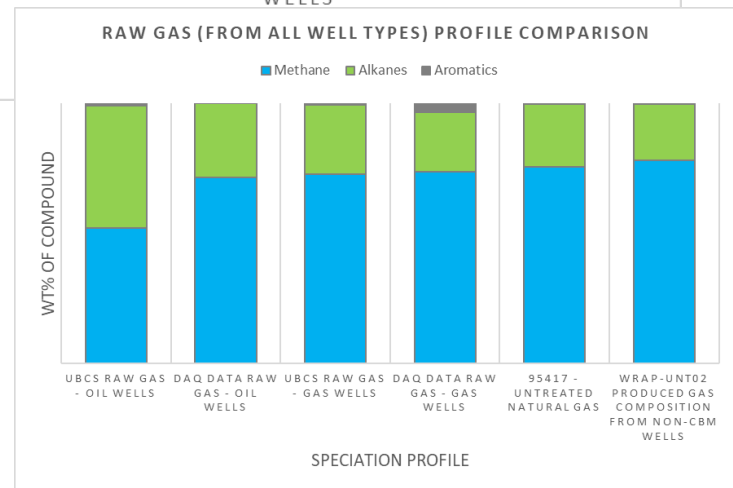


Figure E-2 compares flash gas speciation profiles derived from the four data sources discussed in this report. In the TMSR and WRAP analyses, flash gas profiles (TMSR incorporated both flash and SWB emission composition) were separated into oil and gas wells, so only oil wells are examined here. The WRAP profile on the far right stands out as dramatically different from the other flash gas profiles: this may be because the WRAP “composite” profile for flash gas wells in the Uinta Basin consisted of composition data from one well. The remaining profiles are more similar, with high contributions from heptanes and other heavier alkanes. Contributions from aromatics (BTEX) remain small relative to other compounds in the profiles.

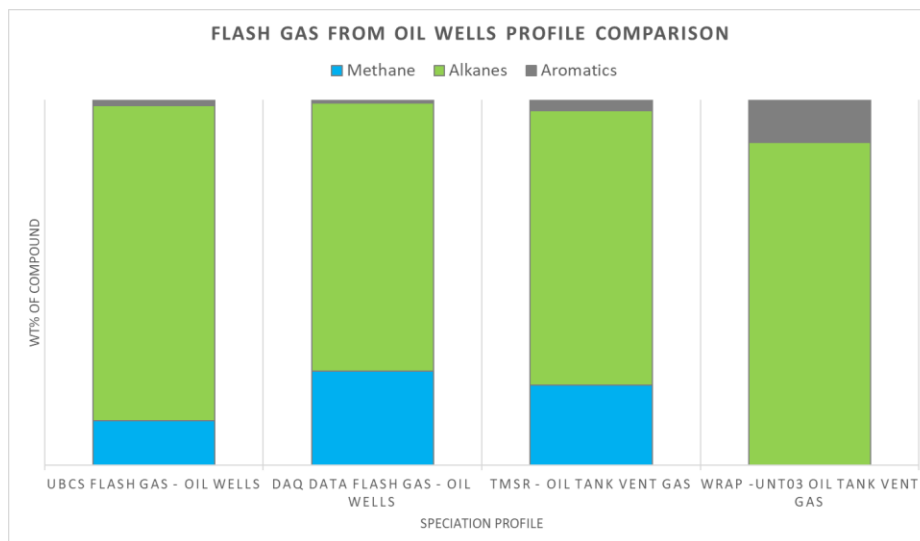
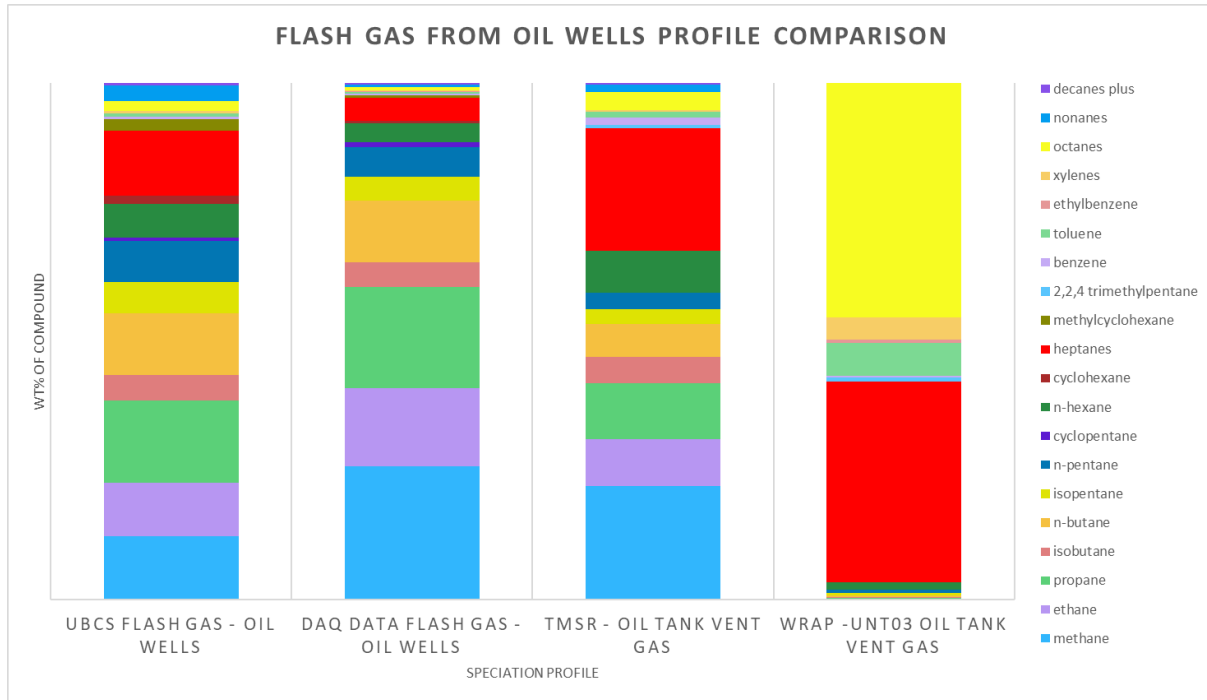


Figure E-2: Flash gas composition from oil wells in the Uinta Basin speciation profile comparison. Full speciation (top) and Methane-alkanes-aromatics (bottom).

Figure E-3 compares flash gas from gas-producing wells in the Basin. The WRAP profile stands out again, and this profile comprises only 5 wells. The remaining profiles all primarily consist of C1-C3. Flash gas from gas wells are notably different than flash gas from oil wells; gas well flash gas tends to have smaller percent of heavier alkanes.

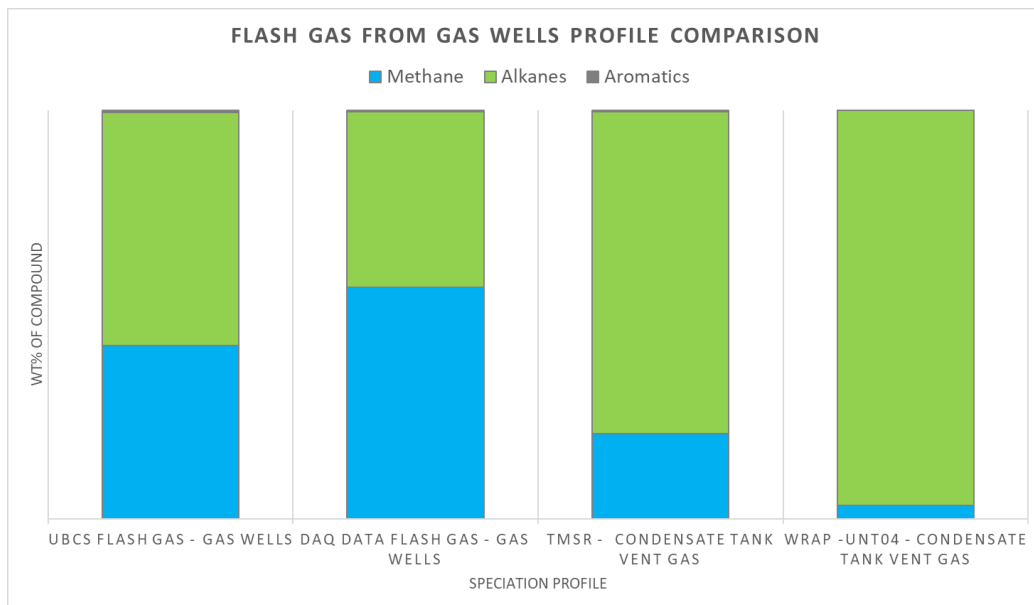
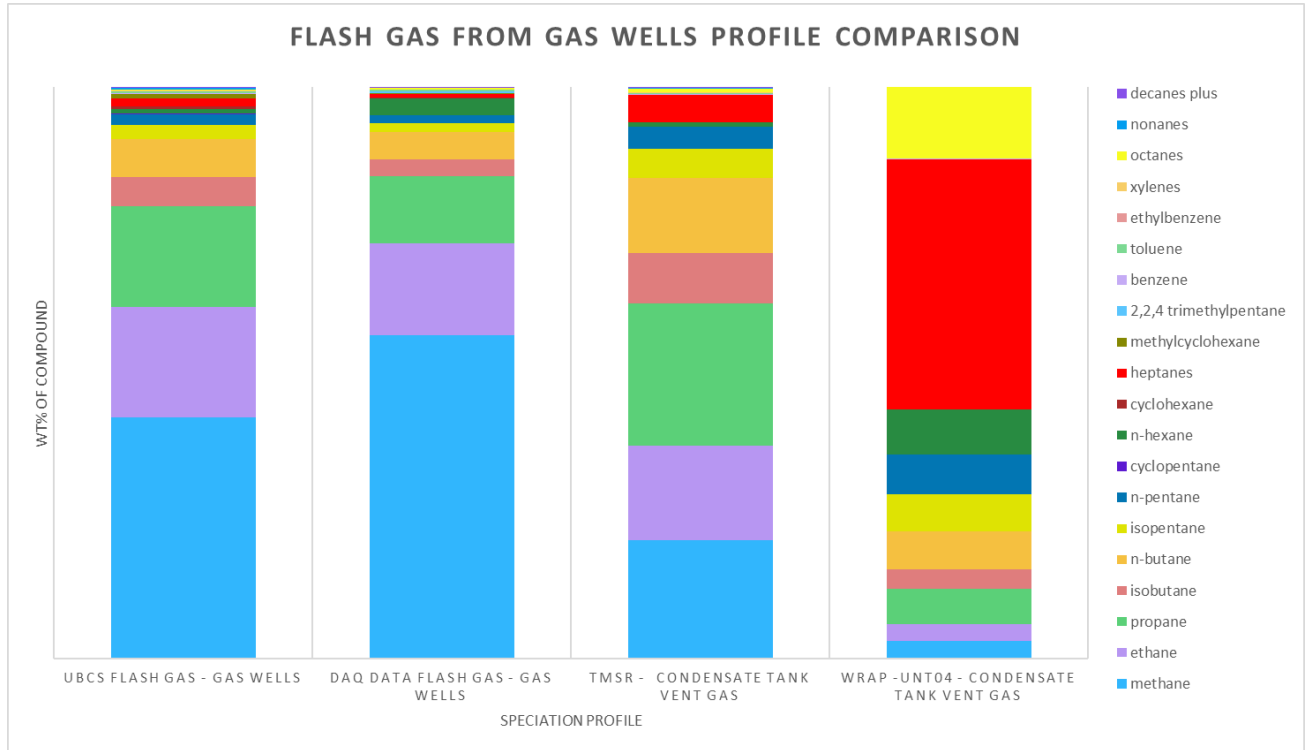


Figure E-3: Flash gas composition from gas wells in the Uinta Basin speciation profile comparison. Full speciation (top) and Methane-alkanes-aromatics (bottom).

Visual comparison of these various speciation profiles helps us understand how they differ in their compositions, but as stated earlier the UBCS profiles have the advantage of consistency of pressurized liquid sample collection and analysis and using the same process simulator software and is the most contemporaneous data set. One goal of this project was to determine which profiles are able to best model the observed ozone in the Uinta Basin. A quick way to look at ozone creation propensity is to adjust each compound in the profile for its MIR, as was done in REPORT C: [DEVELOPMENT OF COMPOSITION SPECIATION PROFILES](#). A complete photochemical model sensitivity test, however, will be required to determine the appropriate profiles for ozone modeling in the Uinta Basin. That work is scheduled to begin in 2020.

Report F: Verification Sampling

Alliance Source Testing

The top half of the page features a background image of an industrial facility, likely a refinery or chemical plant, with several tall distillation columns and complex piping. The sky is a mix of blue and orange, suggesting a sunset or sunrise. Overlaid on the left side of this image is the Alliance Source Testing logo, which consists of the word "Alliance" in a large, bold, white sans-serif font with a stylized flame icon above the 'i'. Below "Alliance" is the text "SOURCE TESTING" in a smaller, all-caps, white sans-serif font.

Alliance
SOURCE TESTING

Uinta Basin Report II

Utah Division of Air Quality

195 North 1950 West

Salt Lake City, Utah

Test Dates:

June 2019

Summary

Summary

Uinta Basin Composition Study - Verification Sampling - Purpose

The purpose of the study extension was to compare the FGOR values and flash gas compositions resulting from VMG model predictions to the physically measured FGOR and flash gas composition values. Five (5) pressurized waxy crude oil samples with respectively high FGOR values were chosen from a subset of the wells originally sampled for this portion of the study. The extended liquid composition results from the samples were input into the VMG software model to produce the theoretical FGOR and flash gas composition values. In a separate experiment, the liquid samples were conditioned to separator temperature and pressure and physically flashed into a closed vessel at storage tank temperature and atmospheric pressure. The FGOR values were derived by physically measuring the volumes of the flashed gas. The composition of the flash gas was determined using a gas chromatograph.

Alliance Source Testing (AST) utilized the analyses shown in Table F-1. Section 2 provides a more comprehensive presentation and discussion of the testing methodology.

TABLE F-1
TESTING METHODOLOGY

Parameter	GPA Test Methods	Notes/Remarks
Pressurized Liquid Collection	GPA 2174	Obtaining Liquid Hydrocarbon samples
Flash Gas Composition	GPA 2286	Extended Gas Analysis by Gas Chromatography
Pressurized Liquid Composition	GPA 2103M/2186M	Extended Liquid Hydrocarbon Analysis by Gas Chromatography
Simulated Flash Gas Composition & FGOR	NA	VMG – EOS/PSM
Physically Measured FGOR	NA	AST Modified Flash

Results

Table F-2 shows the FGOR results from the physical experiment and the VMG model. Tables F-3 (WT%) & F-4 (MOL%) show the flash gas component concentrations from the extended GC analysis and the VMG model. The nitrogen was removed from the extended liquid analysis that was input into VMG based on the Noble Energy Pressurized Hydrocarbon Liquids Sampling and Analysis Study²⁰ recommendations that nitrogen is most likely a sampling artifact, therefore no nitrogen is present in the VMG predicted flash gas composition.

²⁰ https://noblecolorado.com/wp-content/uploads/2018/12/SPL_PHLA-Study_Final-Report_020718.pdf

TABLE F-2
FLASH GAS TO OIL RATIO COMPARISONS

Sample	Physically Measured FGOR (scf/bbl)	VMG Predicted FGOR (scf/bbl)
VII-7	27.8	32.7
VII-9	35.8	42.8
V-3	12.8	15.7
V-4	39.7	46.3
V-6	44.4	55.6

TABLE F-3
FLASH GAS COMPONENT CONCENTRATION COMPARISONS

WT% Comparisons										
COMPONENT	Well - F		Well - D		Well - J		Well - M		Well - O	
	GPA – 2286 (MOD- FLA)	VMG- Ver								
	WT%	WT%								
CARBON DIOXIDE	1.6006	0.8183	1.4356	0.5637	1.1111	0.6813	1.7562	1.5284	1.9953	0.6200
NITROGEN	1.2709	0.0000	1.8108	0.0000	1.4924	0.0000	1.6996	0.0000	2.8619	0.0000
METHANE	21.1644	7.4341	24.9399	6.2074	39.5462	18.1884	21.0902	9.0082	26.6431	7.2600
ETHANE	20.6420	7.9974	20.6035	7.1391	18.9435	10.9771	21.6398	9.5855	20.6041	8.1674
PROPANE	24.5392	14.4977	20.9808	11.7560	18.0389	14.4887	24.4625	15.2860	20.8442	13.4258
ISOBUTANE	6.0881	4.0759	4.9014	4.4260	4.0309	4.6508	4.4147	3.6337	4.3751	4.6308
N-BUTANE	11.5176	13.9312	9.8404	11.8047	6.6500	9.9152	11.0706	13.5570	9.1302	12.6612
ISOPENTANE	2.7009	5.1340	3.5698	6.6210	2.3240	4.8592	2.6875	4.5950	3.0018	6.4090
N-PENTANE	4.5492	10.4665	4.5745	10.2444	2.4936	6.1902	4.6636	9.4726	3.8542	9.8644
CYCLOPENTANE	0.1856	0.5506	0.1315	0.4032	0.1606	0.4946	0.1956	0.5004	0.1195	0.4013
N-HEXANE	1.7430	8.6914	2.0297	9.0522	1.0340	5.1455	1.9814	7.3241	1.7657	8.0354
CYCLOHEXANE	0.3102	1.7716	0.3020	1.6267	0.2573	1.4743	0.3333	1.5880	0.2919	1.6247
"HEPTANES"	2.3404	16.2355	3.2763	20.8155	2.3904	14.5020	2.6177	17.0448	2.8971	18.4568
METHYLCYCLOHEXAN E	0.2989	2.0825	0.3331	2.2737	0.2909	1.8469	0.3116	1.8282	0.3210	2.1089
2,2,4 TRIMETHYLPENTANE	0.0003	0.0174	0.0003	0.0264	0.0006	0.0392	0.0003	0.0251	0.0002	0.0232
BENZENE	0.0740	0.3527	0.1103	0.5061	0.0384	0.1394	0.0812	0.3069	0.0918	0.4565
TOLUENE	0.0716	0.5409	0.1137	0.8536	0.0549	0.3864	0.0767	0.5056	0.1704	1.2681
ETHYLBENZENE	0.0038	0.0375	0.0039	0.0392	0.0056	0.0527	0.0037	0.0357	0.0042	0.0352
XYLENES	0.0326	0.3043	0.0439	0.4495	0.0422	0.3152	0.0330	0.2921	0.0424	0.4005
OCTANES	0.4788	1.4355	0.5765	1.9249	0.5005	1.9636	0.4921	1.4956	0.5422	1.5859
NONANES	0.1166	3.2661	0.1303	2.9066	0.1376	3.3180	0.1177	2.1206	0.1310	2.2948
DECANES+	0.2715	0.3591	0.2916	0.3602	0.4565	0.3714	0.2713	0.2665	0.3125	0.2699

TABLE F-4
FLASH GAS COMPONENT CONCENTRATION COMPARISONS

MOLE% Comparisons										
COMPONENT	Well - F		Well - D		Well - J		Well - M		Well - O	
	GPA – 2286 (MOD-FLA)	VMG- Ver	GPA – 2286 (MOD- FLA)	VMG- Ver	GPA – 2286 (MOD-FLA)	VMG- Ver	GPA – 2286 (MOD-FLA)	VMG- Ver	GPA – 2286 (MOD-FLA)	VMG- Ver
	MOLE %	MOLE %	MOLE %	MOLE %	MOLE %	MOLE %	MOLE %	MOLE %	MOLE %	MOL%
CARBON DIOXIDE	1.1688	0.9445	1.0009	0.6965	0.6489	0.6075	1.2753	1.6576	1.3470	1.9953
NITROGEN	1.4578	0.0000	1.9833	0.0000	1.3694	0.0000	1.9389	0.0000	3.0352	2.8619
METHANE	42.3946	23.5382	47.6985	21.0421	63.3633	44.4900	42.0128	26.8005	49.3410	26.6431
ETHANE	22.0602	13.5097	21.0234	12.9113	16.1937	14.3255	22.9989	15.2149	20.3578	20.6041
PROPANE	17.8831	16.7002	14.5985	14.4981	10.5153	12.8936	17.7288	16.5453	14.0438	20.8442
ISOBUTANE	3.3660	3.5620	2.5874	4.1411	1.7826	3.1400	2.4273	2.9839	2.2364	4.3751
N-BUTANE	6.3679	12.1748	5.1946	11.0449	2.9409	6.6942	6.0870	11.1326	4.6669	9.1302
ISOPENTANE	1.2030	3.6144	1.5181	4.9905	0.8280	2.6428	1.1904	3.0397	1.2361	3.0018
N-PENTANE	2.0262	7.3687	1.9453	7.7216	0.8884	3.3668	2.0657	6.2664	1.5871	3.8542
CYCLOPENTANE	0.0850	0.3987	0.0575	0.3126	0.0589	0.2767	0.0891	0.3405	0.0506	0.1195
N-HEXANE	0.6500	5.1230	0.7227	5.7124	0.3084	2.3431	0.7348	4.0565	0.6087	1.7657
CYCLOHEXANE	0.1184	1.0692	0.1101	1.0511	0.0786	0.6874	0.1266	0.9006	0.1030	0.2919
"HEPTANES"	0.8286	8.2015	1.1108	11.2576	0.6842	5.6595	0.9234	8.0906	0.9489	2.8971
METHYLCYCLOHEXANE	0.0978	1.0773	0.1041	1.2593	0.0761	0.7381	0.1014	0.8887	0.0971	0.3210
2,2,4 TRIMETHYLPENTANE	0.0001	0.0077	0.0001	0.0126	0.0001	0.0135	0.0001	0.0105	0.0001	0.0002
BENZENE	0.0304	0.2293	0.0433	0.3523	0.0126	0.0700	0.0332	0.1875	0.0349	0.0918
TOLUENE	0.0250	0.2982	0.0379	0.5038	0.0153	0.1646	0.0266	0.2619	0.0549	0.1704
ETHYLBENZENE	0.0011	0.0179	0.0011	0.0201	0.0014	0.0195	0.0011	0.0160	0.0012	0.0042
XYLENES	0.0099	0.1456	0.0127	0.2303	0.0102	0.1165	0.0099	0.1313	0.0119	0.0424
OCTANES	0.1354	0.6355	0.1555	0.9114	0.1133	0.6656	0.1383	0.6219	0.1417	0.5422
NONANES	0.0293	1.2753	0.0313	1.2139	0.0277	0.9983	0.0295	0.7774	0.0305	0.1310
DECANES+	0.0614	0.1082	0.0629	0.1165	0.0825	0.0868	0.0610	0.0755	0.0653	0.3125

Testing Methodology

Testing Methodology

The testing program was conducted in accordance with the test methods listed in Table F-1. Method descriptions are provided below.

GPA 2174: Obtaining Liquid Hydrocarbon Samples for Analysis by Gas Chromatography

Samples were collected from a location (e.g., sample probe, sight glass fitting) with routine oil circulation to avoid collecting stagnate HC liquids from the bottom of the separator. Several of the samples were collected from a sample port on the oil leg upstream of the dump valve on the heater treater. A sample collection rate of 60 ml/min or less (start sample collection at a slow rate and increase to target sampling rate) was used for all sampling. The sample collection temperature and pressure were monitored and recorded at the start and conclusion of each sample collection event using highly calibrated gauges on the sample probe. No anomalous pressure changes occurred during the sampling. All samples were collected in constant pressure cylinders. The sample probe was completely purged with the pressurized oil before introduction of the liquid into the cylinder. The cylinders were filled to approximately 80% volume. An onsite compressibility check was performed by pressurizing the back-pressure side of the cylinder with helium after the cylinder was filled to ensure that an unseen gas plug was not introduced into the sample. None of the samples compressed to any extent. The probe assembly and constant pressure cylinders were kept around 70°F until the sampling occurred.

The separator pressure and temperature were measured using a sample probe with highly accurate gauges. The approximate time of the last dump cycle was recorded. The beginning and end time of the sampling event was recorded. The storage tank temperature was recorded for the waxy crude samples that required heated storage tanks. Well names, probe pressure, probe temperature, gauge pressure, gauge temperature, ambient conditions, sample times, sampler's initials, dates, number of tanks onsite, and any important sampling notes or changes were recorded.

GPA 2286: Method for the Extended Analysis of Natural Gas and Similar Gaseous Mixtures by Temperature Programmed Gas Chromatography

The flash gas samples were analyzed on a GC equipped with a flame ionization detector (FID) and a thermal conductivity detector (TCD). The GC was calibrated with several certified external standards and response factors for both detectors were determined. The required components measured were C1-C10, N₂, O₂, CO₂, and BTEX. The flash gas was extracted from the flash gas collection vessel (Tedlar bag) and introduced into the GC sample loop at a constant purge rate. The gas in the sample loop was allowed to relax to atmospheric pressure before injection into the GC. The gas concentrations were reported in mole % and mass %.

GPA 2103M/2186M: Tentative Method for the Analysis of Natural Gas Condensate Mixtures Containing Nitrogen and Carbon Dioxide by Gas Chromatography

The pressurized liquid sample analysis was done by an AST modified version of GPA 2103M/2186M. Modifications were made to the laboratory instrumentation for the analysis of the pressurized waxy crude oil. AST added a heat traced network of tubing to the gas chromatograph's (GC) plumbing. Heat traced tubing temperatures were set to the temperature of the well's heated storage tank to guarantee the sample was a flowing liquid right before injection but not hot enough to become two phases (gas/liquid) in the plumbing. The methodology modifications included an ASTM D7169 simulated distillation analysis to extend the report to C36+, an ASTM D6730 detailed hydrocarbon analysis on the flame ionization detector (FID) for improved speciation, the thermal conductivity detector (TCD) analysis was C1 - C6+ and CO₂ with the air removed, and the C10+ molecular weight and density fractions were calculated from the GC analysis.

The waxy crude liquid samples were heated to the storage tank temperatures, pressurized to 1000 psig, and injected on the GC. The C1 - C6+ and CO2 concentrations were measured on the TCD. The C6+ peak on the TCD is back flushed. A calibration curve and response factors for C1 - C5 and CO2 were established on the TCD using a pressurized 'natural' liquid calibration standard made from a sample in the DJ Basin. The C1 - C5 and CO2 sample concentrations were determined by multiplying the sample peak areas and the individual response factors from the calibration curve. The C6 - C10 concentrations are determined by an ASTM D6730 detailed hydrocarbon analysis run on the FID. A small amount of the pressurized liquid was flashed, diluted with carbon disulfide, and run on a second GC-FID by ASTM D7169. The ASTM D7169 simulated distillation run extended out to C100 and allowed the final report to be extended to C36+.

Flash Gas Composition by VMGThermo EOS/PSM

VMGThermo was used to determine the flash gas composition, Reid Vapor Pressure (RVP) & API gravity of flashed liquids, and FGOR from the pressurized liquid. Using VMGThermo's Advanced Peng Robinson and Advanced Peng Robinson for Natural Gas 2 property packages the calculations were performed for reporting purposes and quality assurance checks (bubble points) of laboratory analysis.

Using VMGThermo's advanced fluid characterization methodology, PIONA, the complete fluid could be modeled accurately from the pure component 'light ends' through the carbon number analysis to C36+. VMGThermo was then used to flash the fluid to storage tank conditions which determined the flash gas composition, and various properties of the flashed liquid.

Flash Gas to Oil Ratio - Modified Physical Flash

A modified setup was used to physically measure the FGOR since the typical instrumentation used per guidance in Colorado Department of Public Health & Environment Policy Memo 17-01, "Flash Gas Liberation Analysis Method for Pressurized Liquid Hydrocarbon Samples", flash liberation analysis can be easily clogged by the waxy crude oil samples. The pressurized oil sample, contained in a floating piston cylinder, was heated to the measured separator temperature for a minimum of one (1) hour. The conditioned oil was then released into a zero-volume flexible flash vessel at storage tank temperature and pressure. A water bath was used to heat the flash vessel to the storage tank conditions. The oil was allowed to flash at atmospheric pressure and storage tank temperature for one hour. The pressure in the lab was within 0.1 psi of the atmospheric pressure in the field. The actual cf/bbl was determined by measuring the mass and density of the oil and the volume of the gas. The actual cf/bbl was converted to scf/bbl for the FGOR determination.

Report G: Process Simulator Comparison and Analysis

Utah Division of Air Quality

The estimation of flash gas composition and FGOR is a key exercise in characterizing air emissions from atmospheric tanks at upstream oil and gas facilities. These emission estimates are often a requirement for obtaining air permits from State, Federal, and Tribal air agencies, determining regulatory applicability, and creating emission inventories. Emission inventories, and the speciation of those emissions, are critical for photochemical ozone modeling to support pragmatic, effective policy analysis. As such, this study sought to explore the various methodologies used by industry and laboratories to obtain these tank emissions characteristics, and to assist operators in obtaining high integrity data for their air permit applications.

There is currently no standardized methodology for the analysis of flash gas. Laboratories often refer to PS Memo 17-01 from the Colorado Department of Public Health and Environment, Flash Gas Liberation Analysis Method for Pressurized Liquid Hydrocarbon Samples²¹. Both Utah State University's lab and Alliance Source Testing used this method for analyzing flashed gas as part of this study.

However, due to the highly viscous and waxy nature of Uinta Basin crude oil, the instrumentation typically deployed for flash gas analysis often becomes blocked as the crude solidifies in unheated conditions, bringing into question the certainty of the flash gas characterization results. Noting this, AST and four other laboratories contacted as part of the initial contracting for this study, suggested that flash gas characteristics be estimated using a Process Simulation Model that employs an Equation of State (EOS/PSM). AST took precautions, as discussed in Report A and F, to prevent such solidifying. In this discussion, analysis performed according to PS Memo 17-01 will be referred to as "physical flash," while use of any EOS/PSM will be referred to as "modeled flash." Table G-1 identifies the cases compared in this report. The goal of this analysis is to examine differences between flash gas composition, FGOR, and VOC weight percent among several modeled and physical flashes from the same 5 oil wells described in Report F. These 5 wells were selected for resampling because initial testing yielded very large FGOR values for oil-producing sites and so warranted additional analysis. These are waxy-crude wells, which may cause EOS/PSM to respond differently than less viscous condensate, such as those modeled in the Noble Energy Pressurized Hydrocarbon Liquids Sampling and Analysis Study (2018)²². This report is focused on comparing estimating methods for tank emissions specifically from waxy crude oil production sites, because the subset of 5 wells resampled for verification fall into this category.

²¹ <https://www.colorado.gov/pacific/sites/default/files/AP-Memo-17-01-Flash-Gas-Liberation-Analysis.pdf>

²² Pressurized Hydrocarbon Liquids Sampling and Analysis Study Data Assessment and Analysis Report. Southern Petroleum Laboratories, 2018. https://noblecolorado.com/wp-content/uploads/2018/12/SPL_PHLA-Study_Final-Report_020718.pdf

Table G-1: EOS/PSM Description table

Case	EOS/PSM	Data Source	Description
VMG Results - Ver	VMGSim	Verification Sampling	“[VMGSim] is a general process simulator and possesses a complete suite of process unit operations. VMGSim can characterize hydrocarbon systems containing a quantity of undefined fractions using recently integrated PIONA Characterization. For hydrocarbon systems, a good default selection of an equation of state is VMGSim’s Advanced Peng-Robinson (APR).” ²³
VMG Results - HC	VMGSim	Subset of Hydrocarbon Sampling - same wells sampled in "Verification Sampling", but different sample date and operational parameters	
PROMAX	ProMax	Verification Sampling	“ProMax is the process simulator developed by Bryan Research and Engineering, employing both Peng-Robinson and SRK equation of state options. Process information is entered into a process simulation which then calculates the amount and composition of vapors generated upon equilibrium flash to atmospheric pressure at the measured tank temperature. From those vapors, the propane and heavier hydrocarbons are summed to yield the tank flash VOC emissions in tons per year.” ²⁴
CEL	Clearstone Engineering proprietary EOS/PSM	Verification Sampling	“The CEL process simulator was developed for use in a variety of engineering analysis tools; especially where computationally intensive simulations are being performed that require access to low-level flash routines. The software features a selection of equations of state to suit different categories of fluids (e.g., hydrocarbon systems, steam and water, and refrigerants). The Peng-Robinson (PR) and Peng-Robinson Volume Translated (PR-VT) equations of state are implemented for determining the two-phase (vapor-liquid) equilibria and thermo-physical properties of hydrocarbon systems. Hydrocarbon mixtures up to C30 (n-triacontane) can be modelled.” ²⁵

²³ Reservoir Fluid Characterization and PVT Analysis in VMGSim. Herbert Loria. VMG Calgary.

<https://virtualmaterials.com/files/galleries/ReservoirFluidAnalysis.pdf>

²⁴ Air Emissions Modeling Advances for Oil and Gas Production Facilities. Barry L. Burr and Adam M. Georgeson.

<https://www.bre.com/PDF/Air-Emissions-Modeling-Advances-for-Oil-and-Gas-Production-Facilities.pdf>

²⁵ Email, Dave Picard M.Eng., P.Eng. Clearstone Engineering Ltd. November 6th, 2019.

Case	EOS/PSM	Data Source	Description
E&P Tanks	API's E&P Tanks Version 2*	Verification Sampling	E&P TANK uses the Peng-Robinson equation of state to calculate flash loss. The working and standing losses are simulated differently depending upon the nature of the tank. For oil production tanks, the working and standing losses are represented by a distillation column operation, either of which will generate a certain amount of vaporization so that the characteristics of the produced liquid matches the sales oil specifications such as Reid Vapor Pressure (RVP). In addition, a modified AP-42 method may be used instead of the distillation column method for calculating working and standing losses from oil production tanks.
Mod-FLA	none - physical flash	Verification Sampling	The modified physical flash is described in REPORT F: VERIFICATION SAMPLING in subsection "Flash Gas to Oil Ratio – Modified Physical Flash"
VBE	Vasquez-Beggs equation	For “ VBE (VMG-Ver) ”, used VMG-Ver estimated flash gas molecular weight and VOC wt% OR For “ VBE (Mod-Fla) ”, used Mod-Fla measured flash gas molecular weight and VOC wt%	The Vasquez-Beggs equation calculates tank losses as total VOC's from flashing (unlike other estimation tools, which speciate flash gas) and FGOR. VBE does not estimate SWB emissions. VBE is a free alternative to EOS/PSM estimation of flash gas emissions. Its inputs are listed in Table G-3.
Permit	unknown	Permit application lab report	The composition report attached to UDAQ's permit file for this well did not specify whether the flash gas composition was physically measured or modeled.

** as of 12/31/18, API discontinued the sale of E&P Tanks, and no new licenses for the software will be issued. Issues with installing the software will not be supported after 3/31/19.*

The various process simulators compared in this report were chosen based on their availability to UDAQ and their prevalence and usage by the oil and gas community. VMG is the process simulator used by AST to simulate flash gas composition, FGOR, and also estimate the API gravity of the sales oil since this was not sampled contemporaneously. VMG was used on the initial 78 pressurized liquid samples (“Hydrocarbon Sampling”) and the additional 5 pressurized liquid samples (“Verification Sampling” – see PROJECT ORGANIZATION AND REPORTS). ProMax is another sophisticated process simulator similar to VMG. EPA R8 sent the results from “Verification Sampling” and associated operational parameters for the 5 wells to Clearstone Engineering (CEL) to analyze with their proprietary process simulator. E&P Tanks is a process simulator provided by the American Petroleum Institute (API) and was widely used by operators for Oil and Gas Emissions Inventory submissions, but the sale of this EOS/PSM has been discontinued since 2019. UDAQ used a Vasquez-Beggs calculation spreadsheet to estimate FGOR and VOC emissions in tons per year for the 5 “verification sampling” wells. The Vasquez-Beggs calculations

are explored in more detail in COMPARISON OF VASQUEZ-BEGGS EQUATION & AP-42 TANK EMISSIONS ESTIMATIONS. UDAQ had a laboratory composition report on file associated with the permitting process for one of the 5 wells sampled in “verification sampling”, but it is unknown whether results of the report were modeled or physically sampled. The “Permit” results are included here as a representative sample of operator-submitted composition data as part of the permit application process. Mod-FLA is the physically measured flash gas composition and FGOR data point (this is labeled as GPA-2286 in Tables F-3 and F-4 in AST’s REPORT F: VERIFICATION SAMPLING). Methods to obtain physically flashed data are described in REPORT F: VERIFICATION SAMPLING.

Comparison of EOS/PSM Tank Emissions Estimations

Generally speaking, all process simulation test cases were set up in the following manner: pressurized liquid composition data from AST’s laboratory results were added as a stream from the separator to the stock tank (oil or condensate tank), and to model the heated oil tanks, the tank was virtually heated by adding a heat stream to the stock tank. The “heat” stream is especially important for modeling Uinta Basin flash gas composition and FGOR from the waxy crude oil tanks; this ensures that the model can accurately estimate flash emissions coming from a heated tank. All EOS/PSM used the Peng-Robinson equation of state to model the secondary flash associated with temperature increase from the separator to the stock tank. Other inputs are shown in Table G-2.

Flash gas composition is one of the model outputs (flash gas coming from tank), alongside API gravity and Reid Vapor Pressure (of the flashed stock tank oil or condensate) and FGOR (calculated). See Figure G-1.

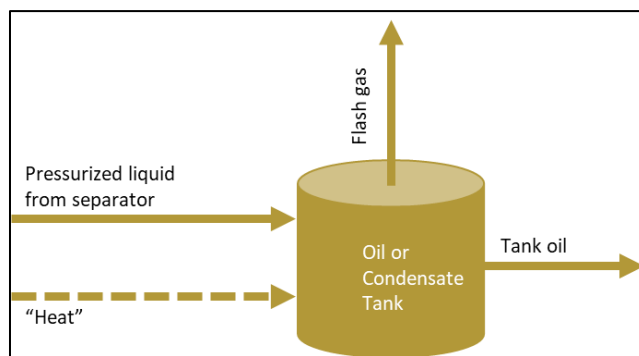


Figure G-1: Typical EOS/PSM configuration for upstream flash gas composition and FGOR estimation.

Process simulators, like any model, produce more certain results when the inputs to the EOS/PSM are also highly certain. AST used high-accuracy, and calibrated, pressure and temperature gauges when sampling from the separator at each well visited in the Uinta Basin, delivering temperatures within ± 0.1 °F and pressures within ± 0.2 psi. The highly-accurate gauges were only applied to the separator, and tank temperatures were read from the tank gauge installed on heated oil or condensate tanks at the well pad. These tank temperature gauges are exposed to constant outdoor conditions in the Uinta Basin, and the certainty of the temperature reading may vary greatly from tank to tank. Pressure of the oil or condensate tank was assumed to be atmospheric.

API gravity and Reid Vapor Pressure (RVP) describe the physical nature of the stock tank oil. These two values were not physically measured as part of this study, due to the difficulty of measuring waxy crude in the laboratory and budget constraints. API gravity and RVP can be estimated using the same EOS/PSM that estimated flash gas composition. Further work is needed to explore whether concurrent API gravity/RVP measurements would improve the accuracy of EOS/PSM flash gas composition estimation.

Input parameters for EOS/PSM test cases are outlined in Table G-2 below. “Prod Rate” (rate of production) is listed in barrels per day and sourced from UDOGM. The rate of production only influences the emissions rate outputs, such as the flow rate of VOCs in tons per year from a given tank. The production rate is an average daily value calculated from the production reported during the month the samples were collected.

Table G-2: Process simulator input parameters

Verification Sampling (VMG-Ver, ProMax, CEL, and E&P Tanks)	Well-ID	Separator T (F)	Separator P (psi)	Tank T (F)	Tank P (psia)	Prod Rate (bbl/day – avg May 2019)
	VII-7	140	59.5	160	12.1	17.77
	VII-9	145	79.1	170	12.1	62.87
	V-3	133	56	160	11.9	15.61
	V-4	129	76.1	160	11.9	36.23
	V-6	122	78.4	170	11.9	33.55
HC Sampling (VMG-HC)	Well-ID	Separator T (F)	Separator P (psi)	Tank T (F)	Tank P (psia)	Prod Rate (bbl/day - avg Jan 2019)
	VII-7	137	67.5	158	12.3	16.32
	VII-9	143	75.9	163	12.3	41.67
	V-3	144	54.8	165	11.9	18.03
	V-4	133	81.7	164	11.9	38.52
	V-6	111	80.4	168	12	23.35
Permit (V-3 Well only)	Well-ID	Separator T (F)	Separator P (psi)	Tank T (F)	Tank P (psia)	Prod Rate (bbl/day – avg April 2013)
	V-3	160	38	160	14.65	207.90

The VOC weight percent of flash gas emissions, Flash Gas to Oil Ratio (FGOR), and Flash Gas VOC emission rate in tons per year (TPY) are useful metrics to determine the potential air quality impact of a given air emissions source. These metrics will be referenced throughout the remainder of this report as variables impacted by different EOS/PSM scenarios and inputs.

Flash emissions with higher VOC content are assumed to have a higher propensity to produce ozone than flash emissions with smaller VOC weight percentages. Pressurized liquids measurements from AST for the 5 verification wells were entered into several EOS/PSM (VMG, ProMax, CEL, and E&P Tanks), and

are compared to the modified physical flash (Mod-Fla) and permit in Figure G-2. The physical flash (Mod-FLA) consistently shows the lowest VOC weight percent for the 5 wells, while various EOS/PSM produced similar, and significantly higher than Mod-FLA, VOC weight percentages. VMG flash gas VOC weight percentages from the original hydrocarbon sampling campaign (VMG-HC) are also displayed in Figure G-2. Flash gas estimates from the same well and under the same simulation (VMG) produced slightly different results. It should be noted that there may have been a loss of temperature to the sample after FGOR was measured and as the flashed gas sample was walked over to the GC instrument to obtain the flash gas composition. It is possible that some of the gas phase constituents moved back to the solid phase during this temperature loss and were therefore not analyzed in the GC as flash gas constituents. Additional comparative analysis between physically measured and modeled flash gas from Uinta Basin heavy crude would reveal more about potential EOS/PSM biases.

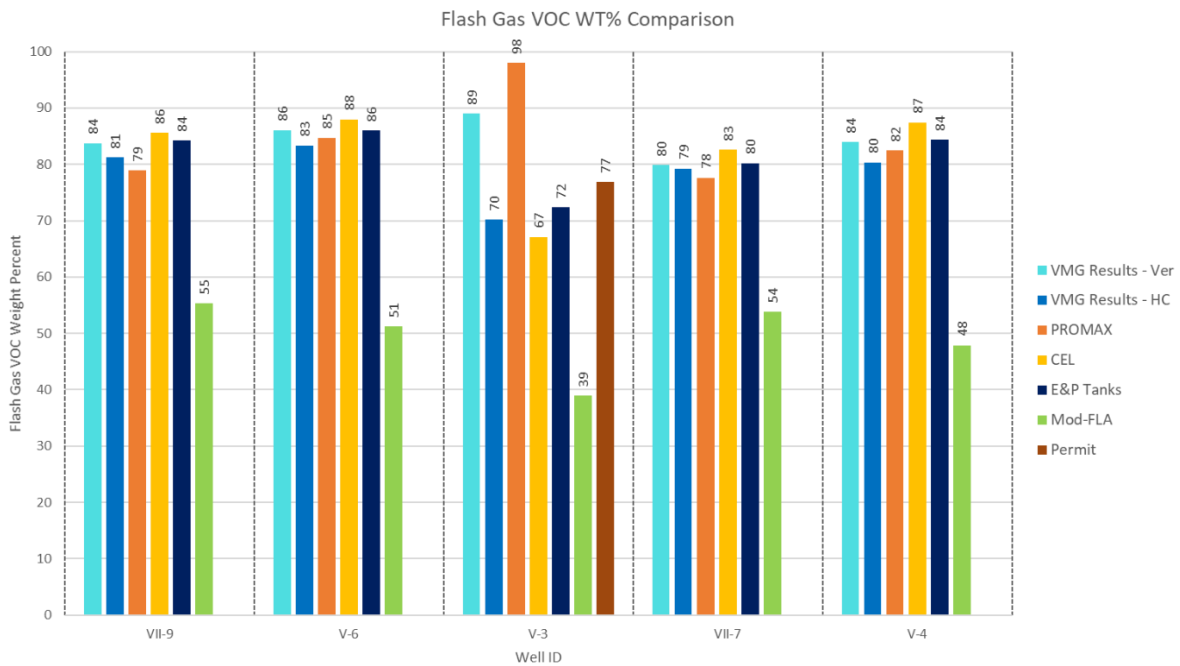


Figure G-2: Percent of flash gas consisting of VOCs according to various flash gas simulations or physical measurements.

FGOR calculations from modeled and physical measurements are also compared for the 5 verification wells (Figure G-3). Engineers use FGOR to calculate emission rates as part of the air permitting process. Many submissions to the Utah Air Agencies Oil and Gas Inventory cited the Vasquez-Beggs Equation (VBE) as their VOC emissions estimation tool, so VBE was also compared in this analysis (Figure G-3). VBE was employed twice; once with inputs from VMG modeling of flash emissions for the 5 verification wells (“VMG-Ver”), and second with inputs from the modified physical flash performed by AST (“Mod-FLA”). VBE [Mod-FLA], with physical flash gas inputs again consistently produces the lowest FGOR for all 5 wells. The large difference between FGOR produced by EOS/PSM and FGOR produced by VBE may be attributed to VBE’s inability to account for a continuously heated tank in the flash gas calculation. VBE’s inputs do not include tank temperature, and the heating of tanks in Uinta Basin oil production is

widespread. The importance of modeling heated tanks for VOC estimations and FGOR from flash gas will be discussed in the next section of this report.

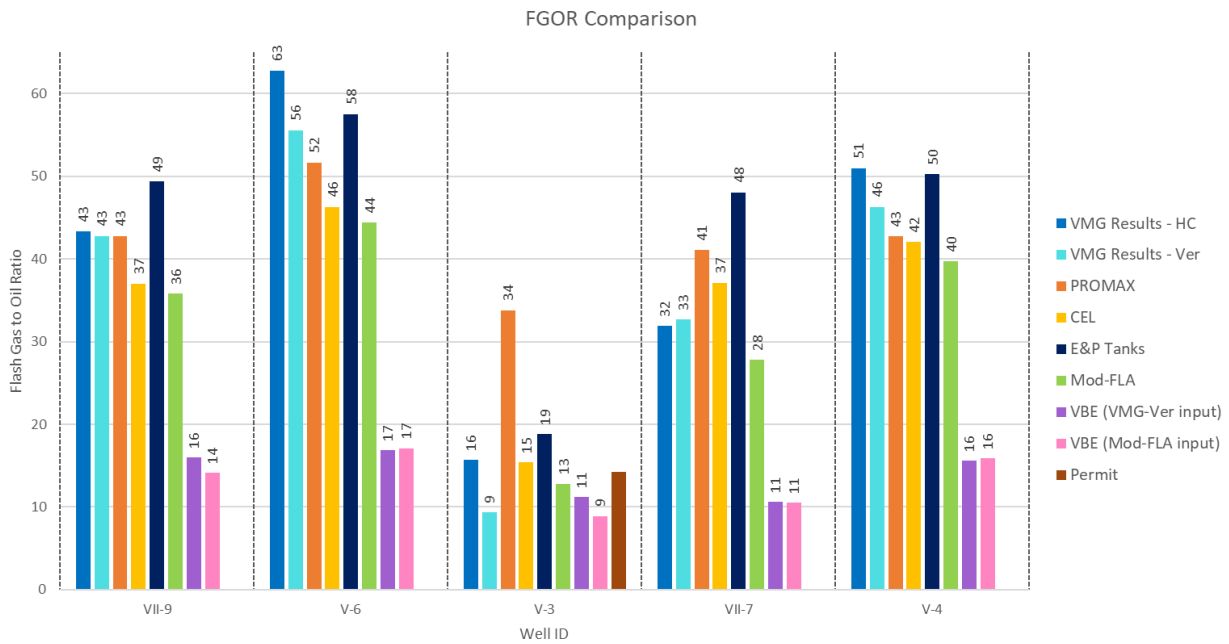


Figure G-3: Flash gas to oil ratios (FGOR) from various sources (see Table G-1).

USU collected pressurized liquids samples from a subset of the Hydrocarbon Sampling campaign and physically flashed them to retrieve FGOR. These results, compared to AST’s physically flashed FGOR retrieval and VMG simulated FGOR, are shown in Figure G-4. More detail about USU’s and AST’s sampling/analysis can be found in REPORT C: CARBONYL SPECIATION IN FLASH GAS-OIL RATIO and REPORT F: FLASH GAS TO OIL RATIO – MODIFIED PHYSICAL FLASH, respectively. These physical measurements represent flashing emissions from heavy waxy crude (far left wells), lighter crude (middle wells), and condensate (right wells). FGOR from gas wells naturally have higher FGOR than oil wells. EOS/PSM estimated FGOR can be either higher or lower than physically measured FGOR, but a clear bias in the simulation cannot be deduced from this small sample size.

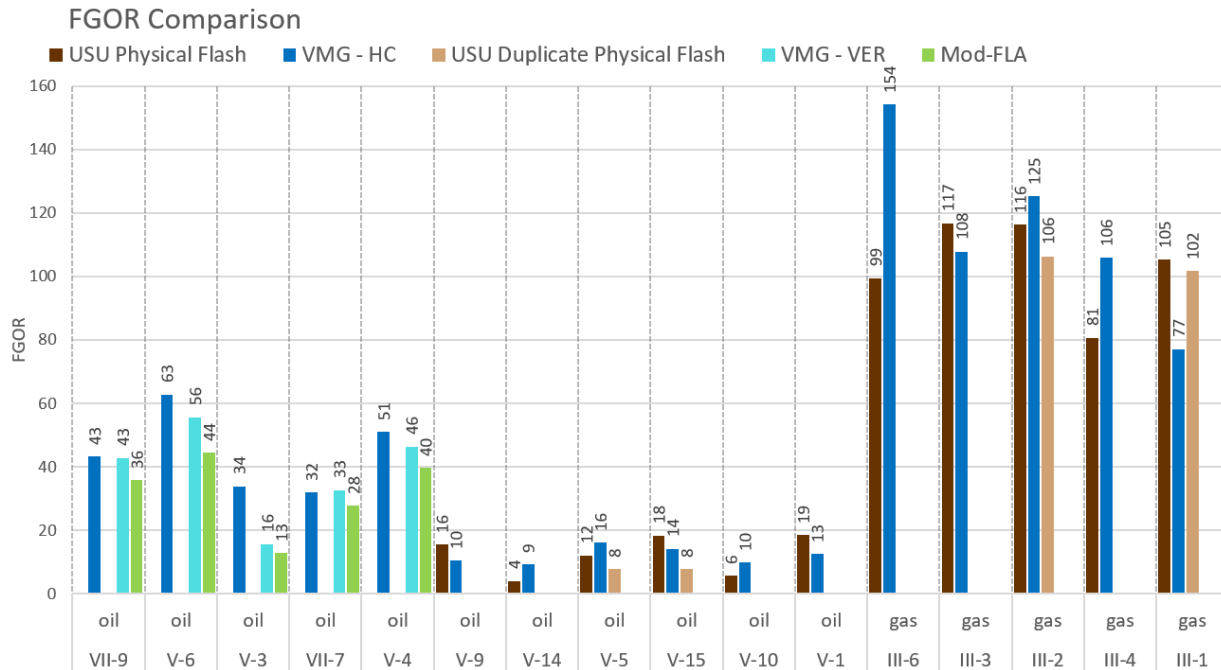


Figure G-4: FGOR measured by USU (wells V-9 to III-1, left to right) or AST (wells VII-9 to V-4, left to right), compared to modeled FGOR by VMG. Physically flashed samples include USU Physical and Duplicate, and Mod-FLA (AST), all referring to a modified flash involving heating of the sample prior to analysis. “VMG-HC” are EOS/PSM results from initial samples taken ~Nov 2018, and “VMG-VER” are EOS/PSM results from the same wells as VMG-HC, but ~ Feb 2019. Well Type (oil or gas well) is noted about the Well ID along the x-axis. These physical measurements represent flashing emissions from heavy waxy crude (far left wells), lighter crude (middle wells), and condensate (right wells).

Air agencies’ interest in the composition of oil and gas emissions is rooted in understanding how those emissions are able to produce ozone and at what rate. Looking at emissions rates of VOCs in tons per year (TPY) is the easiest way to answer this question, but the speciation of those emissions and the variability in reactivity rates in forming ozone are critical for improving performance of photochemical ozone modeling. Many EOS/PSM directly estimate VOC tons per year for a given source (Figure G-5) but UDAQ only had access to ProMax and E&P Tanks for this portion of analysis (VMG and CEL simulations did not include VOC emission rate estimates). The EOS/PSM produce much higher VOC emission rates than the Vasquez-Beggs equation. Again, this may be related to VBE’s inability to account for heated tanks.

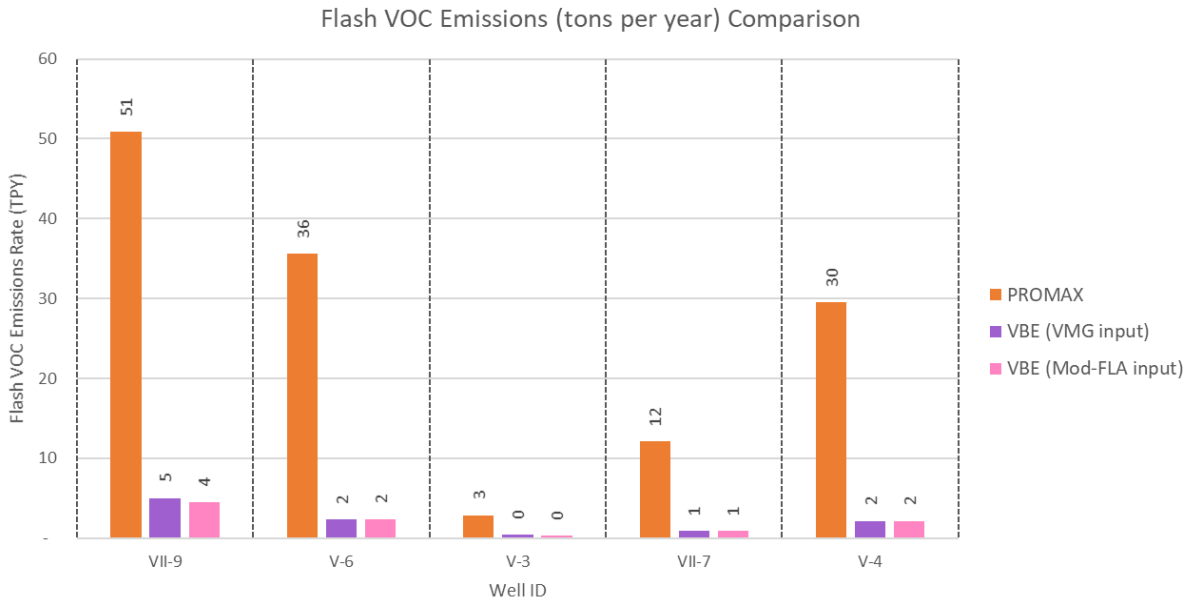


Figure G-5: Flash gas VOC Emission rate estimate according the ProMax and the Vasquez-Beggs equation (VBE). E&P Tanks simulations only provided VOC emission rate estimates for combined SWB and flashing emissions, so those values cannot be compared here. Other EOS/PSM did not include flash gas VOC emission estimations in tons per year, so they are not shown in this figure.

Sensitivity Testing

Industry and regulatory agencies use laboratory or modeled gas composition analyses to estimate a facility’s potential to emit (PTE) of criteria air pollutants (like VOCs) and hazardous air pollutants (like BTEX) to determine regulatory applicability, underscoring the importance of speciation of those emission sources. Depending on the information provided by the operator about the composition of their product, regulatory agencies will use engineering calculations to estimate VOC emissions (in tons per year) from the operator’s source. If the operator is using EOS/PSM to estimate key information about the composition of their product, air agencies are interested in how various EOS/PSM model inputs impact the relevant air quality assessment outputs. Relevant air quality outputs are those that are used in emissions estimations, some examples of which include FGOR and VOC emission rates in tons per year. Many EOS/PSM include calculation blocks that will perform the engineering calculations to estimate emissions for the user, resulting in an emissions rate of VOCs flashing from the tank in tons per year (TPY). As an additional test, VOC weight percent of the modeled flash gas was also examined.

This analysis investigates the sensitivity of EOS/PSM with variable inputs to produce reliable relevant air quality outputs. UDAQ had limited access to the EOS/PSM discussed previously in this report (VMG), but was given full access to ProMax. These sensitivity tests reflect ProMax’s response to various inputs, and the results may or may not apply to other EOS/PSM.

Tank Temperature & Pressure

Temperature and pressure of the storage tank are necessary inputs to EOS/PSM for modeling flash gas composition and other relevant air quality outputs. Storage tanks, especially for oil-producing sites in

the Uinta Basin, are heated. Oil tanks measured in this study varied from 140 to 172°F, and condensate tanks (associated with gas-producing sites) varied from 7 to 120°F (lower temperatures for condensate tanks are associated with unheated storage tanks). Storage tanks are atmospheric and are typically assumed to be at barometric pressure. It is important to input the storage tank pressure as the pressure at the sampling location, *not* the barometric pressure at the laboratory at which other measurements may have occurred. Atmospheric pressures varied from site to site, with minimum pressure of 11.2 and maximum pressure of 12.5 psi. ProMax sensitivity to various tank temperatures [top] and pressures [bottom] are shown in Figure G-6 and Figure G-7.

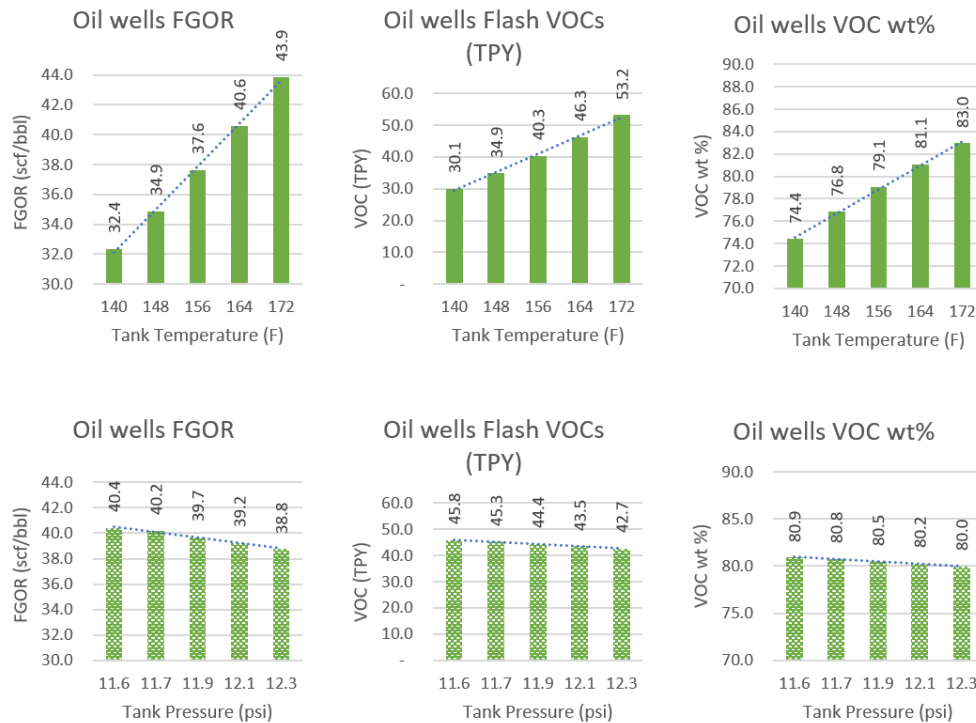


Figure G-6: Impact of oil tank (oil wells) pressure (psi) and temperature (F) on relevant air quality EOS/PSM outputs. Tested using ProMax only.

Generally, FGOR and VOCs increase rapidly with increasing tank temperature. FGOR and VOCs decrease with increasing tank pressure, but with less dramatic impacts than with increasing tank temperature. Simulated API gravity and RVP have opposite trends than FGOR and VOCs with increasing tank pressure and temperature. The Noble Energy Pressurized Hydrocarbon Liquids Sampling and Analysis Study recommends using the minimum anticipated tank pressure and the maximum anticipated tank temperature in EOS/PSM emissions estimations. For Uinta Basin crude, minimum pressure and maximum temperature would yield the highest possible GOR and VOC estimations produced by EOS/PSM (assuming all other inputs are held constant) and would support a Potential to Emit (PTE) estimate.

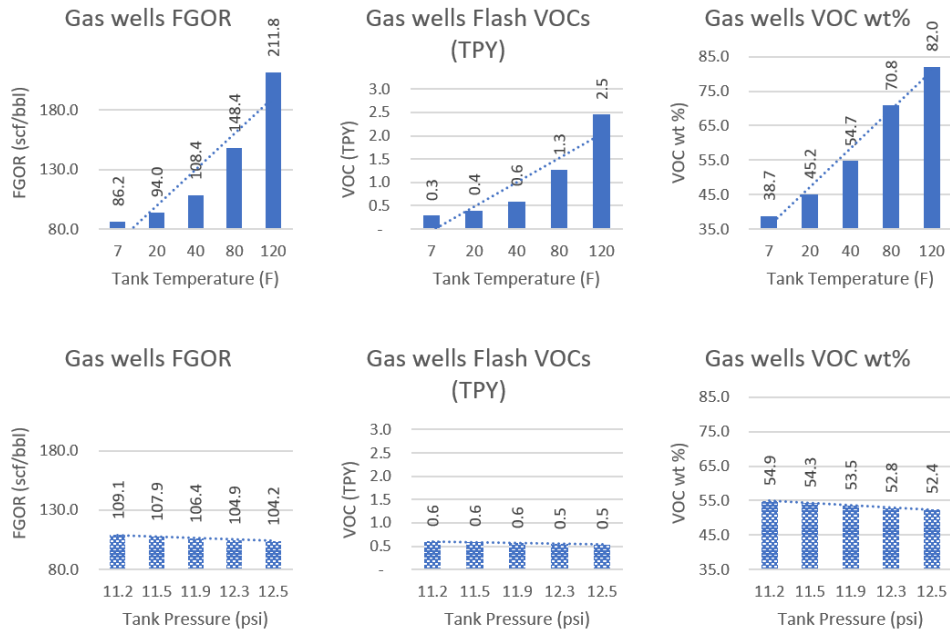


Figure G-7: Impact of condensate tank (gas wells) pressure (psi) and temperature (F) on relevant air quality EOS/PSM outputs. Tested using ProMax only.

Heated vs. Unheated tanks

Heated tanks are widespread in the Uinta Basin due to the waxy nature of its crude and the heat required to keep it in the liquid form for transportation year-round. FGOR, VOC emission rate, and VOC weight percent were first tested for the 5 Verification Sampling wells using ProMax and inputs in Table G-2, and then modeled a second time keeping all inputs the same as the first trial, but setting the tank temperature to ambient (rather than heated). Heated and unheated results are shown in Figure G-8 on the left and right respectively.

The differences between VOC emission rates, VOC weight percentages, and FGOR between heated and unheated tank inputs are dramatic. VOC weight percent of flash gas increase by nearly 50% when the tank is heated, and emission rates increase by 85%. Heating crude to 160°F or higher makes both light and heavy VOCs more likely to volatilize, therefore increasing the emission rate and increasing the VOC weight percent of the flashed gas. Accurate reflection of heated tanks in an EOS/PSM is critical to correctly estimating flash gas emissions. As mentioned in the previous section, the Vasquez-Beggs equation is a common and free tool for estimating flash gas VOC emission rates, but the equation does not account for heated tanks and fails to estimate VOCs resulting from volatilization within a heated storage tank.

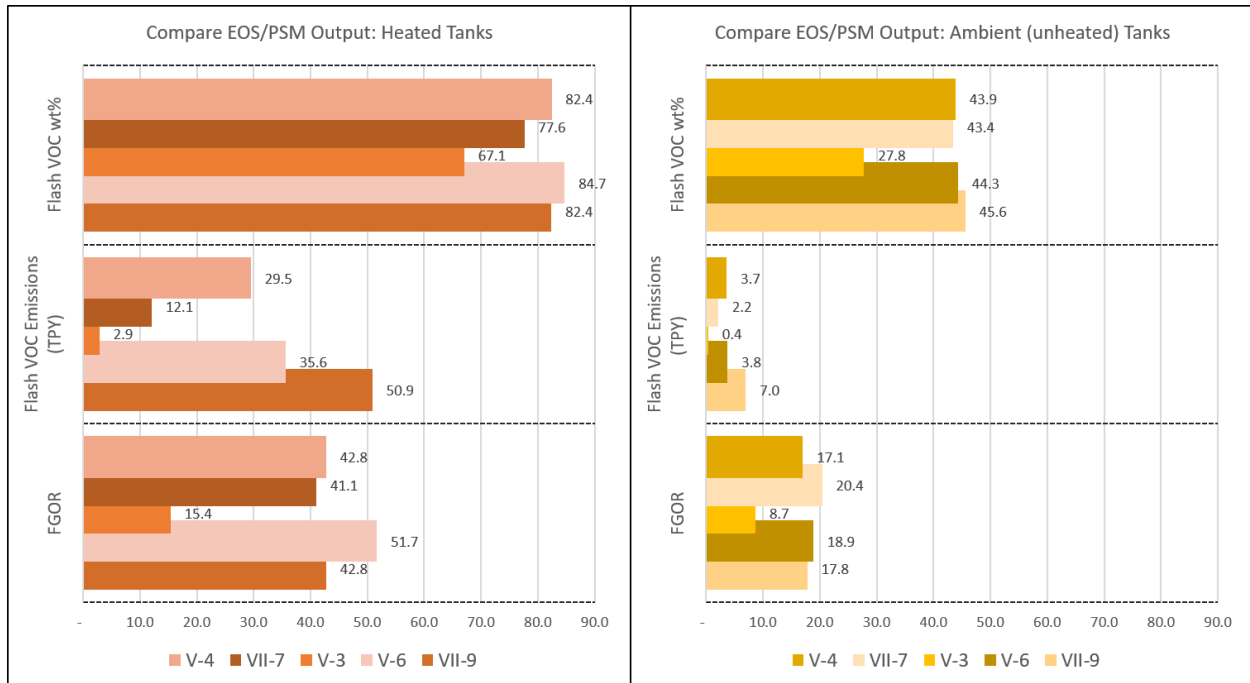


Figure G-8: [Left, orange] EOS/PSM output for 5 wells with tank temperature input as observed on site; [Right, yellow] EOS/PSM output for the same 5 wells with all inputs held constant *except* tank temperature was adjusted to ambient outdoor temperature at the time of measurement. *Tested using ProMax only.*

Pressurized Liquids Input: C1 - C10+ vs C1 -C36+

The pressurized liquid samples analyzed in this study were speciated out to C36+ in an extended liquids analysis, and EOS/PSM matches those species 1-to-1, so flash gas composition was estimated with extent C1 to C36 as well. Operators have often submitted flash gas composition analyses to air agencies with extent only C1 to C10+ or fewer, and the last specie includes an estimation of all heavier compounds amalgamated into “decanes+.” In the Uinta Basin and for the sampling done in this study, pressurized waxy crude typically contains 50% weight percent or more of this “decanes+” category (see APPENDIX C: SAMPLE COLLECTION, LHC COMPOSITION, AND EOS CALCULATIONS DATA) meaning that the molecular weight of more than half of the heavy compounds in a sample may be poorly estimated as decanes. UDAQ tested ProMax’s relevant air quality variables with the 5 Verification Sampling wells, once with full C36 speciation and again with C11-C36 amalgamated to the generic “decanes+.”

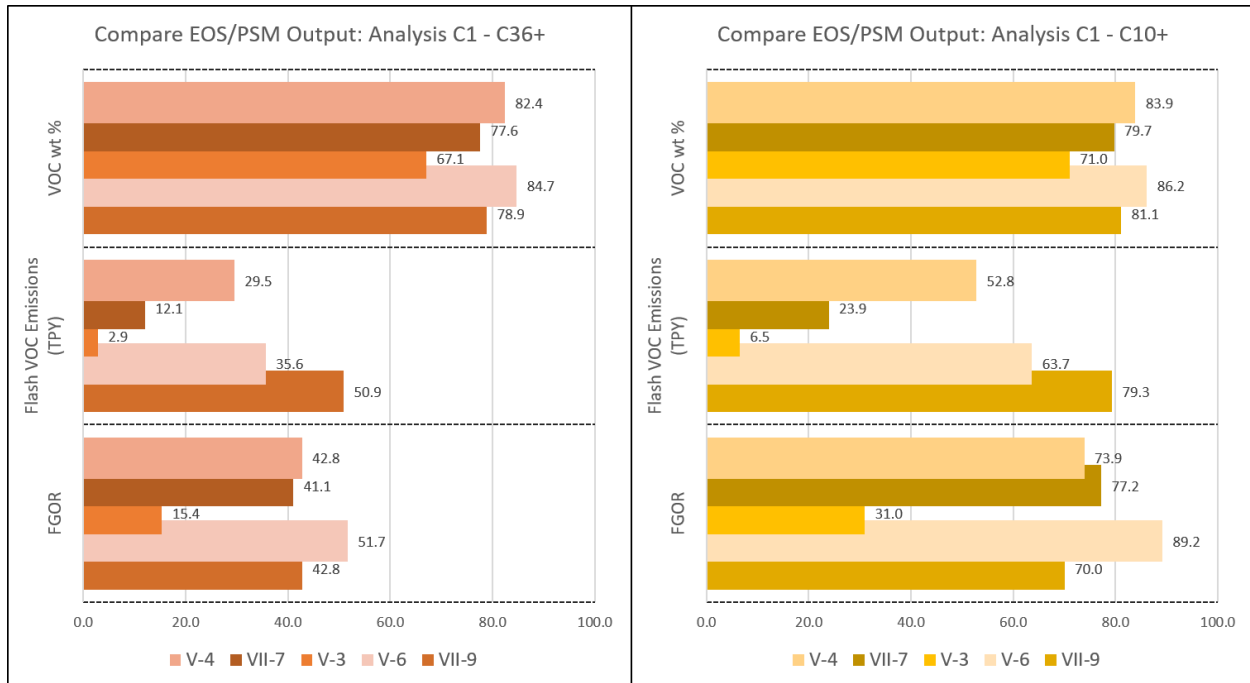


Figure G-9: Relevant air quality EOS/PSM outputs for 5 wells when pressurized liquids composition was entered from C1 to C36+ (orange, left) and C1 to C10+ (yellow, right). Tested using ProMax only.

Figure G-9 shows this comparison with extent C1 to C10+ on the left, and extent C1 to C36+ on the right. C36 extent yields a much lower tank VOC emission rate and FGOR than C10 extent, by 40 – 50%, while the VOC weight percent stays within 5% difference between C36 and C10 extent. With C10 extent, ProMax assumes that all hydrocarbons contained in “decenes+” are actually just decanes (hydrocarbons with 10 carbons in a chain). In a heated tank scenario, both light and heavy hydrocarbons including decanes are more likely to volatilize during a flash event. This volatilization is realized as a relatively higher FGOR and VOC emission rate. The C10 assumption may not be accurate for the composition of heavy crude in the Uinta Basin, as often more than half of the total VOC weight percent is identified as decanes+ in this scenario. Realistically, heavy crude is composed of a multitude of hydrocarbons heavier than decanes, and the C36 extent speciates more of those hydrocarbons. The EOS/PSM interprets these speciated heavies as hydrocarbons with much longer carbon chains than decanes. Longer carbon chains are more available for hydrogen bonding with lighter available hydrocarbons in the tank, and this hydrogen bonding prevents some volatilization in a heated tank environment. The C36 simulation then results in a lower VOC emission rate and lower FGOR as well.

Comparison of Vasquez-Beggs Equation & AP-42 Tank Emissions Estimations

Emissions from tanks are sometimes estimated by an operator without access to a sophisticated EOS/PSM. This is typically accomplished by estimating the tank *flashing* emissions using the Vasquez-Beggs Equation (VBE) in conjunction with AP-42 calculations for estimating *Standing, Working, and Breathing* Emissions (SWB) from the tank.

The Vasquez-Beggs Equation takes several values as inputs (Table G-3). In order to use VBE, a user must have the composition and molecular weight of the flash gas in addition to the API gravity of the stock

tank oil. If flash gas composition was obtained using an EOS/PSM, then API gravity can be retrieved from that same model run. Presumably, the flashing and SWB emissions could also be estimated from the EOS/PSM run, making the VBE calculation unnecessary, but for the sake of comparison, the VMG-Ver flash results were estimated here as well (see “VBE (VMG-Ver)” columns in Table G-3). More likely, operators will have physically flashed in the lab a pressurized liquid sample collected concurrently with an API gravity measurement of the stock tank oil, and entered those data into the VBE (see “VBE (Mod-Fla)” columns in Table G-3). In this study, API gravity of the stock tank oil was not physically measured, so the results (shown in dark gray in Table G-3) reflect a calculation based on an average API gravity of 40 (because EOS/PSM model would not have been available). In the case of VBE, accurate API gravity of the stock tank oil is a crucial input and should be measured if an EOS/PSM is not in use. FGOR and VOC emission rate from flashing between VBE calculations using the physically measured vs modeled flash gas are similar among the same “verification sampling” wells.

		Well ID		VII-9		V-6		V-3			VII-7		V-4	
		Input Category		VBE (VMG-Ver)	VBE (Mod-Fla)	VBE (VMG-Ver)	VBE (Mod-Fla)	VBE (VMG-Ver)	VBE (Mod-Fla)	VBE (Permit)	VBE (VMG-Ver)	VBE (Mod-Fla)	VBE (VMG-Ver)	VBE (Mod-Fla)
VBE Inputs	Stock Tank API Gravity	42.8	40.0	46.4	40.0	40.9	40.0	37.6	43.2	40.0	45.8	40.0		
	Separator Pressure (psig)	79.0	79.1	78.4	78.4	56.0	56.0	38.0	58.0	59.9	76.0	76.1		
	Separator Temperature (°F)	145.0	145.0	122.0	122.0	133.0	133.0	160.0	140.0	140.0	129.0	129.0		
	Separator Gas Gravity at Initial Condition	1.8	0.9	1.9	0.9	1.4	0.9	2.0	1.6	0.9	1.8	0.9		
	Stock Tank Barrels of Oil per day (BOPD)	63.0	63.0	34.0	34.0	16.0	16.0	37.0	18.0	18.0	37.0	37.0		
	Stock Tank Gas Molecular Weight	50.8	32.1	54.4	30.7	39.2	25.7	55.2	47.7	32.0	51.4	29.7		
	Fraction VOC (C3+) of Stock Tank Gas	0.6	0.3	0.7	0.3	0.4	0.2	0.8	0.6	0.3	0.6	0.3		
	Atmospheric Pressure (psia)	12.1	12.1	11.9	11.9	11.9	11.9	11.9	12.1	12.1	11.9	11.9		
VBE Outputs	FGOR	15.97	14.11	16.87	17.08	11.17	8.90	13.50	10.62	10.53	15.56	15.90		
	VOC Emission Rate (TPY) from Flashing	5.04	4.46	2.36	2.39	0.40	0.32	9.86	0.92	0.91	2.16	2.15		

Table G-3: Vasquez-Beggs Equation (VBE) inputs and outputs for VMG-estimated flash gas emissions and physically measured flash gas emissions.

EPA’s AP-42 Chapter 7 outlines calculation methods for SWB emissions, or “Routine Losses from Fixed Roof Tanks.” Programs such as EPA TANKS 4.09D, API E&P Tanks, and EOS/PSM like ProMax and VMG incorporate these AP-42 equations into their software so that operators can easily make SWB emissions estimations. Equation inputs include physical properties of the tank, such as tank height and diameter, tank roof type, tank color, etc. The calculation also requires a nearby city to be entered; this is how annual temperature and pressure profiles are selected for the region in which the tank exists. These attributes determine the emissions resulting from an outdoor liquid storage tank’s exposure to sunlight and average meteorological conditions. It is important to note that AP-42 calculations assume the tank sits at ambient temperature in the select region, but nearly all oil tanks in the Uinta Basin are heated year-round to maintain the waxy crude in a liquid state for transportation. This heating of the tank *must* be accounted for in estimation of flashing and SWB emissions. Figure G-10 shows the differences in flashing and SWB emissions for heated tanks (solid bars) and ambient temperature tanks (dotted bars) when calculating pounds of VOC per barrel of oil or condensate (VOC lb/bbl). The tank temperature influences both SWB and flashing estimations in ProMax. VOC lb/bbl is a crucial input to the Utah Air Agencies Oil and Gas Emissions Inventory for tank emissions estimations.

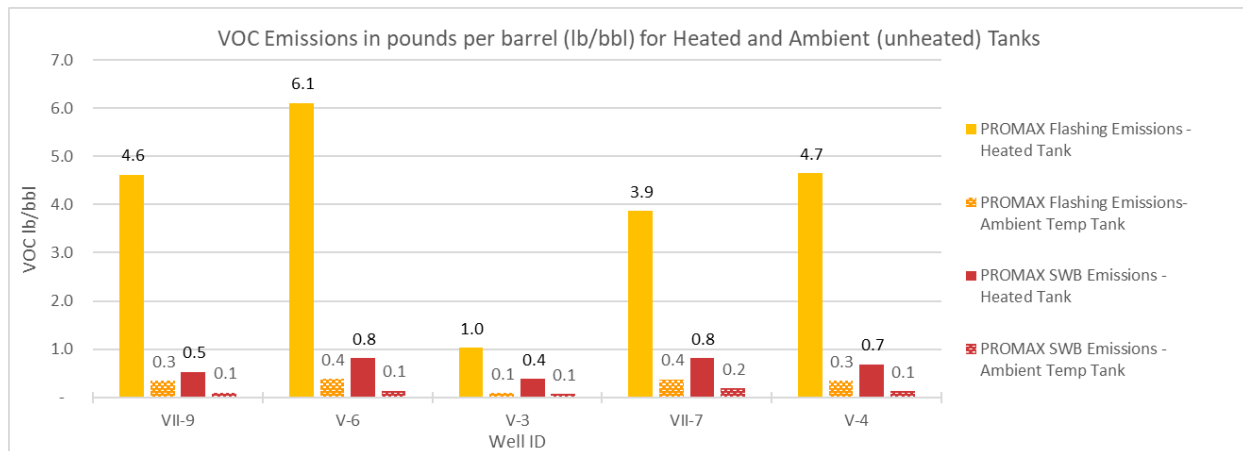


Figure G-10: Flashing (yellow) and SWB (pink) emissions estimated for heated (solid) vs unheated (dotted) tanks using ProMax.

In Figure G-10, ProMax uses a calculation block specifically for calculating flashing (yellow bars) and SWB (dark pink bars) losses over an annual average time period. Heated (solid bars) tank temperature was modeled to be near 170°F year-round, while unheated (dotted bars) used the Salt Lake City annual average temperature, about 67°F. The difference in VOC lb/bbl between modeling a tank heated rather than at ambient temperature is significant. To accurately account for tank emissions from heated oil tanks, EOS-PSM models must use the tank heated temperature.

Comparison to Utah Air Agencies Oil and Gas 2017 Emissions Inventory

Emission factors for flashing and standing, working, breathing (SWB) emissions are required for storage tanks reported in the Utah Air Agencies Oil and Gas Emissions Inventory (OGEI). In order to draw a comparison between the tank emissions calculations in the 2017 inventory and those collected in the Uinta Basin Composition Study for the 5 heavy-crude-producing wells in the Verification sampling campaign, several filters were applied to the 2017 OGEI prior to analysis. Inventory data shown here include all tanks from facilities labeled as “Production Facilities” with throughput labeled as “oil”. Only the top 11 producing companies are shown, which account for 97.6% of the total oil production in the Uinta Basin in 2017.

Figure G-11 shows total number of tanks reported to the 2017 OGEI for each company, separated by tanks with emissions routed to a combustor and tanks with no controls installed. Company VII reported the most tanks to the 2017 inventory. Company IDs are continuous throughout this report, so wells VII-7 and VII-9 are associated with Company VII here, and wells V-3, V-4, and V6 are associated with Company V.

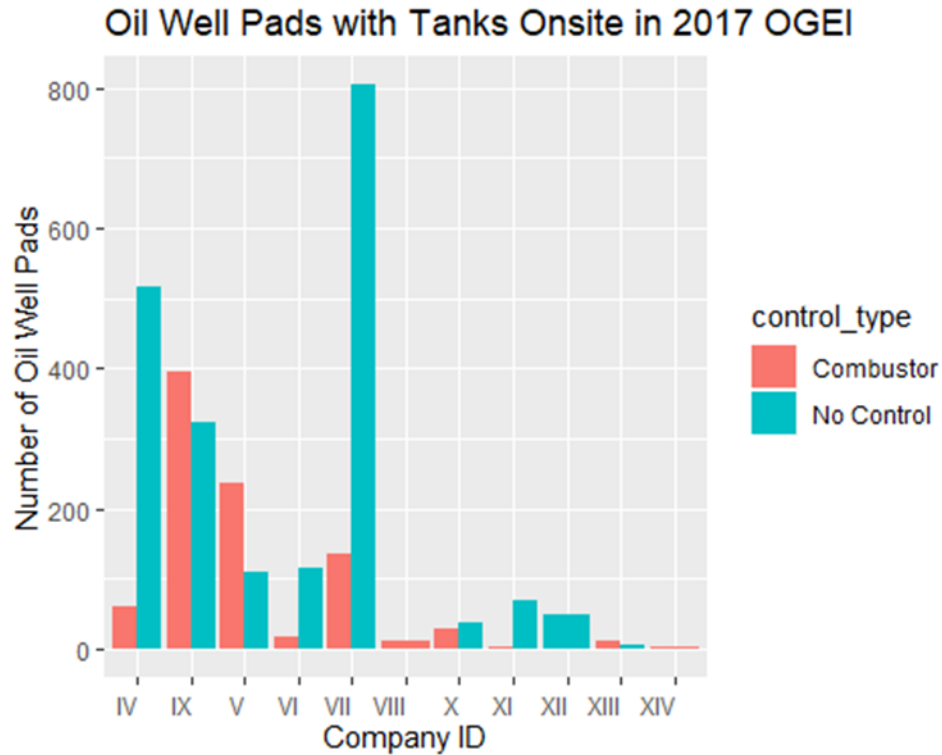


Figure G11: Number of oil well pads reported to the 2017 Oil and gas emissions inventory, sorted by Company ID. Company ID matches Company ID presented in Report B. For instance, wells VII-9 and VII-7 from the verification sampling campaign are associated with Company VII in this figure.

Figure G-12 shows which calculation methods were used by operators in their submissions to the 2017 OGEI. Each bar represents the number of facilities for which the associated calculation method was used in the 2017 inventory. SWB emissions are most frequently calculated using AP-42 guidelines, such as those provided in EPA TANKS 4.09D. Flashing emissions are either calculated from a physical flash (FGOR) and put into VBE, or an EOS/PSM was used to calculate SWB and flashing emissions together. Either ProMax or API’s E&P Tanks account for all EOS/PSM runs in the 2017 OGEI. VBE accounted for a very small proportion of total tanks calculations in 2017. E&P Tanks and TANKS 4.09D are both no longer supported by their developers.

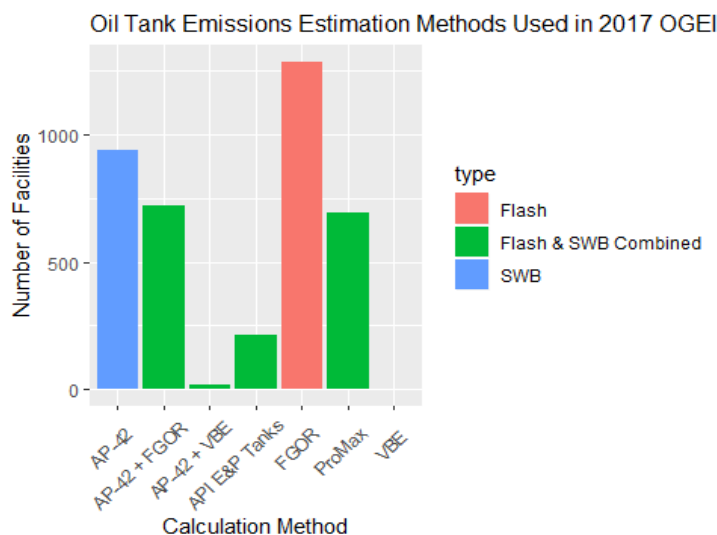


Figure G-12: 2017 OGEI Statewide tanks emission factors calculation methods. Blue bars represent SWB (AP-42) emissions and pink bars represent Flash (FGOR) emissions; these were calculated separately from one another. Green bars are combined calculations for both SWB and flashing emissions. E&P Tanks and TANKS 4.09D (AP-42) are both no longer supported by their developers. Each bar represents the number of oil production facilities for which the associated calculation method was used in the 2017 inventory.

Results from this study are compared to various tanks emissions reported in the OGEI.

The OGEI relies on tank emissions calculations from operators in order to calculate total VOCs from each tank in the Basin, primarily through the collection of pounds of VOC per barrel of oil produced (Figure G-12). Operators submit emission factors to OGEI in VOC pounds per barrel (lb/bbl), with a choice to either calculate emission factors for flashing and SWB separately or combined. For the 5 verification wells, VOC lb/bbl for combined flashing and SWB emissions from the 2017 OGEI are shown in Figure G-13 as hashed bars (pink). These operator-submitted emission factors are compared to VOC lb/bbl estimations for flashing and SWB emissions as calculated by ProMax (yellow) and E&P Tanks (navy); these two EOS/PSM are the first and second most-used calculation methods for all tanks in the 2017 OGEI (Figure G-12). Emission factors submitted by operators often come from one or two laboratory analyses meant to be “representative” of hundreds of wells in the Basin, so the emission factors shown in Figure G-13 may have been calculated from composition data from an entirely different well. While some wells in this subset have much higher VOC lb/bbl than the operator-submitted emission factor, others remain lower, so the operator submitted VOC lb/bbl may be a representative average VOC lb/bbl for that operator’s producing wells. However, this is an extremely small subset of wells in the Basin and the question of sample representativeness may be better addressed with a larger study sample size in the future.

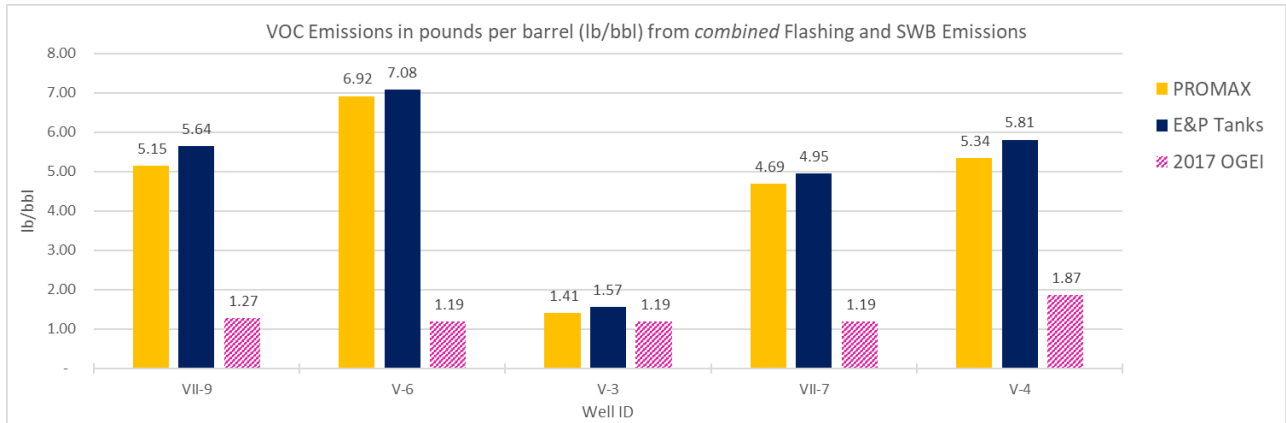


Figure G-13: Flashing and SWB (combined) VOC lb/bbl for the 5 verification wells as calculated by ProMax (yellow) and E&P Tanks (navy), and as submitted for the same wells in the 2017 oil and gas emissions inventory (pink hashed).

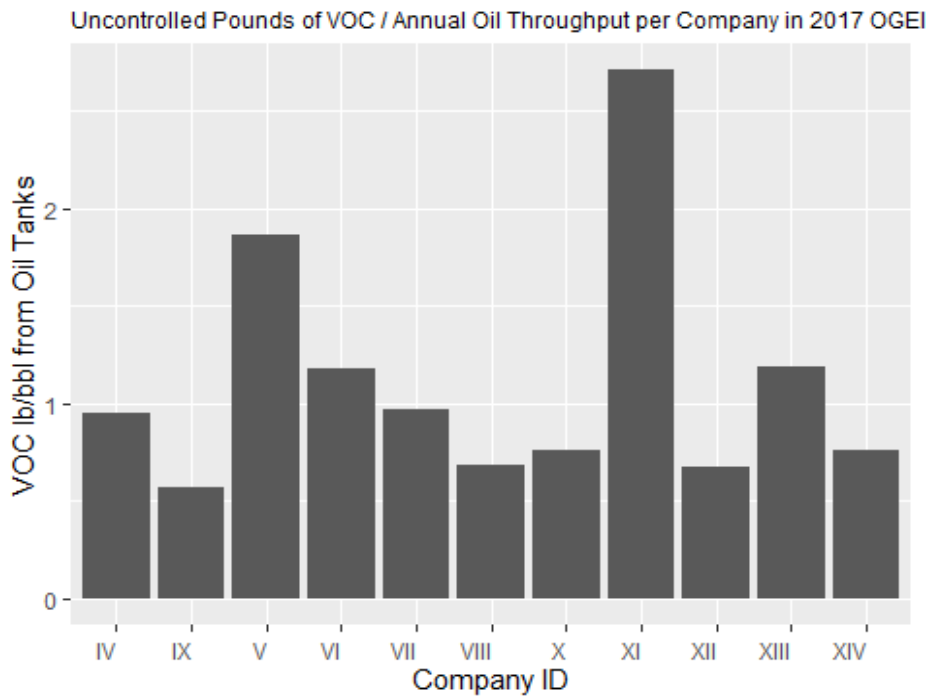


Figure G-14: Uncontrolled VOC emissions from oil tanks divided by oil throughput per company in the 2017 oil and gas inventory. This figure shows a company-wide visualization of pounds of VOC emitted from the tank per barrel of oil produced.

Figure G-13 shows overall, uncontrolled VOC lb/bbl from oil tanks associated with the top producing companies in the 2017 OGEI. All operators show an overall VOC lb/bbl less than 2.8.

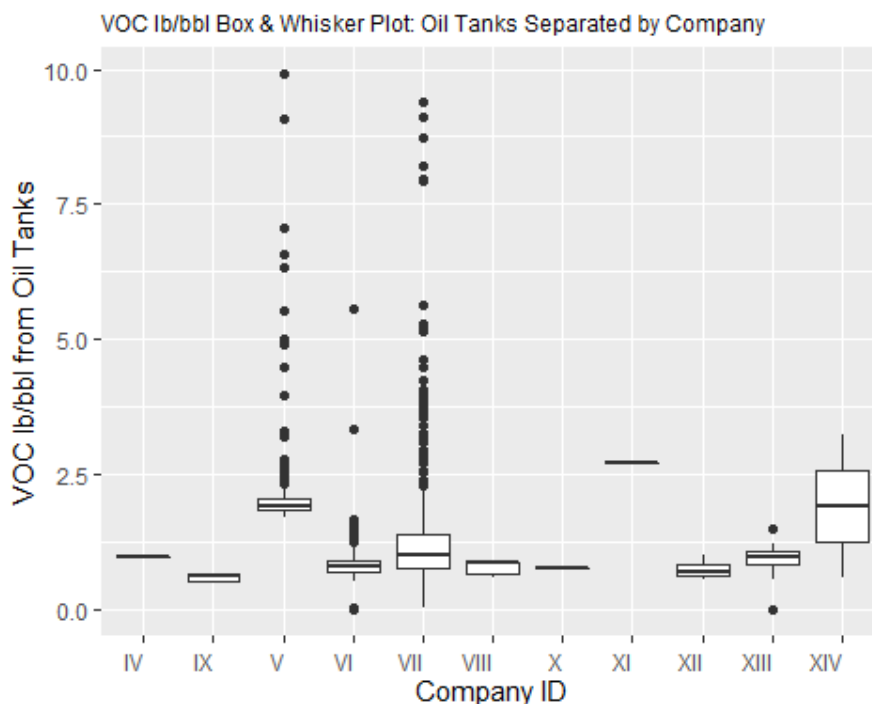


Figure G-15: With some extreme outliers removed to improve clarity of the visualization, this box and whisker plot shows VOC lb/bbl for oil tanks as reported by operators in the 2017 oil and gas inventory.

Figures G-15, G-16, and G-17 show box-and-whisker plots for various parameters. For each plot the data is sorted from least to greatest and then graphed with a box-and-whisker. The box spans the interquartile range (IQR) from the 25th percentile at the bottom (25% of the values are lower than this value) to the 75th percentile at the top of the box. The median value is shown as the horizontal line within the box, the value where 50% of the values are higher than that value and 50% lower. If outliers are present, the whisker on the appropriate side is drawn to 1.5 times the IQR. Small dots are drawn on the chart to indicate where suspected outliers lie. To understand the proportion of number of outliers to number of production facilities, see Figure G-11. When just a median bar is shown (Companies IV, X and XI), the Company used a single VOC lb/bbl emission factor for all their oil production facilities.

As explored above, tank temperatures are very important to estimating accurate VOC emission rates. Figure G-16 shows the tank temperatures used in estimating tank emissions in the 2017 OGEI. Companies IV, V, VII, VIII, IX, XI and XII applied a single tank temperature to estimate emissions from all oil tanks. Heated oil tank temperatures sampled in this study fell in the 160 to 170°F range. Some tank temperatures in the 2017 OGEI, for instance those associated with Company VII, are in the 130°F range. As discussed above and shown in Figure G-6, input tank temperature can have a significant impact on VOC tank emissions estimations.

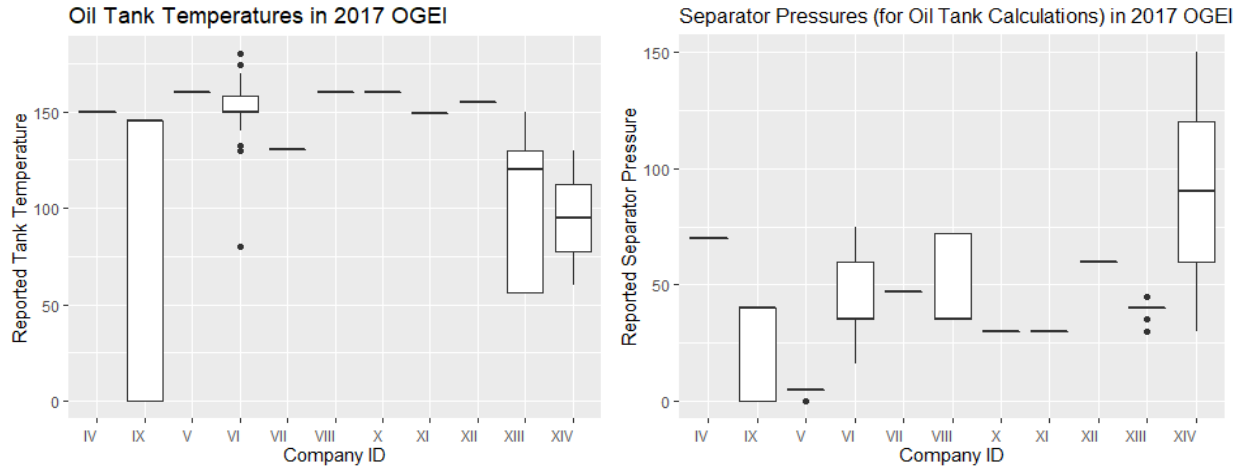


Figure G-16: [Left] Oil tank temperatures as reported in the 2017 oil and gas inventory, separated by company. [Right] Separator temperatures for oil-producing wells as reported in the 2017 oil and gas emissions inventory.

Figure G-17 [Left] shows box and whisker plots for tank temperatures in this study (orange) and in the 2017 oil and gas emissions inventories (yellow). Average tank temperatures in this study were slightly higher than OGEI for oil tanks. Separator pressure is also an important EOS/PSM input, and average pressures observed in this study generally match those reported in OGEI (Figure G-17 [BOTTOM]).

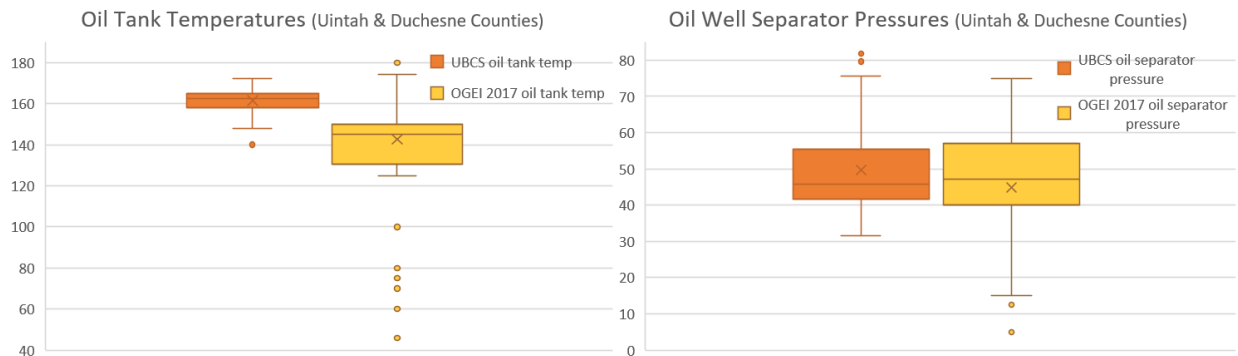


Figure G-17: [Left] Oil tank temperatures as measured in this study (UBCS) and by operators in 2017 OGEI. [Right] Oil well separator pressures as measured in this study (UBCS) and by operators in 2017 OGEI.

Summary

Comparing EOS/PSM outputs for Uinta Basin crude at five wells revealed a few key points. First, accurate temperature of a heated tank is crucial to estimating flashing and SWB VOC emission rates from that tank. Second, analyzing pressurized liquids from C1 to C36+ (extended analysis) yields lower VOC emission rates and FGOR when processed in an EOS/PSM than analyzing pressurized liquids from C1 to C10+. Further analysis could include estimating the uncertainty in EOS/PSM output for Uinta Basin waxy crude oil tanks following a Monte Carlo simulation similar to the analysis performed in the Noble Energy Pressurized Hydrocarbon Liquids Sampling and Analysis Study. Emissions from oil tanks and their representation in the emissions inventory will be further investigated.

Key Findings

Sampling and Composition Analysis in the Uinta Basin

The sampling & analysis protocols initially requested in the scope of work for this study were primarily based on recommendations in the Noble Energy Pressurized Hydrocarbon Liquids Sampling and Analysis Study,²⁶ however, the Noble study focused on light-condensate-producing wells in Colorado. Uinta Basin waxy crude posed several unique challenges to pulling pressurized liquid samples from separators, especially during the wintertime, and analyzing them in the lab because of the oil solidifying in ambient conditions. Here we present recommendations for sampling in these conditions.

Sampling

- Heating the sample probe during pressurized liquid sample collection helps prevent the waxy crude from solidifying.
- Maintaining a constant liquid flow rate (while slowly to avoid flash off of gas) during the probe purging process also helps prevent solidification of the sample.
- Higher quality pressurized liquids samples are more likely to come from 3-phase separators. 2-phase separators can produce quality pressurized liquid samples, but it is necessary to drain all the water from the separator prior to pulling the liquid sample in order to collect a pressurized liquid sample uncontaminated by produced water.
- Pressurized liquid composition can vary greatly between sampling events. Liquids from the same pressurized cylinder were analyzed for composition and found to be similar within 5%, but when two separate samples were collected from the same separator subsequently, composition varied from 24% to 76% different between samples.

Analysis

- Heating the tubing of the gas chromatograph to the site's storage tank temperature prevents the pressurized liquid sample from solidifying before reaching the sampling valve. Heated tubes were considered necessary in order to achieve precise pressurized liquids composition results.
- In physically flashing waxy crude from the Uinta Basin, it is important to keep the pressurized liquid sample, as well as all tubing and valves that transport the liquid, heated to the storage tank temperature during the flash event *and* during transfer to the gas chromatograph for analysis.

Chemical Composition of Oil and Gas Well Emissions

One major goal of this study was to understand the chemical speciation of oil and gas well emissions for air quality modeling applications. These findings describe generally the speciation of tank flash gas and raw separator gas from Uinta Basin wells.

²⁶ Pressurized Hydrocarbon Liquids Sampling and Analysis Study Data Assessment and Analysis Report. *Section 5. Pages 147 – 160*. Southern Petroleum Laboratories, 2018. https://noblecolorado.com/wp-content/uploads/2018/12/SPL_PHLA-Study_Final-Report_020718.pdf

Flash Gas

- Flash gas from oil well tanks contains a higher percentage of heavier hydrocarbons (C6+) than flash gas from gas well tanks.
 - Flash gas from oil well tanks also has a higher ozone reactivity than flash gas from gas well tanks.
- Flash gas analyzed for carbonyls shows that flash gas from oil well tanks tends to contain a higher percentage of formaldehyde than flash gas from gas well tanks. Carbonyl composition measured directly from both oil and gas well tanks largely consists of acetaldehyde.
- Carbonyls relative to other hydrocarbons in flash gas samples are too sparse to have a large impact on the ozone reactivity of the speciation profile (according to MIR values).

Raw gas

- Raw gas from oil well separators contains a higher percentage of heavier hydrocarbons (C6+) than raw gas from gas well separators.
 - Raw gas from oil well separators also has a higher ozone reactivity than raw gas from gas well separators.

Grouping of Composition Data & Application of Speciation Profiles

A new method was developed to analyze composition data for speciation profile development and was applied to composition data gathered in this study.

- To perform statistics on a suite of composition data sampled from various wells, the data should first be transformed into ILR space²⁷, or another Euclidian geometry. Grouping and comparison can occur in this geometry and then the results can be transformed back to simplex geometry (standard weight percent representation).
- The most robust groups as determined by this statistical method are sample type – well type: Flash Gas from Oil Wells, Flash Gas from Gas Wells, Raw Gas from Oil Wells, and Raw Gas from Gas Wells.
- Raw gas profiles can be applied to vented source emissions from non-CBM gas wells for source categories such as equipment and pipeline blowdowns, pigging, pneumatic controllers, pneumatic pumps, and fugitive leaks. (Table H-3)
 - Applying profiles to these diverse categories may lead to inaccuracies in modeling, but these applications represent the best available profiles for these emissions source categories at the time this report was developed.
- Flash gas profiles can be applied to emissions from oil tanks, gas venting associated with well liquid unloading, and truck loading. (Table H-3)
- Groups based on geological formation are still statistically valid groupings, but not enough samples from each formation were collected to make the groupings as robust as the “well type – sample type” groups. Additionally, the geological formation categorical variable is less reliable than well type or sample type.

²⁷ Aitchison, J. (1982), The Statistical Analysis of Compositional Data. Journal of the Royal Statistical Society: Series B (Methodological), 44: 139-160. doi:10.1111/j.2517-6161.1982.tb01195.x

- Composition data from individual wells show that gas composition in emissions is different depending on sample location, and gas composition varies when sampling the same well at different times and operating conditions.

Comparison of Direct (High Flow) to Indirect (Separator) Emissions Measurement

A subset of sites sampled by AST for pressurized liquids and raw gas samples (sample taken from the separator and used as a representation of eventual fugitive or tank emissions, referred to as “indirect”) were also sampled using the high flow device (sample taken of emissions as they are emitted in real time at an active oil or gas site, referred to as “direct”). Composition from both sampling methods were compared.

- Direct emissions measurements of tank emissions (flash gas) show higher aromatics/BTEX and lower C2-C6 content than indirect measurements. This may be due to the measurement of standing-working-breathing emissions that were not modeled for the indirect flash gas estimation.
- Direct and indirect emissions of raw gas differed from one another, likely due to the use of processed gas rather than “field” gas (from the separator) on some of the sites.
- Direct emissions of flash gas contained lower portions of formaldehyde than measured indirectly from flashing the gas in the lab.

EOS/PSM Use for Flash Gas Emissions in the Uinta Basin

Inputs for various EOS/PSM tested in this study were collected and used according to recommendations in the Noble Energy Pressurized Hydrocarbon Liquids Sampling and Analysis Study. To achieve the most robust model results, EOS/PSM inputs for Uinta Basin samples should include the following variables, in the highest possible accuracy:

- Annual average operating pressure and temperature of the separator, collected using highly-accurate, calibrated pressure and temperature probes (it is not recommended to use the temperature/pressure gauge on the separator due to lower accuracy)
- Maximum or annual average storage tank temperature
 - If the tank is heated, collect temperature using an IR temperature gun, the temperature gauge on the storage tank, or the set points on the tank thermostat pneumatic controller.
 - It is important to use the heated tank temperature (not ambient temperature) in modeling flash gas AND standing, working, breathing emissions. Tanks with higher temperatures have higher modeled VOC weight percentages, VOC emission rates, and FGOR. For PTE calculations, the maximum tank temperature should be used. For emission inventory estimates, the annual average tank temperature could be used.
- Barometric pressure at the location of the storage tank

- Pressure can vary slightly across the Uinta Basin, and these changes in pressure can affect the air emissions estimation in the EOS/PSM. VOC emission rates, VOC weight percent of flash gas, and FGOR tend to increase with decreasing tank pressure.
 - An average value that applies in the Uinta Basin is 12 psia.
 - Raw gas composition (C1 to C10+)
 - Extended pressurized liquids composition (C1 to C30+²⁸)
 - Analyzing compounds out to C30+ reduces the amount of uncertainty in binning all C10+ as “decane plus.” Because a significant percent of total composition of pressurized liquids from Uinta Basin oil and gas wells consist of C10+, analysis out to at least C30+ increases the certainty of air emissions calculations. Speciation out to C36+ can decrease the estimate VOC emission rate and FGOR for a given tank (relative to speciation out to C10+).
 - API gravity and Reid Vapor Pressure of the stock tank oil or condensate
 - A sample from the storage tank to derive the Sales Oil API gravity and RVP should be done contemporaneously with pressurized liquid samples from the separator

Composition Results Compared to 2017 Utah Air Agencies Oil and Gas Emissions Inventory

- Emission measurement from the high flow device of 24 sites (23 of which had controlled tanks) showed a majority of observed emissions from thief hatches or pressure relief devices on the tanks. Other emission points included connectors, pneumatics, valves, regulators, and wellheads.
- VOC emission factors for flashing and SWB emissions developed from modeling 5 wells are much larger than emission factors provided for those same wells in the OGEI.

Uinta Basin Oil and Gas Speciation Profiles

The final speciation profiles recommended for photochemical modeling and other air quality applications are printed here. There are 4 speciation profiles for oil and gas wells’ flash and raw gas. There are 2 additional flash gas profiles for oil and gas wells that include carbonyls. The impact of these profiles on ozone modeling in the Uinta Basin will be explored in a subsequent study.

²⁸ AST speciated out to C36+ for this study, but any speciation beyond C30+ will yield similar results in EOS/PSM, according to several EOS/PSM technical personnel.

Table H-1: Uinta Basin Speciation profiles for flash gas and raw gas from oil and gas wells

	Oil Well – Flash Gas	Oil Well – Raw Gas	Gas Well – Flash Gas	Gas Well – Raw Gas
<i>Profile Name</i>	<i>UNTF_OW</i>	<i>UNTR_OW</i>	<i>UNTF_GW</i>	<i>UNTR_GW</i>
METHANE	13.01%	53.38%	47.76%	73.76%
ETHANE	10.74%	11.49%	20.57%	10.39%
PROPANE	16.48%	9.68%	15.68%	5.92%
ISOBUTANE	4.85%	2.22%	4.37%	1.67%
N-BUTANE	12.38%	4.99%	5.25%	2.12%
ISOPENTANE	6.07%	2.32%	2.16%	1.01%
N-PENTANE	8.12%	3.13%	1.52%	0.83%
CYCLOPENTANE	0.61%	0.23%	0.08%	0.05%
N-HEXANE	6.76%	2.14%	0.75%	0.46%
CYCLOHEXANE	1.73%	0.57%	0.37%	0.26%
HEPTANES	10.47%	4.99%	0.33%	1.45%
METHYLCYCLOHEXANE	2.09%	0.81%	0.56%	0.55%
2,2,4 TRIMETHYLPENTANE	0.022%	0.0012%	0.0022%	0.000012%
BENZENE	0.38%	0.16%	0.10%	0.07%
TOLUENE	0.53%	0.26%	0.17%	0.20%
ETHYLBENZENE	0.0005%	0.03%	0.01%	0.01%
XYLENES	0.36%	0.21%	0.08%	0.14%
OCTANES	2.04%	1.81%	0.11%	0.54%
NONANES	2.94%	0.34%	0.12%	0.13%
DECANES+	0.42%	1.26%	0.02%	0.44%
TOTAL	100.00%	100.00%	100.00%	100.00%

Table H-2: Uinta Basin Flash Gas speciation profiles featuring carbonyls

	Oil Well – Flash Gas + carbonyl	Gas Well – Flash Gas + carbonyl
<i>Profile Name</i>	<i>UNTF_OW_C=O</i>	<i>UNTF_GW_C=O</i>
methane	18.352449%	29.781276%
ethane	11.442717%	19.158171%
propane	13.853831%	24.774409%
isobutane	3.743012%	7.324207%
n-butane	8.717217%	10.111346%
isopentane	4.485868%	3.755852%
n-pentane	5.720342%	2.841874%
cyclopentane	0.566515%	0.132872%
n-hexane	6.150359%	0.834259%
cyclohexane	1.728527%	0.373549%

<i>Profile Name</i>	<i>UNTF_OW_C=O</i>	<i>UNTF_GW_C=O</i>
heptanes	14.715750%	0.153740%
methylcyclohexane	2.321627%	0.455461%
2,2,4 trimethylpentane	0.057637%	0.005366%
benzene	0.442477%	0.061007%
toluene	0.702816%	0.082497%
ethylbenzene	0.071685%	0.002748%
xylenes	0.433246%	0.027933%
octanes	2.372057%	0.050819%
nonanes	3.503362%	0.062586%
decanes plus	0.616783%	0.008577%
Formaldehyde	0.000145%	0.000006%
Acetaldehyde	0.000218%	0.000755%
Acetone	0.000000%	0.000000%
Acrolein	0.001259%	0.000673%
Propionaldehyde	0.000014%	0.000004%
Crotonaldehyde	0.000004%	0.000001%
Methacrolein/2-butanone	0.000030%	0.000008%
Benzaldehyde	0.000008%	0.000000%
Valeraldehyde	0.000042%	0.000002%
p-Tolualdehyde	0.000000%	0.000001%
Hexaldehyde	0.000005%	0.000001%
TOTAL	100.00%	100.00%

Table H-3: Proposed application of speciation profiles prepared in this study to various emission source categories

Profile	Application
UNTF_GW: Gas Well – Flash Gas OR UNTF_GW_C=O: Gas Well – Flash Gas + carbonyl	<ul style="list-style-type: none"> • Condensate Tank Emissions • Gas Venting associated with well liquid unloading • Truck loading
UNTF_OW: Oil Well – Flash Gas OR UNTF_OW_C=O: Oil Well – Flash Gas + carbonyl	<ul style="list-style-type: none"> • Oil Tank Emissions • Casinghead gas venting • Truck loading
UNTR_GW: Gas Well – Raw Gas	<ul style="list-style-type: none"> • Fugitives/leaks • Pneumatic Devices and Pneumatic Pumps • Equipment and pipeline blowdowns, pigging, and leaks
UNTR_OW: Oil Well – Raw Gas	<ul style="list-style-type: none"> • Fugitives/leaks • Pneumatic Devices and Pneumatic Pumps • Equipment and pipeline blowdowns, pigging, and leaks • Associated gas venting

Next Steps

- Complete photochemical modeling exercises to determine speciation profile performance and ability to produce ozone in the Uinta Basin
- Collection of additional composition data through permitting process, followed by comparative analysis to the current suite of speciation profiles
- Incorporation of speciation profiles as default profiles in the 2020 OGEI submission process
- Continued assessment of sensitivity/uncertainty of EOS/PSM for Uinta Basin crudes using Monte Carlo simulations, similar to analysis done in Noble Energy Pressurized Hydrocarbon Liquids Sampling and Analysis Study
 - o Determination of EOS/PSM modeling bias for API gravity and RVP of Uinta Basin crude
- Collection and analysis of pressurized liquid samples at well pad facilities to better estimate of emissions from produced water and inform the OGEI.
- Development of an easy-to-use version of composition analysis tool described in REPORT D: SUPPLEMENTAL SPECIATION PROFILE ANALYSIS, available through RStudio.

Acknowledgements

The Utah Division of Air Quality would like to thank the Utah State Legislature for providing funding to complete this study. UDAQ thanks the Ute Tribe for their willingness to participate in this important study to help improve air quality in the Uinta Basin airshed. UDAQ also thanks Utah State University's Bingham Research Center and their team of diligent scientists, especially Dr. Trang Tran and Dr. Seth Lyman, for their expertise and hard work in the field, lab, and office. UDAQ thanks Alliance Source Testing, especially Mike Pearson and Andrew Marmo, and Tom McGrath for their consultation and ideas regarding improved sampling and analysis for the Uinta Basin's especially difficult crude. UDAQ thanks Jared Petersen for his assistance in configuring ProMax for this study. UDAQ thanks Cindy Beeler from EPA Region 8 for her thorough review and consultation on each step of this study, leaving no stone unturned! Thanks for Aaron Zull at EPA for consultation on data visualization. UDAQ thanks Whitney Oswald for kicking off the study. Finally, and most importantly, UDAQ thanks all the operators who allowed samples to be collected at their facilities.

Appendices

Appendix A: Calibration Checks

See Supplemental Documentation section here: <https://documents.deq.utah.gov/air-quality/planning/technical-analysis/DAQ-2020-004666.pdf>

Appendix B: Calibration Gas Certificates of Analysis

See Supplemental Documentation section here: <https://documents.deq.utah.gov/air-quality/planning/technical-analysis/DAQ-2020-004668.pdf>

Appendix C: Sample Collection, LHC Composition, and EOS Calculations Data

Company	C or W	Well Site	P _{bar} (psia)	P _{probe} (psig)	P _{BP} (psia)	P _{SC} (psia)	P _{BP} /P _{SC}	FGOR (scf/bbl)	CO ₂ (mole %)	CH ₄ (mole %)	C ₂ H ₆ (mole %)	C ₃ H ₈ (mole %)	C ₁₀₊ (mole %)	T _{probe} (°F)
I	C	I-1	12.5	189	150.0	201.5	0.744	48.5	0.168%	4.336%	1.222%	1.243%	22.047%	62
I	€	I-2	12.5	187	81.5	199.5	0.409	23.6	0.093%	2.320%	0.910%	0.990%	21.039%	61
I	€	I-3	12.5	166	80.3	178.5	0.450	19.1	0.127%	2.372%	0.696%	0.670%	26.908%	58
I	C	I-4	12.5	76	100.1	88.5	1.131	23.6	0.142%	3.218%	0.500%	0.412%	48.171%	49
I	C	I-5	12.5	207	161.8	219.5	0.737	35.8	0.184%	4.541%	0.787%	0.617%	57.901%	86
I	€	I-6	12.5	326	103.9	338.5	0.307	28.7	0.120%	2.909%	0.799%	0.723%	24.193%	49
I	€	I-7	12.5	125.1	57.5	137.6	0.418	12.5	0.078%	1.523%	0.582%	0.866%	24.953%	76
I	€	I-8	12.5	274	44.9	286.5	0.157	10.2	0.051%	1.261%	0.660%	1.007%	21.818%	59
I	€	I-9	12.5	196	85.3	208.5	0.409	23.6	0.096%	2.342%	1.073%	1.171%	25.705%	70
I	C	I-10	12.5	146.3	119.5	158.8	0.753	35.9	0.098%	3.368%	1.380%	1.385%	28.961%	68
II	C	II-1	11.2	33.8	49.4	45.0	1.098	10.1	0.067%	1.256%	0.593%	0.522%	58.740%	107
II	C	II-2	11.5	44.8	45.9	56.3	0.815	10.4	0.036%	1.317%	0.556%	0.532%	46.967%	75
II	C	II-3	11.5	25	30.8	36.5	0.844	4.6	0.026%	0.845%	0.403%	0.391%	61.130%	87
II	C	II-4	11.4	32.2	37.1	43.6	0.851	5.0	0.024%	0.927%	0.448%	0.420%	68.096%	116
II	€	II-5	11.5	162.6	95.9	174.1	0.551	28.0	0.043%	2.877%	1.189%	1.290%	64.340%	104
II	€	II-6	11.5	164.1	82.8	175.6	0.472	27.8	0.029%	2.140%	1.097%	1.196%	42.606%	94
II	C	II-7	11.2	36.5	50.1	47.7	1.050	21.7	0.038%	1.406%	0.996%	1.341%	42.705%	60
II	€	II-8	11.5	191.5	104.0	203.0	0.512	33.4	0.033%	2.775%	1.287%	1.394%	47.764%	92
II	€	II-9	11.4	72	51.2	83.4	0.614	15.4	0.018%	1.843%	0.869%	0.967%	56.835%	89
III	C	III-1	12.3	191.7	175.1	204.0	0.858	77.1	0.150%	4.703%	2.132%	3.667%	17.508%	72
III	C	III-2	12.3	265.4	244.0	277.7	0.879	125.2	0.242%	6.818%	2.671%	4.292%	17.164%	64
III	C	III-3	12.3	280.3	222.9	292.6	0.762	107.8	0.243%	6.056%	2.704%	4.345%	24.185%	72
III	C	III-4	12.3	253.8	198.6	266.1	0.746	105.9	0.226%	5.480%	2.711%	4.653%	19.038%	65
III	C	III-5	12.3	270.1	198.6	282.4	0.703	84.3	0.188%	5.270%	2.129%	3.113%	13.645%	72
III	C	III-6	12.3	324.0	268.4	336.3	0.798	154.2	0.268%	7.147%	3.017%	5.066%	12.858%	71

Company	C or W	Well Site	P _{bar} (psia)	P _{probe} (psig)	P _{BP} (psia)	P _{SC} (psia)	P _{BP} /P _{SC}	FGOR (scf/bbl)	CO2 (mole %)	CH4 (mole %)	C2H6 (mole %)	C3H8 (mole %)	C10+ (mole %)	T _{probe} (°F)
III	C	III-7	12.3	238.0	180.0	250.3	0.719	91.6	0.173%	4.893%	2.722%	4.514%	23.461%	67
III	C	III-8	12.4	344.7	294.5	357.1	0.825	129	0.297%	8.265%	2.878%	4.442%	23.666%	67
IV	W	IV-1	11.6	51	73.3	62.6	1.171	15.4	0.080%	1.893%	0.518%	0.826%	73.709%	133
IV	W	IV-2	11.6	55.6	86.3	67.2	1.284	12.8	0.084%	2.451%	0.232%	0.347%	77.154%	135
IV	W	IV-3	11.6	32	54.9	43.6	1.259	6.2	0.108%	1.654%	0.173%	0.216%	93.154%	135
IV	W	IV-4 (W2)	11.8	46	77.2	57.8	1.336	31.3	0.069%	1.743%	1.345%	2.007%	66.946%	125
IV	W	IV-5 (W1)	11.9	53.5	94.3	65.4	1.442	74.0	0.120%	1.842%	2.471%	4.122%	57.998%	115
IV	W	IV-6	11.8	47.5	58.1	59.3	0.980	10.1	0.125%	1.501%	0.493%	0.594%	77.255%	128
V	W	V-1	11.8	56.2	60.5	68.0	0.890	12.6	0.034%	1.559%	0.701%	0.810%	76.732%	145
V	W	V-2	11.9	53.5	78.7	65.4	1.203	32.6	0.070%	1.600%	1.278%	1.621%	63.964%	137
V	W	V-3	11.9	55	83.1	66.9	1.242	33.8	0.029%	1.836%	0.879%	1.108%	74.165%	144
V	W	V-4	11.9	81.7	115.1	93.6	1.230	51.0	0.079%	2.411%	1.763%	2.102%	57.634%	133
V	W	V-5	11.9	52	79.5	63.9	1.244	16.1	0.041%	1.729%	0.671%	0.630%	68.263%	153
V	W	V-6	12.0	79.6	116.3	91.6	1.270	62.8	0.080%	2.655%	1.995%	2.286%	56.427%	111
V	W	V-7	11.9	55.4	81.5	67.3	1.211	22.7	0.040%	1.655%	0.984%	1.106%	65.125%	150
V	W	V-8	11.9	56	63.9	67.9	0.941	17.6	0.053%	1.291%	0.912%	1.106%	68.288%	142
V	W	V-9	11.8	36.2	54.6	48.0	1.138	10.4	0.032%	1.057%	0.687%	0.844%	73.180%	158
V	W	V-10	11.8	39.9	63.0	51.7	1.219	9.9	0.029%	1.410%	0.471%	0.729%	78.495%	145
V	W	V-11	12.1	82	113.8	94.1	1.209	46.5	0.186%	2.076%	1.666%	1.970%	59.982%	152
V	W	V-12	12.0	66.2	91.3	78.2	1.168	24.9	0.032%	1.899%	1.007%	1.723%	70.666%	152
V	W	V-13	12.2	67	90.8	79.2	1.146	20.1	0.093%	2.043%	1.126%	1.030%	73.533%	126
V	W	V-14	11.8	43.2	63.2	55.0	1.149	9.2	0.025%	1.309%	0.460%	0.564%	76.138%	185
V	W	V-15	11.7	38	55.5	49.7	1.117	14.2	0.024%	1.030%	0.670%	1.089%	69.676%	160
VI	W	VI-1	12.2	46.1	60.5	58.3	1.038	11.6	0.190%	1.248%	0.493%	0.792%	72.513%	156
VI	W	VI-2	12.2	49.1	57.5	61.3	0.938	12.3	0.436%	1.128%	0.441%	0.826%	72.433%	146
VI	W	VI-3	12.1	45.1	66.6	57.2	1.164	30.3	0.065%	1.207%	1.313%	1.965%	60.842%	139
VI	W	VI-4	12.1	32	38.9	44.1	0.882	14.6	0.300%	0.734%	0.609%	1.243%	68.862%	110

Company	C or W	Well Site	P _{bar} (psia)	P _{probe} (psig)	P _{BP} (psia)	P _{sc} (psia)	P _{BP} /P _{sc}	FGOR (scf/bbl)	CO ₂ (mole %)	CH ₄ (mole %)	C ₂ H ₆ (mole %)	C ₃ H ₈ (mole %)	C ₁₀₊ (mole %)	T _{probe} (°F)
VI	W	VI-5	12.2	40.5	59.1	52.7	1.121	14.6	0.281%	1.195%	0.578%	1.106%	70.545%	137
VI	W	VI-6	12.2	46.5	66.2	58.7	1.128	16.1	0.313%	1.298%	0.502%	1.085%	69.066%	153
VI	W	VI-7	12.2	44.4	50.0	56.6	0.883	12.0	0.245%	0.928%	0.504%	1.005%	72.391%	152
VI	W	VI-8	12.2	42.7	54.6	54.9	0.995	11.8	0.195%	1.084%	0.517%	0.911%	72.660%	152
VI	W	VI-9	12.2	45	57.8	57.2	1.010	9.6	0.238%	1.124%	0.336%	0.676%	72.820%	162
VI	W	VI-10	12.2	42.4	50.6	54.6	0.927	10.6	0.505%	0.979%	0.418%	0.743%	73.642%	159
VI	W	VI-11	12.2	44.3	52.9	56.5	0.936	14.8	0.282%	0.949%	0.580%	1.196%	70.308%	143
VI	W	VI-12	12.2	46.3	66.5	58.5	1.137	14.6	0.377%	1.228%	0.603%	1.003%	71.366%	162
VI	W	VI-13	12.2	44.8	62.9	57.0	1.104	10.5	0.105%	1.323%	0.342%	0.739%	71.791%	156
VI	W	VI-14	12.2	45.5	65.1	57.7	1.128	15.2	0.346%	1.246%	0.639%	1.124%	71.458%	142
VI	W	VI-15	12.2	52.1	70.2	64.3	1.092	17.7	0.188%	1.307%	0.697%	1.177%	67.936%	163
VII	W	VII-1	12.2	55.4	82.2	67.6	1.216	24.6	0.048%	1.669%	1.272%	1.434%	67.242%	151
VII	W	VII-2	12.2	44.1	69.7	56.3	1.238	20.6	0.046%	1.590%	1.040%	1.238%	65.104%	125
VII	W	VII-3	12.2	40.1	66.4	52.3	1.270	29.6	0.081%	1.365%	1.178%	1.566%	61.680%	129
VII	W	VII-4	12.2	31.5	46.4	43.7	1.062	7.3	0.015%	1.178%	0.540%	0.614%	79.915%	136
VII	W	VII-5 (W4)	12.2	39.1	42.1	51.3	0.821	8.6	0.043%	1.014%	0.673%	0.828%	79.748%	125
VII	W	VII-6	12.2	40.7	54.4	52.9	1.028	22.2	0.023%	1.305%	0.929%	2.042%	65.828%	111
VII	W	VII-7	12.3	67.5	89.2	79.8	1.118	31.9	0.069%	1.918%	1.345%	1.868%	66.102%	137
VII	W	VII-8 (W3)	12.3	70.8	66.5	83.1	0.800	18.1	0.041%	1.342%	1.031%	1.214%	71.075%	159
VII	W	VII-9	12.3	75.7	109.4	88.0	1.243	43.3	0.069%	2.387%	1.597%	2.037%	61.344%	143
VII	W	VII-10	12.3	44.6	70.2	56.9	1.234	28.9	0.061%	1.420%	1.215%	1.832%	63.226%	134
VII	W	VII-11	12.2	37.8	45.1	50.0	0.902	20.1	0.024%	0.946%	0.912%	1.969%	67.010%	125
VII	W	VII-12	12.2	33.3	48.9	45.5	1.075	23.8	0.027%	1.099%	0.953%	1.897%	67.373%	113
VII	W	VII-13	12.2	43.1	57.1	55.3	1.033	14.3	0.051%	1.421%	0.899%	0.982%	73.473%	120
VII	W	VII-14	12.2	42.1	52.0	54.3	0.958	15.0	0.044%	1.276%	0.769%	1.241%	70.451%	116
VII	W	VII-15	12.2	58.2	78.5	70.4	1.115	31.8	0.044%	1.925%	1.372%	2.238%	70.131%	120

Appendix D: AST Hydrocarbon Composition Data

Hydrocarbon Composition Data Determined by Alliance Source Testing

Hydrocarbon Composition Data for Flash Gas

Table E-1a. Hydrocarbon composition of flash gas (weight percent) at oil wells associated with the Green River formation . Well IDs are anonymized. Red indicates an outlier well detected by the z-score method.

Compound	IV-2	V-12	VI-5	VI-14	VI-7	VI-11	VI-13	VI-4	VI-6	VI-15	VI-9	VI-10	VII-9	VII-11	VII-12	VII-6	VII-14	VII-7	VII-13
Methane	39.830	11.539	12.555	12.998	13.192	14.544	19.675	7.173	12.380	11.332	21.533	16.769	8.549	6.826	6.308	8.809	13.400	9.339	10.794
Ethane	5.425	9.935	8.899	9.897	9.636	9.948	6.990	8.857	7.195	9.202	8.793	9.955	9.735	10.156	8.736	9.649	11.963	10.766	13.056
Propane	7.549	18.898	14.985	17.018	15.742	16.422	13.543	17.851	15.548	15.733	15.758	16.031	14.957	22.281	18.827	21.341	18.764	16.873	15.716
Isobutane	2.543	5.896	4.096	4.566	4.305	4.603	3.734	5.162	4.706	4.579	4.383	4.337	4.157	8.605	7.156	7.080	5.688	4.367	3.991
n-Butane	5.922	12.935	10.974	12.240	11.775	12.334	9.840	13.790	12.934	12.225	11.386	11.625	14.004	17.687	16.224	16.727	13.620	14.353	12.173
Isopentane	3.518	6.482	5.819	6.443	6.021	6.340	5.494	7.294	7.263	6.399	6.211	6.212	4.990	8.074	7.636	6.828	6.246	4.914	4.253
n-Pentane	4.659	6.786	7.008	7.432	7.789	8.159	6.014	8.807	8.343	7.941	7.474	7.596	10.602	8.929	9.188	8.310	7.120	9.791	8.928
Cyclopentane	0.397	0.950	0.716	0.896	0.811	0.919	0.782	0.921	1.096	0.852	1.180	0.901	0.596	0.656	0.704	0.606	0.644	0.541	0.395
n-Hexane	5.063	4.545	6.699	5.126	5.826	6.290	11.381	5.864	5.703	7.292	8.651	6.797	9.881	6.408	5.947	5.571	6.766	6.470	6.907
Cyclohexane	1.430	1.809	1.523	1.655	1.801	1.837	1.556	1.967	1.950	1.964	1.946	1.842	1.790	1.214	1.436	1.158	1.409	1.531	1.503
Heptanes	14.900	11.396	20.309	13.779	13.977	9.380	13.088	12.230	14.540	12.956	3.141	7.215	12.531	3.502	11.196	9.645	5.808	14.372	14.720
Methylcyclohexane	2.066	2.104	1.608	1.638	1.966	1.850	1.489	2.009	1.516	2.382	1.873	2.044	1.996	1.400	1.647	1.355	1.886	1.713	1.783
2,2,4 Trimethylpentane	0.044	0.037	0.060	0.044	0.057	0.074	0.045	0.062	0.077	0.079	0.089	0.054	0.031	0.026	0.027	0.042	0.076	0.027	0.021
Benzene	0.337	0.327	0.266	0.271	0.402	0.288	0.257	0.325	0.152	0.348	0.250	0.538	0.339	0.254	0.277	0.184	0.205	0.283	0.297
Toluene	0.494	0.531	0.386	0.380	0.411	0.307	0.398	0.502	0.345	0.513	0.477	0.537	0.556	0.299	0.404	0.204	0.354	0.454	0.593
Ethylbenzene	0.036	0.062	0.090	0.076	0.071	0.078	0.130	0.086	0.104	0.060	0.167	0.115	0.041	0.039	0.043	0.027	0.000	0.027	0.029
Xylenes	0.307	0.346	0.377	0.364	0.444	0.396	0.227	0.471	0.442	0.435	0.540	0.316	0.291	0.155	0.221	0.116	0.422	0.209	0.326
Octanes	1.936	2.065	1.054	1.845	2.065	2.568	1.914	2.771	2.128	2.083	2.409	3.236	1.722	1.642	1.347	1.003	2.324	1.383	1.806
Nonanes	3.181	2.992	2.292	2.995	3.341	3.209	3.119	3.454	3.236	3.266	2.752	3.285	2.959	1.595	2.415	1.217	2.930	2.314	2.412
Decanes plus	0.362	0.367	0.286	0.336	0.370	0.455	0.326	0.404	0.341	0.360	0.985	0.595	0.273	0.253	0.262	0.129	0.374	0.274	0.297
TOTAL	100																		

Table D-1b. Z-scores calculated for hydrocarbon composition of flash gas at oil wells associated with the Green River formation. Well IDs are anonymized. Red indicates an outlier with an absolute z-score larger than $z_{th}=3$.

Compound	IV-2	V-12	VI-5	VI-14	VI-7	VI-11	VI-13	VI-4	VI-6	VI-15	VI-9	VI-10	VII-9	VII-11	VII-12	VII-6	VII-14	VII-7	VII-13
Methane	3.5	-0.3	-0.1	-0.1	0.0	0.1	0.8	-0.8	-0.2	-0.3	1.1	0.4	-0.7	-0.9	-1.0	-0.6	0.0	-0.6	-0.4
Ethane	-2.4	0.3	-0.3	0.3	0.1	0.3	-1.4	-0.3	-1.3	-0.1	-0.4	0.3	0.2	0.4	-0.4	0.1	1.5	0.8	2.2
Propane	-2.9	0.8	-0.5	0.2	-0.3	0.0	-1.0	0.4	-0.3	-0.3	-0.2	-0.2	-0.5	1.9	0.7	1.6	0.7	0.1	-0.3
Isobutane	-1.7	0.7	-0.6	-0.3	-0.5	-0.2	-0.9	0.2	-0.2	-0.3	-0.4	-0.4	-0.6	2.6	1.6	1.5	0.5	-0.4	-0.7
n-Butane	-2.6	0.1	-0.7	-0.2	-0.4	-0.2	-1.1	0.4	0.1	-0.2	-0.5	-0.4	0.5	1.9	1.3	1.5	0.3	0.6	-0.2
Isopentane	-2.3	0.3	-0.3	0.3	-0.1	0.2	-0.6	1.0	1.0	0.2	0.1	0.1	-1.0	1.7	1.3	0.6	0.1	-1.1	-1.7
n-Pentane	-2.4	-0.9	-0.7	-0.4	-0.1	0.2	-1.4	0.6	0.3	0.0	-0.3	-0.3	2.0	0.7	0.9	0.3	-0.6	1.4	0.7
Cyclopentane	-1.7	0.9	-0.2	0.6	0.2	0.7	0.1	0.7	1.5	0.4	1.9	0.6	-0.8	-0.5	-0.3	-0.8	-0.6	-1.1	-1.7
n-Hexane	-1.0	-1.3	0.0	-0.9	-0.5	-0.2	2.8	-0.5	-0.6	0.4	1.2	0.1	1.9	-0.2	-0.4	-0.7	0.0	-0.1	0.1
Cyclohexane	-0.9	0.6	-0.5	0.0	0.6	0.7	-0.4	1.3	1.2	1.2	1.2	0.8	0.6	-1.7	-0.8	-1.9	-0.9	-0.5	-0.6
Heptanes	0.8	0.0	2.1	0.5	0.6	-0.5	0.4	0.2	0.7	0.3	-2.0	-1.0	0.2	-1.9	-0.1	-0.4	-1.3	0.7	0.8
Methylcyclohexane	1.0	1.1	-0.7	-0.6	0.6	0.2	-1.2	0.7	-1.1	2.1	0.2	0.9	0.7	-1.5	-0.6	-1.7	0.3	-0.3	-0.1
2,2,4 Trimethylpentane	-0.3	-0.7	0.4	-0.4	0.3	1.1	-0.3	0.5	1.2	1.3	1.8	0.1	-1.0	-1.2	-1.1	-0.4	1.2	-1.1	-1.5
Benzene	0.5	0.4	-0.3	-0.3	1.3	-0.1	-0.4	0.4	-1.7	0.6	-0.5	2.9	0.5	-0.5	-0.2	-1.3	-1.1	-0.1	0.0
Toluene	0.6	1.0	-0.4	-0.5	-0.2	-1.2	-0.3	0.7	-0.8	0.8	0.5	1.1	1.3	-1.3	-0.2	-2.2	-0.7	0.2	1.6
Ethylbenzene	-0.8	-0.1	0.5	0.2	0.1	0.2	1.5	0.5	0.9	-0.2	2.4	1.2	-0.6	-0.7	-0.6	-1.0	-1.6	-1.0	-0.9
Xylenes	-0.3	0.1	0.4	0.2	0.9	0.5	-1.0	1.2	0.9	0.9	1.8	-0.2	-0.4	-1.6	-1.0	-1.9	0.7	-1.1	-0.1
Octanes	0.0	0.2	-1.6	-0.2	0.2	1.1	-0.1	1.4	0.3	0.2	0.8	2.3	-0.4	-0.6	-1.1	-1.7	0.6	-1.0	-0.3
Nonanes	0.6	0.3	-0.8	0.3	0.9	0.7	0.5	1.1	0.7	0.8	-0.1	0.8	0.3	-2.0	-0.6	-2.6	0.2	-0.8	-0.6
Decanes plus	0.0	0.0	-0.5	-0.2	0.0	0.5	-0.3	0.2	-0.2	-0.1	3.5	1.3	-0.6	-0.7	-0.6	-1.4	0.0	-0.6	-0.4

Table D-2a. Hydrocarbon composition of flash gas (weight percent) at oil wells associated with the Green River - Wasatch formation. Well IDs are anonymized. Red indicates outlier wells detected by the z-score method.

Compound	IV-1	IV-6	IV-4	IV-3	V-6	V-3	V-9	V-14	V-1	V-4	V-5	VI-11	VI-3	VI-12	VI-2	VI-1	VII-8	VII-5	VII-15	VII-3	VII-13	VII-4
Methane	20.087	27.013	8.543	59.370	6.996	0.146	15.686	24.771	19.857	8.449	17.605	10.414	5.889	13.192	16.755	17.231	13.089	17.896	8.845	6.905	25.460	28.304
Ethane	8.314	12.175	10.853	7.834	9.181	1.476	13.968	12.073	13.334	10.657	10.293	9.561	10.448	9.636	9.531	9.664	15.509	15.462	10.528	9.659	20.316	16.192
Propane	13.244	12.975	18.310	7.989	13.291	9.643	15.256	13.492	15.336	15.673	9.712	19.565	17.439	15.742	17.046	14.370	18.705	15.991	19.979	14.234	17.223	14.832
Isobutane	3.906	2.703	5.458	1.504	4.618	5.178	3.660	3.578	4.184	5.116	2.777	5.843	6.104	4.305	4.783	3.929	4.507	3.474	5.940	5.306	3.230	3.873
n-Butane	10.724	7.735	14.042	3.307	12.022	20.284	9.350	8.570	9.514	14.210	6.730	16.192	12.579	11.775	13.649	10.785	13.874	8.841	14.908	13.254	8.767	6.766
Isopentane	5.658	3.146	6.409	0.950	6.951	12.910	4.477	4.506	4.613	7.622	4.109	8.559	6.822	6.021	7.015	5.861	4.734	3.331	5.885	6.969	2.340	2.905
n-Pentane	8.163	5.717	9.081	1.185	10.210	15.962	6.072	5.981	6.418	11.687	5.952	9.595	7.697	7.789	8.927	7.582	9.299	4.952	7.469	10.090	4.792	3.369
Cyclopentane	0.469	0.387	0.440	0.296	0.414	1.208	0.353	0.875	0.495	0.472	0.323	0.990	0.553	0.811	0.940	0.928	0.537	0.266	0.536	0.266	0.208	0.269
n-Hexane	6.907	6.805	6.005	2.187	8.175	10.849	6.198	6.621	4.989	9.499	8.921	5.546	5.650	5.826	5.952	5.225	7.718	7.145	4.625	9.644	4.651	3.590
Cyclohexane	1.542	1.459	1.306	0.386	1.719	3.931	1.458	2.172	1.563	2.039	1.873	1.965	2.115	1.801	2.143	1.943	1.679	1.080	1.329	1.337	0.753	0.947
Heptanes	12.560	11.181	13.152	10.155	16.156	5.072	14.633	5.083	8.382	3.486	19.186	2.758	15.169	13.977	2.698	12.590	2.670	15.101	12.533	14.899	8.611	14.344
Methylcyclohexane	2.013	1.835	1.554	0.393	2.399	4.591	1.874	2.835	2.211	2.695	2.725	2.425	3.000	1.966	2.325	1.979	2.011	1.160	1.641	1.796	0.880	1.518
2,2,4 Trimethylpentane	0.034	0.047	0.032	0.000	0.034	0.070	0.055	0.051	0.070	0.047	0.033	0.057	0.045	0.057	0.063	0.048	0.038	0.018	0.066	0.027	0.011	0.059
Benzene	0.394	0.414	0.507	0.000	0.488	0.835	0.466	0.413	0.212	0.580	0.673	0.419	1.032	0.402	0.593	0.354	0.250	0.000	0.327	0.480	0.160	0.130
Toluene	0.224	0.349	0.345	0.096	0.816	1.084	0.635	0.684	0.525	1.220	1.002	0.490	0.973	0.411	0.562	0.485	0.422	0.208	0.466	0.379	0.294	0.386
Ethylbenzene	0.000	0.000	0.000	0.000	0.025	0.063	0.049	0.111	0.000	0.047	0.041	0.079	0.052	0.071	0.133	0.086	0.000	0.000	0.000	0.000	0.015	0.000
Xylenes	0.172	0.278	0.279	0.111	0.443	0.446	0.335	0.515	0.481	0.588	0.557	0.313	0.378	0.444	0.355	0.479	0.233	0.167	0.450	0.194	0.167	0.286
Octanes	2.127	2.453	1.599	1.355	2.099	2.466	1.998	2.704	3.634	2.083	2.527	1.981	1.763	2.065	2.068	2.685	1.503	1.673	1.527	2.087	0.894	2.169
Nonanes	3.094	2.949	1.851	2.268	3.611	3.346	3.101	3.629	3.598	2.852	4.490	2.406	2.043	3.341	3.334	3.376	2.463	2.892	2.622	2.197	1.120	0.000
Decanes plus	0.367	0.381	0.234	0.615	0.352	0.440	0.378	1.334	0.585	0.977	0.471	0.842	0.249	0.370	1.127	0.398	0.759	0.342	0.322	0.277	0.109	0.060
TOTAL	100																					

Table D-2b. Z-scores calculated for hydrocarbon composition of flash gas at oil wells associated with the Green River-Wasatch formation. Well IDs are anonymized. Red indicates an outlier with an absolute z-score larger than $z_{th}=3$.

Compound	IV-1	IV-6	IV-4	IV-3	V-6	V-3	V-9	V-14	V-1	V-4	V-5	VI-11	VI-3	VI-12	VI-2	VI-1	VII-8	VII-5	VII-15	VII-3	VII-13	VII-4
Methane	0.3	0.8	-0.7	3.5	-0.8	-1.4	-0.1	0.6	0.2	-0.7	0.1	-0.5	-0.9	-0.3	0.0	0.0	-0.3	0.1	-0.7	-0.8	0.7	0.9
Ethane	-0.8	0.3	-0.1	-0.9	-0.5	-2.6	0.7	0.2	0.6	-0.1	-0.2	-0.4	-0.2	-0.4	-0.5	-0.4	1.2	1.1	-0.2	-0.4	2.4	1.3
Propane	-0.6	-0.6	1.1	-2.2	-0.5	-1.7	0.1	-0.5	0.1	0.2	-1.7	1.5	0.8	0.2	0.7	-0.2	1.2	0.3	1.6	-0.2	0.7	-0.1
Isobutane	-0.3	-1.3	1.0	-2.4	0.3	0.8	-0.5	-0.6	-0.1	0.7	-1.3	1.4	1.6	0.0	0.4	-0.3	0.2	-0.7	1.4	0.9	-0.9	-0.3
n-Butane	-0.1	-0.9	0.7	-2.1	0.2	2.4	-0.5	-0.7	-0.5	0.8	-1.2	1.3	0.3	0.1	0.6	-0.1	0.7	-0.6	1.0	0.5	-0.7	-1.2
Isopentane	0.0	-1.0	0.3	-1.8	0.6	2.9	-0.4	-0.4	-0.4	0.8	-0.6	1.2	0.5	0.2	0.6	0.1	-0.3	-0.9	0.1	0.6	-1.3	-1.1
n-Pentane	0.2	-0.6	0.5	-2.1	0.8	2.7	-0.5	-0.5	-0.4	1.3	-0.5	0.6	0.0	0.0	0.4	0.0	0.5	-0.9	-0.1	0.8	-0.9	-1.4
Cyclopentane	-0.3	-0.6	-0.4	-0.9	-0.5	2.3	-0.7	1.2	-0.2	-0.3	-0.8	1.6	0.0	0.9	1.4	1.3	0.0	-1.0	0.0	-1.0	-1.2	-1.0
n-Hexane	0.2	0.2	-0.2	-2.1	0.8	2.1	-0.1	0.1	-0.7	1.5	1.2	-0.5	-0.4	-0.3	-0.3	-0.6	0.6	0.3	-0.9	1.5	-0.9	-1.4
Cyclohexane	-0.2	-0.3	-0.5	-1.8	0.1	3.3	-0.3	0.7	-0.1	0.5	0.3	0.4	0.7	0.2	0.7	0.4	0.0	-0.8	-0.5	-0.5	-1.3	-1.0
Heptanes	0.4	0.1	0.5	-0.1	1.1	-1.1	0.8	-1.1	-0.5	-1.4	1.7	-1.6	0.9	0.7	-1.6	0.4	-1.6	0.9	0.4	0.8	-0.4	0.7
Methylcyclohexane	-0.1	-0.3	-0.6	-2.0	0.4	3.0	-0.2	0.9	0.2	0.7	0.8	0.4	1.1	-0.1	0.3	-0.1	-0.1	-1.1	-0.5	-0.3	-1.4	-0.7
2,2,4 Trimethylpentane	-0.5	0.2	-0.7	-2.3	-0.5	1.4	0.6	0.4	1.4	0.2	-0.5	0.7	0.1	0.7	1.0	0.3	-0.3	-1.4	1.2	-0.9	-1.7	0.8
Benzene	-0.1	0.0	0.4	-1.7	0.3	1.7	0.2	0.0	-0.8	0.7	1.0	0.0	2.5	-0.1	0.7	-0.2	-0.7	-1.7	-0.4	0.3	-1.0	-1.2
Toluene	-1.1	-0.7	-0.7	-1.5	0.9	1.8	0.3	0.5	-0.1	2.2	1.5	-0.2	1.4	-0.5	0.0	-0.2	-0.4	-1.1	-0.3	-0.6	-0.8	-0.5
Ethylbenzene	-0.9	-0.9	-0.9	-0.9	-0.2	0.7	0.3	1.8	-0.9	0.3	0.1	1.1	0.4	0.9	2.4	1.2	-0.9	-0.9	-0.9	-0.9	-0.5	-0.9
Xylenes	-1.3	-0.5	-0.5	-1.7	0.7	0.7	-0.1	1.2	0.9	1.7	1.5	-0.3	0.2	0.7	0.0	0.9	-0.8	-1.3	0.7	-1.1	-1.3	-0.4
Octanes	0.1	0.7	-0.8	-1.3	0.1	0.7	-0.1	1.1	2.8	0.0	0.8	-0.2	-0.5	0.0	0.0	1.1	-1.0	-0.7	-1.0	0.0	-2.1	0.2
Nonanes	0.4	0.2	-0.9	-0.5	0.9	0.6	0.4	0.9	0.9	0.1	1.8	-0.4	-0.7	0.6	0.6	0.6	-0.3	0.1	-0.1	-0.6	-1.7	-2.9
Decanes plus	-0.4	-0.4	-0.8	0.4	-0.5	-0.2	-0.4	2.6	0.3	1.5	-0.1	1.1	-0.8	-0.4	1.9	-0.3	0.8	-0.5	-0.5	-0.7	-1.2	-1.4

Table D-2. Hydrocarbon composition of flash gas (weight percent) at oil wells associated with the Wasatch formation. Well IDs are anonymized. Red indicates outlier samples screened out to maintain average values with RSD < 33.3%.

Compound	V-13	V-7	V-10	V-15	V-11	V-2	V-8	VII-10	VII-2
Methane	16.664	11.421	22.647	11.055	6.829	7.408	11.823	7.535	12.791
Ethane	14.529	10.717	10.510	10.370	9.415	9.805	13.042	10.363	12.723
Propane	14.208	12.834	14.819	15.990	13.632	14.311	16.608	16.984	15.129
Isobutane	4.990	3.628	3.814	4.887	6.333	4.535	4.956	5.296	4.312
n-Butane	9.358	9.073	8.525	10.413	12.474	12.462	12.901	14.812	11.284
Isopentane	5.101	4.913	3.893	5.444	7.710	6.841	6.767	6.332	4.840
n-Pentane	5.395	6.765	4.762	5.836	8.267	9.882	9.819	10.203	8.108
Cyclopentane	0.193	0.388	0.533	0.748	0.290	0.287	0.383	0.416	0.378
n-Hexane	6.818	6.262	4.029	4.983	6.752	7.579	8.704	6.368	6.825
Cyclohexane	1.652	1.782	1.457	1.684	2.300	1.511	1.820	1.479	1.473
Heptanes	10.116	22.208	15.686	18.993	14.379	16.120	3.013	13.740	15.555
Methylcyclohexane	2.348	2.507	1.847	2.328	3.351	1.939	2.560	1.835	1.787
2,2,4 Trimethylpentane	0.000	0.000	0.052	0.097	0.036	0.017	0.039	0.000	0.026
Benzene	1.307	0.869	0.239	0.422	1.220	0.491	0.473	0.286	0.371
Toluene	1.121	1.265	0.414	0.779	1.511	0.718	0.845	0.484	0.488
Ethylbenzene	0.059	0.070	0.089	0.068	0.038	0.025	0.000	0.000	0.000
Xylenes	0.658	0.629	0.428	0.330	0.619	0.356	0.473	0.250	0.241
Octanes	2.269	1.235	2.468	2.163	1.475	1.803	2.144	1.443	1.393
Nonanes	2.811	3.088	3.301	2.997	3.067	3.543	2.696	1.948	2.048
Decanes plus	0.405	0.347	0.486	0.415	0.303	0.368	0.935	0.226	0.226
TOTAL	100								

Table D-3. Hydrocarbon composition of flash gas (weight percent) at gas wells associated with the Mesa Verde formation. Well IDs are anonymized.

Compound	III-1	III-7	III-5	III-3	III-8	III-6	III-2	III-4
Methane	33.578	24.477	37.889	30.166	38.241	26.122	31.540	27.503
Ethane	20.302	20.015	21.023	19.789	19.618	17.467	18.486	19.749
Propane	23.333	26.320	21.312	24.576	22.614	26.537	23.721	25.707
Isobutane	6.366	8.214	5.937	7.179	6.107	8.138	7.244	7.694
n-Butane	8.621	11.482	7.442	9.978	8.165	11.321	10.066	10.572
Isopentane	3.186	4.053	2.264	3.577	2.444	4.149	3.859	4.008
n-Pentane	2.421	3.052	1.671	2.749	1.771	3.371	2.837	2.832
Cyclopentane	0.128	0.129	0.085	0.147	0.080	0.151	0.116	0.123
n-Hexane	0.721	0.770	0.742	0.761	0.393	1.087	0.890	0.712
Cyclohexane	0.348	0.393	0.420	0.345	0.180	0.492	0.364	0.319
Heptanes	0.205	0.163	0.143	0.119	0.006	0.154	0.160	0.130
Methylcyclohexane	0.442	0.546	0.644	0.367	0.236	0.654	0.436	0.379
2,2,4 Trimethylpentane	0.002	0.008	0.008	0.006	0.002	0.005	0.008	0.005
Benzene	0.059	0.073	0.091	0.053	0.033	0.082	0.056	0.056
Toluene	0.088	0.116	0.156	0.057	0.049	0.122	0.069	0.076
Ethylbenzene	0.004	0.003	0.005	0.002	0.002	0.003	0.002	0.003
Xylenes	0.039	0.041	0.041	0.021	0.020	0.029	0.027	0.025
Octanes	0.071	0.053	0.060	0.037	0.013	0.045	0.053	0.048
Nonanes	0.077	0.078	0.056	0.064	0.019	0.064	0.058	0.051
Decanes plus	0.008	0.012	0.010	0.009	0.006	0.009	0.008	0.008
TOTAL	100							

Table D-4. Hydrocarbon composition of flash gas (weight percent) at gas wells associated with the Wasatch - Mesa Verde formation. Well IDs are anonymized. Red indicates outlier samples screened out to maintain average values with RSD < 33.3%.

Compound	I-5	I-10	I-1	I-4	II-4	II-2	II-3	II-7	II-1
Methane	73.387	53.373	57.967	77.893	66.492	59.471	65.752	21.840	32.469
Ethane	14.462	23.544	18.982	10.979	18.525	19.667	17.625	19.909	17.682
Propane	6.315	12.529	10.903	4.257	7.203	8.952	7.164	20.025	11.100
Isobutane	1.600	3.114	3.293	1.165	1.593	2.345	1.772	7.178	3.752
n-Butane	1.442	3.112	3.408	1.055	1.923	2.672	2.071	9.706	4.501
Isopentane	0.687	1.344	1.692	0.590	0.739	1.269	0.960	5.595	2.711
n-Pentane	0.399	0.826	1.112	0.345	0.563	0.928	0.707	4.658	1.840
Cyclopentane	0.039	0.042	0.048	0.035	0.032	0.039	0.040	0.286	0.161
n-Hexane	0.315	0.657	0.918	0.280	0.362	0.687	0.557	3.507	2.460
Cyclohexane	0.214	0.219	0.289	0.238	0.210	0.377	0.328	1.843	0.984
Heptanes	0.181	0.315	0.274	1.939	0.857	1.222	0.912	0.000	12.838
Methylcyclohexane	0.284	0.362	0.524	0.350	0.393	0.779	0.649	2.717	2.512
2,2,4 Trimethylpentane	0.003	0.000	0.003	0.003	0.004	0.008	0.003	0.025	0.031
Benzene	0.163	0.088	0.112	0.191	0.057	0.112	0.090	0.694	0.493
Toluene	0.267	0.169	0.215	0.338	0.120	0.296	0.206	1.243	1.701
Ethylbenzene	0.006	0.009	0.006	0.008	0.021	0.021	0.015	0.027	0.105
Xylenes	0.093	0.106	0.079	0.130	0.108	0.214	0.155	0.324	1.226
Octanes	0.068	0.104	0.092	0.088	0.388	0.459	0.384	0.042	1.208
Nonanes	0.063	0.074	0.069	0.112	0.345	0.407	0.514	0.166	2.100
Decanes plus	0.011	0.012	0.011	0.004	0.066	0.077	0.095	0.214	0.127
TOTAL	100								

Hydrocarbon Composition Data for Raw Gas

Table D-5a. Hydrocarbon composition of raw gas (weight percent) at oil wells associated with the Green River formation. Well IDs are anonymized. Red indicates outlier wells detected by the z-score method.

Compound	IV-2	V-12	VI-5	VI-14	VI-7	VI-11	VI-13	VI-4	VI-6	VI-15	VI-9	VI-10	VII-9	VII-11	VII-12	VII-6	VII-14	VII-7	VII-13
Methane	89.888	58.443	55.172	39.763	43.161	50.272	55.874	46.593	49.888	42.102	54.622	54.311	52.533	35.367	53.669	53.457	57.535	49.603	44.263
Ethane	2.930	11.136	10.610	7.944	8.717	9.685	7.131	9.927	7.906	9.556	7.117	8.659	14.475	11.463	12.767	11.774	11.376	14.101	13.494
Propane	1.031	10.538	10.548	9.545	10.755	9.457	8.196	11.177	9.937	9.955	7.438	8.623	10.466	14.469	12.287	12.621	9.429	11.259	9.071
Isobutane	0.246	2.389	2.217	2.560	2.814	2.162	2.061	2.622	2.339	2.583	1.652	1.957	1.881	4.770	3.043	3.010	2.151	2.074	1.972
n-Butane	0.472	4.463	4.911	6.805	7.092	5.180	4.854	6.396	5.656	6.541	3.833	4.876	5.407	9.118	5.701	6.267	4.031	5.945	5.900
Isopentane	0.232	1.925	2.266	4.556	4.047	2.868	2.873	3.430	3.179	4.064	2.078	2.775	1.715	4.805	2.201	2.281	1.962	1.993	2.437
n-Pentane	0.309	1.974	2.578	6.078	4.848	3.740	3.307	4.221	3.814	5.424	2.490	3.408	3.595	5.501	2.489	2.685	2.359	4.115	5.613
Cyclopentane	0.031	0.270	0.246	0.761	0.515	0.432	0.419	0.426	0.478	0.585	0.333	0.375	0.203	0.413	0.163	0.195	0.234	0.226	0.262
n-Hexane	0.317	0.997	1.468	4.593	3.085	2.660	2.183	2.430	2.657	3.982	2.210	2.350	2.548	2.680	1.054	1.238	1.464	2.934	4.794
Cyclohexane	0.106	0.479	0.449	1.343	0.923	0.819	0.740	0.685	0.877	1.195	0.869	0.737	0.517	0.660	0.266	0.313	0.457	0.576	0.923
Other hexanes	0.345	2.147	2.117	6.454	4.508	3.574	3.470	3.404	3.703	5.295	3.052	3.402	1.783	4.144	1.573	1.712	2.457	2.071	3.032
Heptanes	0.576	1.512	1.975	4.184	3.679	3.182	2.905	2.725	3.463	3.634	4.498	2.832	1.955	2.526	1.233	1.176	1.833	2.126	3.792
Methylcyclohexane	0.244	0.679	0.686	1.173	1.086	1.009	0.885	0.845	0.915	1.334	1.267	0.943	0.613	0.838	0.490	0.473	0.767	0.660	1.089
2,2,4 Trimethylpentane	0.000	0.001	0.002	0.003	0.003	0.002	0.002	0.002	0.002	0.003	0.003	0.002	0.001	0.002	0.001	0.001	0.001	0.001	0.001
Benzene	0.031	0.118	0.103	0.290	0.205	0.178	0.144	0.142	0.091	0.294	0.109	0.231	0.118	0.161	0.063	0.070	0.090	0.137	0.222
Toluene	0.068	0.198	0.207	0.300	0.305	0.307	0.242	0.236	0.255	0.335	0.350	0.243	0.185	0.208	0.141	0.095	0.181	0.195	0.380
Ethylbenzene	0.027	0.022	0.037	0.025	0.033	0.039	0.040	0.040	0.039	0.023	0.065	0.034	0.011	0.015	0.022	0.020	0.028	0.009	0.012
Xylenes	0.193	0.114	0.261	0.142	0.178	0.223	0.234	0.254	0.214	0.130	0.379	0.203	0.106	0.141	0.132	0.156	0.219	0.082	0.144
Octanes	1.033	1.111	1.867	1.847	2.088	2.290	2.120	2.219	2.332	1.637	3.775	1.977	1.197	1.534	1.609	1.154	1.871	1.108	1.570
Nonanes	0.546	0.173	0.408	0.216	0.258	0.212	0.319	0.327	0.230	0.218	0.421	0.309	0.181	0.259	0.148	0.300	0.212	0.225	0.300
Decanes plus	1.375	1.310	1.872	1.418	1.699	1.708	2.002	1.899	2.025	1.109	3.437	1.753	0.510	0.924	0.948	1.004	1.344	0.562	0.730
TOTAL	100	100	100	100	100	100	100	100	100	100	100	100	100	100	100	100	100	100	100

Table D-6b. Z-scores calculated for hydrocarbon composition of raw gas at oil wells associated with the Green River formation. Well IDs are anonymized. Red indicates an outliers with absolute z-scores larger than $z_{th}=3$.

Compound	IV-2	V-12	VI-5	VI-14	VI-7	VI-11	VI-13	VI-4	VI-6	VI-15	VI-9	VI-10	VII-9	VII-11	VII-12	VII-6	VII-14	VII-7	VII-13
Methane	3.4	0.6	0.3	-1.1	-0.8	-0.1	0.4	-0.5	-0.2	-0.9	0.2	0.2	0.1	-1.5	0.2	0.1	0.5	-0.2	-0.7
Ethane	-2.5	0.4	0.2	-0.7	-0.5	-0.1	-1.0	0.0	-0.8	-0.2	-1.0	-0.5	1.6	0.5	1.0	0.6	0.5	1.4	1.2
Propane	-3.3	0.3	0.3	-0.1	0.3	-0.1	-0.6	0.5	0.0	0.0	-0.9	-0.5	0.2	1.7	0.9	1.0	-0.2	0.5	-0.3
Isobutane	-2.5	0.1	-0.1	0.3	0.6	-0.2	-0.3	0.3	0.0	0.3	-0.8	-0.5	-0.5	2.9	0.8	0.8	-0.2	-0.3	-0.4
n-Butane	-2.9	-0.6	-0.3	0.8	1.0	-0.2	-0.3	0.6	0.1	0.6	-0.9	-0.3	0.0	2.1	0.1	0.5	-0.8	0.3	0.3
Isopentane	-2.2	-0.7	-0.4	1.7	1.2	0.1	0.1	0.6	0.4	1.2	-0.6	0.0	-0.9	1.9	-0.5	-0.4	-0.7	-0.7	-0.3
n-Pentane	-2.2	-1.1	-0.7	1.7	0.8	0.1	-0.2	0.4	0.1	1.2	-0.8	-0.1	0.0	1.3	-0.8	-0.6	-0.8	0.3	1.4
Cyclopentane	-1.8	-0.4	-0.6	2.4	1.0	0.5	0.4	0.5	0.8	1.4	-0.1	0.2	-0.8	0.4	-1.1	-0.9	-0.7	-0.7	-0.5
n-Hexane	-1.8	-1.2	-0.8	1.8	0.6	0.2	-0.2	0.0	0.2	1.3	-0.2	0.0	0.1	0.2	-1.1	-1.0	-0.8	0.4	2.0
Cyclohexane	-1.8	-0.7	-0.7	2.1	0.8	0.4	0.2	0.0	0.6	1.7	0.6	0.2	-0.5	-0.1	-1.3	-1.2	-0.7	-0.3	0.8
Other hexanes	-1.9	-0.6	-0.7	2.4	1.0	0.4	0.3	0.2	0.4	1.6	0.0	0.2	-0.9	0.8	-1.0	-0.9	-0.4	-0.7	0.0
Heptanes	-1.9	-1.0	-0.6	1.4	1.0	0.5	0.3	0.1	0.8	0.9	1.7	0.2	-0.6	-0.1	-1.3	-1.3	-0.7	-0.5	1.1
Methylcyclohexane	-2.1	-0.6	-0.5	1.2	0.9	0.6	0.2	0.0	0.3	1.7	1.5	0.4	-0.8	0.0	-1.2	-1.3	-0.3	-0.6	0.9
2,2,4 Trimethylpentane	-1.5	-0.5	-0.1	1.5	1.1	0.8	0.3	0.3	-0.1	1.8	1.1	0.8	-1.3	0.2	-0.8	-0.8	-0.3	-1.3	-1.2
Benzene	-1.6	-0.4	-0.6	1.9	0.8	0.4	0.0	-0.1	-0.8	2.0	-0.5	1.1	-0.4	0.2	-1.1	-1.0	-0.8	-0.1	1.0
Toluene	-2.0	-0.4	-0.3	0.8	0.9	0.9	0.1	0.0	0.3	1.2	1.4	0.1	-0.6	-0.3	-1.1	-1.7	-0.6	-0.5	1.8
Ethylbenzene	-0.1	-0.5	0.7	-0.2	0.3	0.8	0.8	0.9	0.8	-0.4	2.7	0.4	-1.3	-1.0	-0.5	-0.6	0.0	-1.5	-1.2
Xylenes	0.1	-1.0	1.1	-0.6	-0.1	0.5	0.7	1.0	0.4	-0.8	2.8	0.3	-1.1	-0.6	-0.7	-0.4	0.5	-1.5	-0.6
Octanes	-1.2	-1.1	0.1	0.1	0.4	0.8	0.5	0.6	0.8	-0.3	3.1	0.3	-1.0	-0.4	-0.3	-1.0	0.1	-1.1	-0.4
Nonanes	2.7	-1.1	1.3	-0.6	-0.2	-0.7	0.4	0.5	-0.5	-0.6	1.5	0.3	-1.0	-0.2	-1.3	0.2	-0.7	-0.5	0.2
Decanes plus	-0.1	-0.2	0.6	-0.1	0.4	0.4	0.8	0.7	0.8	-0.5	2.9	0.4	-1.4	-0.8	-0.7	-0.7	-0.2	-1.3	-1.1

Table D-6a. Hydrocarbon composition of raw gas (weight percent) at oil wells associated with the Green River - Wasatch formation. Well IDs are anonymized.

Compound	IV-1	IV-6	IV-4	IV-3	V-6	V-3	V-9	V-14	V-1	V-4	V-5	VI-11	VI-3	VI-12	VI-2	VI-1	VII-8	VII-5	VII-15	VII-3	VII-13	VII-4
Methane	70.023	77.959	68.031	92.295	42.410	55.772	51.032	51.501	67.701	38.827	60.727	47.195	41.585	48.628	48.022	49.698	56.940	55.570	61.248	56.989	51.533	64.938
Ethane	7.494	8.968	13.563	3.369	12.675	10.715	11.130	12.282	11.059	11.089	11.251	8.721	15.194	9.198	8.110	9.165	14.561	14.740	12.100	14.946	13.516	12.591
Propane	5.363	4.824	8.825	1.474	10.295	8.582	9.099	10.548	7.184	9.115	6.377	10.325	14.249	9.547	9.516	8.739	9.607	10.038	9.440	9.705	8.059	7.748
Isobutane	0.984	0.888	1.432	0.265	2.820	2.221	2.093	2.385	1.518	2.559	1.383	2.544	3.996	2.269	2.392	2.036	1.512	2.044	1.930	2.065	1.528	1.653
n-Butane	2.445	1.995	2.992	0.452	6.536	4.636	4.951	4.875	2.982	6.826	2.882	6.351	7.124	5.593	6.105	5.035	4.272	4.035	3.547	4.733	4.170	2.733
Isopentane	0.917	0.620	0.828	0.149	3.232	2.433	2.430	2.005	1.255	3.661	1.529	3.272	3.202	3.137	3.374	3.033	1.350	1.567	1.423	1.825	1.554	1.110
n-Pentane	1.390	0.965	1.161	0.174	4.621	3.096	3.234	2.414	1.646	5.573	2.110	3.855	3.491	4.112	4.201	4.092	2.633	2.188	1.687	2.760	3.770	1.290
Cyclopentane	0.121	0.067	0.056	0.012	0.154	0.255	0.194	0.237	0.117	0.197	0.110	0.415	0.209	0.452	0.451	0.489	0.156	0.125	0.149	0.098	0.195	0.086
n-Hexane	1.438	0.677	0.596	0.121	3.168	1.740	2.742	1.537	1.131	4.062	2.065	2.446	1.895	2.940	2.859	3.126	1.853	1.452	1.109	1.624	4.248	0.791
Cyclohexane	0.403	0.173	0.115	0.033	0.571	0.506	0.718	0.542	0.277	0.759	0.504	0.813	0.567	0.872	0.914	0.954	0.418	0.335	0.353	0.279	0.824	0.243
Other hexanes	1.309	0.564	0.590	0.140	2.885	2.556	2.844	2.191	1.336	3.609	2.041	3.742	2.487	3.937	3.875	4.158	1.386	1.521	1.609	1.492	2.491	1.106
Heptanes	2.526	0.695	0.529	0.211	3.709	1.944	3.406	2.075	1.242	6.361	2.639	3.255	1.678	3.321	3.609	3.584	1.612	1.747	1.460	1.254	3.768	1.121
Methylcyclohexane	0.824	0.224	0.161	0.068	1.053	0.745	1.121	0.885	0.407	1.069	0.846	1.275	0.754	1.069	1.123	1.096	0.548	0.634	0.571	0.403	1.009	0.467
2,2,4 Trimethylpentane	0.001	0.000	0.000	0.000	0.001	0.001	0.002	0.001	0.001	0.001	0.001	0.003	0.001	0.003	0.003	0.003	0.001	0.001	0.001	0.000	0.000	0.001
Benzene	0.145	0.068	0.051	0.013	0.195	0.070	0.332	0.132	0.054	0.241	0.225	0.216	0.343	0.263	0.277	0.229	0.100	0.080	0.117	0.097	0.252	0.047
Toluene	0.173	0.063	0.047	0.012	0.476	0.177	0.507	0.354	0.118	0.527	0.410	0.356	0.275	0.306	0.301	0.316	0.170	0.222	0.188	0.105	0.380	0.156
Ethylbenzene	0.029	0.008	0.006	0.005	0.029	0.030	0.031	0.049	0.011	0.032	0.053	0.048	0.024	0.035	0.040	0.033	0.017	0.028	0.027	0.006	0.011	0.027
Xylenes	0.147	0.057	0.054	0.038	0.365	0.261	0.237	0.552	0.110	0.283	0.416	0.271	0.162	0.214	0.224	0.196	0.193	0.265	0.198	0.081	0.132	0.294
Octanes	2.711	0.559	0.492	0.312	3.071	1.777	2.196	2.905	0.973	1.976	2.457	2.578	1.196	2.155	2.410	2.104	1.397	1.983	1.405	0.576	1.649	1.614
Nonanes	0.378	0.156	0.146	0.195	0.474	0.553	0.417	0.719	0.174	2.095	0.499	0.323	0.380	0.280	0.282	0.267	0.406	0.286	0.251	0.343	0.241	0.508
Decanes plus	1.180	0.471	0.325	0.662	1.258	1.928	1.286	1.810	0.704	1.138	1.477	1.995	1.187	1.668	1.911	1.649	0.869	1.141	1.188	0.619	0.670	1.473
TOTAL	100																					

Table D-7b. Z-scores calculated for hydrocarbon composition of raw gas at oil wells associated with the Green River formation. Well IDs are anonymized.

Compound	IV-1	IV-6	IV-4	IV-3	V-6	V-3	V-9	V-14	V-1	V-4	V-5	VI-11	VI-3	VI-12	VI-2	VI-1	VII-8	VII-5	VII-15	VII-3	VII-13	VII-4
Methane	1.0	1.6	0.9	2.8	-1.2	-0.1	-0.5	-0.5	0.8	-1.5	0.3	-0.8	-1.2	-0.7	-0.7	-0.6	0.0	-0.1	0.3	0.0	-0.4	0.6
Ethane	-1.3	-0.8	0.8	-2.7	0.5	-0.2	0.0	0.4	0.0	0.0	0.0	-0.9	1.4	-0.7	-1.1	-0.7	1.2	1.2	0.3	1.3	0.8	0.5
Propane	-1.3	-1.5	0.1	-2.8	0.7	0.0	0.2	0.8	-0.6	0.2	-0.9	0.7	2.3	0.4	0.4	0.1	0.4	0.6	0.3	0.4	-0.2	-0.3
Isobutane	-1.2	-1.4	-0.7	-2.2	1.2	0.4	0.2	0.6	-0.5	0.8	-0.7	0.8	2.7	0.4	0.6	0.1	-0.5	0.1	0.0	0.2	-0.5	-0.4
n-Butane	-1.1	-1.4	-0.8	-2.3	1.3	0.2	0.4	0.3	-0.8	1.4	-0.8	1.2	1.6	0.7	1.0	0.4	0.0	-0.2	-0.5	0.2	-0.1	-0.9
Isopentane	-1.0	-1.3	-1.1	-1.8	1.2	0.4	0.4	0.0	-0.7	1.6	-0.5	1.2	1.2	1.1	1.3	1.0	-0.6	-0.4	-0.6	-0.2	-0.4	-0.9
n-Pentane	-1.0	-1.3	-1.2	-1.9	1.4	0.3	0.4	-0.2	-0.8	2.0	-0.5	0.8	0.5	1.0	1.1	1.0	-0.1	-0.4	-0.8	0.0	0.7	-1.1
Cyclopentane	-0.6	-1.0	-1.0	-1.4	-0.3	0.4	0.0	0.3	-0.6	0.0	-0.6	1.6	0.1	1.9	1.9	2.1	-0.3	-0.5	-0.4	-0.7	0.0	-0.8
n-Hexane	-0.5	-1.2	-1.3	-1.7	1.1	-0.2	0.7	-0.4	-0.8	1.9	0.1	0.4	-0.1	0.9	0.8	1.0	-0.1	-0.5	-0.8	-0.3	2.0	-1.1
Cyclohexane	-0.4	-1.2	-1.4	-1.7	0.2	0.0	0.8	0.1	-0.9	0.9	0.0	1.1	0.2	1.3	1.5	1.6	-0.3	-0.6	-0.6	-0.8	1.2	-1.0
Other hexanes	-0.7	-1.4	-1.3	-1.7	0.6	0.3	0.6	0.0	-0.7	1.2	-0.1	1.3	0.3	1.5	1.4	1.7	-0.7	-0.6	-0.5	-0.6	0.3	-0.9
Heptanes	0.1	-1.2	-1.3	-1.5	0.9	-0.3	0.7	-0.2	-0.8	2.8	0.2	0.6	-0.5	0.7	0.9	0.9	-0.5	-0.4	-0.6	-0.8	1.0	-0.9
Methylcyclohexane	0.2	-1.5	-1.7	-1.9	0.9	0.0	1.1	0.4	-1.0	0.9	0.3	1.5	0.0	0.9	1.1	1.0	-0.6	-0.3	-0.5	-1.0	0.8	-0.8
2,2,4 Trimethylpentane	0.0	-1.0	-1.4	-1.4	-0.1	-0.1	0.4	0.2	-0.6	-0.2	0.1	1.9	-0.1	1.7	2.0	1.6	-0.7	0.0	-0.1	-1.1	-0.8	-0.4
Benzene	-0.2	-0.9	-1.1	-1.5	0.3	-0.9	1.7	-0.3	-1.1	0.8	0.6	0.6	1.8	1.0	1.2	0.7	-0.6	-0.8	-0.4	-0.6	0.9	-1.1
Toluene	-0.6	-1.3	-1.4	-1.6	1.5	-0.5	1.7	0.7	-0.9	1.8	1.0	0.7	0.1	0.3	0.3	0.4	-0.6	-0.2	-0.5	-1.0	0.8	-0.7
Ethylbenzene	0.2	-1.3	-1.4	-1.5	0.2	0.2	0.3	1.6	-1.1	0.4	1.8	1.5	-0.1	0.6	0.9	0.5	-0.6	0.1	0.0	-1.4	-1.0	0.1
Xylenes	-0.6	-1.3	-1.3	-1.4	1.2	0.4	0.2	2.7	-0.9	0.5	1.6	0.4	-0.4	0.0	0.1	-0.2	-0.2	0.4	-0.1	-1.1	-0.7	0.6
Octanes	1.2	-1.5	-1.5	-1.8	1.6	0.0	0.5	1.4	-1.0	0.3	0.9	1.0	-0.7	0.5	0.8	0.4	-0.4	0.3	-0.4	-1.4	-0.1	-0.2
Nonanes	-0.1	-0.7	-0.7	-0.6	0.1	0.3	0.0	0.7	-0.6	4.2	0.2	-0.3	-0.1	-0.4	-0.4	-0.4	-0.1	-0.4	-0.4	-0.2	-0.5	0.2
Decanes plus	-0.1	-1.5	-1.8	-1.1	0.1	1.4	0.2	1.2	-1.0	-0.1	0.5	1.6	0.0	0.9	1.4	0.9	-0.7	-0.1	0.0	-1.2	-1.1	0.5

Table DE-7. Hydrocarbon composition of raw gas (weight percent) at oil wells associated with the Wasatch formation. Well IDs are anonymized.

Compound	V-13	V-7	V-10	V-15	V-11	V-2	V-8	VII-10	VII-2
Methane	58.240	41.818	65.084	54.773	46.121	47.929	46.992	47.962	56.924
Ethane	16.175	11.276	8.450	11.643	14.805	13.778	12.861	15.785	14.271
Propane	8.391	8.920	7.418	9.752	9.965	10.200	8.574	13.003	9.488
Isobutane	1.957	2.264	1.679	2.228	2.877	2.430	1.903	2.714	1.959
n-Butane	2.958	5.501	3.550	4.141	4.902	5.885	4.366	6.533	4.557
Isopentane	1.463	3.280	1.561	1.963	2.842	2.859	2.304	2.282	1.687
n-Pentane	1.499	4.520	1.877	2.078	3.122	3.962	3.567	3.569	2.908
Cyclopentane	0.059	0.234	0.203	0.251	0.123	0.113	0.147	0.126	0.114
n-Hexane	1.127	4.168	1.243	1.244	2.253	2.445	3.437	1.936	2.051
Cyclohexane	0.365	1.063	0.454	0.500	0.687	0.392	0.703	0.332	0.378
Other hexanes	1.378	4.301	1.735	2.444	2.729	2.296	3.117	1.652	1.586
Heptanes	1.401	4.911	1.744	1.970	2.651	2.407	6.428	1.321	1.470
Methylcyclohexane	0.671	1.555	0.677	0.882	1.222	0.670	1.114	0.386	0.363
2,2,4 Trimethylpentane	0.001	0.002	0.001	0.002	0.001	0.001	0.001	0.000	0.000
Benzene	0.337	0.557	0.107	0.167	0.441	0.149	0.233	0.096	0.129
Toluene	0.411	0.815	0.198	0.364	0.673	0.354	0.497	0.119	0.132
Ethylbenzene	0.051	0.036	0.024	0.044	0.034	0.033	0.023	0.011	0.011
Xylenes	0.402	0.301	0.216	0.466	0.377	0.338	0.261	0.137	0.119
Octanes	1.562	2.669	1.508	2.477	2.449	2.288	2.368	0.997	0.937
Nonanes	0.439	0.503	0.566	0.738	0.526	0.373	0.274	0.337	0.237
Decanes plus	1.113	1.305	1.704	1.874	1.203	1.099	0.831	0.702	0.679
TOTAL	100								

Table D-8. Hydrocarbon composition of raw gas (weight percent) at gas wells associated with the Mesa Verde formation. Well IDs are anonymized.

Compound	III-1	III-7	III-5	III-3	III-8	III-6	III-2	III-4
Methane	70.254	72.933	75.188	72.075	71.856	65.089	72.827	68.052
Ethane	10.288	10.956	10.062	10.356	10.691	9.571	10.739	10.276
Propane	7.075	7.041	5.760	7.046	7.348	6.715	7.370	7.294
Isobutane	1.858	1.883	1.536	1.809	1.833	1.665	1.876	1.951
n-Butane	2.711	2.627	2.049	2.625	2.602	2.427	2.661	2.902
Isopentane	1.228	1.096	0.956	1.154	1.059	0.940	1.096	1.386
n-Pentane	1.079	0.853	0.798	1.019	0.924	0.815	0.910	1.254
Cyclopentane	0.071	0.050	0.047	0.063	0.060	0.050	0.052	0.086
n-Hexane	0.609	0.418	0.430	0.516	0.541	0.594	0.353	0.746
Cyclohexane	0.351	0.208	0.228	0.274	0.280	0.466	0.166	0.438
Other hexanes	1.021	0.761	0.746	0.870	0.885	0.867	0.652	1.241
Heptanes	0.776	0.343	0.469	0.546	0.543	2.277	0.291	1.017
Methylcyclohexane	0.757	0.298	0.410	0.519	0.499	2.595	0.271	0.855
2,2,4 Trimethylpentane	0.000	0.000	0.000	0.000	0.000	0.001	0.000	0.000
Benzene	0.066	0.053	0.069	0.052	0.056	0.074	0.036	0.089
Toluene	0.204	0.079	0.127	0.126	0.135	0.857	0.073	0.322
Ethylbenzene	0.017	0.005	0.010	0.009	0.006	0.048	0.007	0.019
Xylenes	0.178	0.054	0.122	0.091	0.066	0.420	0.079	0.202
Octanes	0.773	0.182	0.404	0.472	0.333	2.952	0.247	0.970
Nonanes	0.166	0.031	0.152	0.066	0.046	0.243	0.070	0.316
Decanes plus	0.518	0.131	0.439	0.311	0.236	1.334	0.226	0.584
TOTAL	100							

Table D-9. Hydrocarbon composition of raw gas (weight percent) at gas wells associated with the Wasatch - Mesa Verde formation. Well IDs are anonymized. Red indicates outlier samples screened out to maintain average values with RSD < 33.3%.

Compound	I-5	I-10	I-1	I-4	II-4	II-2	II-3	II-7	II-1
Methane	88.349	74.267	76.395	91.560	77.558	71.682	77.693	71.937	78.422
Ethane	5.542	10.926	9.705	4.062	9.692	9.246	10.129	11.331	10.443
Propane	1.759	5.229	4.250	1.062	4.605	4.737	4.784	6.207	4.312
Isobutane	0.458	2.930	1.184	0.278	1.212	1.345	1.277	1.947	1.232
n-Butane	0.468	1.657	1.367	0.277	1.509	2.176	1.557	2.469	1.246
Isopentane	0.266	0.894	0.758	0.170	0.740	1.132	0.758	1.407	0.700
n-Pentane	0.177	0.618	0.589	0.115	0.590	1.174	0.591	1.114	0.492
Cyclopentane	0.018	0.031	0.038	0.013	0.035	0.096	0.032	0.047	0.026
n-Hexane	0.122	0.335	0.420	0.104	0.356	0.797	0.327	0.382	0.302
Cyclohexane	0.159	0.155	0.294	0.146	0.240	0.391	0.194	0.240	0.168
Other hexanes	0.299	0.674	0.762	0.244	0.656	1.307	0.611	0.751	0.596
Heptanes	0.250	0.452	0.941	0.254	0.546	1.176	0.424	0.440	0.433
Methylcyclohexane	0.338	0.363	0.969	0.327	0.527	0.820	0.379	0.407	0.358
2,2,4 Trimethylpentane	0.000	0.000	0.000	0.000	0.000	0.001	0.000	0.000	0.000
Benzene	0.139	0.034	0.123	0.142	0.079	0.154	0.066	0.108	0.082
Toluene	0.453	0.136	0.544	0.417	0.190	0.357	0.141	0.241	0.204
Ethylbenzene	0.022	0.013	0.018	0.014	0.014	0.049	0.010	0.011	0.011
Xylenes	0.312	0.187	0.203	0.172	0.143	0.323	0.101	0.128	0.124
Octanes	0.329	0.452	0.806	0.283	0.554	1.339	0.436	0.325	0.369
Nonanes	0.112	0.147	0.143	0.058	0.159	0.421	0.135	0.109	0.098
Decanes plus	0.426	0.498	0.491	0.304	0.596	1.277	0.355	0.400	0.380
TOTAL	100								

Appendix E: Uinta Basin Profiles as Column-wise and Throughput-Weighted Averages

Column-wise Average Results

	Gas well - flash gas		Gas well - raw gas		Oil well – flash gas		Oil well – raw gas	
METHANE	46.0%	±36.8%	73.1%	±7.4%	13.8%	±13.7%	52.4%	±17.0%
ETHANE	18.6%	±5.6%	10.3%	±1.2%	4.0%	±10.4%	11.4%	±5.0%
PROPANE	16.4%	±16.9%	6.0%	±2.4%	5.5%	±15.9%	9.6%	±3.8%
ISOBUTANE	4.72%	±5.2%	1.70%	±0.9%	2.36%	±4.7%	2.24%	±1.3%
N-BUTANE	6.11%	±7.8%	2.17%	±1.1%	5.39%	±12.1%	5.05%	±2.9%
ISOPENTANE	2.35%	±2.7%	1.02%	±0.5%	2.72%	±5.9%	2.44%	±1.9%
N-PENTANE	1.71%	±2.1%	0.85%	±0.5%	3.50%	±7.9%	3.29%	±2.5%
CYCLOPENTANE	0.09%	±0.1%	0.05%	±0.0%	0.50%	±0.6%	0.26%	±0.3%
N-HEXANE	0.77%	±1.0%	0.48%	±0.3%	3.22%	±6.6%	2.30%	±2.1%
CYCLOHEXANE	0.36%	±0.4%	0.27%	±0.2%	0.59%	±1.7%	0.61%	±0.5%
HEPTANES	1.23%	±6.3%	1.54%	±1.3%	10.40%	±11.6%	5.34%	±4.6%
METHYL-CYCLOHEXANE	0.60%	±1.1%	0.67%	±1.2%	0.88%	±2.0%	0.84%	±0.6%
2,2,4 TRIMETHYL-PENTANE	0.0063%	0.0140%	0.0003%	0.0006%	0.0418%	0.0466%	0.0015%	0.0017%
BENZENE	0.11%	0.22%	0.08%	0.06%	0.43%	0.40%	0.18%	0.21%
TOLUENE	0.25%	0.79%	0.25%	0.42%	0.55%	0.56%	0.29%	0.30%
ETHYLBENZENE	0.01%	0.05%	0.02%	0.03%	0.09%	0.05%	0.03%	0.03%
XYLENES	0.15%	0.59%	0.16%	0.20%	0.25%	0.36%	0.23%	0.21%
OCTANES	0.20%	0.61%	0.71%	1.39%	1.07%	2.00%	1.88%	1.32%
NONANES	0.26%	1.03%	0.15%	0.21%	1.23%	2.87%	0.38%	0.58%
DECANES	0.03%	0.08%	0.52%	0.69%	0.54%	0.46%	1.33%	1.11%

Profiles with Weighted Averages Based on Throughput (UDOGM, annual value collected from 6/2018 to 05/2019)

Profiles with Weighted Averages Based on Throughput								
	Gas well - flash gas n=17		Gas well - raw gas n=17		Oil well – flash gas n=50		Oil well – raw gas n=50	
	Mean	St Dev	Mean	St Dev	Mean	St Dev	Mean	St Dev
METHANE	38.66%	17.42%	73.17%	8.47%	12.50%	12.47%	52.17%	32.48%
ETHANE	19.41%	4.88%	10.23%	2.16%	10.62%	4.66%	11.88%	3.34%
PROPANE	18.04%	3.64%	5.86%	2.61%	15.66%	4.83%	9.62%	14.24%
ISOBUTANE	5.46%	1.29%	1.66%	0.83%	4.83%	2.14%	2.28%	4.67%
N-BUTANE	7.18%	2.83%	2.18%	1.16%	11.97%	5.15%	4.98%	6.96%
ISOPENTANE	3.07%	1.76%	1.07%	0.55%	5.99%	3.16%	2.39%	3.26%
N-PENTANE	2.35%	2.65%	0.90%	0.54%	7.89%	4.33%	3.19%	2.78%
CYCLOPENTANE	0.13%	0.26%	0.05%	0.04%	0.59%	0.52%	0.23%	0.17%
N-HEXANE	1.33%	2.22%	0.48%	0.34%	6.55%	3.37%	2.22%	2.31%
CYCLOHEXANE	0.65%	2.46%	1.12%	0.66%	1.75%	0.81%	3.16%	1.20%
HEPTANES	1.23%	2.65%	0.70%	0.94%	12.37%	10.13%	2.60%	6.67%
METHYLCYCLOHEXANE	1.05%	0.55%	0.64%	1.02%	2.20%	1.14%	0.85%	1.93%
2,2,4 TRIMETHYLPENTANE	0.01%	0.00%	0.00%	0.00%	0.04%	0.05%	0.00%	0.02%
BENZENE	0.22%	0.23%	0.09%	0.07%	0.49%	0.63%	0.20%	0.51%
TOLUENE	0.45%	0.33%	0.26%	0.37%	0.69%	0.66%	0.33%	1.12%
ETHYLBENZENE	0.02%	0.03%	0.02%	0.03%	0.05%	0.07%	0.03%	0.05%
XYLENES	0.20%	0.25%	0.17%	0.19%	0.40%	0.27%	0.25%	0.63%
OCTANES	0.21%	1.27%	0.69%	1.28%	2.03%	0.99%	1.89%	0.65%
NONANES	0.29%	0.73%	0.17%	0.23%	2.93%	1.14%	0.45%	1.07%
DECANES	0.07%	0.94%	0.54%	0.71%	0.45%	0.49%	1.29%	0.16%
Sum	100%		100%		100%		100%	

Appendix F: EOS/PSM Comparison Tables

	Well VII-9				
	Mod-FLA	VMG Results - Ver	VMG Results - HC	PROMAX	CEL
COMPONENT	WT%	WT%	WT%	WT%	WT%
CARBON DIOXIDE	1.6006	0.8183	0.6433	1.0779	0.0000
NITROGEN	1.2709	0.0000	0.0000	0.0000	0.0000
METHANE	21.1644	7.4341	8.4944	10.0632	6.5446
ETHANE	20.6420	7.9974	9.6726	9.9664	7.1383
PROPANE	24.5392	14.4977	14.8604	15.1908	13.3137
ISOBUTANE	6.0881	4.0759	4.1303	4.3874	3.8041
N-BUTANE	11.5176	13.9312	13.9140	14.6014	13.5194
ISOPENTANE	2.7009	5.1340	4.9584	4.9364	5.1447
N-PENTANE	4.5492	10.4665	10.5338	9.8793	10.7080
CYCLOPENTANE	0.1856	0.5506	0.5921	0.5593	0.6538
N-HEXANE	1.7430	8.6914	9.8171	7.8521	8.9292
CYCLOHEXANE	0.3102	1.7716	1.7784	7.1934	2.3444
OTHER HEXANE					8.4019
"HEPTANES"	2.3404	16.2355	12.4499	5.4744	7.0503
METHYLCYCLOHEXANE	0.2989	2.0825	1.9834	1.9836	2.6185
2,2,4 TRIMETHYLPENTANE	0.0003	0.0174	0.0312	0.0158	0.0176
BENZENE	0.0740	0.3527	0.3364	0.3654	0.2455
TOLUENE	0.0716	0.5409	0.5521	0.5520	0.8013
ETHYLBENZENE	0.0038	0.0375	0.0409	0.0377	0.0558
XYLENES	0.0326	0.3043	0.2889	0.3252	0.5047

OCTANES	0.4788	1.4355	1.7114	3.2616	4.8638
NONANES	0.1166	3.2661	2.9401	1.3169	1.4991
DECANES	0.2715	0.3591	0.2709	0.9600	1.1200
TOTAL	100.0000	100.0000	100.0000	100.0000	99.2787
VOC WT %	55.3	83.8	81.2	78.9	85.6
FGOR	35.8	42.8	43.3	42.8	37.0
API Gravity	-----	42.4	42.4	49.7	-----
RVP	-----	3.1	3.1	3.4	-----

	Well V-6				
	Mod-FLA	VMG Results - Ver	VMG Results - HC	PROMAX	CEL
COMPONENT	WT%	WT%	WT%	WT%	WT%
CARBON DIOXIDE	1.4356	0.5637	0.5582	0.6244	0.4851
NITROGEN	1.8108	0.0000	0.0000	0.0000	0.0000
METHANE	24.9399	6.2074	6.9570	6.9105	5.3308
ETHANE	20.6035	7.1391	9.1298	7.7355	6.2246
PROPANE	20.9808	11.7560	13.2164	11.8483	10.5776
ISOBUTANE	4.9014	4.4260	4.5926	4.6822	4.0799
N-BUTANE	9.8404	11.8047	11.9545	12.4650	11.3163
ISOPENTANE	3.5698	6.6210	6.9120	6.8360	6.6303
N-PENTANE	4.5745	10.2444	10.1534	10.5285	10.4965
CYCLOPENTANE	0.1315	0.4032	0.4120	0.4492	0.4745
N-HEXANE	2.0297	9.0522	8.1293	9.3262	9.4364
CYCLOHEXANE	0.3020	1.6267	1.7098	8.7858	2.1544
OTHER HEXANE					9.6085
"HEPTANES"	3.2763	20.8155	16.0663	7.7556	8.9935
METHYLCYCLOHEXANE	0.3331	2.2737	2.3852	2.5148	2.8966

2,2,4 TRIMETHYLPENTANE	0.0003	0.0264	0.0337	0.0281	0.0280
BENZENE	0.1103	0.5061	0.4849	0.5913	0.3552
TOLUENE	0.1137	0.8536	0.8112	1.0068	1.2698
ETHYLBENZENE	0.0039	0.0392	0.0250	0.0458	0.0592
XYLENES	0.0439	0.4495	0.4407	0.5584	0.7577
OCTANES	0.5765	1.9249	2.0868	4.4668	5.8470
NONANES	0.1303	2.9066	3.5911	1.6643	1.7122
DECANES	0.2916	0.3602	0.3501	1.1766	1.2660
TOTAL	100.0000	100.0000	100.0000	100.0000	100.0000
VOC WT %	51.2	86.1	83.4	84.7	88.0
FGOR	44.4	55.6	62.8	51.7	46.3
API Gravity	-----	46.1	46.1	51.4	-----
RVP	-----	3.0	3.0	3.0	-----

	Well V-3					
	Mod-FLA	Permit	VMG Results - Ver	VMG Results - HC	PROMAX	CEL
COMPONENT	WT%	WT%	WT%	WT%	WT%	WT%
CARBON DIOXIDE	1.1111	0.0990	0.6813	0.0535	0.7590	0.5255
NITROGEN	1.4924	0.3220	0.0000	0.3444	0.0000	0.0000
METHANE	39.5462	2.7470	18.1884	0.1459	20.6670	13.8168
ETHANE	18.9435	7.8160	10.9771	1.4704	11.4999	8.7818
PROPANE	18.0389	15.6810	14.4887	9.6049	12.8563	12.6695
ISOBUTANE	4.0309	5.4000	4.6508	5.1569	4.7630	4.3046
N-BUTANE	6.6500	16.4480	9.9152	20.2031	10.1965	9.8540
ISOPENTANE	2.3240	8.8880	4.8592	12.8588	4.8967	5.1629
N-PENTANE	2.4936	14.0240	6.1902	15.8986	6.2317	6.7995
CYCLOPENTANE	0.1606	0.4120	0.4946	1.2031	0.5545	0.6530

N-HEXANE	1.0340	9.1810	5.1455	10.8061	5.2610	5.8798
CYCLOHEXANE	0.2573	1.2410	1.4743	3.9157	7.6135	2.2116
OTHER HEXANE		8.1110				9.1536
"HEPTANES"	2.3904	6.1630	14.5020	5.0515	4.9886	6.7274
METHYLCYCLOHEXANE	0.2909	1.1920	1.8469	4.5726	2.0467	2.6484
2,2,4 TRIMETHYLPENTANE	0.0006	0.0000	0.0392	0.0695	0.0416	0.0449
BENZENE	0.0384	0.5110	0.1394	0.8314	0.1659	0.1048
TOLUENE	0.0549	0.3890	0.3864	1.0793	0.4613	0.6616
ETHYLBENZENE	0.0056	0.0000	0.0527	0.0627	0.0623	0.0921
XYLENES	0.0422	0.0420	0.3152	0.4445	0.3989	0.6218
OCTANES	0.5005	1.2270	1.9636	2.4561	3.6759	5.8406
NONANES	0.1376	0.0960	3.3180	3.3328	1.6612	1.9388
DECANES	0.4565	0.0100	0.3714	0.4384	1.1984	1.5069
TOTAL	100	100.0000	100.0000	100.0000	100.0000	100.0000
VOC WT %	38.9	89.0	70.2	98.0	67.1	76.9
FGOR	12.8	9.3	15.7	33.8	15.4	14.2
API Gravity	-----	39.0	49.4	49.4	48.4	-----
RVP	-----	"<0.1"	4.1	4.1	2.3	-----

	Well VII-7				
	Mod-FLA	VMG Results - Ver	VMG Results - HC	PROMAX	CEL
COMPONENT	WT%	WT%	WT%	WT%	WT%
CARBON DIOXIDE	1.7562	1.5284	0.8568	1.7156	1.3155
NITROGEN	1.6996	0.0000	0.0000	0.0000	0.0000
METHANE	21.0902	9.0082	9.2590	10.2132	7.7339
ETHANE	21.6398	9.5855	10.6738	10.4582	8.3920
PROPANE	24.4625	15.2860	16.7281	15.0353	13.9368

ISOBUTANE	4.4147	3.6337	4.3300	3.8393	3.4165
N-BUTANE	11.0706	13.5570	14.2302	14.2890	13.3683
ISOPENTANE	2.6875	4.5950	4.8716	4.7173	4.7722
N-PENTANE	4.6636	9.4726	9.7067	9.6798	10.1072
CYCLOPENTANE	0.1956	0.5004	0.5362	0.5593	0.6249
N-HEXANE	1.9814	7.3241	6.4143	7.5169	8.0238
CYCLOHEXANE	0.3333	1.5880	1.5176	7.3201	2.2542
OTHER HEXANE					8.0248
"HEPTANES"	2.6177	17.0448	14.2484	5.7749	6.9024
METHYLCYCLOHEXANE	0.3116	1.8282	1.6986	2.0176	2.4857
2,2,4 TRIMETHYLPENTANE	0.0003	0.0251	0.0272	0.0265	0.0273
BENZENE	0.0812	0.3069	0.2805	0.3620	0.2243
TOLUENE	0.0767	0.5056	0.4497	0.6000	0.8132
ETHYLBENZENE	0.0037	0.0357	0.0272	0.0419	0.0582
XYLENES	0.0330	0.2921	0.2073	0.3671	0.5338
OCTANES	0.4921	1.4956	1.3713	3.2387	4.5347
NONANES	0.1177	2.1206	2.2941	1.3005	1.4031
DECANES	0.2713	0.2665	0.2713	0.9268	1.0471
TOTAL	100.0000	100.0000	100.0000	100.0000	100.0000
VOC WT %	53.8	79.9	79.2	77.6	82.6
FGOR	27.8	32.7	31.9	41.1	37.1
API Gravity	-----	42.2	42.2	49.7	-----
RVP	-----	3.2	3.2	3.0	-----

	Well V-4				
	Mod-FLA	VMG Results - Ver	VMG Results - HC	PROMAX	CEL
COMPONENT	WT%	WT%	WT%	WT%	WT%

CARBON DIOXIDE	1.9953	0.6200	0.7309	0.6883	0.4821
NITROGEN	2.8619	0.0000	0.0000	0.0000	0.0000
METHANE	26.6431	7.2600	8.3871	8.0928	5.5892
ETHANE	20.6041	8.1674	10.5795	8.7954	6.4646
PROPANE	20.8442	13.4258	15.5588	13.2026	11.2496
ISOBUTANE	4.3751	4.6308	5.0788	4.8501	4.0855
N-BUTANE	9.1302	12.6612	14.1056	13.2503	11.8098
ISOPENTANE	3.0018	6.4090	7.5658	6.5575	6.4608
N-PENTANE	3.8542	9.8644	11.6015	10.0521	10.2819
CYCLOPENTANE	0.1195	0.4013	0.4684	0.4480	0.4899
N-HEXANE	1.7657	8.0354	9.4291	8.2497	8.8326
CYCLOHEXANE	0.2919	1.6247	2.0244	8.0925	2.3042
OTHER HEXANE					9.1768
"HEPTANES"	2.8971	18.4568	3.4610	6.7704	8.4759
METHYLCYCLOHEXANE	0.3210	2.1089	2.6753	2.3347	2.9075
2,2,4 TRIMETHYLPENTANE	0.0002	0.0232	0.0471	0.0245	0.0263
BENZENE	0.0918	0.4565	0.5760	0.5384	0.3348
TOLUENE	0.1704	1.2681	1.2108	1.5073	2.0625
ETHYLBENZENE	0.0042	0.0352	0.0465	0.0413	0.0589
XYLENES	0.0424	0.4005	0.5841	0.5030	0.7550
OCTANES	0.5422	1.5859	2.0677	3.7271	5.4537
NONANES	0.1310	2.2948	2.8315	1.3481	1.5528
DECANES	0.3125	0.2699	0.9701	0.9257	1.1458
TOTAL	100.0000	100.0000	100.0000	100.0000	100.0000
VOC WT %	47.9	84.0	80.3	82.4	87.5
FGOR	39.7	46.3	51.0	42.8	42.1
API Gravity	-----	43.3	43.3	51.3	-----
RVP	-----	3.1	3.1	3.2	-----

